UNIVERSITÀ DELLA CALABRIA

UNIVERSITA' DELLA CALABRIA

Dipartimento di Chimica e Tecnologie Chimiche

Dottorato di Ricerca in

Scienze della Vita

CICLO

XXXIII

Development of new bio-materials and technologies for the green regeneration of RAP

Settore Scientifico Disciplinare CHIM/02

Coordinatore: Ch.mo Prof. Maria Carmela Cerra

Firma _____

Supervisore/Tutor: Ch.mo Prof. Cesare Oliviero Rossi

Firma_____

Dottorando: Dott.ssa Valeria Loise

Firma _____

Sono stati anni lunghi e faticosi, ma sicuramente ad oggi i più stimolanti. Per questo voglio ringraziare la mia famiglia, costante faro nella notte, per avere gioito e sofferto con me sempre durante il lungo percorso formativo che mi ha portato a raggiungere questo importantissimo traguardo. Grazie ai vostri insegnamenti e ai continui stimoli fornitimi, oggi sono fiera della persona che sono diventata.

Un grazie anche alla mia ziuccina, che nonostante la distanza è al mio fianco pronta ad emozionarsi e incoraggiarmi.

Menzione d'onore per Pino che si è sorbito più e più volte i miei discorsi in inglese e i racconti di fine giornata. A lui un grazie particolare per non avermi fatto impazzire durante il lockdown, e per aver reso le lunghe interminabili giornate casalinghe sempre piacevoli e divertenti.

Un pensiero speciale va a tutti i miei preziosissimi amici, da ognuno di voi ho imparato qualcosa e di questo ne sono grata.

In fine i capisaldi della mia vita, la mia dolcissima Carotina e il mio prezioso angelo custode. Ovunque la vita mi porterà sarete sempre nel mio cuore, è stato e sarà per sempre l'onore più grande della mia vita far parte e aver fatto parte delle vostre vite.

Contents

ABSTRACT

Il presente lavoro di ricerca ha avuto come scopo lo sviluppo di nuovi rigeneranti green per il fresato d'asfalto, noto anche come reclaimed asphalt pavement (RAP). Questa ricerca nasce dalla necessità di aumentare l'uso del RAP nelle pavimentazioni stradali. L'uso del RAP ha sia un impatto economico positivo, infatti non è necessario usare inerti e bitume fresco, ma soprattutto ha un alto un impatto in termini di ecosostenibilità, il RAP da rifiuto da smaltire diventa di fatto materia prima, implementando l'economia circolare e l'end waste. Infatti il riuso del fresato d'asfalto consentirebbe di non trattare più questo materiale come uno scarto, con tutti le relative problematiche ambientali derivabili, ma bensì come una risorsa. Inoltre sono state sviluppate ed implementate tecniche di indagine chimico-fisiche e nuove metodologie per determinare i meccanismi di azione di un rigenerante sulla struttura del bitume e distinguere in modo univoco un rigenerante da un semplice flussante. Tale tesi è stata la base scientifica che ha permesso di definire una norma europea e nazionale da seguire per le aziende che commercializzano rigeneranti bituminosi. Spesso infatti il fresato d'asfalto viene trattato con agenti che non modificano la struttura colloidale del bitume riportandola alla loro struttura originaria, ma che semplicemente hanno una mera attività flussante (abbassare la viscosità del sistema). Le "classiche" metodologie di indagine generalmente basate su parametri fisici-meccanici ed ingegneristici, non sono sufficienti per discriminare l'azione di un rigenerante da quella di un flussante. Tale approccio finora comunemente usato ha avuto un forte impatto sulla durata e qualità delle pavimentazioni stradali, effetto devastante dal punto di vista economico, sociale e soprattutto ambientale.

ABSTRACT

The present research aimed to develop a procedure and methodologies that could uniquely distinguish between a fluxing agent and a rejuvenating agent. Recently, it has been realized that the reclaimed asphalt pavement (RAP) was a resource of considerable importance. In fact, it contains an appreciable amount of binder, which under certain conditions can be recycled for the construction of new pavements, thus reducing not only costs but also the use of raw materials. Therefore, this allows to consider the RAP more as a resource than a waste. Most of the time, the bitumen obtained from the RAP is treated with agents that have a mere flux function (lowering the viscosity of the system). These agents do not modify the colloidal structure of the bitumen. Therefore, they are not able to restore the structure of the aged bitumen to that of the neat bitumen. Furthermore, the investigation methodologies generally used to counter the regenerating effect of an additive are based

on physical-mechanical and engineering parameters. These parameters are almost always insufficient to discriminate the action of a regenerant from that of a flux. For this reason, chemical-physical investigation techniques have been developed and implemented to determine the action mechanisms of a rejuvenator on the inner structure of the bitumen. In this way, it was possible to uniquely discriminate between a real rejuvenator and a fluxing agent. Finally, this thesis was the scientific basis that allowed the definition of a new European and National standard to be followed for companies that market bituminous regenerants.

Chapter 1

Introduction

A project funded by the European Community, which began in 2009 and ended in 2012, has highlighted how even a recycling of just 15% of the road pavement brings significant environmental benefits compared to the use of the warm mix. The study also analysed the release of metals and polycyclic aromatic hydrocarbons (PAH) from unused reclaimed asphalt. Highlighting how toxic responses were obtained in leachate tests due to the presence of unknown substances. That is, responses due not to the 16 types of PAH generally sought in waste products from road scarification and not even due to the 12 metals analysed (including nickel, cobalt, zinc, etc.). The team of researchers who conducted the analyses on the ecotoxicity of leachate hypothesized that the high values are due to a synergistic effect of several substances, which could give rise to degradation products [1]. Moreover, as reported in the National Cooperative Highway Research Program Synthesis of Highway Practice 54 [2] the first experiments for the recycling of road pavements date back to 1915, although, as reported in the document, there was little research carried out in this field until the early 1970s. The major push towards research aimed at recycling asphalt pavements came following the 1973 Arab oil embargo, which led to an increase in the price of crude oil [3]. In a publication of U.S. Department of Transportation dated back to 2011 [3] it is specified that:

The same materials used to build the original highway system can be re-used to repair, reconstruct, and maintain them. Where appropriate, recycling of aggregates and other highway construction materials makes sound economic, environmental, and engineering sense;

proving that asphalt recycling is a good practice to be pursued. In fact, a paper by the European Asphalt Pavement Association highlights that since asphalt pavements are built with natural resources (mainly aggregates and bitumen), the reuse of these pavements is of fundamental importance for sustainable development [4].

According to the World Commission on Environment and Development (WCED) [5] sustainability can be defined as:

Development that meets the needs of the present generation without compromising the ability of future generations to meet their own needs.

Chapter 2

2.1 Materials

2.1.1 Historical overview of bitumen

The use of bitumen has very ancient origin, in fact already 40 000 years ago it was used to fix handles to tools. Most of the bitumen artifacts found are distributed in the Middle East, where natural deposits are present. In addition, traces of its use as a mortar for the construction of palace in Mesopotamia and Elam have been found. However, it was also known for its waterproofing properties, so much so that it was used for the famous handing gardens of Babylon. Finally, its use as a building material was so common that bitumen is mentioned in the Bible both as a material for the construction of the Tower of Babel and for the construction of Noa's ark [6]. Instead, is attested of between 625 and 640 B.C. a bituminous mortar was used for the construction of the processional road of Babylon. While the Romans, between the I and IV centuries built a road system in Great Britain, used as a matrix for the modern British road system. The use of bitumen as a material for road pavements almost disappeared until the early 19^{th} century, when new natural deposits were discovered in Europe. Moreover, in the early 1900s, when the discovery of vacuum distillation allowed to have large quantities of bitumen from crude oil, the use of bitumen from natural source was shelved [7]. In any case, the first "modern" road pavement built with bitumen dates back to 1870 by the Belgian chemist Edmund J. DeSmedt. In addition, in the same year J. D. Rockefeller founded the first crude oil company, called Standard Oil Company and now known as Esso.

2.1.1.1 Nomenclature

Crude oil: is a complex mixture of hydrocarbons. Its physical and chemical properties are variable depending to extraction areas. Generally, it is found in the liquid state but crude oils with high molecular mass aliphatic hydrocarbons (paraffines) are solid at ambient temperature.

It is principally composed of:

i. Aliphatic Hydrocarbons (paraffin C_nH_{2n+2} with n up to 35)
ii. Cycloalkanes (naphthenes typically C5-C7)
iii. Aromatic and Polyaromatic compounds.

Bitumen: hydrocarbon product produced by refining process of crude oil by removing its lighter fractions.

From a chemical point of view, the molecular weight distribution analysis of bitumen shows that it is made up of a complex mixture of about 300-2000 chemical compounds (medium value 500-700), which makes a complete chemical characterization extremely difficult. For this reason, bitumen is generally roughly fractionated, such us to identify two main macro components:

i. Asphaltenes;
ii. Maltenes, also known as Petrolens.

From the last macro component, it is possible to obtain Resins and Oil, which are classified as Saturated Oil and Aromatic oil respectively, in order to obtain the famous S.A.R.A. (Saturate, Aromatic, Resin, Asphaltene) classification [8].

Asphalt: road paving material consisting of bitumen, mineral aggregates and fillers, Bitumen constitutes less than 7% of the finished product [9].

Reclaimed asphalt pavement (RAP): mixture of aggregate and asphalt binder. RAP is obtained through the asphalt milling process, or as waste from asphalt production plants or even as an unwanted load returned from the laying site [10,11].

2.1.2 Bitumen structure

Asphaltenes (percentage in bitumen varies from 5-25%) are amorphous brown/black solids, insoluble in n-heptane, with dimension between 5-30 µm and a hydrogen/carbon ratio ranging from 0.98 to 1.6. They are constituted by complex mixtures of hydrocarbons, characterized by condensed aromatic compounds. Asphaltene contains oxygen, nitrogen, sulphur and heavy metals, such as V, Ni etc, with aliphatic chains more than 30 carbon atoms long, pyrrolic and pyridinic rings as shown in Fig.1 [10].

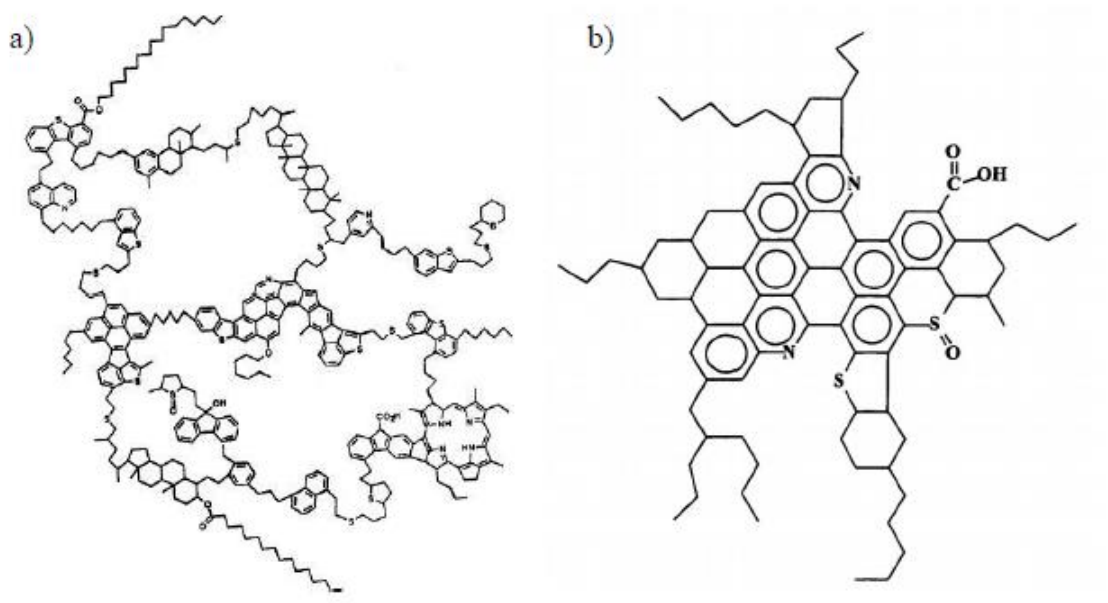

Figure 1 Asphaltene hypotetical structure: a) Archipelago structure: $C_{412}H_{509}O_9S_{17}N_7$ with H/C ratio 1.23 and molecolar weight 6239 g/mol, b) Continent structure: $C_{84}H_{100}O_3S_2N_2$ with H/C ratio 1.19 and molecolar weight 1276 g/mol [12,13]

Bitumen characteristics strongly depends on them. In particular a higher asphaltene content is responsible of a more viscous and harder bitumen.

Resins (percentage in bitumen varies from 10 to 25%) are dark brown solid (or semi-solid) compounds soluble in n-heptane, the adhesive properties of bitumen depend on them. Resins consist mainly of carbon and hydrogen, however small quantities of oxygen, nitrogen and sulphur could be seen. Their principal role is as dispersing agents for the asphaltene macromolecular structures and oils, which are mutually insoluble. Resins molecular weight ranges from 500 to 5000 Dalton, with particle sizes of 1-5 nm and a hydrogen/carbon ratio of 1.3 - 1.4. When bitumen is oxidized resins gains oxygen molecules acquiring a structure similar to asphaltenes. Bitumen characteristics is determined largely by resins asphaltenes ratio [10,14].

Aromatic oils (percentage in bitumen varies from 40 to 65%) are dark brown viscous liquids containing low molecular weight aromatic compounds. Their weight is in the range between 570 and 980 g/mol. They have a high solvent power relative to high molecular weight hydrocarbons. Together with saturated oils aromatic oils are considered as the plasticizing agents of bitumen. Moreover, their hydrogen/carbon ratio ranging between 1.4 – 1.6.

Saturated oils are white/yellow viscous liquids essentially composed by long chain saturated hydrocarbons and naphtenes. They are non-polar compounds with molecular weight ranging between 300-1500 Dalton and constitutes about 5 - 20% of the bitumen.

2.1.3 Reclaimed Asphalt Pavement (RAP)

Thanks to the precious content of bitumen and aggregates, RAP is considered a very promising material as a valid alternative to virgin materials not only for restoration but also for the construction of road pavements. At present, the use of RAP is regulated by state agencies that allow its use no more than 40% [15]. Moreover, its use has often been underestimated due to the high stiffness of the binder which could cause premature fatigue and cracking at low temperatures [16]. However, the reuse of the RAP could contribute to the creation of a virtuous circle, in which the remaining 60% of the unused material would be returned to the circulation. In fact, the recycling of this material would contribute not only to the optimization of the use of natural resources, but also to the creation of a virtuous circle for the environment from the point of view of energy consumption and more. In addition to an undeniable reduction in the production costs of new asphalts [3]. Very often, the materials needed for road pavement construction are not available on site, which would involve transporting materials over long distances with the consequent use of fuel for trucks and the emission of greenhouse gases. Furthermore, the production of new road pavements involves reaching high temperatures both to dry the aggregates and to obtain good workability of the bitumen. The emission of greenhouse gases and harmful pollutants doubles for every 10°C increase in the production temperature of the new asphalt mix [3,17]. Finally, it was found that the use of RAP can reduce energy consumption by approximately 23% [18].

Chapter 3

3.1 Aging mechanism of bitumen and rejuvenating agents

Bitumen is subject to aging processes that affect its properties, this is the main cause of the deterioration of road pavements. For this reason, it is of fundamental importance to study the mechanisms that occur during the aging of bitumen and to understand how aging alters the internal structures of the bitumen, in order to optimize the use of RAP. Furthermore, the reuse of RAP is strictly dependent on the ability to restore precisely those characteristics that make bitumen an excellent material for the construction of road pavements. Hence, the study of agents that can restore the characteristics of aged bitumen has become one of the crucial topics of research in the field of asphalts. Precisely for these reasons, the first part of this thesis was dedicated to an in-depth research of the state of the art on the knowledge about the aging of bitumen and on what has been done so far in the field of rejuvenating agents. However, this paragraph is intended to be an introduction to the aging mechanisms of bitumen and the action of rejuvenators on it, some parts taken from the review work will be briefly reported. First of all, it should be noted that the aging of bitumen "*is a more complex process involving different sub-mechanisms usually taking place in different time-scales. It can already take place during asphalt construction through volatilization of light components in the maltene. Then, long-term aging occurs in the field as a consequence of different processes:*

1. *Oxidative, due to changes in composition through a reaction between bitumen constituents and*

atmospheric oxygen;

2. *Evaporative, due to the evaporation of low-molecular weight components in the maltene. These*

compounds have higher vapor pressure and are somehow volatile so they can escape the maltene

phase causing not only a change of its composition, but also an overall reduction of its amount in

the bitumen;

3. *Structural ageing, by a chemical reaction between molecular components causing polymerization*

with consequent formation of a structure within the bitumen (thixotropy)."

The main function of a rejuvenator should be to restore the original rheological properties of the bitumen, *"very first action to restore the original bitumen rheological properties is to shift back the ratio between solid asphaltenes and fluid maltenes to higher maltene contents. However, a rheological rejuvenating agent can exert its action in different sub-mechanisms:*

1. *Softening (usually called fluxing) agent: flux oil, lube stock, slurry oil, etc. can lower the viscosity of the aged binder;*
2. *Real rejuvenator: it helps to restore the physical and chemical properties".*

Unfortunately, *"literature does not make a clear distinction among the types of mechanism exerted by the specific rejuvenator: this term is usually given to any king of additive, which allows a certain restoring of the original rheological properties, no matter the effective mechanism involved".* All information was collected in a review [19] entitled "A Review on Bitumen Rejuvenation: Mechanisms, Materials, Methods and Perspectives", published on international journal Applied Science, and it is reported later in chapter 5.

Chapter 4

4.1 Experimental Techniques

4.1.1 Nuclear Magnetic Resonance.

Nuclear magnetic resonance (NMR) spectroscopy is a non-destructive analytical chemistry technique used to obtain structural information by identifying the different functional groups that make up the matrix under examination. For this reason, it is a widely used technique in quality control.

4.1.1.1 Basic Concepts

Nucleus of spin I has 2I+1 energy level [20] equally spaced with a separation

$$\Delta E = \mu H_0 / I \qquad \textbf{eq.1,}$$

where H_0 is the applied magnetic field; μ the nuclear magnetic moment given by

$$\mu = \frac{\gamma \hbar I}{2\pi} \qquad \textbf{eq.2;}$$

and γ and $\hbar$ are magnetogyric ratio and reduced Planck constant respectively. Having an ensemble of nuclei, it is possible to define a magnetization vector $\boldsymbol{M}$ from the sum of all the nuclear magnetic moments. The frequency of radiation that induces a transition between adjacent levels is

$$\nu_0 = \frac{\Delta E}{h} = \gamma H_0 / 2\pi \qquad \textbf{eq.3.}$$

At equilibrium, nuclei are distributed among the energy levels according to a Boltzmann distribution.

Assuming to excite the nuclei, if the pulse provided were along the direction of the applied magnetic field, then would create a component of the vector $\boldsymbol{M}$ perpendicular to H_0, called transverse.

At the same time the component called longitudinal of the vector $\boldsymbol{M}$ disappears, that is the one along the direction of the field H_0.

If the pulse was turned off, then the nuclear spin system would return to equilibrium. The time for the transverse magnetization to disappear is indicated as T_2, on the contrary the time for the longitudinal magnetization to reappear is called T_1 (see Figure 2).

The physical meaning of these two relaxation times is profoundly different, and in general $T_2 \approx T_1$ in a solution, while $T_2 << T_1$ in a solid.

In fact, T_1 considers the energy exchange of the nuclear spin with neighboring molecules (lattice). This exchange of energy depends on the momentum and the interaction between the nuclear spins and their surroundings. More in detail, the momentum will be influenced by variations in temperature and viscosity of the matrix examined, while the interaction nuclear spin/surrounding will be influenced by local magnetic fields. Regarding T_2, after a pulse perpendicular to H_0 the nuclear spins are aligned along one direction, i.e. they are in phase coherence [21], with each other.

Quickly the spins undergo a phase shift due to the spin-spin interactions, that is to the interactions between the single magnetic moments experienced by each spin. This leads to a gradual reduction of the transverse magnetization vector.

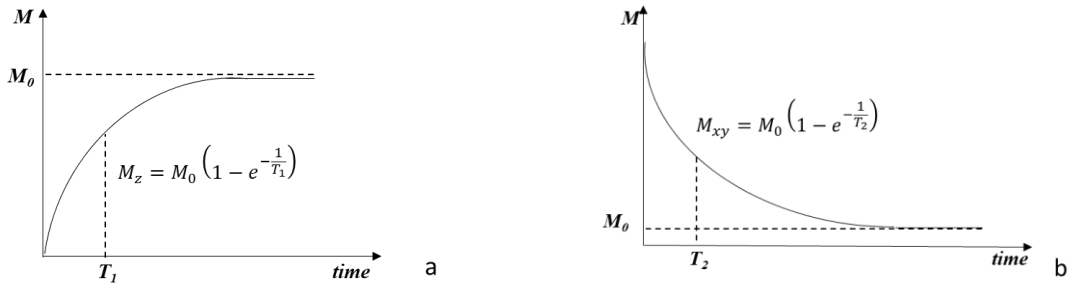

Figure 2 Relaxation time T_1 a and Relaxation time T_2 b.

Moreover, the transverse decay of the magnetization is also influenced by the variations of the applied field H_0 which leads to a T_{2i} due to the inhomogeneity of the field. Therefore, the overall transverse relaxation time will be:

$$T_2^* = T_2 + T_{2i}$$

Free Induction Decay (FID)

Suppose a 90° pulse is applied perpendicular to the applied field and a coil is placed along this perpendicular direction, then the transverse magnetization, in accordance with Faraday's law,

generates an electric current acquired by the coil itself.

$$\varepsilon = -\frac{d\Phi_H}{dt} \qquad \textbf{eq.4.}$$

When the pulse is stopped the transverse magnetization will relax. Plotting the induced current as a function of time, a sine wave is obtained which attenuates exponentially according to the time constant T_2^* (Figure 3). This signal is the so called Free Induction Decay (FID) [22].

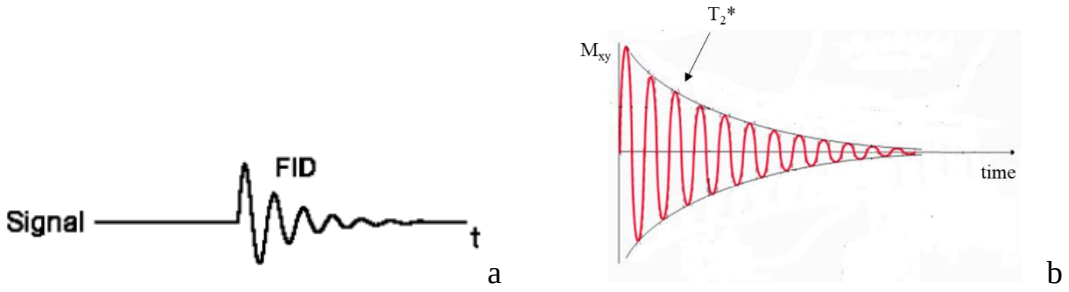

Figure 3 a Time diagram of FID, and b T_2^* relaxation time.

4.1.2 Spin-Spin Relaxation time measurement: Spin Echo Sequences.

The relaxation time that is commonly useful to investigate is T_2 , as it is related to the internal structure of the sample. The problem therefore arises of "cleaning" the signal from field inhomogeneities in such a way as to obtain $T_2^* = T_2$.

An ingenious method for overcoming the inhomogeneity problem was first, proposed by Hahn [23] who called it the spin-echo method. In this method a 90° pulse is applied, after which the FID is allowed to decay away for time τ, subsequently another pulse at 180° is applied (Figure 4). A free induction "echo" forms at time τ after this last pulse, or in other word at 2τ after the firs pulse.

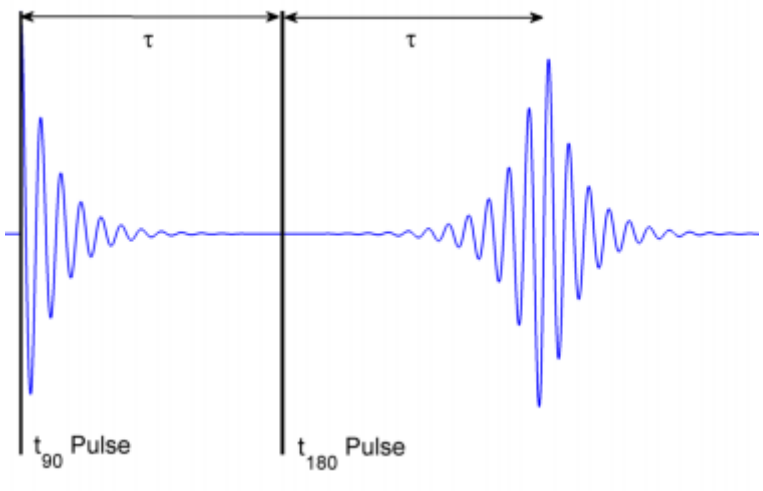

Figure 4 Spin-echo sequence proposed by Hahn.

To understand what caused the spins to return in phase in such a way as to generate another FID signal, it is necessary to investigate what happens to the spins that are affected by different fields due to the field inhomogeneity [24]. Following a 90◦ pulse, spins in a region in which there is relatively high magnetic field precess faster, while those in a region in which there is a relatively low magnetic field precess slower. By a time τ later, the phases of the magnetization across different regions disagree sufficiently to degrade the overall magnetization. The application of a 180° pulse has the effect of reversing these spins precession motion. The result is that a time τ after the 180◦ pulse, all the spins are back in phase and the total magnetization reaches a maximum, producing a spin echo (Figure 5) [25].

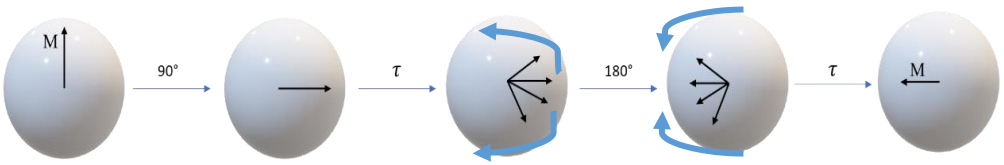

Figure 5 Behavior of Magnetization during Hanh Pulse sequence.

In this way, the magnetization decays exponentially with $^{2\tau}/_{T_2}$, where τ is the time between the pulse.

This is true only if the field inhomogeneity and the diffusion rates of the nuclei are small, otherwise the exponential decay will have to take these two factors into account, as reported in the eq.5 below in which T_{2i} is the term for the field inhomogeneity and $\frac{2}{3}D\tau^3$ is the term for the diffusion rate.

$$M(2\tau) = M_0 \times e^{-\frac{2\tau}{T_2}} \times e^{-\left((T_{2i})^2 \frac{2}{3} D\tau^3\right)} \qquad \textbf{eq.5.}$$

The refocusing of the total magnetization depends on the ability that each nucleus has to remain in a constant magnetic field for the duration of the sequence. If the diffusion, that is the movement of the nuclei, leads them to move from one part with a certain inhomogeneity of field to another with different inhomogeneity, then the amplitude of the echo is reduced [26].

Carr and Purcell [27] showed that a simple modification of Hahn's spin-echo method reduces drastically the effect of diffusion on the determination of T_2. This method may be described as a 90°, τ, 180°, 2 τ, 180°, 2 τ, 180°, 2 τ,…… sequence (or, more commonly, a Carr—Purcell sequence).

4.1.3 Inverse Laplace Transform of the echo decay.

If the FID of Carr-Purcell sequence has a mono-exponential decay, the relaxation time T_2 of the sample can be obtained by fitting the n echos to the following equation:

$$A_n = A_o e^{-2n\tau/T_2} \qquad \textbf{eq.6};$$

where A_n is the amplitude of nth echo, and A_o is a constant depending on the sample magnetization, filling factor and other experimental parameters.

The Laplace transform is a powerful tool for solving ordinary and partial differential equations, linear difference equations and linear convolution equations. The Laplace transform F(s) of a function f (t) [28,29] is defined by:

$$F(s) = \int_0^\infty f(t)e^{-st}\,dt = L[f(t)] \quad \textbf{eq.7}$$

The transformation process from the domain s to the time domain t is called the inverse Laplace transform (see eq.8), in this case, the transformation process from the frequency domain to the time domain.

$$f(t) = L^{-1}[F(s)] \qquad \textbf{eq.8}$$

Large variations of $f(t)$ for very large t, produce small variations of the transform $F(s)$.

Normally, the T_2 relaxation time varies all over the sample due to the sample heterogeneity or surface relaxation differences; then a multiexponential attenuation of the Carr-Purcell FID should be observed. Hence, if inside the sample a continuous distribution of relaxation times exists, the amplitude of the nth echo in the echo train is given by:

$$A_n = A_0 \int_0^\infty P(T_2)e^{-2n\tau/T_2}\,dT_2 \qquad \textbf{eq.9};$$

where $P(T_2)$ is the Inverse Laplace transform (ILT) of the unknown function that fit the echo amplitude curve. Hence $P(T_2)$ could be interpreted as a distribution of rate constants, strictly, a probability density function, PDF. The ILT allows to have information related to the structural organization of the examined samples.

4.1.4 Pulsed Gradient Spin Echo – Nuclear Magnetic Resonance (PGSE-NMR)

The inner nanostructure of bitumen can be investigated through a particular kind of NMR, that is Pulse Gradient Spin Echo (PGSE-NMR), which allows to have information on the Brownian motion of the particles (self-diffusion). Self-diffusion is the result of the thermal motion that induce random-walk, i.e. rotational and translational motion. In particular, in solution translational motion is commonly referred to as self-diffusion and is defined with a self-diffusion coefficient D. The magnitude of this coefficient is given by:

$$D = k_B T/f \qquad \textbf{eq.10};$$

where T is the temperature, k_B is the well-known Boltzmannn's constant and f is a frictional factor.

The friction factor expresses the resistance exerted by a fluid on a object that moves inside it. In the case of a sphere of radius r in a medium of viscosity η, this factor is given by the Stokes equation:

$$f = 6\pi\eta r \qquad \textbf{eq.11}.$$

In this way, the self-diffusion coefficient can be obtained through the Stokes-Einstein [30] equation (eq.12).

$$D = k_B T/6\pi\eta r \qquad \textbf{eq.12.}$$

The function expressing the probability that molecules experience a displacement Z in a time t is given by:

$$P(Z,t) = (4\pi Dt)^{-3/2} \times e^{\frac{-Z^2}{4Dt}} \qquad \textbf{eq.13;}$$

where D is the self-diffusion coefficient.

The PGSE is the basic NMR sequence for the determination of D [31,32]. The most common PGSE experiment is based on a pulse sequence consisting of a 90° RF pulse at t = 0 followed by a 180° RF pulse at t = τ; this results in a spin-echo at t = 2τ. In addition to RF pulses, a pulsed magnetic field gradient is inserted on each side of the 180° RF pulse, causing the attenuation of echo intensities. The parameters associated with the RF and magnetic field gradient pulse sequence are shown in Figure 6.

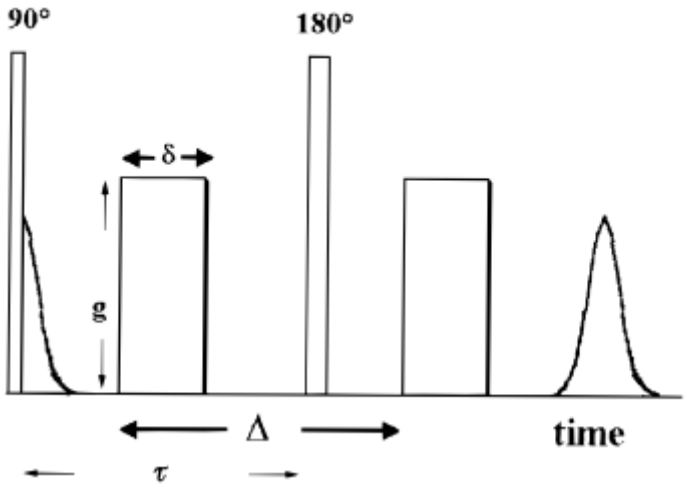

Figure 6 Schematic representation of Pulsed field Gradient Spin-Echo (PGSE-NMR) sequence.

In the case of free Gaussian diffusion, the theoretical expression of echo attenuation, R, is given by the well-known Stejskal-Tanner equation:

$$R = \frac{I(g)}{I(0)} = exp\left[-(\gamma\delta g)^2 D(\Delta - {}^{\delta}/_{3})\right] \qquad \textbf{eq.14}$$

Here $I(g)$ and $I(0)$ are the signal intensities at t = 2τ in the presence of gradient pulses of strength g and in the absence of any gradient pulses, respectively. The time between 90° and 180° RF pulses is τ, γ is the magnetogyric ratio, δ is the duration of the gradient pulses, Δ is the time between the leading edges of the gradient pulses (time of the diffusion), and D is the self-diffusion coefficient.

4.2 Atomic Force Microscopy (AFM)

Atomic force microscopy is a relatively novel method, in fact the first AFM was developed by researchers at Stanford University and at IBM San Jose Research Laboratory in the late 1980s. AFM was born as a development of scanning tunneling microscopy invented in 1982 by Binning and Rohrer [33,34]. An AFM is profoundly different from other microscopic techniques, which concentrate beams of light or electrons on the surface of the sample under examination in order to reconstruct a 2D image. Instead it builds a height map of the sample surface, detecting the force acting between a sharp probe and the surface of the sample, i.e. the AFM probe physically interacts with the sample.

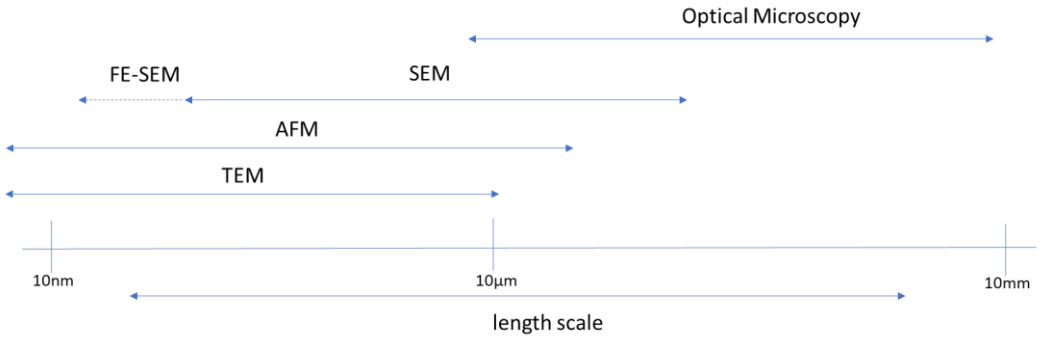

Figure 7 Comparison of length-scales of various microscopes

Since this type of microscopy is based on a mechanical scanning of the surface, it is not convenient in terms of analysis times to go beyond 100x100 μm^2 of surface to be analyzed. Moreover, to carry out an AFM analysis the sample does not need particular analysis conditions (such as vacuum). Finally, unlike Scanning Electron Microscopy (SEM) and Transmission Electron Microscopy (TEM) which can be used only for conductive samples, or which are rendered so with a metallic layer, AFM can be used on any type of sample without needing it to be "prepared" for the analysis [35].

An atomic force microscope consists of a tip attached to a very flexible cantilever and an optical level system: a laser diode and photodiode (Figure 8).

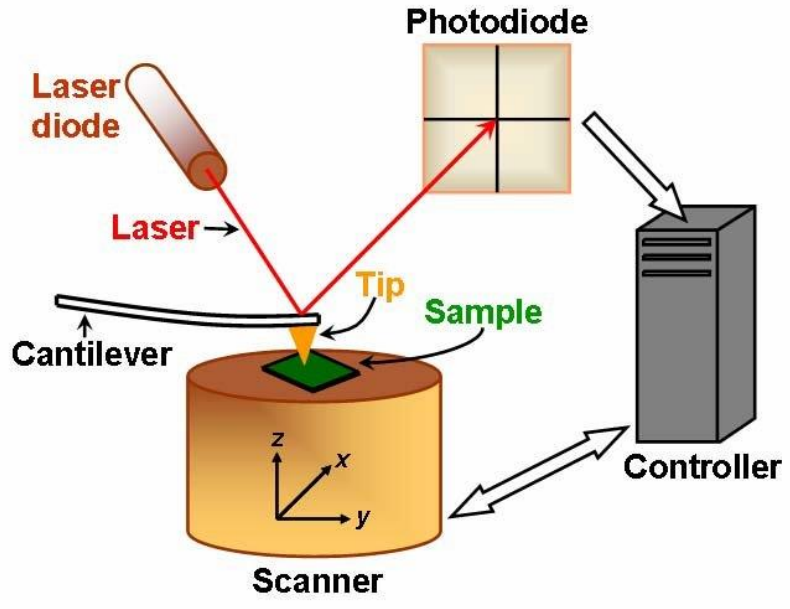

Figure 8 Simplified schematic of an atomic force microscope

A piezoelectric scanner moves the tip on the surface of the sample under examination under the tip, while the optical lever detects the movements of the lever, due to the force between the tip and the sample [34,35]. The microscope can operate in three different ways: contact mode; non-contact mode and intermittent-contact mode.

Contact Mode

In this operation mode the Van der Waals forces that are established between the sample and the tip cause the cantilever to bend, when the latter is pushed against the sample, rather than forcing the atoms of the tip close to those of the sample [36]. In addition, two other forces influence the cantilever movement, namely capillary force and the force exerted by the cantilever itself. The first of these two forces is due to the presence of a thin layer of water, due to environment humidity, which generates an attractive force between the tip and the sample. However, it is assumed that the water layer is homogeneous.

The second force can be seen as the force of a compressed spring. However, the magnitude and sign

(i.e. repulsive or attractive) of the cantilever force depends upon the deflection of the cantilever and upon its spring constant. The sum between the capillary force and cantilever force must be balanced by the Van der Waals force.

Contact operation mode is usually used on hard samples since the intense friction and capillary forces between the tip and the sample during the scanning procedure may damage the sample surface.

Non-contact Mode

No-contact mode is a vibrational mode in which the tip is never brought in physical contact with the surface. To prevent the contact, the probe is kept vibrating. When the cantilever, which vibrates at its resonant frequency, approaches the surface of the sample, it can detect changes in resonant frequency and amplitude of vibration. The frequency of vibration can be described through its spring constant k_0 (eq.15).

$$f_0 = \sqrt{\frac{k_0}{m}} \qquad \textbf{eq.15.}$$

Because of the Van Der Waals force between the tip and the sample surface, the cantilever vibration at its resonant frequency near the sample surface experiences a shift in spring constant from its intrinsic spring constant (k_0). This is called the effective spring constant (k_{eff}) for which it holds:

$$k_{eff} = k_0 - F' \qquad \textbf{eq.16;}$$

where $F' = \frac{\partial f}{\partial z}$ is the force gradient.

Therefore, when the force gradient is positive the force constant k_{eff} is smaller than k_0 (the tip moves closer to the surface), vice versa when the force gradient is negative k_{eff} is larger than k_0 (the tip moves more away from the surface) [37].

Intermitted-contact Mode

This method, also known as tapping mode, the cantilever tip is positioned close to the sample surface so that it can "taps" it during its vibration. First, when the tip is distant from the sample (i.e. not subjected to Van der Waals forces), the resonance curve (amplitude of vibration as a function of frequency) of the cantilever is constructed. Subsequently, a working frequency is set, close to the vibration frequency, which will be kept constant during the analysis. As the tip approaches the sample it begins to feel the force gradient due to the Van der Waals interactions. This causes a shift of the resonance curve towards lower frequencies (Figure 9). Since the working frequency remains constant, there is an increase in the amplitude of oscillation until, as the tip approaches the sample more and more, the tip touches the surface of the sample intermittently [38].

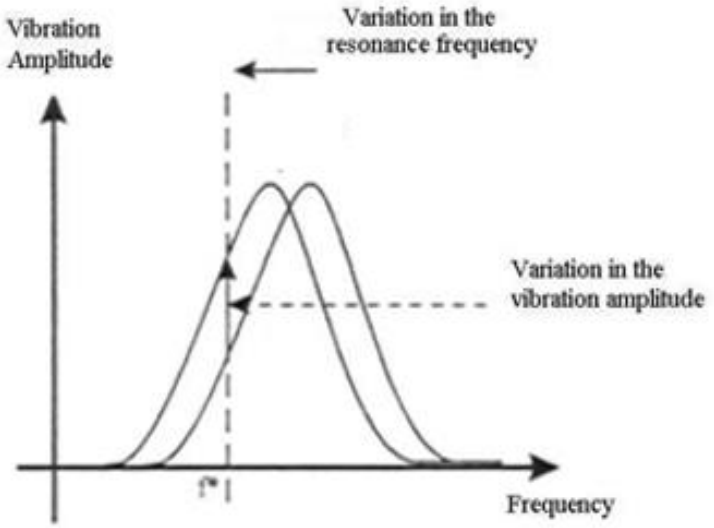

Figure 9 As the tip / sample distance decreases, the resonance curve shifts and the amplitude of vibration increases

Moreover, the tapping mode provides qualitative information on the mechanical properties of the sample surface, through the so-called phase imaging. In fact, it is possible to distinguish between areas of the surface that have different mechanical properties, through the acquisition of the dephasing between the oscillation of the tip and the oscillating signal acquired by the photodiode. The measurement of the dephasing provides information on the energy of the cantilever dissipated during contact with the sample. If the sample has hard zones and soft zones, then the energy dissipated by the cantilever coming into contact with the rigid zone will be less than that dissipated by when it

comes into contact with the soft zone. Soft areas will appear in the phase image as dark areas, while hard areas as light areas (Figure 10).

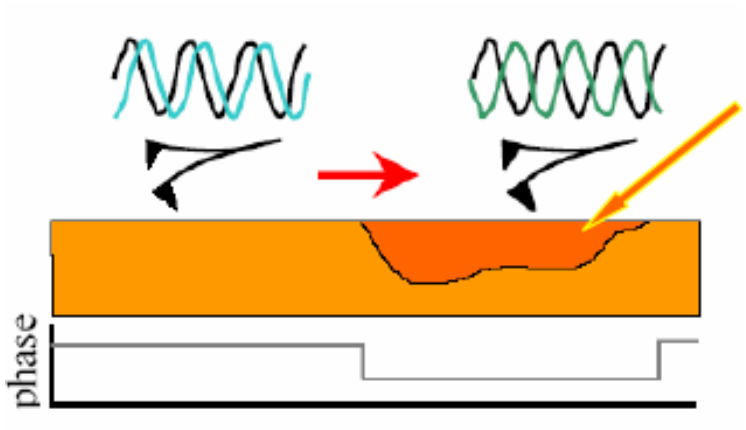

Figure 10 Dephasing of the cantilever signal with respect to that recorded by the photodiode as a function of the mechanical properties of the sample.

Application of AFM to bitumen

In 1996 Loeber et al. [39] published a research in which they explained the use of the AFM technique applied to bitumen, this was the first work in this sense. They observed the presence of periodic structures called bee-structures and noticed that at higher magnifications these same structures were no longer visible. They gave way to a three-dimensional network, formed by interconnected aggregate particles, or asphaltenes interconnected through resins. Since then, many studies have been carried out on the characterization of bitumen using AFM. In an interesting study conducted in 2006 by Masson et al. [40], it emerged that not all bitumens have repetitive bee-structures. In fact, they observed different types of structures depending on the bitumen analyzed. They were therefore identified (see Figure 11):

- Catana Phase, when the bee-structures are not independent from each other;
- Peri-phase, a darker layer surrounding the catana phase;
- Para-phase, the clearest layer in which the catana and the peri phase are immersed.

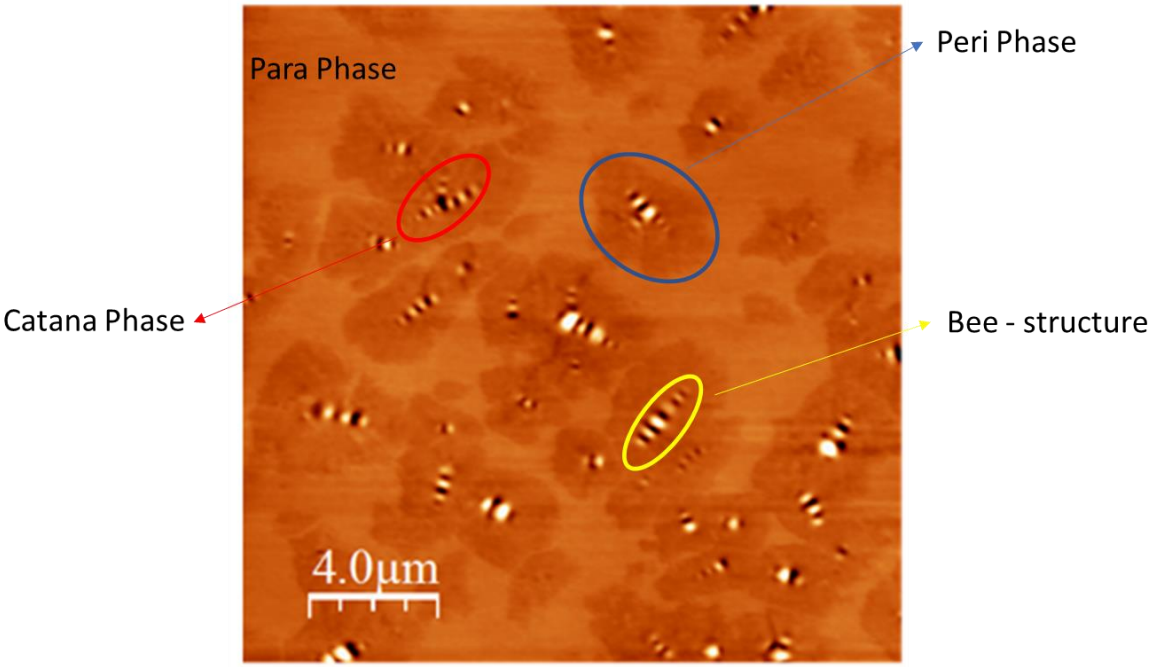

Figure 11 AFM imagine of the bitumen structure.

Furthermore, in this study the authors found that there is no correlation between the SARA of a bitumen and the structures observed by AFM. Furthermore, it was pointed out that AFM analysis is strongly influenced by the sample preparation method. For this reason, the bitumen samples that have been the subject of this thesis were all prepared by heating the sample placed on the support for analysis in a preheated oven at 100 ° C for 10 min. Subsequently, they were left in the stove with the door open for another 15 min in order to cool them.

4.3 Fundamentals Rheology of Viscoelastic Matter.

Rheology, according to Bingham's definition that first coined the term, is the study of deformation and flow of materials.

Traditionally, fluids deform irreversibly under a certain load, conversely, solids deform under a load and recover their original shape when the load is removed. However, there are materials defined as soft matter that are halfway between the behavior of a liquid and that of a solid. Soft matter systems are typically “viscoelastic” materials, that display a combination of viscous (fluid-like) and elastic (solid-like) behavior. This characteristic of a material depends on the observation time of its properties [41].

In order to define what is meant by deformation and flow in the rheological field, consider a small solid cube having sides of length l and area A, as shown in Figure 12.

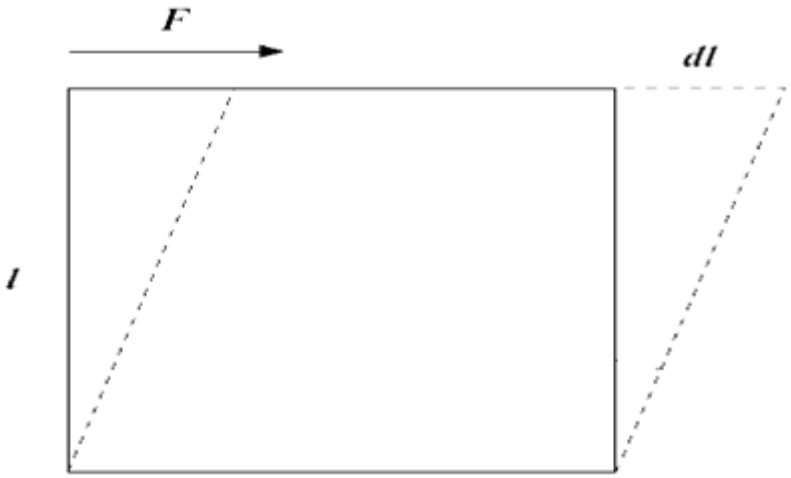

Figure 12 A small element of material subject to a shear force

Suppose that the bottom surface is held in place, and that we apply a shear force F parallel to plane of the top surface. The shear stress σ is given by:

$$\sigma = {}^{F}/_{A} \qquad \textbf{eq.17.}$$

In this way, the shear strain γ (eq.18) is the response of the small solid cube to the applied shear force, i.e. relative deformation.

$$\gamma = {}^{dl}/_{l} \qquad \textbf{eq.18.}$$

For a perfectly elastic solid, stress and strain are linearly proportional, Hook's law:

$$\sigma = G'\gamma \qquad \textbf{eq.19,}$$

where G', named elastic modulus, is a measure of the elastic energy stored in the material when it is deformed. Hooke's Law implies reversibility – the deformation immediately returns to zero when the shear stress is removed. Now imagine applying the same shear stress to the same cubic element of a Newtonian fluid. In this case, the material flows continuously – the strain continues to increase for as long as the stress is applied. If the stress is increased, the fluid flows faster. Newton's law of viscosity states that:

$$\sigma = \eta\dot{\gamma} \qquad \textbf{eq.20;}$$

where $\dot{\gamma} = {}^{d\gamma}/_{dt}$ is the strain rate and η is the viscosity, related to the dissipation of energy in the flow. Therefore, η can be thought of as the tendency of a material to resist flow. However, although stress and strain are tensor quantities, for the general purpose of this chapter they will be treated as scalar quantities. This implies neglect any material anisotropy [41][42]. At this point it is appropriate to

specify what is meant by Newtonian fluid. By analyzing fluids from a viscosity point of view, it is possible to make a distinction between Newtonian and non-Newtonian fluids. Thus, as seen in eq. 20 for Newtonian fluids there is a direct proportionality between shear stress and shear rate. Instead, as regards the non-Newtonian fluids, these show a divergent trend from linearity at high shear rate values, as shown in the figure below.

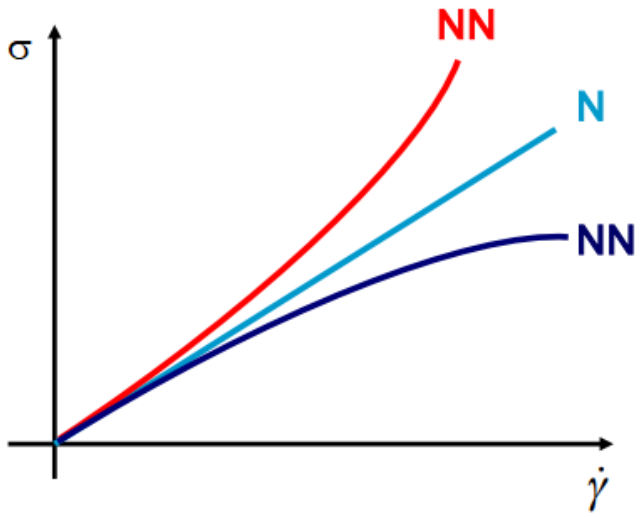

Figure 13 relationship between shear stress and shear rate (Newtonian and non-Newtonian fluids)

This implies that the viscosity is a function of the shear rate. Therefore, it is possible to construct a graph of viscosity as a function of shear rate. If the viscosity is increasing there are non-Newtonian shear-thickening fluids, on the contrary if the viscosity is decreasing there are non-Newtonian fluids of the shear-thinning type (see Figure 13).

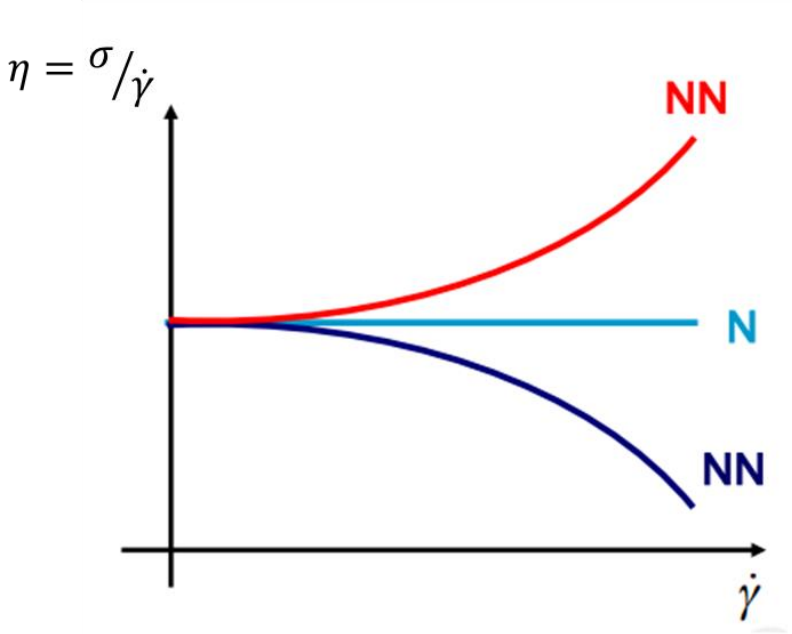

Figure 14 thixotropic and antithixotropic fluids

Moreover, a further distinction can be made when shear stress decreases monotonically, at a constant shear rate, then we have a thixotropic fluid. Conversely, when shear stress increase, then we have an antithixotropic fluids (also known as rheopectic fluids) [43].

Furthermore, when a thixotropic fluid is subjected to a shear rate ranging from $\dot{\gamma} = 0$ to $\dot{\gamma}_0$ and back, then the shear stress will show a hysteresis loop (see Figure 15). However, if the shear rate cycle were repeated, then the hysteresis loop would be reduced to reproduce the trend for $\sigma_0(\dot{\gamma})$ [44].

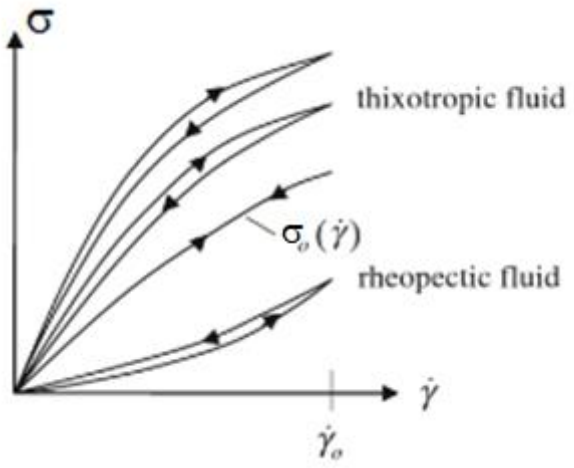

Figure 15 trend of shear stress for a thixotropic fluid

Since bitumen is a viscoelastic material, future treatments will be limited to the specific case.

The simplest model of a viscoelastic material is originally due to Maxwell [45], and is mechanically equivalent to a spring in series with a viscous damper (a dashpot) (see Figure 16). When a load is applied the dashpot will open, but once the load is removed the dashpot will not close, i.e. recovery will not take place as in the case of the spring alone.

Figure 16 The spring-dashpot representation, the viscous and elastic elements are combined in series

Based on this representation of viscoelastic systems it is possible to apply different static and dynamic tests to investigate the mechanical properties of materials.

For the development of this thesis work, dynamic tests were carried out, since the bitumen is always subject to dynamic rather than static loads. Specifically, dynamic tests in oscillatory regime were used. In these types of tests, sinusoidal stresses are applied to determine mechanical parameters such as elastic and viscous modulus.

For a perfectly elastic solid, the strain is exactly in phase with the stress (Figure 17A). For a perfectly viscous liquid, the strain is 90° out of phase (Figure 17C). In the case of a viscoelastic material (Figure 17B), the strain is somewhere in between, i.e. $\frac{\pi}{2} > \delta > 0$ [46].

.

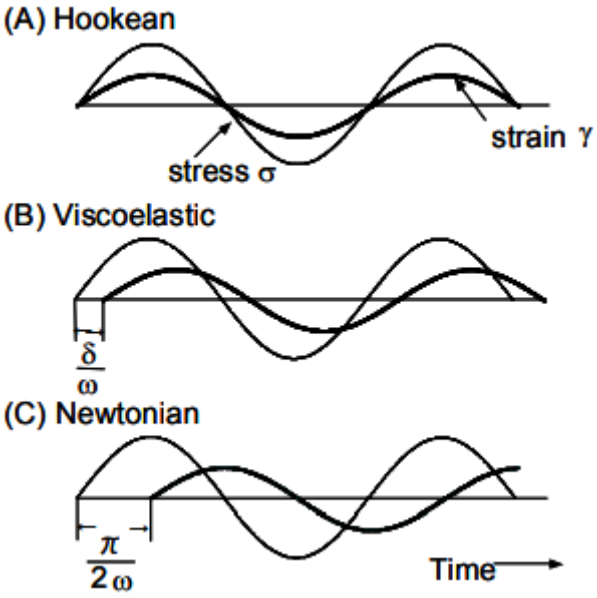

Figure 17 Relationship between stress and strain in oscillatory regime, for a perfectly elastic solid (A), for viscoelastic material (B) and for perfectly viscous liquid (C).

Thus, in viscoelastic materials a phase shift is created between stress and strain. The phase angles between the stress and the strain is an extremely useful parameter, in fact the tangent of the angle is defined as the ratio between the energy lost and that stored during the deformation. Amplitude attenuation of the sinusoidal strain and delay of the strain wave are known to be dependent on the viscoelastic properties of the material. The more the phase angle is close to the value of 90 °, the more the viscous component of the material under examination is predominant. On the contrary, the more the phase angle is close to 0° the more the elastic component of the material is predominant (eq.21).

$$tan\delta = \frac{G''}{G'} \qquad \textbf{eq.21,}$$

where G''represents the viscous component of material behavior (loss modulus), and G'represents the elastic component of material behavior (storage modulus).

Typical rheological tests on bitumen samples are carried out using a controlled shear stress rheometer equipped with a parallel plate geometry (gap 2 mm, / = 25 mm) and a Peltier system (±0.1°C) for temperature control. Dynamic tests, carried out in conditions of linearity where measured material functions are independent of the amplitude of applied load and are the only function of microstructure [47], are adopted for material characterization. Aimed at investigating the material phase transition, temperature sweep tests are performed at 1 Hz increasing temperature

from 25 °C to 120 °C at 1 °C/min and applying the proper stress values to guarantee linear viscoelastic conditions (previously determined by stress sweep tests) at all tested temperatures.

4.3.1 Deborah number

As mentioned before, the response of soft matter to an applied deformation or stress is time-dependent. In 1964 Reiner [48] proposed a dimensionless number (eq.22), labelled ad Deborah number (D_e), as a measure of the solid or liquid behavior of a material, the idea behind Deborah's issue is that everything flows if you wait long enough.

$$D_e = {}^{\lambda}/_{t_0} \quad \textbf{eq.22;}$$

Where λ is the relaxation time and t_0 is the observation time. If the material behaves as solids, that is it cannot relax the applied stress, then the relaxation time is long and the Deborah number is large. On the other hand, if the material behaves as viscous liquid, that is the stress applied will be dissipated, then the relaxation time is short and the Deborah number is small.

Through Deborah number it is possible to classify the materials into three categories:

- D_e >> 1, solid-like materials;
- D_e << 1, liquid-like materials;
- $D_e \approx 1$, viscoelastic materials.

4.4 X-ray Diffraction

X-ray diffraction is a powerful nondestructive analysis that provides information on structure, crystal defects, preferred crystal orientations, more in general on structural parameters on the sample under examination [49]. X-rays have a wavelength ranging from 10 to 10^{-3} nm and overlapping with γ-rays in the shorter wavelengths and with UV in the longer wavelength [50,51]. They are produced by applying a high voltage between two electrodes so that the electrons pass from the cathode to the anode. The electrons that lose all their kinetic energy in the collision with the anode originate the X-rays at maximum energy (or shortest wavelength), which can be calculated through equations 23 and 24.

$$eV = h\nu_{max} \qquad \textbf{eq.23,}$$

$$\lambda_s = \frac{c}{\nu_{max}} = \frac{hc}{eV} \qquad \textbf{eq.24;}$$

Where λ_s is the shortest wavelength and ν_{max} is the maximum frequency.

The continuous X-ray spectrum is due to electrons losing their kinetic energy in a series of collision. However, it is important to note that only less than 1% of the kinetic energy turns into X-rays, most of it dissipates in the form of heat. [50,52]. Therefore, when a beam of X-ray hits a material two phenomena can occur. The first, called absorption, when an incident electron has enough energy to eject an electron from the inner shell, the electron will leave a hole in its place. If such hole is filled by an electron from an outer shell, an X-ray photon is produced. This latter X-ray photon has energy equal to the energy difference between the level of the ejected electron and that of the electron that has taken its place. The second phenomenon, called scattering, generates scattered X-rays with the same with the same wavelength as the same beam [50,52,53]. The diffraction pattern is a function of the structure of the sample, or its electronic distribution. Diffraction patterns can be observed only when the Bragg condition is satisfied:

$$n\lambda = 2dsin\theta \qquad \textbf{eq.25;}$$

Where λ is the wavelength of the incident beam; n is an integer (called the order of reflection); d is the distance between each adjacent crystal plane; θ is the incident angle (see Figure 18) [51].

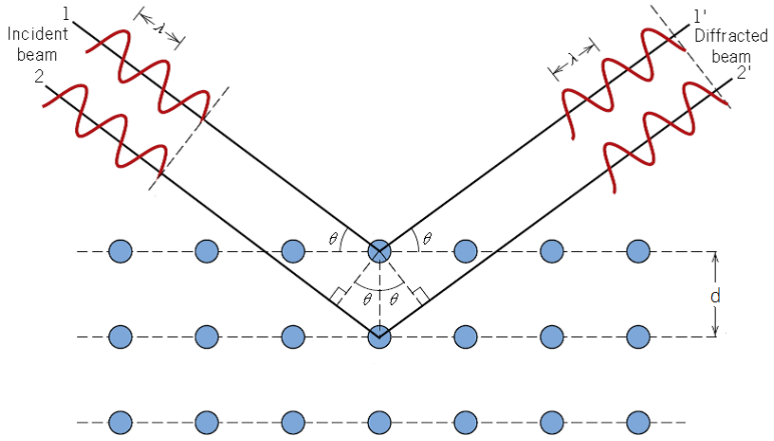

Figure 18 Bragg condition: incident X-ray and the scattered one form an angle θ with the crystalline plane.

X-ray diffraction can be used both on single crystals (regular geometric arrangement that is infinitely repeated in the three spatial dimensions) and on polycrystalline aggregates, in the latter case the material is referred to as powder (such as ceramic, polymer, …). When a powder is analysed it will be referred to as PXRD (powder X-ray diffraction). In this case it is possible to observe the diffraction of all the possible interatomic planes of each single crystallite, each at its own angle of refraction θ [54].

BIBLIOGRAPHY

1. Mollenhauer, K.; Mouillet Re-road – End of life strategies of asphalt pavements. *Eur. Comm. DG Res.* **2011**, 1–22.

2. National, T.; Highway, C. *National Cooperative Highway Research Program Fiscal Year 2014*; 2014; ISBN 0309028590.

3. Copeland, a Reclaimed Asphalt Pavement in Asphalt Mixtures: State of the Practice. *Rep. No. FHWA-HRT-11-021* **2011**, McLean, Virginia.

4. EAPA Arguments to stimulate the government to promote asphalt reuse and recycling. *Eur. Asph. Pavement Assoc.* **2008**, 1–14.

5. Visser, W.; Brundtland, G.H. Our Common Future ('The Brundtland Report'): World Commission on Environment and Development. *Top 50 Sustain. Books* **2013**, 52–55, doi:10.9774/gleaf.978-1-907643-44-6_12.

6. Connan, J. Use and trade of bitumen in antiquity and prehistory: Molecular archaeology reveals secrets of past civilizations. *Philos. Trans. R. Soc. B Biol. Sci.* **1999**, *354*, 33–50, doi:10.1098/rstb.1999.0358.

7. Lesueur, D. The colloidal structure of bitumen: Consequences on the rheology and on the mechanisms of bitumen modification. *Adv. Colloid Interface Sci.* **2009**, *145*, 42–82, doi:10.1016/j.cis.2008.08.011.

8. Ashoori, S.; Sharifi, M.; Masoumi, M.; Mohammad Salehi, M. The relationship between SARA fractions and crude oil stability. *Egypt. J. Pet.* **2017**, *26*, 209–213, doi:https://doi.org/10.1016/j.ejpe.2016.04.002.

9. Caputo, P.; Abe, A.A.; Loise, V.; Porto, M.; Calandra, P.; Angelico, R.; Rossi, C.O. The role of additives in warm mix asphalt technology: An insight into their mechanisms of improving an emerging technology. *Nanomaterials* **2020**, *10*, 1–17, doi:10.3390/nano10061202.

10. Hunter, R.; Self, A.; Read, J. *The Shell Bitumen Handbook*; Hunter, R., Ed.; 6th ed.; ICE Publishing: London, 2015; ISBN 0727758373.

11. Al-Qadi, I.L.; Elseifi, M.; Carpenter, S.H. Reclaimed asphalt pavement - A literature review.

Fed. Highw. Adm. **2007**, *07*, 23.

12. Mullins, O.C. Review of the Molecular Structure and Aggregation of Asphaltenes and Petroleomics. *SPE J.* **2008**, *13*, 48–57, doi:10.2118/95801-PA.

13. Dickie, J.P.; Yen, T.F. Macrostructures of the asphaltic fractions by various instrumental methods. *Anal. Chem.* **1967**, *39*, 1847–1852, doi:10.1021/ac50157a057.

14. Yarranton, H.W.; Fox, W.A.; Svrcek, W.Y. Effect of Resins on Asphaltene Self-Association and Solubility. *Can. J. Chem. Eng.* **2007**, *85*, 635–642, doi:https://doi.org/10.1002/cjce.5450850510.

15. Zaumanis, M.; Mallick, R.; Frank, R. Evaluation of Rejuvenator's Effectiveness with Conventional Mix Testing for 100% Reclaimed Asphalt Pavement Mixtures. *Transp. Res. Rec. J. Transp. Res. Board* **2013**, *2370*, 17–25, doi:10.3141/2370-03.

16. Zaumanis, M.; Mallick, R.; Poulikakos, L.; Frank, R. Influence of six rejuvenators on the performance properties of reclaimed asphalt pavement (RAP) binder and 100% recycled asphalt mixtures. *Constr. Build. Mater.* **2013**, *71*, 538–550.

17. Pradyumna, T.A.; Mittal, A.; Jain, P.K. Characterization of Reclaimed Asphalt Pavement (RAP) for Use in Bituminous Road Construction. *Procedia - Soc. Behav. Sci.* **2013**, *104*, 1149–1157, doi:10.1016/j.sbspro.2013.11.211.

18. Chiu, C.-T.; Hsu, T.-H.; Yang, W.-F. Life cycle assessment on using recycled materials for rehabilitating asphalt pavements. *Resour. Conserv. Recycl.* **2008**, *52*, 545–556, doi:https://doi.org/10.1016/j.resconrec.2007.07.001.

19. Loise, V.; Caputo, P.; Porto, M.; Calandra, P.; Angelico, R.; Rossi, C.O. A review on Bitumen Rejuvenation: Mechanisms, materials, methods and perspectives. *Appl. Sci.* **2019**, *9*, doi:10.3390/app9204316.

20. Levitt, M.; Försterling, F. Spin dynamics: Basics of Nuclear Magnetic Resonance, Second Edition. *Med. Phys. - MED PHYS* **2010**, *37*, doi:10.1118/1.3273534.

21. Spin-lattice and spin-spin relaxation Available online: ucl.ac.uk/nmr/sites/nmr/files/L5_3SH_web_shortened.pdf (accessed on Oct 26, 2020).

22. van Duynhoven, J.; Voda, A.; Witek, M.; Van As, H. Chapter 3 - Time-Domain NMR Applied to Food Products. In; Annual Reports on NMR Spectroscopy; Academic Press, 2010; Vol. 69, pp. 145–197.

23. Hahn, E. Spin Echoes. *Phys. Rev.* **1950**, *80*, 580–594, doi:10.1063/1.3066708.

24. Slichter, C.P. *Principles of Magnetic Resonance*; Springer-Verlag Berlin Heidelberg: New York, 1980;

25. Check, P. Pulsed Nuclear Magnetic Resonance: Spin Echoes. *MIT Dep. Phys.* **2017**, 1–14.

26. FARRAR, T.C.; BECKER, E.D. Chapter 2 - Free Induction and Spin Echoes. In *Pulse and Fourier Transform NMR*; FARRAR, T.C., BECKER, E.D., Eds.; Academic Press: San Diego, 1971; pp. 18–33 ISBN 978-0-12-249650-9.

27. Carr, H.Y.; Purcell, E.M. Effects of Diffusion on Free Precession in Nuclear Magnetic Resonance Experiments. *Phys. Rev.* **1954**, *94*, 630–638, doi:10.1103/PhysRev.94.630.

28. Widder, D. V. *Advanced Calculus*; 2nd ed.; Dover Publications: New York, 2012;

29. Bellman, R.; Roth, R. *The Laplace Transform*; WORLD SCIENTIFIC, 1984;

30. Stilbs, P. Fourier transform pulsed-gradient spin-echo studies of molecular diffusion. *Prog. Nucl. Magn. Reson. Spectrosc.* **1987**, *19*, 1–45, doi:https://doi.org/10.1016/0079-6565(87)80007-9.

31. Angelico, R.; Murgia, S.; Palazzo, G. Reverse Wormlike Micelles: A Special Focus on Nuclear Magnetic Resonance Investigations. *RSC Soft Matter* **2017**, *2017-Janua*, 31–62, doi:10.1039/9781782629788-00031.

32. Antalek, B. Using pulsed gradient spin echo NMR for chemical mixture analysis: How to obtain optimum results. *Concepts Magn. Reson.* **2002**, *14*, 225–258, doi:https://doi.org/10.1002/cmr.10026.

33. Binnig, G.; Rohrer, H.; Gerber, C.; Weibel, E. Surface Studies by Scanning Tunneling Microscopy. *Phys. Rev. Lett.* **1982**, *49*, 57–61, doi:10.1103/PhysRevLett.49.57.

34. Sokolov, I. Atomic Force Microscopy in Cancer Cell Research. In *Cancer Nanotechnology-Nanomaterials for Cancer Diagnosis and Therapy*; 2007; Vol. 1, pp. 43–59.

35. Eaton, P.; West, P. Atomic Force Microscopy. *At. Force Microsc.* **2010**, *9780199570*, 1–256, doi:10.1093/acprof:oso/9780199570454.001.0001.

36. Shahbazian-Yassar, R. Atomic Force Microscopy (AFM) BT - Encyclopedia of Tribology. In; Wang, Q.J., Chung, Y.-W., Eds.; Springer US: Boston, MA, 2013; pp. 129–133 ISBN 978-0-387-92897-5.

37. An Introduction to Non-Contact Mode AFM Under Ambient Atmosphere Available online: https://www.azonano.com/article.aspx?ArticleID=5071 (accessed on Oct 29, 2020).

38. Howland, R.; Benatar, L.; Symanski, C. *A Practical Guide to Scanning Probe Microscopy*; DIANE Publishing Company, 1998; ISBN 9780788171260.

39. Loeber, L.; Sutton, O.; Morel, J.; Valleton, J.M.; Muller, G. New direct observations of asphalts and asphalt binders by scanning electron microscopy and atomic force microscopy. *J. Microsc.* **1996**, *182*, 32–39, doi:10.1046/j.1365-2818.1996.134416.x.

40. Masson, J.-F.; Leblond, V.; Margeson, J. Bitumen morphologies by phase-detection atomic force microscopy. *J. Microsc.* **2006**, *221*, 17–29, doi:10.1111/j.1365-2818.2006.01540.x.

41. Macosko, C.W.; Larson, R.G.; (Firm), K. *Rheology: Principles, Measurements, and Applications*; Advances in interfacial engineering series; VCH, 1994; ISBN 9781560815792.

42. Morrison, F.A.; Morrison, A.P.C.E.F.A. *Understanding Rheology*; Raymond F. Boyer Library Collection; Oxford University Press, 2001; ISBN 9780195141665.

43. Chhabra, R.P.; Richardson, J.F. Chapter 1 - Non-Newtonian fluid behaviour. In *Non-Newtonian Flow in the Process Industries*; Chhabra, R.P., Richardson, J.F., Eds.; Butterworth-Heinemann: Oxford, 1999; pp. 1–36 ISBN 978-0-7506-3770-1.

44. Irgens, F. Chapter 1 - Classification of Fluids. In *Rheology and Non-Newtonian Fluids*; 2014 ISBN 978-3-319-01052-6.

45. Maxwell, J.C. On the dynamical theory of gases. *Phil. Trans. R. Soc.* **1867**, *157*, 49–88.

46. Chapter 3 - Linear Viscoelasticity. In *An Introduction to Rheology*; Barnes, H.A., Hutton, J.F., Walters, K., Eds.; Rheology Series; Elsevier, 1989; Vol. 3, pp. 37–54.

47. Steffe, J.F. *Rheological Methods in Food Process Engineering*; Freeman Press, 1996; ISBN 9780963203618.

48. Reiner, M. The Deborah Number. *Phys. Today* **1964**, *17*, 62, doi:10.1063/1.3051374.

49. Chapter 3 - Methods for Assessing Surface Cleanliness. In *Developments in Surface Contamination and Cleaning, Volume 12*; Kohli, R., Mittal, K.L., Eds.; Elsevier, 2019; pp. 23–105 ISBN 978-0-12-816081-7.

50. Waseda, Y.; Matsubara, E.; Shinoda, K. Chapter 1 - Fundamental Properties of Xrays. In *X-Ray Diffraction Cristallography*; Waseda, Y., Matsubara, E., Shinoda, K., Eds.; Springer

Science & Business Media, 2011; pp. 1–21 ISBN 3642166350.

51. He, B.B. Chapter 1 - Introduction. In *Two-dimensional X-ray Diffraction*; He, B.B., Ed.; John Wiley & Sons, Ltd, 2018; pp. 1–28 ISBN 9781119356080.

52. Suryanarayana, C.; Grant Norton, M. Chapter 1 - X-Rays and Diffraction. In *X-Ray Diffraction - A Practical Approach*; Suryanarayana, C., Grant Norton, M., Eds.; Springer Science & Business Media, 2013; pp. 1–18 ISBN 1489901485.

53. Warren, B.E. Chapter 1 - X-Ray Scattering by Atoms. In *X-Ray Diffraction*; Warren, B., Ed.; Courier Corporation, 2012 ISBN 0486141616.

54. Snyder, R.L. X-Ray Diffraction. In *X-ray Characterization of Materials*; John Wiley & Sons, Ltd, 1999; pp. 1–103 ISBN 9783527613748.

Chapter 5

A Review on Bitumen Rejuvenation: Mechanisms, Materials, Methods and Perspectives

Applied Sciences 2019,9; doi:10.3390/app920431

applied sciences

MDPI

Review

A Review on Bitumen Rejuvenation: Mechanisms, Materials, Methods and Perspectives

Valeria Loise [1], Paolino Caputo [1,*], Michele Porto [1], Pietro Calandra [2,*], Ruggero Angelico [3] and Cesare Oliviero Rossi [1]

[1] Department of Chemistry and Chemical Technologies, University of Calabria, Via P. Bucci, Cubo 14/D, 87036 Rende (CS), Italy; valeria.loise@unical.it (V.L.); michele.porto@unical.it (M.P.); cesare.oliviero@unical.it (C.O.R.)

[2] CNR-ISMN, National Council of Research, Institute for the Study of Nanostructured Materials, Via Salaria km 29.300, 00015 Monterotondo Stazione (RM), Italy

[3] Department of Agricultural, Environmental and Food Sciences (DAAA), University of Molise, Via De Sanctis, 86100 Campobasso (CB), Italy; angelico@unimol.it

* Correspondence: paolino.caputo@unical.it (P.C.); pietro.calandra@ismn.cnr.it (P.C.); Tel.: +39-0984-493381 (P.C.); +39-0690-672409 (P.C.)

Received: 12 September 2019; Accepted: 7 October 2019; Published: 14 October 2019

Abstract: This review aims to explore the state of the knowledge and the state-of-the-art regarding bitumen rejuvenation. In particular, attention was paid to clear things up about the rejuvenator mechanism of action. Frequently, the terms rejuvenator and flux oil, or oil (i.e., softening agent) are used as if they were synonymous. According to our knowledge, these two terms refer to substances producing different modifications to the aged bitumen: they can decrease the viscosity (softening agents), or, in addition to this, restore the original microstructure (real rejuvenators). In order to deal with the argument in its entirety, the bitumen is investigated in terms of chemical structure and microstructural features. Proper investigating tools are, therefore, needed to distinguish the different mechanisms of action of the various types of bitumen, so attention is focused on recent research and the use of different investigation techniques to distinguish between various additives. Methods based on organic synthesis can also be used to prepare ad-hoc rejuvenating molecules with higher performances. The interplay of chemical interaction, structural changes and overall effect of the additive is then presented in terms of the modern concepts of complex systems, which furnishes valid arguments to suggest X-ray scattering and Nuclear Magnetic Resonance relaxometry experiments as vanguard and forefront tools to study bitumen. Far from being a standard review, this work represents a critical analysis of the state-of-the-art taking into account for the molecular basis at the origin of the observed behavior. Furnishing a novel viewpoint for the study of bitumen based on the concepts of the complex systems in physics, it constitutes a novel approach for the study of these systems.

Keywords: Bitumen; rejuvenator; oils; flux agents; physical chemistry techniques; structure; RAP

1. Introduction to Bitumen and Ageing

Asphalts are well-known materials used for road pavement throughout the world. They are heterogeneous systems where one phase is constituted by macro-meter sized inorganic particles called aggregates, and the other one is the binding agent (bitumen). The latter, in turn, is a micro heterogeneous complex viscous fluid constituted by nano-meter sized aggregates of polar molecules (asphaltenes) hierarchically organized with different levels of aggregations [1], and dispersed in a more apolar continuous phase of saturated paraffins, aromatic oils and resins called maltene [2,3].

Asphalts are, therefore, biphasic systems, with the predominant phase (93–96%, *w*/*w*) made by the macro-meter sized inorganic aggregates (size from microns to millimeters) hold together by small amounts of binding bitumen which constitutes the second phase. Although the bitumen constitutes the minor part of the asphalt, it however plays the most important role, giving consistency to the overall material, which is necessary for practical purposes: even slight changes in the bitumen will affect the overall properties of asphalt. Even the usability of asphalt can be traced back to the properties of its bitumen. This work will focus the attention on bitumen as a key ingredient in asphalt. Where necessary, however, some extensions will cover asphalt and related aspects. The aggression of chemicals normally presents in the environment, or ageing can oxidize some of the organic components in the bitumen so that the increase in polar functional groups can cause immobilization of an excessive number of macromolecules and ultimately bitumen embrittlement and asphalt cracks. Other processes causing ageing are loss of volatiles and changes in a molecular organization driven by the spontaneous tendency to reach a stable (equilibrium) thermodynamic state, which obviously depends on the conditions [4]. As a consequence of the mentioned processes taking place in bitumen, the final asphalt is susceptible to fracturing or cracking in thermal or mechanical stresses. Ageing of bitumen, therefore, constitutes a serious problem. Aged asphalt can be re-used in mixtures with new binders, answering the economic need for low-cost production and fully facing obvious environmental concerns. Therefore, recent research has been focused on reclaimed asphalt pavements (RAPs), which really are environmentally friendly alternatives and constitute an economically viable way to afford the costs of binder and aggregates. However, their use is still limited (less than 20% in the new mixtures), due to their low rheological performances (high stiffness and low stress relaxation ability [5] which can cause unexpected premature failure [6]. To overcome these problems, opportune actions must be taken to improve the mechanical and chemical properties of aged bitumen or RAP/bitumen mixtures. The addition of opportune additives is certainly one of the most effective. For example, a compound able to tune the red-ox state of the polar molecules contained in the bitumen can avoid the degrading process. The restoring of a favorable asphaltene/maltene relative ratio by providing more maltene is another solution, since the viscosity of bitumen is related to the fraction of asphaltene [7]. Another strategy can be directed to the stabilization of the supramolecular aggregates mainly made by asphaltene formed in the maltene phase [8,9] acting on their interfacial tension and consequently better dispersing them. In all these cases, a rejuvenator is usually dealt with. With this work, the recent studies carried out in this field will be highlighted in order to shed light on the possible mechanisms of actions of a rejuvenator and to furnish a panoramic view considering both theoretical considerations and applicative aspects. This works will show the state-of-the-art in the use of rejuvenators in bitumen, taking care to highlight also some applications to the rejuvenation of recycled asphalt for a more complete view of the problematics. Differently from standard review papers, this work, prior to presenting all the state-of-the-art works dealing with rejuvenators (Section 4), it proposes a clear, new and marked distinction between different "rejuvenators" according to their effect and influence at the microscopic length-scale individuating techniques and methods of analysis for their distinction (Section 3 "mechanisms of ageing and rejuvenating" and sub-paragraphs). Then, the work will show methods for the synthesis of ever more performing rejuvenators (Section 5) and suggest vanguard techniques of investigation (Section 6).

2. Methods for Bitumen Characterizations

The characteristics of bitumen are not trivial at all: it is an organic high-viscosity viscoelastic binding agent which is itself a composite system constituted by nano-meter sized aggregates of polar molecules (asphaltenes) dispersed in a more apolar continuous phase of saturated paraffins, aromatic oils and resins called maltene [2,3]. Usually, these fractions can be determined by the so-called S.A.R.A. determination (Saturates, Aromatics, Resins and Asphaltenes) [10]. In this method, the sample of bitumen is dissolved in peroxide-free tetrahydrofuran solvent (usually to reach a 2% (*w*/*v*) solution). Saturated components of the sample are developed in *n*-heptane solvent while the aromatics in a 4:1

mixture of toluene and *n*-heptane. Afterwards, the rods are dipped into a third tank, (usually 95 to 5% mixture of dichloromethane and methanol). This organic medium proved suitable to develop the resin fraction, whereas, the asphaltene fraction is left on the lower end of the rods. However, it must also be pointed out that asphaltenes are not classified using their molecular structure, but they are defined traditionally on the basis of the procedure required to extract them from heavy oils [11]. Bitumen are a not well-defined mixture of constituents so different methods of analysis exist where solvents are added to bitumen to determine its chemical properties. For example, Zenke [12] offered a method for not only determining the number of maltenes and asphaltenes of bitumen, but also distinguishing light-, middle-, and high-solubility of asphaltenes. However, for an effective study, the general viewpoint of their overall assembly becomes more important than the detailed chemical speciation of the various molecules involved. Based on this, a testing method for determination of the quality of bitumen, called "simplified laboratory method", was developed in order to gain fast and easy information. S.A.R.A. determination and the attempts by Zenke are examples of this approach to gain chemical information. Bitumen are also regarded in terms of their performances, for which a rheological description of the materials is often given. Empirical approaches are always followed to determine the performances within a chosen temperature range [13,14] for convenient use [15,16]. Due to the general description of the bitumen performances in rheological terms (penetration index, softening point, ductility, viscosity), and due to the need of quick, easy and low-cost methods to characterize the bitumen, the lack of detailed knowledge of the supramolecular assembly characterizing the bitumen structure at the various levels of complexity caused the fact that a rational correlation of the bitumen structure with its performances is actually missing. Attempts at more sophisticated investigative tools are present. Scattering experiments, and in particular X-ray scattering ones, would be advisable to probe the structure from the Å to the meso-scale. As a matter of fact, remarkable attempts have been made since the '60s [17], but the bitumen complex organization has hindered the development of such structural study in details. The structural investigation has been, therefore, generally carried out by Atomic Force Microscopy (AFM) [18], by Confocal Laser Scanning Microscopy [19], by Optical Microscopy [20], and Fluorescence Microscopy [21], but all these methods were used to probe the micro-scale (not going deeper to the nano-scale) and the surface. Attempts at gaining information on the nano-scale structure of the bulk have been limited, and the results remained quite hypothetical [22]. Even the "colloidal structure" is just empirically derived by the contents of aromatics, resins, asphaltenes and saturates [23]. This is probably due, in our opinion, to the always-urgent need of improving performances for applicative purposes so that basic research, highlighting the specific intermolecular interactions and the molecular organization at the base of the observed behavior has been sometimes overlooked. Therefore, there is still a lack of information on how many additives affect the supra-molecular structure and the distribution of aggregates within the bituminous colloidal network and how this can reflect on the overall material properties. This makes the relationship between molecular interactions and the final material structure/properties (which is ultimately the final objective of physical chemistry) still quite vague. This problem was already faced recognizing that bitumen are characterized by intermolecular associations at different length-scales: asphaltene molecules are aggregated to form stacks by self-interactions and these aggregates are stabilized by polar resins, due to their amphiphilic chemical nature and the overall structures are then dispersed in a paraffin-like apolar matrix. These characteristics render the material a truly complex system, so an approach based on the complex systems theory is, therefore, necessary foreseeing different levels of complexity, each of them potentially showing emerging properties arising from the opportune organization of the molecules. It has been, in fact, recently highlighted that asphaltenes tend to form stacks of about 18 Å, organized at higher levels of complexity in anisotropic aggregates of about 200 Å × 28 Å, which, again, are assembled to form micrometer-size elongated aggregates characterized by the so-called "bee-structure" [24]. However, asphaltenes are unable to create a continuous network [25]. These recent findings opened the door to a better comprehension of the bitumen structure from X-ray scattering data, making this technique a method of election [26] for the structural investigation of such systems. In this context, it was shown

that the influence of additives is exerted by their preferential localization in the maltene phase or close to the asphaltene clusters, depending on the additive chemical characteristics, thus, finally affecting the overall rheological properties. An additive can play, therefore, important roles: it can exert its effect at the inorganic/organic interface, or, at a lower level of complexity, within the maltene/asphaltene aggregates, whereas, a redox additive works at the chemical state of the single polar molecules, i.e., at an even lower level of complexity. Another mechanism exerted by the additive is the formation of a network inside the maltene giving elasticity to the bitumen [27] or a simple change of physical phase transition with fluxing at a higher temperature while conferring rigidity at lower ones [28]. The so-called "antistripping agents" act by stabilization of eventual supramolecular asphaltene aggregates in the maltene phase [8,9]. As regards the additive chemical nature, selected polymers have been used (low-density polyethylene, ethylene-vinyl-acetate, SBS-polyphosphoric acid (PPA), Elvaloy, etc.) [29], as well as smaller molecules falling in the categories of organosilane and phospholipids [30] or paraffinic synthetic waxes, derivate of fatty amines and surfactants [31], antioxidants [32], etc. Once introduced the chemical and the structural characteristics of a bitumen, the next paragraphs will highlight the modifications taking place during ageing and how the original state can be restored by the introduction of the concept of rejuvenator.

3. Mechanisms of Ageing and Rejuvenating

3.1. Ageing

Due to the ageing process of bitumen and its corresponding increase in viscosity, the stiffness of asphalt pavement increases during its lifetime. The general, zero-order, description of aging is given in terms of an overall mechanism where some of the maltene medium is transformed into the asphaltene phase, resulting in higher asphaltene and lower maltene contents. This leads to a higher viscosity and lower ductility, due to the stronger polar-polar interactions between asphaltenes. In simpler words, "when the asphaltene micelles are not sufficiently mobile to flow past one another under the applied stress, the resistance of asphalt binder to cracking or fracture is decreased" as beautifully depicted by J. Petersen [4]. However, ageing is a more complex process involving different sub-mechanisms usually taking place in different time-scales. It can already take place during asphalt construction through volatilization of light components in the maltene. Then, long-term aging occurs in the field as a consequence of different processes:

1. Oxidative, due to changes in composition through a reaction between bitumen constituents and atmospheric oxygen;
2. Evaporative, due to the evaporation of low-molecular weight components in the maltene. These compounds have higher vapor pressure and are somehow volatile so they can escape the maltene phase causing not only a change of its composition, but also an overall reduction of its amount in the bitumen;
3. Structural ageing, by a chemical reaction between molecular components causing polymerization with consequent formation of a structure within the bitumen (thixotropy) [33].

The processes involved are schematically depicted in Figure 1.

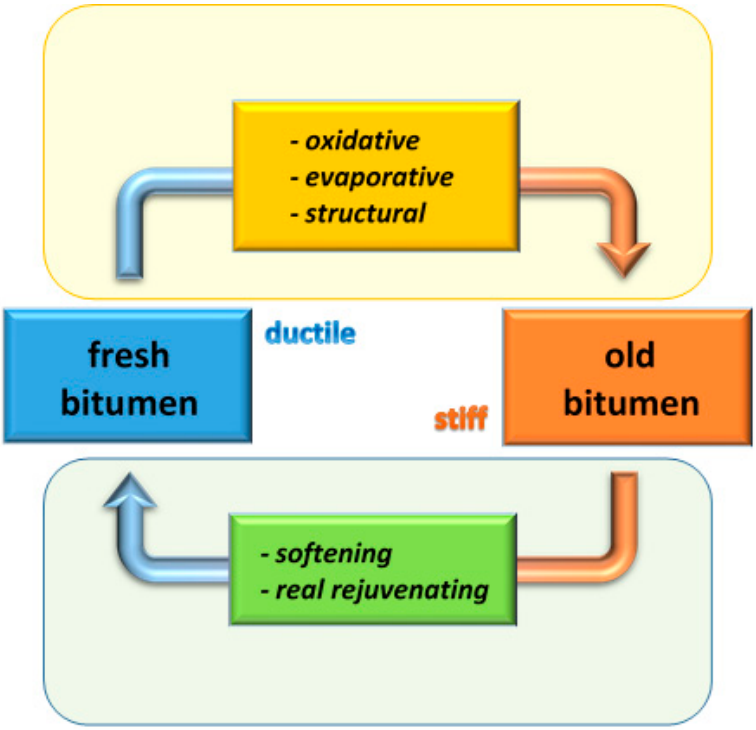

Figure 1. Scheme showing the main processes involved in bitumen ageing and its rejuvenation.

3.2. Rejuvenation

A rejuvenator has been defined as that agent capable of restoring the original rheological properties of a bitumen. Therefore, it is assumed that the primary action of a rejuvenator should be to bring the bitumen to lower stiffness and viscosity and higher ductility. Despite the above description of bitumen ageing showing different and somehow interconnected mechanisms, taking place, simultaneously, the very first action to restore the original bitumen rheological properties is to shift back the ratio between solid asphaltenes and fluid maltenes to higher maltene contents. However, a rheological rejuvenating agent can exert its action in different sub-mechanisms (see the schematic diagram of Figure 1):

1. Softening (usually called fluxing) agent: flux oil, lube stock, slurry oil, etc. can lower the viscosity of the aged binder;
2. Real rejuvenator: it helps to restore the physical and chemical properties [33].

As it will be seen (see Section 4), literature does not make a clear distinction among the types of mechanism exerted by the specific rejuvenator: this name is usually given to any king of additive, which allows a certain restoring of the original rheological properties, no matter the effective mechanism involved. Instead, we are keen on making a clear distinction: given the aim of this contribution to go deeper into the details and to make clear all the aspects involved, it will be now defined a rheological rejuvenator as any type of additive causing a certain restoring of the rheological characteristics. In the specific, if the rejuvenator is also able to restore even the bitumen inner structure, then it will be defined as a real rejuvenator. If, on the other hand, the rheological rejuvenator makes the bitumen more ductile and less viscous/brittle by simply furnishing oily components to maltene without restoring the original complex structure (hierarchical structures of asphaltenes), then it will be called as softening (more often fluxing) agent. It can be seen that in this distinction, the term "rheological rejuvenator" has a more general sense and is associated with the concept of "rejuvenator" usually present in the literature. For this reason, in the following, when simply naming "rejuvenator" it will be referred to rheological rejuvenator, to resemble the classical meaning of rejuvenator usually adopted. Instead, when dealing with real rejuvenator effect, the terminology "real rejuvenator" will be stressed. Rheological rejuvenators are, however, usually based on oils: lubricating oil extracts and extender

oils. They contain an adequate amount of maltene constituents, naphthenic or polar aromatic fractions, which re-balance the composition of the aged binder in favour of such compounds or those usually lost during construction and service. Rejuvenator must fulfil two requirements:

1. They should have a high proportion of aromatics, which are necessary to keep the asphaltenes dispersed;
2. They should contain a low content of saturates, which are highly incompatible with the asphaltenes.

3.2.1. Down to the Nano-Scale

Of course, the effectiveness of a rejuvenation action depends on the uniform dispersion of the rejuvenator within the bitumen. In fact, after its mixing with aged bitumen and the obvious homogenization, diffusional processes taking place at longer times and shorter length-scales must complete the job. This aspect was first faced by Lee et al. in 1983 [34] who mixed a dye with the rejuvenator to estimate the homogenization of the overall product by visual inspection. The authors concluded that mechanical mixing could give a uniform distribution of the rejuvenators within the bitumen. However, our perplexity holds in the fact that visual inspection cannot probe the uniformity of dispersion at the sub-micro scale, which instead is the final goal of an efficient mixing allowing complete rejuvenator action. According to a work by Carpenter and Wolosick [35] published few years before, the diffusion of a rejuvenator into an aged binder is a complex, multi-step mechanism consisting of four steps (the curious reader is redirected to the reading of that article for details), but basically the requirement of a complete homogenization of the rejuvenator down to the nano-scale was already pointed out. However, their results were later confirmed by Noureldin and Wood [36], and Huang et al. [37]. The complete homogenization, down to the sub-micro scale cannot happen without being diffusion-driven and diffusion-limited—a dynamical process whose rate is given by the viscosity of the medium. This indeed, has been shown by Karlsson and Isacsson [38], who highlighted that the diffusion rate is governed by the viscosity of the maltene phase rather than the viscosity of the recycled binder as a whole, an aspect which was somehow observed previously by Oliver [39] who had suggested that the diffusion could be sped up by diluent oil fractions addition and/or raising the temperatures.

3.2.2. Distinguishing Softening Agents and Real Rejuvenators

From the point of view of the physical performances, softening (fluxing) and real rejuvenating, which constitute two different mechanisms, can be distinguished experimentally. Whereas, the stiffness or rigidity of a bitumen, usually empirically determined by simplified and fast methods generally by immediate techniques developed for characterizing mechanical and rheological properties and used especially in the field of engineering [40], the distinction of the two effects of fluxing and real rejuvenating needs the exploitation of methods with a substantial physical basis. In this ambit, small amplitude oscillatory rheometry is a useful technique using specific specimen geometries and mathematical interpretation of the data to achieve physical quantities: the complex modulus G^*. G^* is a measure of the total energy required to deform the specimen and is defined as:

$$|G^*|^2 = (G')^2 + (G'')^2 \quad (1)$$

where G' is the elastic modulus (or storage modulus), a measure of the energy stored in the material during oscillation, and G'' is the viscous modulus (or loss modulus), a measure of the energy dissipated as heat. Martin Radenberg et al. [41] highlighted the difference between a "rejuvenating" (here associated with our conception of real rejuvenating) effect and a "fluxing" agent from a rheological perspective using the so-called black diagrams, which depict the magnitude of the complex modulus G^* versus the phase angle (δ, defined as $\tan \delta = G''/G'$) obtained from the dynamic tests. In black diagrams, frequency and temperature are eliminated. This method was previously suggested by Airey and Brown [42] to assess and compare the rheological properties of bitumen. The characterization of

the two different actions of rejuvenator has been recently carried out by NMR. Although bitumen is a complex material, ambitious studies are facing structural characterization by probing relaxation times. Application of Low-Field NMR has been used for the determination of physical properties of petroleum fractions [43,44], and the Inverse Laplace Transform (ILT) analysis of the NMR echo signal decay gives the T_2 relaxation time which can be connected to different domains characterized by different rigidities [45]. The chemical reasoning for this lies on the molecular constraint, causing dynamic hindrance and lowering T_2, an effect that can be considered quite general and already found also in different systems [46]. These attempts have given interesting and encouraging results, which deserve to be tailored. We support efforts in this direction since the comprehension of the microscopic/molecular processes at the basis of the observed behavior of a material is of fundamental importance for the improvement of materials characteristics in specific applications.

4. The State-Of-The-Art

4.1. General Requirements

As a general requirement, additives should be non-hazardous and stable over a wide range of temperatures, from production to application. In addition, they must not experience any exudation or evaporation, in order to ensure good performance over the designed lifetime of the asphalt pavement. Further specific requirements depend on the local country specification. Bocci et al. for example [47], focus on the use of a specific bio-based rejuvenator to produce asphalt concrete using a high amount of RAP without scarifying the mix performance and complying with the Italian specifications. In particular, the paper presents the results from a trial section on a highway connecting Ancona to Perugia, in the center of Italy.

In any case the use of "forbidden" chemicals should not be the goal of the work: for example, Tine et al. [48] take care in clarifying that the additives they studied in their work (a liquid process oil with a typical viscosity at 40 °C of 700 mm^2/s) conform to all current Registration, Evaluation, Authorisation and restriction of Chemicals, (REACH) and Polycyclic Aromatic Hydrocarbons (PAHs) limits. Another additive they used (a tall oil distillate originating from pine trees) is "not classified as dangerous according to Directive 67/548/EEC and its amendments and according to EU legislation". In our opinion, any work should clarify the environmental/safety/legal issues connected to the additives presented.

In this sense, Król et al. [49], and Somé et al. [50] show that the addition of some particular bio-additives has a large potential application as reversible fluxing agents in bitumen industry, RAP technology and Warm Mix Asphalt (WMA). They used vegetable oil produced using various raw materials (Rapeseed oils, Soybean oil, Sunflower oil, Linseed oil, etc.) and combined in bituminous binders generally as a modifier/additive (up to 10%). Interestingly, not only they used vegetable oils, but they also perform chemical action to prepare other additives (they use methyl esters of fatty acid obtained by transesterification of vegetable oils). The aspect of a couple the use of raw/cheap materials with chemical actions to increase their performances is intriguing and promising. The chemical actions that can be performed for the optimization of additive performances will be discussed in Section 5.

The rejuvenating benefits can be utilized to allow for higher RAP addition using traditional hot mix asphalt (HMA) configuration or in the warm mix asphalt (WMA) technology since the additives, changing the viscosity of the binder, allow for the lowering of the asphalt mixture production temperature. Critical issue related to the application of the additive fluxing of the bitumen is the final viscosity of the bitumen and stiffness of the mixture placed in the pavement. In fact, while fluxing is desired during mixture production, placement and compaction, it is no longer appreciated once the road is open to traffic. Considering the examples of Król et al. [49], and Somé et al. [50], the suitability criterion for vegetable oils and the corresponding methyl esters for obtaining environment-friendly bitumen fluxes is their reactivity to the oxypolymerization reaction, which raises the viscosity of the stock, thus, contributing to its hardening and drying. The efficiency of polymerization depends on the

number of double bonds and their position in the aliphatic chain of fatty acid. Oxypolymerization of the fatty acids present in the vegetable stocks is a multistage process and leads to the crosslinking of their structural units. The principle of using additives susceptible to oxypolimerization has been recently exploited for preparing additives, increasing the bitumen viscosity [51].

This paragraph, from the next sub-paragraph on, is devoted to showing the works involving rejuvenators as additives in bitumen. Some applications to the rejuvenation of partly recycled asphalt will also be shown for a more complete view of the problematics also because for practical uses sometimes rejuvenation must be exerted on recycled asphalt (RAP, reclaimed asphalt pavement). They have been grouped according to the experimental methods that can be used for the rejuvenation evaluation. In addition, particular care has been taken in using the same names and formalisms used by the various Authors, for a better comparison with the original works.

4.2. Rejuvenation Probed by IR

Zargar et al. in 2012 [52] explored the possibility of using a waste cooking oil (WCO) as rejuvenator in the aged bitumen, in order to reduce the expense of highway renovation. They added various amounts of a WCO mainly composed by Oleic acid (C18:2n9c, 43.7%), Palmitic acid (C16:0, 38.4%) and Linoleic acid (C18:2n6c, 11.4%) to an aged bitumen monitoring the changes in standard parameters like penetration index, softening point, Brookfield viscosity and dynamic shear viscosity. The comparison among pristine, aged and rejuvenated bitumen gave self-consistent results furnishing clear clues: the aged bitumen, which is stiffer than the virgin one as result of oxidation processes, can be substantially driven to the performances typical of the virgin bitumen by progressive addition of waste cooking oil. The restoring of the virgin performances takes place at WCO content of 3%, but they can even be improved (n penetration index, softening point and viscosity) by further addition of WCO up to 5%. See, for example, Figure 2 where the penetration value versus various rejuvenator amounts is reported. These results were interpreted at the molecular basis with the aid of Fourier transform infrared spectroscopy (FT-IR) which probes the amount of oxidized functional groups, and specifically C=O and S=O. The increase of polar functional group signal intensity, and specifically C=O and S=O ones, in FT-IR spectra when the bitumen is aged correlates with its stiffness increase. This suggests that the loss in bitumen performances is due to the oxidation process. Even, this increase correlates with an increase in asphaltenes fraction, i.e., the most polar component of the bitumen. On the other hand, the addition of WCO implies a substantial restoring of the pristine C=O and S=O signal, together with the pristine asphaltene/maltene ratio, although the process seems not to be complete/quantitative. Typical IR spectra, together with the most important band attributions, are reported in Figure 3. In conclusion, WCO appears to have a rejuvenating effect because it reduces the oxidation (asphaltene content) compared to an aged bitumen, even if it is not capable of restoring the correct ratio maltene asphaltenes. However, it is interesting to point out that the rejuvenated bitumen has less tendency to ageing compared to original bitumen and has lower volatility than the virgin bitumen reasonably, due to the lower volatility of bio-oil as a consequence of its high content in saturated hydrocarbons. Unfortunately, the Authors do not give details on the FT-IR experiments.

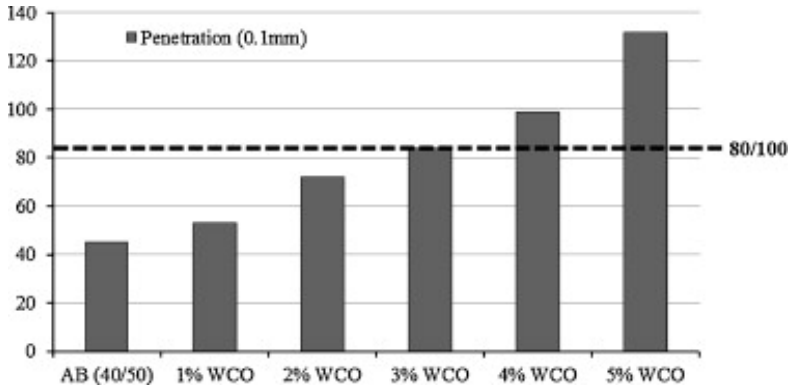

Figure 2. Penetration value versus different rejuvenated waste cooking oil (WCO) bitumen's (AB, aged bitumen) (reprinted from Reference [52] with the permission of Elsevier).

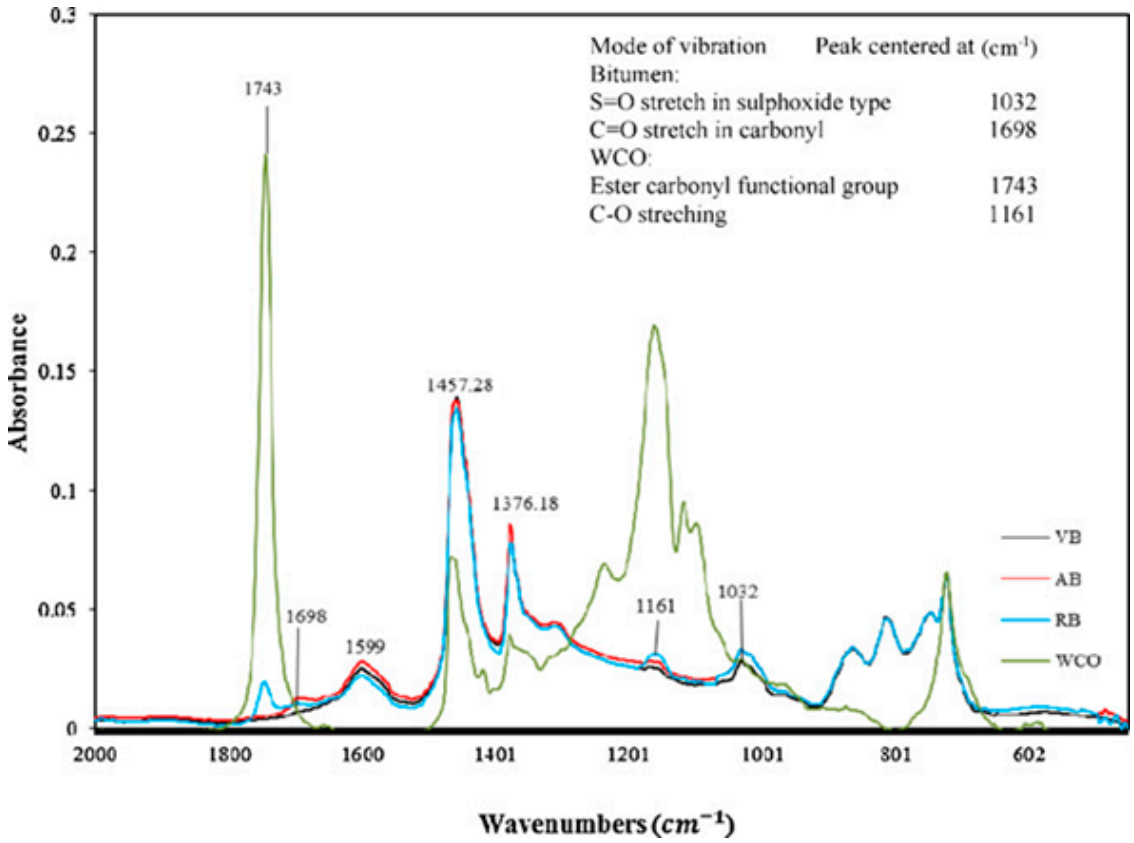

Figure 3. FTIR analysis of virgin aged and rejuvenated bitumen (VB, virgin bitumen; AB, aged bitumen; RB, rejuvenated bitumen) (reprinted from Reference [52] with the permission of Elsevier).

To avoid FT-IR artefacts, due to differences in the optical path (different thickness of samples) or in experimental procedures, Nayak and Sahoo [53] wisely consider the relative amount of ketonic bond with respect to the signals of functional groups which are not expected to change, like the bending of C–H bonds. This peak is pointed out in Figure 4.

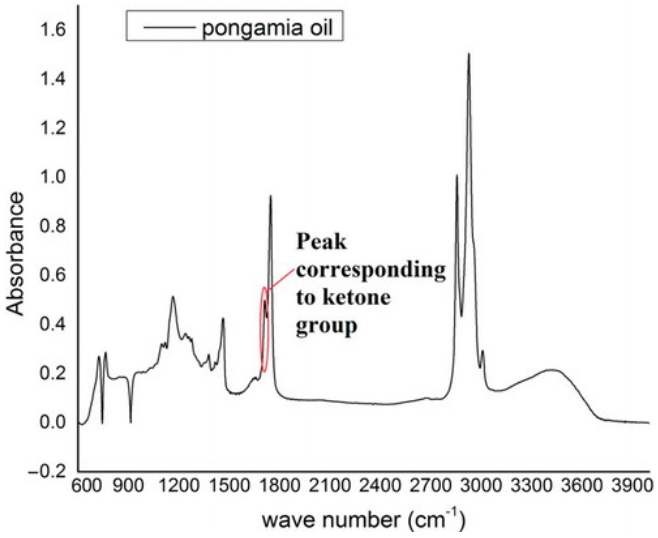

Figure 4. FTIR spectrum for pongamia oil (reprinted from Reference [53] with the permission of Taylor and Francis).

This criterion of using a relative intensity was proposed by De la Roche et al. [54], but the use of the relative area is consistent with the consideration by Lamontagne et al. [55].

In any case, Nayak and Sahoo studied the rejuvenating effect of two different types of oils (the pongamia oil and a composite castor oil made of 70% castor oil and 30% coke-oven gas condensate). The results confirm the clues by Zargar et al. showing an increase of the C=O relative signal when the bitumen is aged. Moreover, they found that the C=O relative signal slightly tends to decrease when the composite oil is added, but more markedly increases when pongamia oil is added. The reason lies in the fact that the ketone group is present in pongamia oil itself, and therefore, it is not necessarily due to ageing process. This result should be interpreted as an invitation in being prudent when performing FT-IR experiments and when interpreting its results.

4.3. Thermal Stability Helps in Probing Rejuvenation

By monitoring viscoelasticity, creep and response, FT-IR, Thermogravimetric Analysis (TGA) and Differential Scanning Calorimetry (DSC), Nayak and Sahoo proved that successful rejuvenation takes place when these oils are added to the bitumen. It is interesting to notice that both oils have good thermostability performances. The virgin binder showed a visible mass loss at temperatures below 200 °C; instead, all the rejuvenated binders along with aged binder showed significant mass loss beyond 200 °C, but such temperatures are much higher than those typically adopted in hot mix asphalt preparation, rendering this difference not significant for practical purposes.

Also, Elkashef et al. [56] used thermal stability analysis to evaluate the effect of rejuvenating soybean oil on reclaimed asphalt pavement (RAP). Acknowledging the importance of studying thermal stability of rejuvenated binders to assure that eventual loss of rejuvenating additive (typically characterized by low molecular mass) does not modify asphalt performance, they carried out thermogravimetric analysis on the RAP, on the blend made by RAP and the pristine bitumen (PG58-28), and finally, on the mixture formed by RAP, soybean oil (12%) and the pristine bitumen. Coupled to Thermogravimetry (TG), an FT-IR spectrometric investigation on the gases produced by heating was also carried out. The Authors' results obtained by Thermogravimetry (TG) can be summarized in Table 1.

Table 1. TG results of the studied asphalt binders (reprinted from Reference [56] with the permission of Springer Nature).

Sample	IDT (°C)	Char Yield (%)	Residue (%)
RAP	316	30	7
RAP + PG58-28	309	26	6
RAP + 12% Mod PG58-28	309	26	6

This table shows the Initial Decomposition Temperature (IDT), defined as the temperature where 2% mass loss occurs; the char yield percentage is the mass remaining at the temperature of 550 °C, and the percentage residue is the remaining percentage of asphalt material at the end of the analysis. From this table it is clear that the RAP binder shows the highest thermal stability, confirming that the stiffness is due to asphaltene amount that is more thermally stable, whereas, the other two binders show the same behavior, having an IDT few degrees lower. Elkashef et al. also compared the spectra (at a temperature of 390 °C) of the gases evolved from the three different binders, taking into account for the blank constituted by the bare soybean oil. It turned out that the spectrum of the binder containing the rejuvenator shows a relatively intense peak typical of the rejuvenator itself. Although this observation can be thought as trivial, a pseudo-quantitative analysis, carried out at different temperatures by normalizing the FT-IR spectra at the same C-H stretching peak height (2930 cm^{-1}), allowed the Authors to conclude that FT-IR spectrometry can be used as a tool to probe the rate of mass loss of the rejuvenator. In fact, a higher mass loss triggered by a temperature increase implies higher relative intensities of the characteristic functional groups of the rejuvenator itself (C=O stretching at 1736 cm^{-1} and the two C-O stretching at 1015 and 1153 cm^{-1}).

4.4. Rejuvenation May Be Uncorrelated with IR Functional Groups: Need of Chromatography

Cavalli et al. [57] found an interesting aspect. In fact, these Authors pointed out that, despite the addition of rejuvenators, the bitumen physico-chemical oxidation did not reverse: mechanical changes were not caused by chemical changes at functional groups level, but by a rearrangement of polar/nonpolar components. They took into account for three different commercial bio-based rejuvenators: a natural seed oil (called rejuvenator "A"), a cashew nut shell oil (called rejuvenator "B") and a rejuvenator based on tall oil (rejuvenator "C"). After highlighting by FT-IR that rejuvenator A and C have a rather similar chemical nature (see Figure 5 which reports the FT-IR spectra of the bare three rejuvenators), they performed FT-IR spectra on samples of RAP containing 5% of each rejuvenating and compared them to the spectrum of a virgin bitumen 50/70. The results are shown in Figure 6: the peaks corresponding to the ageing of binders, due to oxidation do not disappear although rejuvenators were added to the RAP binder. Chemical structures of RAP +5% C and RAP +5% A were found to be similar, suggesting that the chemical effect of rejuvenator C and A on RAP binder is similar.

The Authors also determined the chemical ageing index (CAI). This is given by the sum of carbonyl index (CI) and sulfoxide index (SI) defined, as suggested in Marsac et al. [58], as the area of the carbonyl and sulphoxide signal, respectively, normalized, to the peaks related to the asymmetric vibration of CH_2 and CH_3 (around 1455 cm^{-1}) and to the symmetric deformation vibration of CH_3 (around 1376 cm^{-1}) as the latter areas do not change significantly. It must be noted that here the Authors use the same indices as Nayak and Sahoo, by considering the area of the FT-IR signals (and not the bare intensities) and normalizing them to signals related to the C-H functional group since they are expected to be hardly sensitive to the chemical environment.

By using these indices, the Authors found that the unaged binders RAP + 5% A and RAP + 5% C have a higher CAI index than the plain RAP. Most probably due to the fact that seed oil and tall oil themselves contain carboxylic groups C=O, they found the same clues derived by Nayak and Sahoo who found that the ketone group is present in their rejuvenator (pongamia oil) itself.

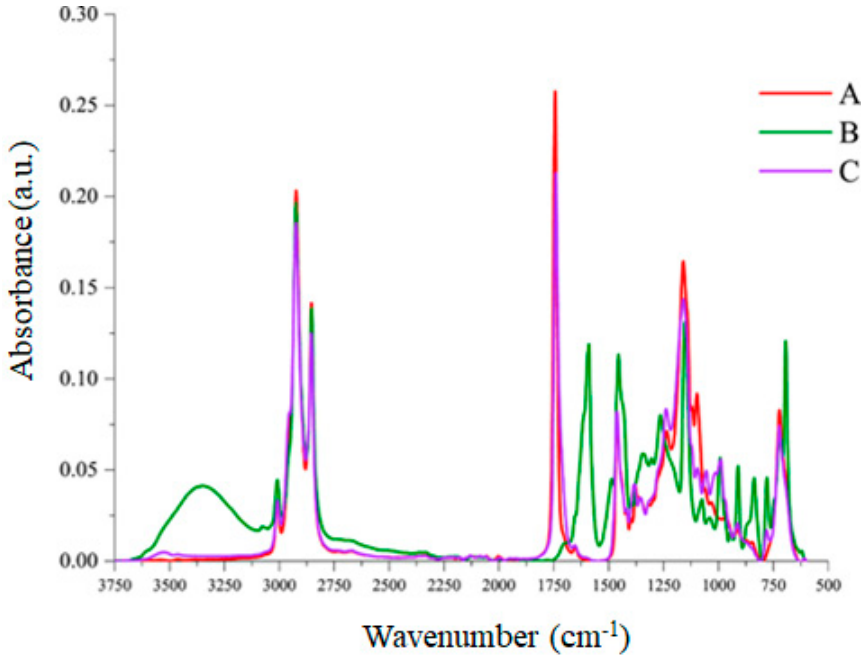

Figure 5. ATR-FT-IR spectra of the plain rejuvenators A, B and C before ageing) (reprinted from Reference [57] with the permission of Elsevier).

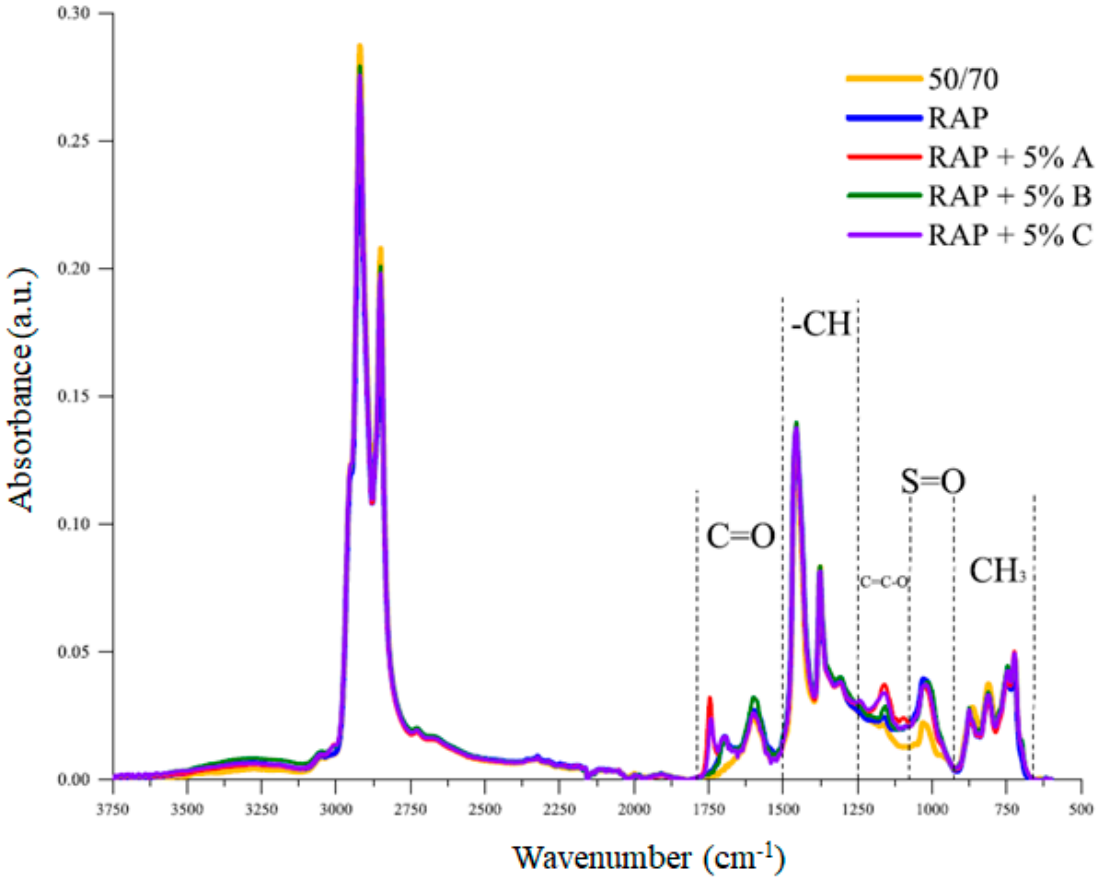

Figure 6. ATR-FTIR spectra of the virgin binder 50/70, the RAP binder and the RAP binders with rejuvenators A, B and C (5% by mass of RAP binder each) (reprinted from Reference [57] with the permission of Elsevier).

Elkashef et al. [59] also used the FT-IR-ATR analysis to explore the effect of soybean-derived rejuvenator on two different kinds of performance grade bitumen. The types of bitumen, PG 64-28 and PG 58-28, were aged by Rolling Thin Film Oven Test (RTFOT, similar but slightly different in parameters values from TFOT technique) and pressure-aging-vessel (PAV) methods, and then they were doped with 0.75% of soybean-derived rejuvenator.

Figure 7a shows the increase in the carbonyl index with ageing. The soybean additive does not influence the ageing behavior of the binder. Regarding the sulfoxide index, (shown in Figure 7b) it increases with the aging of PG 58-28. On the contrary, it decreases dramatically to the last step of PG 64-28 ageing (PAV). The drop is also present for the aged doped binder. Ageing was probed by FT-IR-ATR in both the control and modified asphalt binders. As a result, the carbonyl and sulfoxide functional groups increase with ageing. The time evolution of these two functional groups, leads to the conclusion that the modification does not cause any significant influence on the ageing behavior of the asphalt binders. Cavalli et al. also investigated the molecular size distribution with Gel Permeation Chromatography (GPC) in order to evaluate if the rejuvenator modified molecular properties of RAP binder. They used two kinds of detector: one is the refractive index (RI) detector, and the second one is a variable wavelength detector with UV signal (UV). From RI detector, RAP + 5% A and RAP + 5% C (see Figure 8) displayed a shift from the large to the middle size as compared to RAP binder.

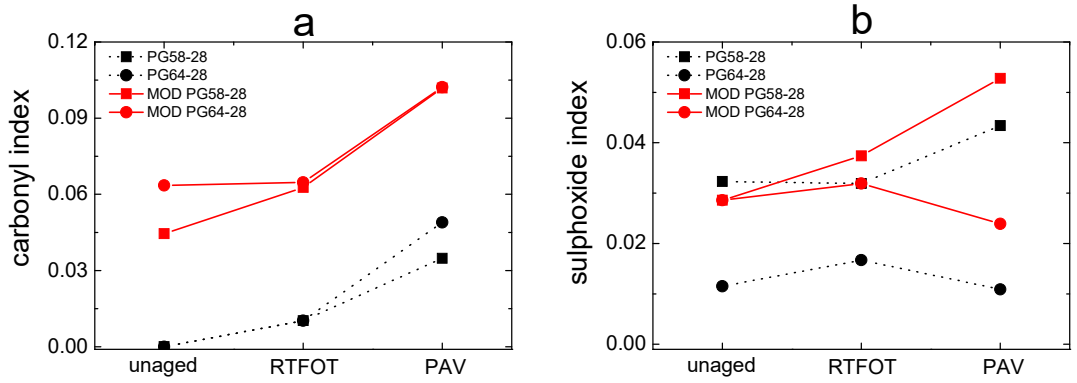

Figure 7. Carbonyl index (**a**) and sulfoxide index (**b**) (data taken from Reference [59]).

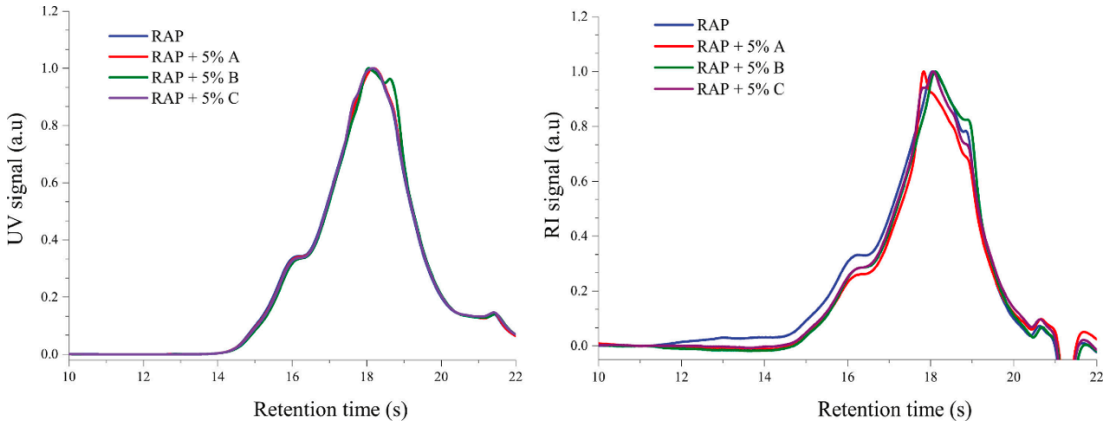

Figure 8. GPC spectra with UV (**left**) and RI-signals (**right**) of the RAP binder and the RAP binder with rejuvenator A, B and C (5% by mass of RAP binder each) (reprinted from Reference [57] with the permission of Elsevier).

Comparing the FT-IR spectra and the results obtained with GPC they hypothesized the presence of an ether group (C-O-C) in the RAP modified with A and C, whereas, from UV detector a shift towards the smaller molecular sizes has been observed in RAP + 5% B. In summary rejuvenators could partially change the molecular size distribution of the RAP binders.

The idea of combining FT-IR to obtain information on functional groups and GPC test to obtain information on molecular weight distribution was also exploited by Zhu et al. [60] who studied the effect of a bio-rejuvenator made by a by-product in cotton-oil production and dibutyl phthalate (7.5 wt% in the bio-rejuvenator) as plasticizer. In fact, they carried out a comparison between the FT-IR spectra of pure bio-rejuvenator; pristine bitumen; bitumen aged by Thin Film Oven Test (TFOT - 5 h, 163 °C) followed by a pressure-aging-vessel (PAV) test (aging temperature in the PAV test 90 °C, pressure 2.1 MPa, duration of the test 20 h); PAV was added with 5% or 10% bio-rejuvenator. Moreover, they carried out FT-IR spectra on an asphalt modified with styrene-butadiene-styrene (SBS); SBS-modified PAV, and 5% or 10% bio-rejuvenator on SBS-modified PAV. The peak-area intensity of the oxygenated groups (CO and SO) was used to probe the degree of aging and rejuvenation of the asphalt. Here, again, the Authors calculated the I_{co} and the I_{so} indexes. As expected, for pristine bitumen and SBS-modified asphalt, the carbonyl and sulfoxide indexes increase after aging. As it can be seen by a perusal of Figure 9, both indexes decrease with the addition of the bio-rejuvenator.

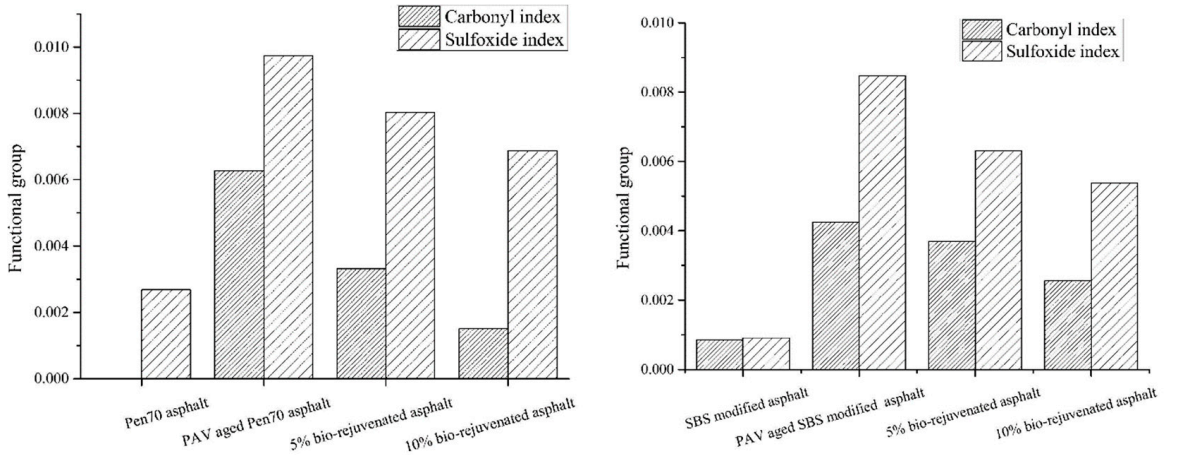

Figure 9. Carbonyl and sulfoxide indexes of virgin, aged, and bio-rejuvenated asphalt (reprinted from Reference [60] with the permission of Elsevier).

However, the carbonyl and sulfoxide indexes of the PAV-aged asphalt cannot be restored to their original levels. The Authors applied the GPC to the system under consideration to shed light on the effect of the rejuvenator on the molecular size distribution. The chromatogram reported in Figure 10a shows that the dw/dlogM versus Mw (weight-average molecular weight) curves for the bio-rejuvenator. Mw of the bio-rejuvenator is about 1000 g/mol, and the narrow and sharp peak indicates that the molecular-distribution dispersity of the bio-rejuvenator is low.

Figure 10b shows that the PAV-aging process causes a decrease in the low and medium-weight molecular content of the pristine bitumen while increasing its high-weight molecular content. Adding the rejuvenator helps in improving the properties of the PAV-aged bitumen by increasing the medium-weight molecular content and decreasing the low-weight molecular content. Figure 10c shows a similar phenomenon with the single-peak in the PAV-aged SBS-modified asphalt splitting into two peaks after bio-rejuvenation. In order to characterize the molecular mass distribution, the Authors used analysis of polydispersity, defined as the Mw-to-Mn ratio (Mw, weight average molecular weight; Mn, number-average molecular weight). The results are reported in Figure 11. Both Mw and polydispersity of the virgin asphalt were found to increase after PAV ageing, due to the various chemical reactions in the asphalt/polymer. On the other hand, the values of the PAV-aged virgin and SBS-modified bitumen show that the rejuvenation effect can be primarily attributed to the changes in the molecular polydispersity of the asphalt.

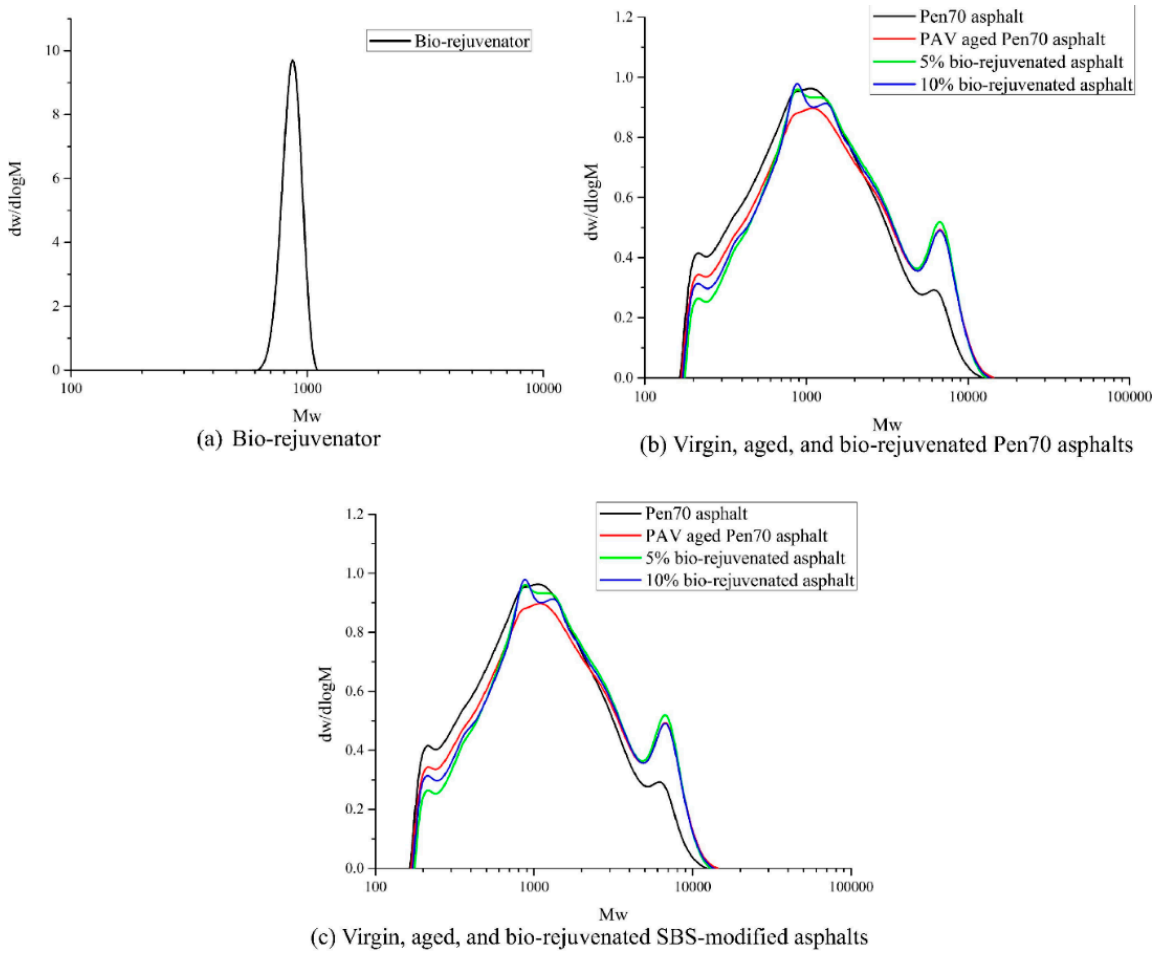

Figure 10. GPC curves of bio-rejuvenator and virgin, aged, and bio-rejuvenated asphalt (reprinted from Reference [60] with the permission of Elsevier).

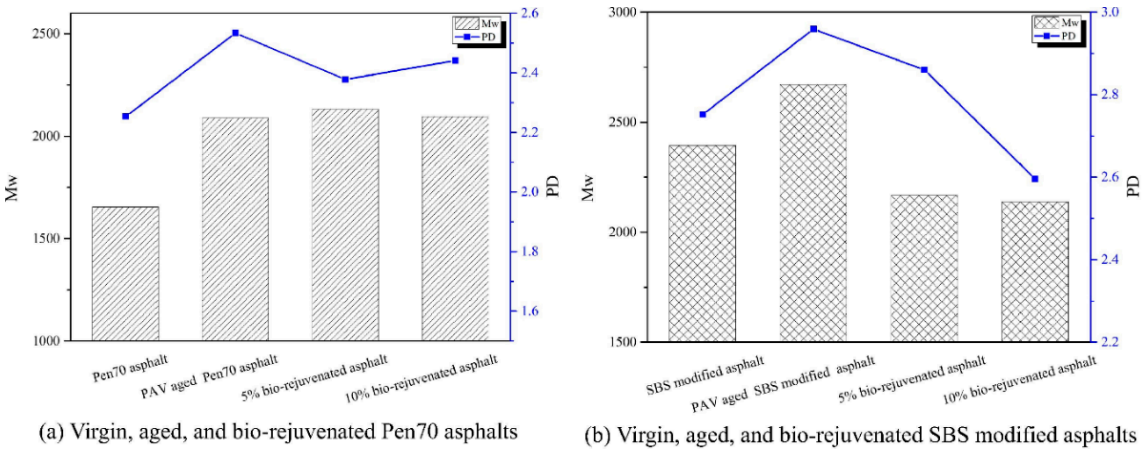

Figure 11. GPC Mw and PD results of virgin, aged, and bio-rejuvenated asphalt (for bio-rejuvenator: Mw = 861, PD = 1.0082) (reprinted from Reference [60] with the permission of Elsevier).

Conversely, for the PAV-aged SBS-modified asphalt, Mw decreases with the increase in the dosage of the bio-rejuvenator from 0 to 10%. Both the 5% and 10%-bio-rejuvenated asphalt exhibit lower PDs than the PAV-aged SBS-modified asphalt. However, there is no clear difference between the Mw values of the 5% and 10%-bio-rejuvenated asphalt.

In order to understand the role played by the rejuvenator on the RAP bitumen, Elkashef et al. [61] used the GC-MS (Gas Chromatography-Mass Spectroscopy). They considered a rejuvenator produced from soybean oil, but they did not furnish further details. First, they analyzed the pure rejuvenator: its total ion chromatogram (see Figure 12a) shows five distinct and well-resolved peaks. The pure rejuvenator was then subjected to RTFOT-aging and PAV-aging following the same protocol as that used for asphalt binders aging to assess the chemical stability of the rejuvenator with aging. The total ion chromatogram for the RTFOT-aged and PAV-aged rejuvenator samples are shown in Figure 12 (panels b and c, respectively): they clearly show that the aged rejuvenator gives the same peaks at the same retention times and with similar relative intensity as the unaged rejuvenator. This indicates that the chemical composition of the rejuvenator is preserved during aging.

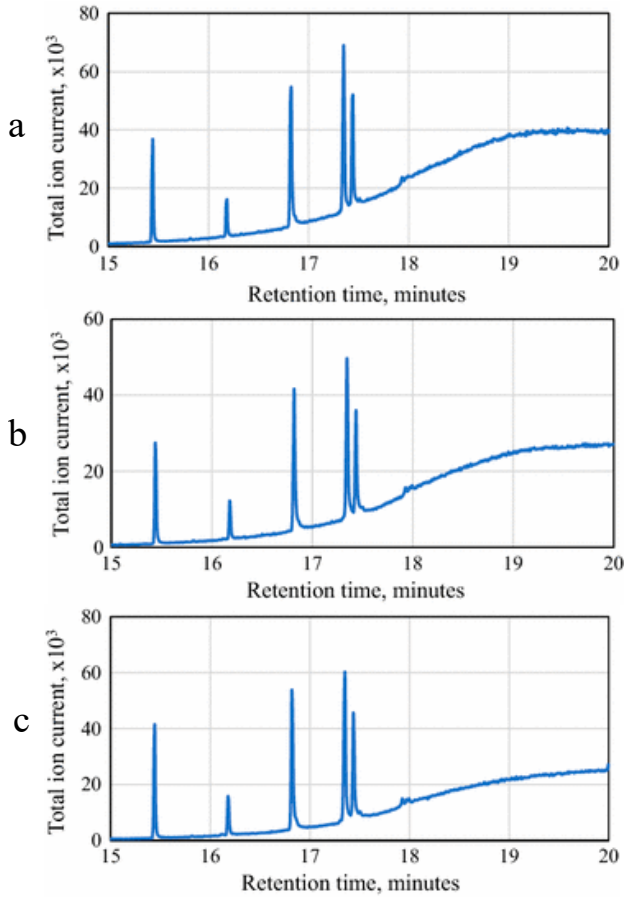

Figure 12. Total ion chromatogram for the used rejuvenator (**a**), the RTFOT-aged rejuvenator (**b**) and the pressure-aging-vessel (PAV)-aged rejuvenator (**c**) (reprinted from Reference [61] with the permission of Elsevier).

Subsequently, they submitted rejuvenated RAP (unaged, RTFOT-aged and PAV-aged) to pyrolysis to analyze the evolved gases using Gas Chromatography coupled with Mass Spectrometry (GC-MS) (see Figure 13). The total ion chromatogram of the unaged rejuvenated binder shows the rejuvenator's peaks in addition to other smaller peaks attributed to the binder itself. However, the structure of the rejuvenator added to the binder appears to change with aging.

It is, therefore, clear that the rejuvenator interacts with the RAP binder, with the consequent structure modification of the rejuvenator itself. Strikingly, the two peaks at 17.3 and 17.4 min are reduced in intensity with aging, and they entirely disappear in the PAV-aged binder.

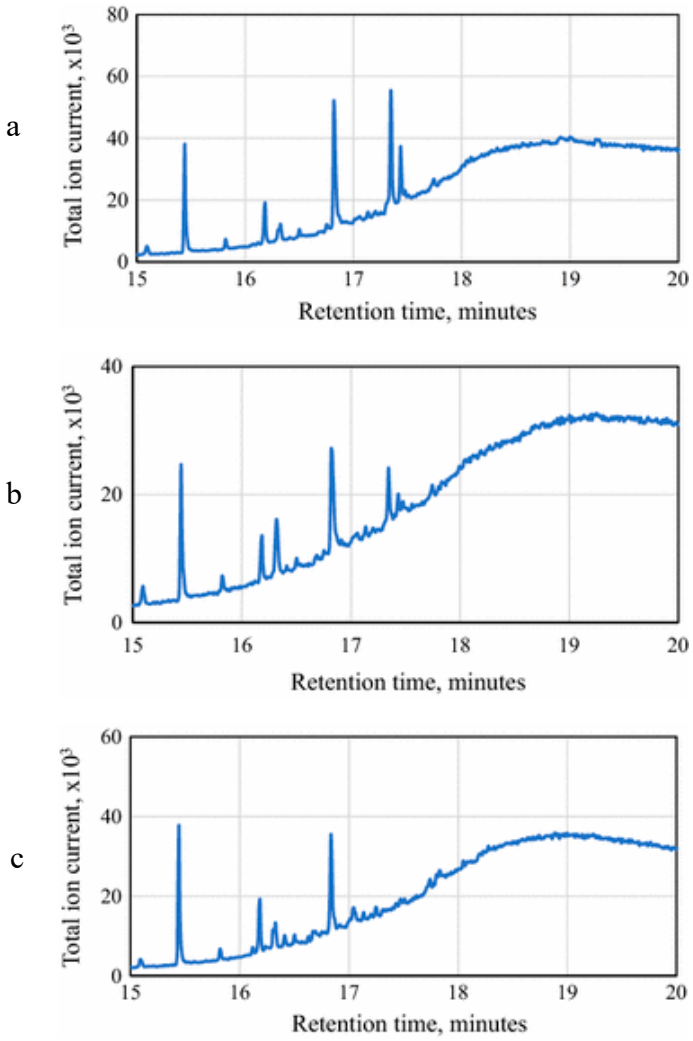

Figure 13. Total ion chromatogram for (**a**) unaged, (**b**) RTFOT-aged and (**c**) PAV-aged rejuvenated RAP (reprinted from Reference [61] with the permission of Elsevier).

4.5. Images Techniques as Useful Complementary Tools

Mokhtari et al. [62] have exploited the potential of FT-IR to investigate the effect of two different rejuvenators: a petroleum oil (called "A"), and a product derived from refined tall oil (called "B"). Rejuvenator "A" was added to 15% or 30% by weight on PAV, while the rejuvenator "B" was added to 10% or 20% by weight on PAV. These two dosage rates are the lower and upper limits of each rejuvenator type. Once the spectra were acquired, in order to determine if the use of the rejuvenators minimizes the oxidation, the I_{co} and I_{so} indices were calculated although the normalization seems to us to take place only over the C-H signal at 1459 cm^{-1}. As expected, PAV-aged samples show an increase in the I_{so} value, as well as in the I_{co} index.

On the contrary, by perusal of Figure 14 it can be seen that both rejuvenators at both concentrations show a significant decrease in I_{so} values, while the decrease with respect to the I_{co} index is moderate. However, both additives have proved to be effective in counteracting the oxidation of the carbonyl groups, as well as the sulfoxide groups. The Authors also thought to compare the FT-IR results with a Cryo-Scanning Electron Microscopy (Cryo-SEM) investigation for evaluating fracture surface properties of rejuvenator-restored through a digital image processing technique to quantify cracks developed on the fractured surface, due to the aging process. The choice of this technique comes from the Authors' consideration that the evaluation of the microstructural assessment of asphalt with SEM would not be confident, due to presence of volatile components in asphalt and its susceptibility

to electron beam damage. Instead, the use of Cryo attachment to SEM, implying a lowering of the samples' temperature well below the glass point, allows observing samples with greater beam and lower temperature sensitivity. They have acquired images with varying magnifications in different parts of the samples, to indicate the fracture surface characteristics of each sample. It is possible to notice that the asphalt sample has a rough and fractured surface with many fragments, due to the high stiffness caused by the aging process. Rejuvenator "A" makes the fracture surface of aged asphalt smoother with some remaining minor cracks or fragments. However, no further improvement of the surface texture can be observed when rejuvenator "A" amount was increased from 15 to 30%. Even adding rejuvenator "B" (10%) makes the fracture surface smoother, although at a minor extent, since significant amounts of fragments still holds. Instead, increasing the rejuvenator "B" amount from 10 to 20%, results in a significant improvement of the surface.

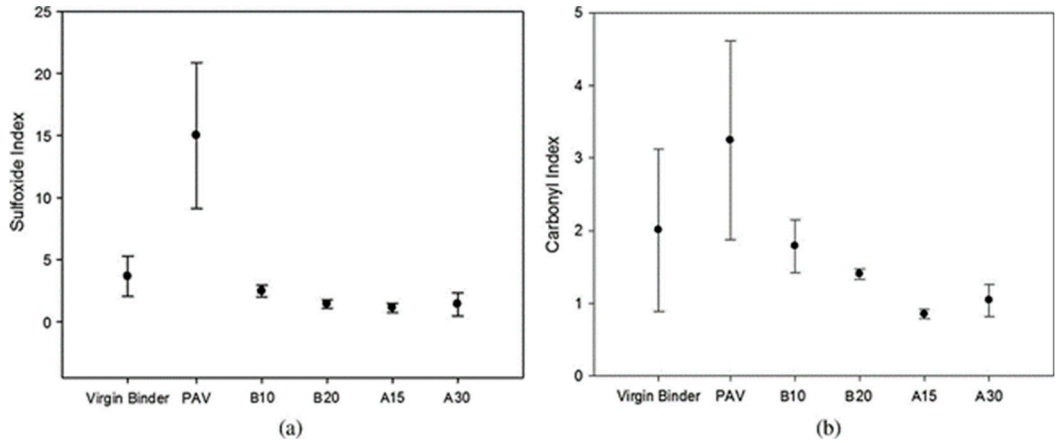

Figure 14. Calculated index values for various asphalt types (**a**) sulfoxide index, (**b**) carbonyl index (reprinted from Reference [62] with the permission of Elsevier).

An interesting aspect can be found in the work of Mokhtari et al., who notes that in order to identify the length and the gravity of the cracks, a digital analysis of the images was carried out using an edge detection technique. Briefly, various algorithms developed using MATLAB software DIP image toolbox were used to generate fracture models, including the crack propagation throughout the samples. Comparison with real samples allowed the selection of the best algorithm and a Fracture Index (F.I.) was defined in order to quantify the fracture capability of aged and restored asphalt samples.

As expected, as it can be seen from Figure 15, PAV-aged asphalt has the highest F.I., confirming more pronounced brittleness of the aged asphalt with respect to the aged asphalt with rejuvenators.

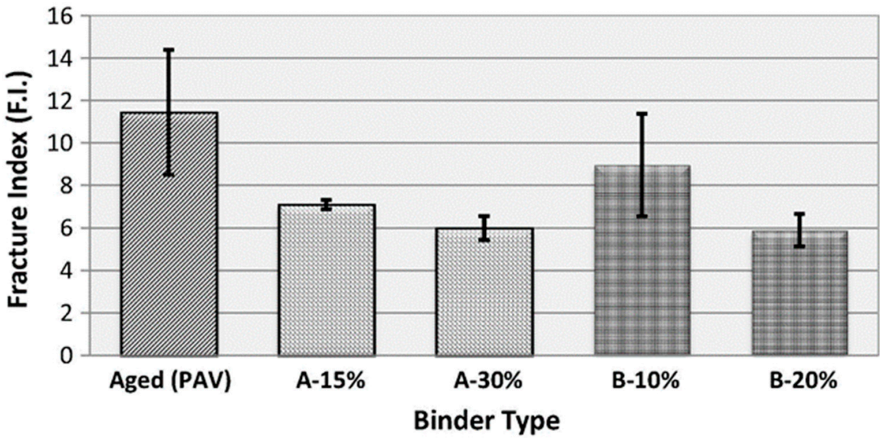

Figure 15. The comparative plot of fracture index for various asphalt types (reprinted from Reference [62] with the permission of Elsevier).

Figure 15 shows that the addition of 10% of the rejuvenator "B" could not significantly soften the aged asphalt. However, although 10% of the rejuvenator "B" was not completely effective in softening the PAV-aged asphalt, 20% of that rejuvenator shows the highest efficiency in preventing undesirable cracks at low temperatures. Moreover, both A-15% and A-30% asphalts were soft enough to prevent surface fractures.

Other authors have also focused their attention on the use of image techniques to better understand the structural changes induced by the use of rejuvenators. Indeed, Yu et al. [5] have used the AFM technique to analyze the materials' surface morphology. They have investigated two types of bitumen which are called by the Authors as asphalt binders, named AAD (PG 58–28) and ABD (PG 58–10), and two types of rejuvenators: one comes from fast and convenience food frying oil, here named WV oil, the other is an aromatic extract containing approximately 75% of aromatic oil and resin compounds with small amount of saturate oil. AFM images are shown in Figure 16.

The two virgin binders displayed different morphologies: virgin ABD has a dispersed phase with flake-like structures (with an average size of fewer than 2 μm in diameter) spreading over a smooth matrix continuous phase; virgin AAD, instead, clearly shows the elliptical domains with "bee-structures" (with axes of a few microns). The Authors attribute these differences to the chemical composition of the two samples, in particular, worth of note is the high wax content of the bitumen AAD (1.94%) with respect to the ABD bitumen (0.81%). Upon aging, in ABD, the size of the flake-like microstructures decreased while the quantity increased; on the other hand, in AAD, the "bee-structures" are still present with no obvious morphological changes. The addition of the aromatic extract in the aged ABD bitumen, instead, produces marked changes, giving elliptical domains with "bee-structures" at the middle of the domains. On the other hand, the use of the aromatic extract in the aged bitumen AAD gives smaller-sized "bee-structures". Even, the less noticeable contrast between the 'bee-structures' and the matrix suggests that the amplitude of the undulated "bee-structures" is smaller than that of the virgin and aged ones. On the contrary, the addition of WV oil in both aged binders do not produce a significant morphological modification.

The Authors conclude that the addition of the rejuvenator can cause big morphological changes, even bigger than those coming from the aging; however, this behavior is not general, depending on the specific rejuvenator. This because the asphalt binders' effect depends on its chemical behavior, and therefore, on the complicated molecular interactions which can establish with the other chemical species in the bitumen (and also the eventual inorganic particles). This is generally true for any additive. This conclusion is in accordance with the clues of a recent paper by Calandra et al. [1] which highlights the physical and chemical reasons for this. In this work, the Authors carried out a deep structural investigation by X-ray scattering on bare and additivated bitumen and found that asphaltene clusters hierarchically self-assemble to form aggregates at various levels of complexity, with different sizes up to the micrometer-sized domains dispersed in the maltene, and hold up by interactions of different strengths. The eventual presence of an additive triggers the formation of further intermolecular interaction in competition with those responsible for this self-assembly, causing a change of the size and shape of these aggregates.

The potential of the AFM has been exploited by Kuang et al. [23] to discriminate the effect of Dodecyl Benzene Sulfonic Acid (DBSA) as a solubilizer together with conventional rejuvenator (a blend of fluid catalytic cracking slurry—FCC—and bitumen with penetration of 70 grade) in two different aged (TFOT and PAV) bitumen.

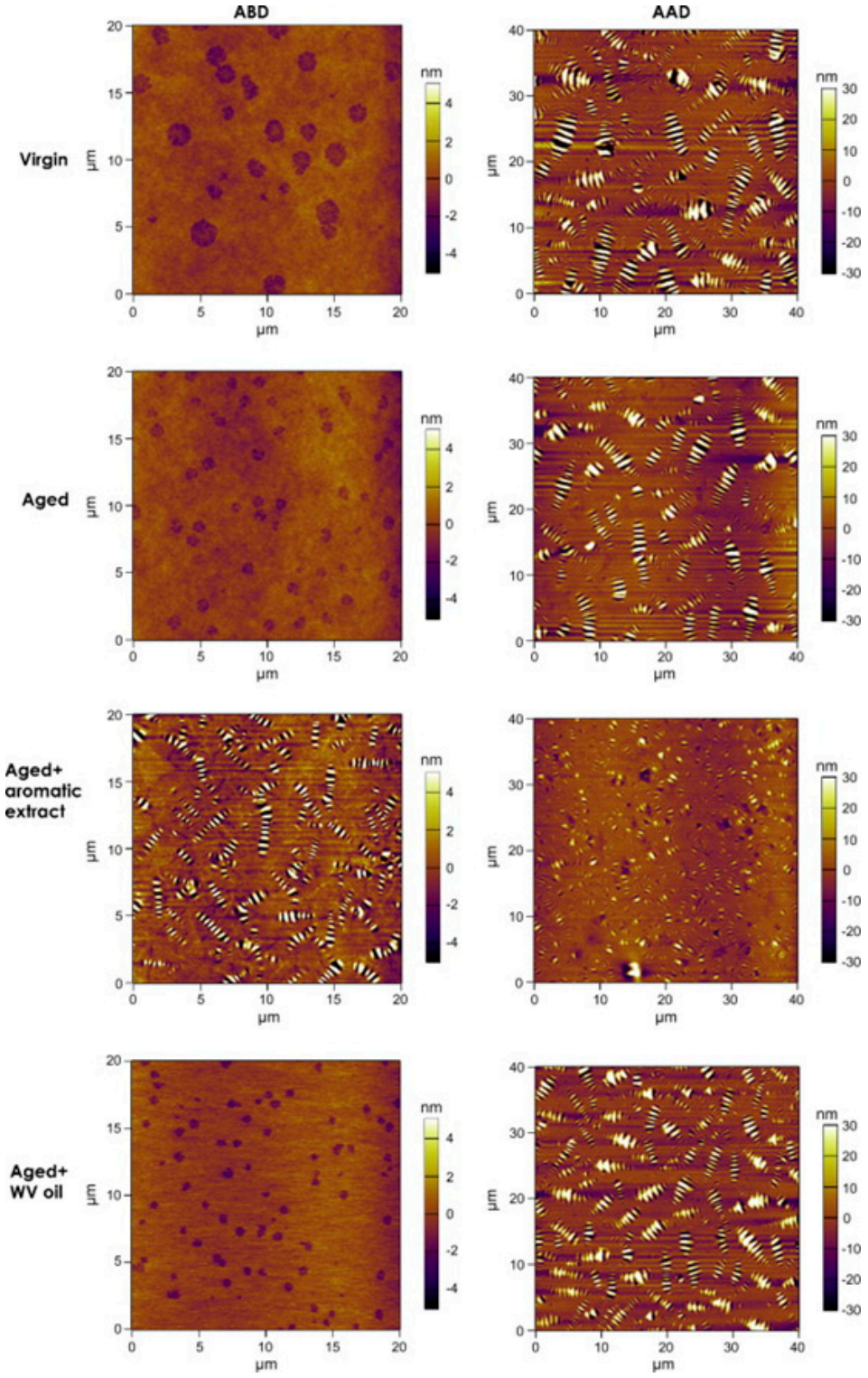

Figure 16. Topographic images of virgin (**top row**), aged (**2nd row**), aromatic extract (**3rd row**), and WV oil rejuvenated (**4th row**) ABD (left, 20 × 20 µm^2) and AAD (right, 40 × 40 µm^2) measured at room temperature (~20 °C). The colour scales range over 10 nm and 60 nm for ABD and AAD based samples, respectively (reprinted from Reference [5] with the permission of Elsevier).

Kuang et al. compared first the effect of aging on the virgin bitumen, whose clues are reported in Figure 17. This figure shows the AFM images of virgin bitumen, Thin Film Oven Test (TFOT) aged bitumen and PAV aged bitumen. The Authors have observed that the aging of the bitumen leads

to a change in the colloidal structure, and differently from Yu et al., an increase in the size of the bee-structures (see Figure 17). Then, they compared the effect of adding the conventional rejuvenating (CR) and the solubilised rejuvenating (SR) on the aged bitumen TFOT and PAV. The comparison in TFOT-aged bitumen and PAV-aged bitumen are reported in Figure 17. They found that in any case the surface of both TFOT and PAV bitumen become smoother with the introduction of CR or SR. However, in the case of TFOT there is no evident difference between the effect of CR and SR showing that, in this case, DBSA does not affect much the surface smoothing action exerted by the rejuvenator. On the other hand, an evident effect can be detected in the case of PAV. By inspection of Figure 18 (lower panel) and comparison with Figure 17, it is possible to notice how the addition of CR on the aged PAV bitumen does not bring marked morphological changes, just a slight reduction in the size of the bee-structures. On the contrary, the addition of SR helps asphaltenes of PAV aged bitumen to be re-dispersed, and this contributes to the performance improvement.

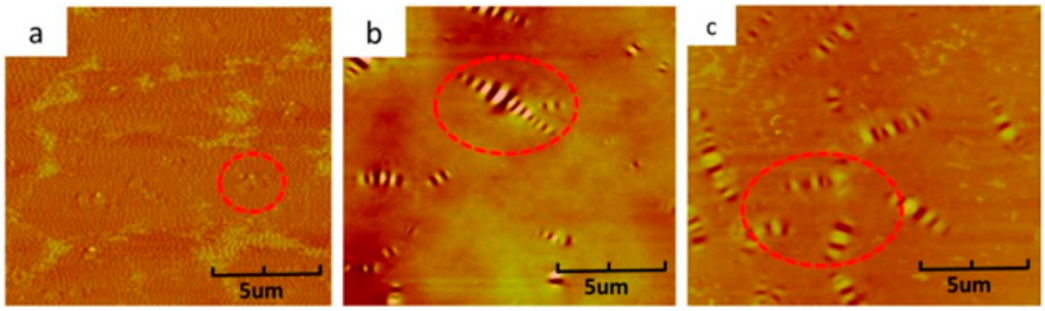

Figure 17. Atomic Force Microscopy (AFM) images of virgin bitumen, TFOT aged bitumen and PAV aged bitumen: (**a**) Virgin bitumen, (**b**) TFOT aged bitumen, (**c**) PAV aged bitumen (reprinted from Reference [23] with the permission of MDPI open access journal).

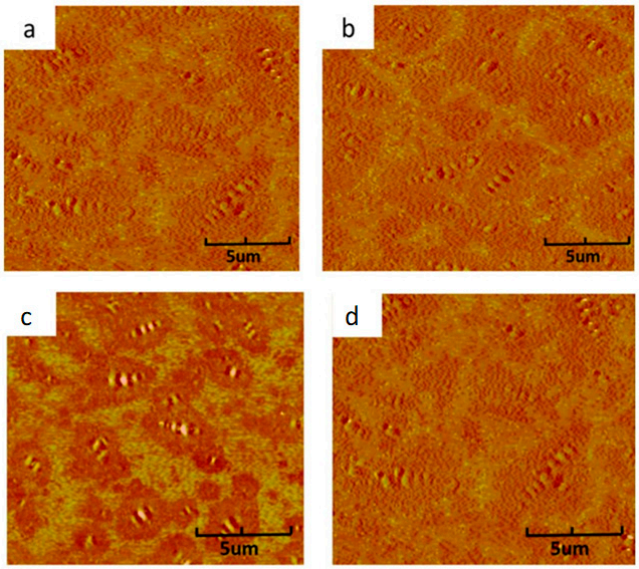

Figure 18. Upper panel: (**a**) Regenerated TFOT aged bitumen with 10 wt% CR, (**b**) regenerated TFOT aged bitumen with 10 wt% SR; lower panel: (**c**) Regenerated PAV aged bitumen with 10 wt% CR, (**d**) regenerated PAV aged bitumen with 10 wt% SR (reprinted from Reference [23] with the permission of MDPI open access journal).

For the Authors DBSA (1.5% by weight of rejuvenator) can react with asphaltenes via its sulfonic group to form a solvation layer covering on the surface of asphaltenes clusters, thus, interfering with the colloidal structure transformation of aged bitumen. Therefore, PAV aged bitumen can be recovered

from Gel to Sol-Gel by 10 wt% SR, and the dimension of a bee-like structure formed by asphaltenes can be approximately that of virgin bitumen.

Also, Nahar et al. [63] have explored the potentiality of AFM techniques to investigate the effect of rejuvenator on the aged bitumen. They used a bitumen aged through Rotational Cylinder Ageing Tester (RCAT) for testing two types of rejuvenators, namely, BM1 and CM1. They analyzed the pristine, aged and doped aged bitumen by means rheology and AFM.

From the rheological analysis, they were able to observe that the aged bitumen P1 shows higher complex shear modulus and lower phase angle compared to the pristine bitumen. Obviously, ageing makes the bitumen stiffer (Figure 19a) and less viscous (Figure 19b). The neat rejuvenators show very distinct behaviors. In fact, the rheology of the BM1 rejuvenator shows a lower viscosity compared to bitumen, while CM1 rejuvenator has different rheological characteristics. Indeed, it displays a much lower shear modulus at low frequencies. There is even a behavior of dilatant fluid or shear thickening at a frequency of about 3–5 Hz. The Authors thought that this was due to the presence of suspended particles like structures in rejuvenator CM1 or the formation of such structures at higher shear rates. However, the addition of rejuvenator BM1 into the aged bitumen causes a decreasing of the complex shear modulus, while the phase angle increases to the value of the virgin bitumen. CM1 rejuvenator on the aged bitumen leads to a lower complex shear modulus than pristine bitumen for both the concentrations tested. On the contrary, as expected, the phase angle is almost equal to (10% *w*/*w* CM1) or higher than the pristine bitumen (25% *w*/*w* CM1). It is worth noting that in a blend with aged bitumen any signature of the dilatant nature of the pure rejuvenator CM1 is completely lost.

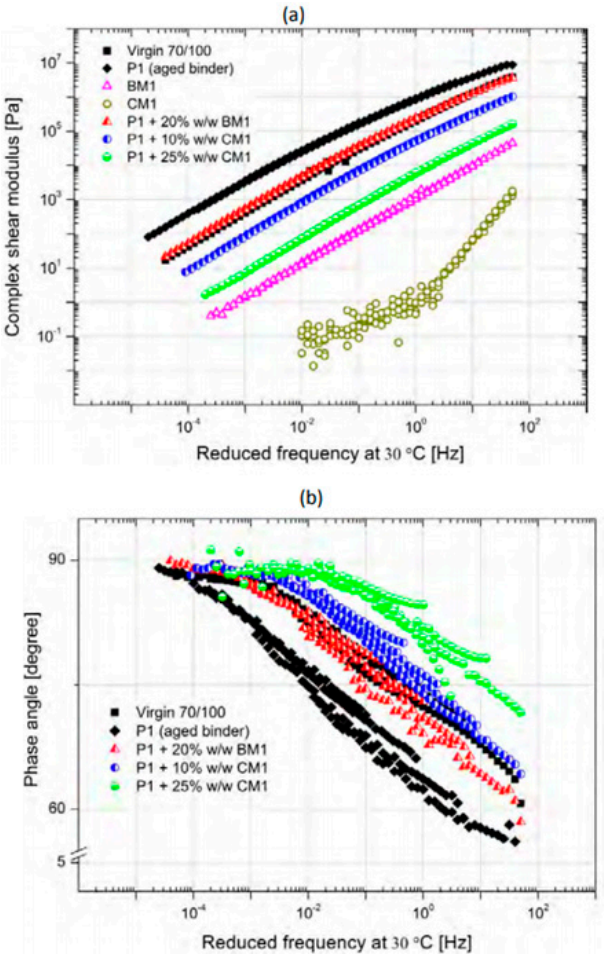

Figure 19. (**a**) Complex shear modulus of pristine, aged, doped aged and rejuvenator; (**b**) phase angle of pristine, aged and doped aged bitumen (reprinted from Reference [63] with the permission of SAGE Publications).

In our opinion, the AFM analysis conducted by Nahar et al. is commendable. To our eyes, it seems to be almost the most complete job among all the AFM-based works we have examined. In fact, the authors were not limited to the identification of domains and bee structures, having identified new types of structures (e.g., tertiary and quaternary) providing an accurate description. Figure 20(ai) shows the AFM phase image for the pristine bitumen. It is possible to estimate the length of the domains long axes which falls into the range 2–6 µm. The topography images show "wrinkling" in the middle of the domain. Finally, the domains result to be buried about 2–5 nm with respect to the average height of the continuous phase. On the contrary, the aged bitumen is very different from the pristine one. Figure 21 shows the same elliptical domain (i) and matrix (ii) of pristine bitumen. Moreover, it is possible to observe the tertiary phase, which consists of fine dark arcs and spots dispersed throughout the matrix (iii). This tertiary phase displays the lowest phase shift, and it is the softest phase. From the topography (shown in Figure 20 (ii)), it turns out that the elliptical domains are 5–8 nm lower (buried) the matrix surface, on average, while the tertiary phase protrudes above the matrix phase by 3–5 nm.

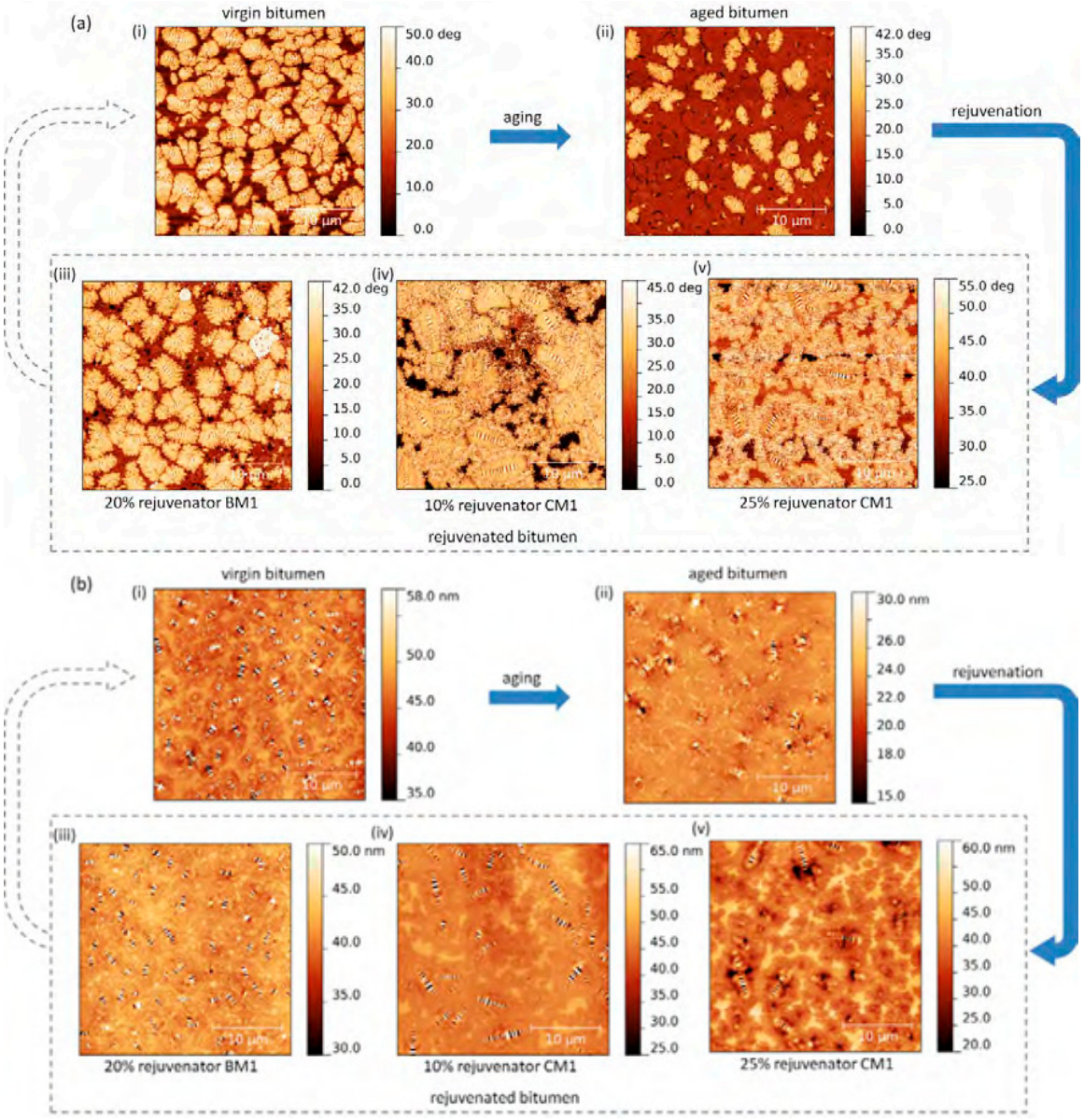

Figure 20. AFM (**a**) phase images, (**b**) topography images of pristine, aged and doped aged bitumen (reprinted from Reference [63] with the permission of SAGE Publications).

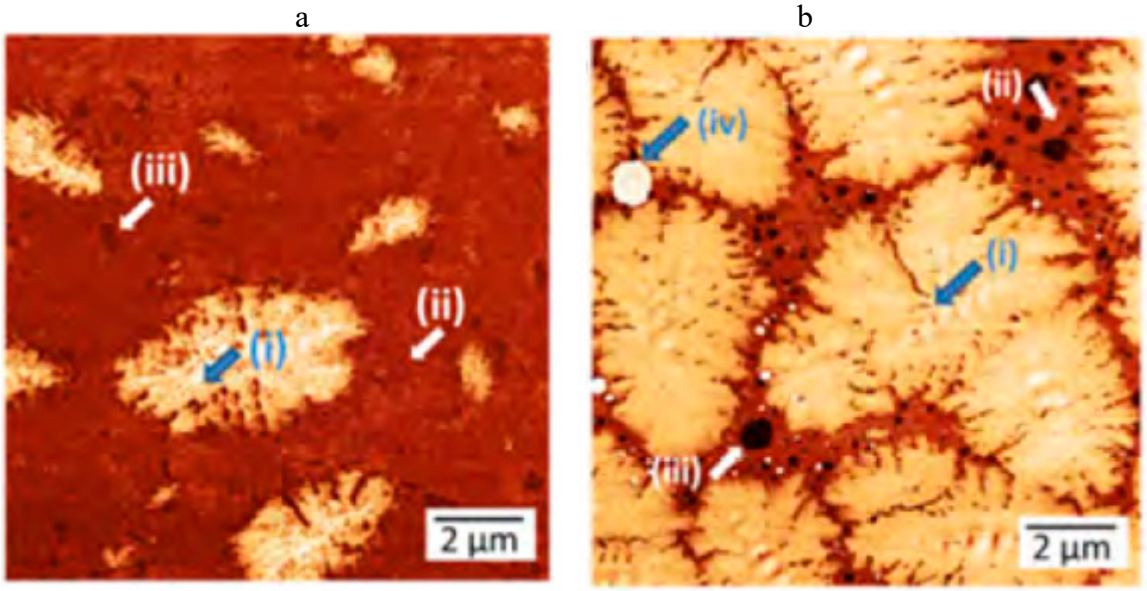

Figure 21. AFM phase image of aged bitumen (**a**) and aged bitumen doped with 20% of BM1 (**b**) with (i) elliptical domains, (ii) matrix, (iii) tertiary phase and (iv) quaternary phase (adapted from Reference [63]).

From Figure 20(aiii), it is possible to notice that the addition of 20% of BM1 to aged bitumen restores the microstructure. However, now it is possible to distinguish a new phase at the boundary of the domains and at the interstitial spaces of consecutive domains. A new quaternary phase is found, see Figure 21(biv). This new phase has the highest phase shift (highest stiffness), and it appears in almost circular shapes with sizes in the range 15.2–4 µm.

As it can be seen from Figure 20 (iv) and (v), the addition of the CM1 additive at both concentrations causes a change in morphology: needle-like particles, 20–90 nm wide and 50–250 nm long, appear. The network becomes the main phase at a microstructural level at the increasing of CM1 concentration.

In order to understand if the microstructure evolves with time, the Authors analyzed the samples, again, after seven days. The aged bitumen and the aged doped with 20% BM1 did not show any change over time. On the contrary, the aged bitumen doped with 10 and 25% of CM1 evolve over time (see Figure 22). The biggest change can be observed for the blend with the lower (10%) concentration of CM1 rejuvenator (see Figure 22(aii)). Over time, some effects can be highlighted: needles are expelled from the matrix phase, disconnected domains only comprising the network phase are born, and the wrinkling in the elliptical domains tends to decrease. The network phase, in this period, has formed a kind of bilayer around the elliptical domains, consisting of 200–300 nm stiffer layer (higher phase shift, light colour in Figure 22(bii)), surrounded by a 1 µm somewhat softer layer. Both layers display the typical pattern of randomly oriented needles, typical of the network phase. The higher stiffness layer may be just a denser packed region of the network phase. On the contrary, for the higher concentration of CM1 rejuvenator (25%) the effect of the time on microstructure is less obvious. Indeed, it is possible to notice islands solely consisting of the needle network, as well as the bilayer of 15 needles surrounding the elliptical domains. It is noticeable that, here, the stiffer (white) region of the needle network phase is the more prominent phase. Also, at a 25% concentration of CM1, the wrinkling in the elliptical domains remains over time, though the oscillation amplitude has decreased.

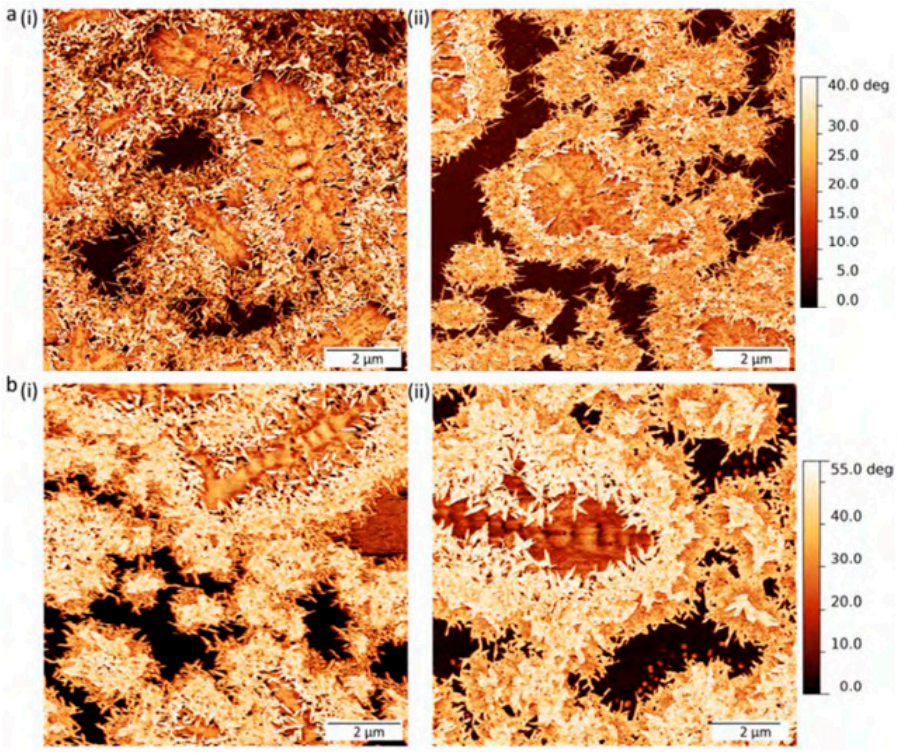

Figure 22. Time evolution of microstructure of aged bitumen doped with CM1. AFM phase images; (**a**) 10% CM1 and (**b**) 25% CM1, (i) after preparation (ii) after seven days (reprinted from Reference [63] with the permission of SAGE Publications).

Kuang et al. [64] evaluated the effect of composite rejuvenator in comparison with a common rejuvenator by means of dynamic shear rheometer (DSR) and atomic force microscopy (AFM). The composite rejuvenator, named RRA, was laboratory-prepared by blending the light weight oil rich in aromatics with a chemical compound containing polar group. The common rejuvenator, denoted as CRA, was also prepared in a laboratory. They used for these researches the bitumen SK-70, whose physical properties are listed in Table 2.

Table 2. Physical properties of SK-70 bitumen (reprinted from Reference [64] with the permission of Springer Nature).

Index	Value
Penetration (25 °C, dmm)	73
Ductility (15 °C, cm)	>150
Softening point/°C	45.2
Viscosity (135 °C, Pa·s)	0.6

The aged binder was prepared through the aging of SK-70 by Thin Film Oven Test (TFOT). Aged bitumen was doped with 4; 6; 8 and 10 wt% of the two kinds of rejuvenator.

The results are shown in Figure 23: the composite rejuvenator (RRA) has a greater effect with respect to the common rejuvenator (CRA). When the content of RRA is 10 wt%, the values of penetration, ductility, softening point and viscosity are very close to the values of pristine SK-70. Therefore, the Authors believe that the rejuvenator RRA is able to restore the colloidal structure by increasing the aromatics content. In addition, the polar groups of RRA can react with the asphaltene in aged bitumen, decreasing the asphaltenes content themselves. On the contrary, according to them, chemical reactions between the common rejuvenator and asphaltenes molecules do not take place, due to the lack of polar groups in common rejuvenator.

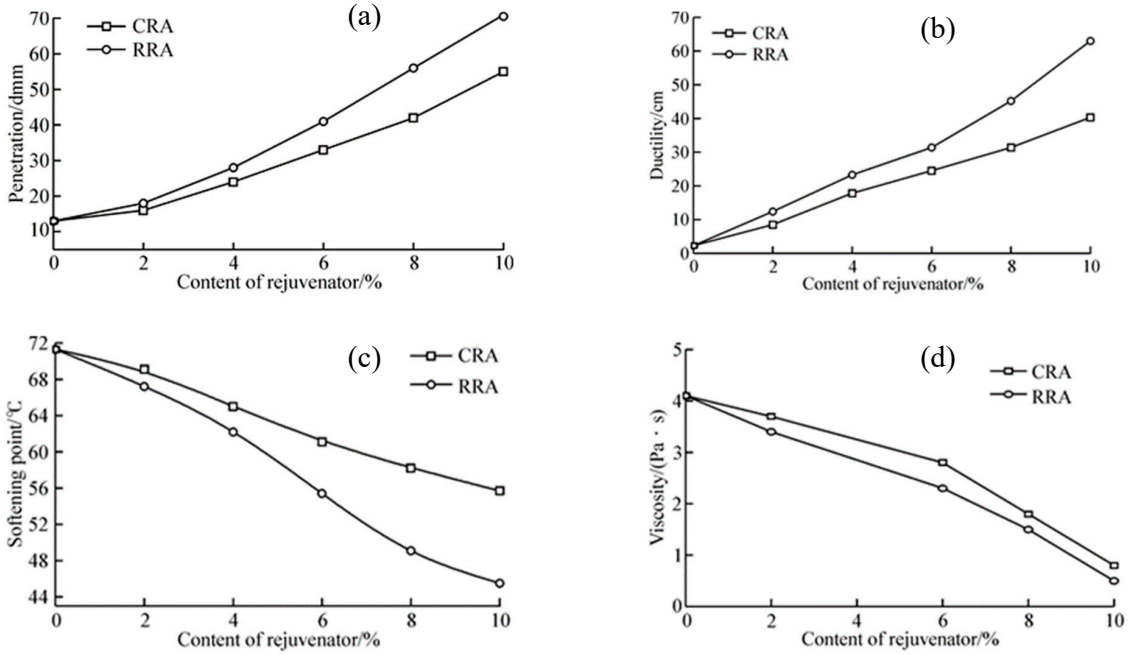

Figure 23. Effect of rejuvenators on penetration (**a**), ductility (**b**), softening point (**c**) and viscosity (**d**) (reprinted from Reference [64] with the permission of Springer Nature).

From the rheological analysis, it results that the rutting factor, shown in Figure 24a as a function of temperature, of the aged binder is greater than the virgin one. The addition of 10 wt% of RRA and CRA causes a decrease in the rutting factor, but sample with RRA gives a trend similar to the pristine one. Obviously, the aged bitumen is very brittle and easy to crack under load at low temperature, in fact, has a high fatigue factor (see Figure 24b) compared to virgin bitumen. The poor regenerative power of CRA is evident. Aged asphalt with 10 wt% CRA and aged asphalt shows similar fatigue factor curves. Nevertheless, the addition of 10 wt% of RRA improves the fatigue resistance considerably, being the fatigue factor trend close to that of virgin bitumen. In order to evaluate the effect of rejuvenators on the bitumen structure, the Authors carried out AFM analysis. From topographic images, the virgin asphalt (see Figure 25a) seems to be rather smooth; instead, the aged asphalt, (see Figure 25b) appears to be more wrinkled. Even, the surface of aged asphalt doped with 10 wt% of CRA seems to be rougher with flocculated structure just like that of the aged asphalt, see Figure 25c. The addition of RRA restores a smooth surface like that of virgin asphalt, Figure 25d. The disappearance of the flocculated structure is due to the dissolution of asphaltenes. Therefore, it can be concluded that aged asphalt can experience good recover of its original microstructure by means of the composite rejuvenator: an effective rejuvenation of the aged asphalt performance can be claimed.

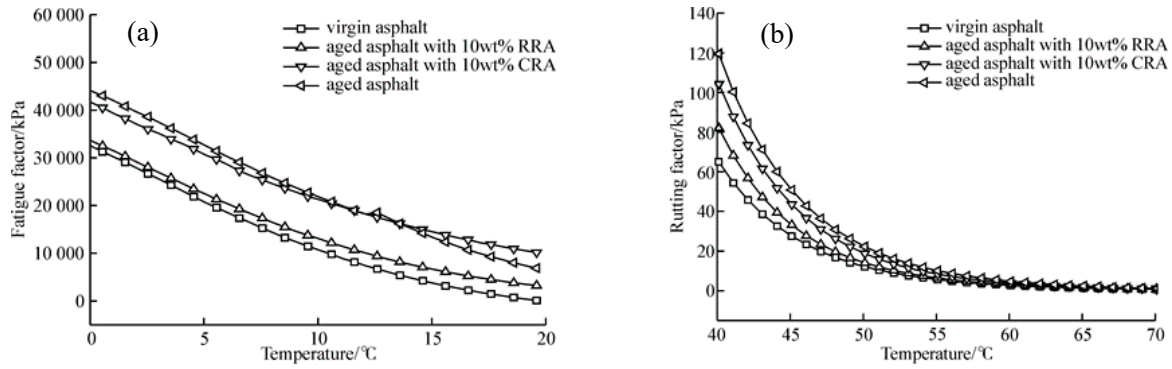

Figure 24. Effect of the rejuvenators on the Rutting factor (**a**) and on the Fatigue factor (**b**) (reprinted from Reference [64] with the permission of Springer Nature).

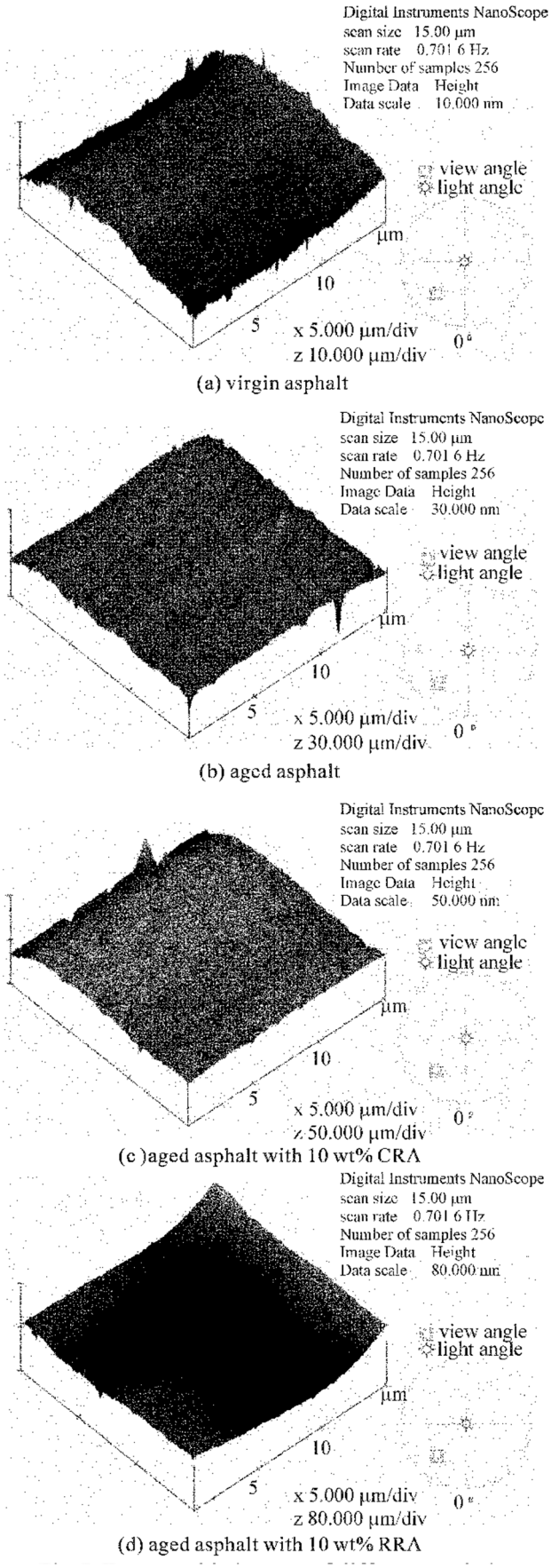

Figure 25. Topographic AFM images of samples (reprinted from Reference [64] with the permission of Springer Nature).

5. Perspectives

5.1. Improving Rejuvenators Characteristics

As already discussed above, a rejuvenator is commonly made by simple oil waste for their low-cost and obvious environmental concerns. In fact, oil waste is the by-product of edible oils surely more produced in the world. Therefore, its re-utilization may provide a feasible method to minimize the amount of generated waste, providing a positive environmental impact. From a chemical point of view, the oil subjected to elevated temperature changes its chemical composition, producing molecules with high anti-oxidant properties, which are certainly advantageous, for example, in the exhausted oil utilization as rejuvenating of bitumen. However, the waste oils have some disadvantageous, such as poor low temperature fluid properties, a propensity to oxidative degradation, a susceptibility to hydrolysis in acid media, which limits its application. For this reason, it is actually of greatest interest the proposal of chemical modifications of their structure to improve its physicochemical properties. In particular, if search should be narrowed only to vegetable oil waste (i.e., Waste Cooking Oils (WCO), then soybean oil, canola oil, coconut oil, castor oil, etc.), esterification, [65] hydrogenation [66], epoxidation [67], acylation [24] are only some examples of adopted chemical transformations to enhance the performance of these oils. In fact, the major components of vegetable oil waste are triglycerides esters of glycerol with saturated and unsaturated long-chain fatty acids, therefore, the transesterification reaction may represent the most valid method to change their properties, and it progresses through hydrolysis and successive esterification of the hydrolyzed products as schematically shown in Scheme 1.

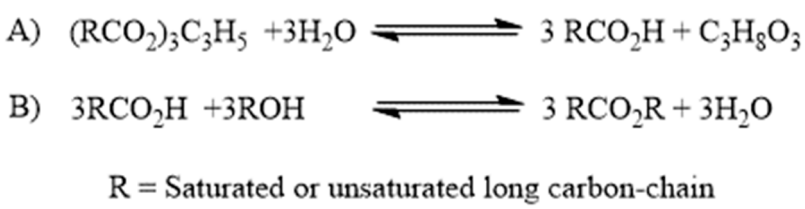

Scheme 1. (A) Hydrolysis reaction to form long-chain fatty acids; (B) esterification reaction to produce esters of long carbon-chain fatty acids.

This procedure paves the way to subsequent chemical modifications. An example is reported from Xiang et al. [68] that carried out the transesterification reaction by the treatment of exhausted oils with NaOH in CH_3OH to obtain methyl esters of fatty acids. The latter were transformed in variously substituted triester derivatives by the first epoxidation of unsaturated bounds present on of carbon backbone of R and a subsequent opening of oxirane ring to produce a final matrix with increased physicochemical properties, (i.e., better anti-wear ability, improved oxidation stability, etc.). However, it is evident that in proposing new synthetic methodologies of structural transformations, the chemists should take into account cheap and eco-friendly procedures. For this reason new perspectives on this typology of reaction may be, for example, the introduction of low-cost catalysts (i.e., Lanthanide salts, Fe salts, Zn salts, Cu salts, etc.), which are known to be employed in many chemical manipulations [69,70] in combination with green solvents, such as ionic liquid, Deep Eutectic Solvents (generally named DES) or water or Microwave irradiation [71,72]. For example, in order to transform oil waste into more performing products, it is possible to suggest a synthesis process to open oxirane rings, formed on the unsaturated bounds of R chain, in mild conditions, introducing transformable functional groups, such as nitriles or nitro that may be subsequently oxidized in environmentally friendly solvents. Another suggested modification may be the introduction of acyl groups with alkyl or aromatic chains on the unsaturated scaffold of the carbon-chain [73–75]. The presence of alkyl or aromatic groups could lead to forming secondary interaction, such as Wan der Waals or π-π interactions that may confer to the modified oils a major branched substructure, varying the physicochemical characteristics, increasing the chemical stability of the substrates and obtaining their better performance.

An alternative to the chemical catalysts could be the enzymatic catalysis, as proposed by Avisha and co-workers [76]. Candida rugosa lipase was used to hydrolyze oil wastes in a water solution with successive esterification by Amberlyst 15(H) resin catalyst. In addition, orange lipase deriving from waste was used from Okino-Delgado et al. in transesterification reaction, realizing remediated oils with higher performance profile [77]. However, the enzymatic catalysis through the commercial and the homemade lipase is considerably less convenient than the chemical one, because of higher reaction costs, specific reaction conditions, less manageability, the greater facility of degradation. On the other hand, the negative impact of oil waste on the environment and humans directs the scientists to propose its re-use to reduce the produced amount. Then, the chemical manipulation of the exhausted oils fits perfectly in the contest of its recycling. Obviously, it is important to always make a cost/benefit ratio. In fact, it is correct to think that chemical modification of an oil matrix has a major cost than its use as such, but it is equally true that with a view to having products, such as bitumen rejuvenating ones with enhanced physicochemical properties, the future of research in this field is to invest in rebirth of oil waste by innovative synthetic methods.

5.2. New/Novel Rejuvenators

The overall characteristics of a bitumen are, as a matter of fact, the consequence of its complex structure. The term "complex" does not refer to "complicated" or "hard to describe" but, instead, the term is used on a physical basis. The peculiar aspect involved in this topic will be better clarified in the next paragraph. Aging perturbs and changes the complex organization of a bitumen through various mechanisms whose consequence is to change the overall complex organization of the material and not, strictly speaking, one single specific aspect of the molecular organization of the bitumen. That is why, if only one specific structural feature is looked at, it may not correlate the dynamic behavior. In this respect, novel rejuvenators can be thought of. A typical class of molecule usually related to complex behavior is that of surfactant, and more generally that of amphiphiles. Amphiphiles, simultaneously possessing polar and apolar moieties within their molecular architecture, can give a wide scenario of possible intermolecular interactions: polar–polar, polar–apolar, apolar–apolar interactions, eventual directional H-bonds, steric hindrance, etc. For this reason, some of them are a surfactant, i.e., surface-active agents, when dissolved in water: they expose to the air their apolar part while binding water through their polar head, thus, decreasing the surface tension [78,79]. The same principle holds when trying to mix polar and apolar substances. Bypassing their natural tendency to remain separated, they actually can be effectively mixed if an amphiphile is present. Thanks to its capability to simultaneously linking both the polar and the apolar phases, the amphiphile act as a bridging molecule between the two. The two phases can be, therefore, homogenized to such an extent that the system can become homogeneous at the macro-scale although heterogeneous at the nano-scale, with the formation of local domain of one phase stabilized by one or more layers of opportunely oriented amphiphilic molecules and dispersed in the other phase [80]. Micelles, vesicles, bicontinuous structures and liquid crystals are only examples of stabilization of the systems through the formation of local intermolecular assemblies. This principle can be used, in our opinion, to the bitumen cases also. Let us consider that, in the micellar model, the bitumen is constituted by polar aggregates stabilized by polar resins and dispersed in a more apolar matrix. In this case, an amphiphilic molecule can bind on a side the asphaltene cluster, and on the other side, the apolar maltene phase. The overall outcome of these simultaneous interactions would be to disperse the asphaltene clusters contrasting aging better, or even, drawing back to rejuvenation. On the other hand, it must be admitted that the general mechanism of action shown by amphiphiles is already well-known and used for several issues in various fields: amphiphiles have been proved to be effective in stabilizing organic molecule clusters within an apolar solvent [81,82], as well as metal clusters [83], nanoparticles [84], and ionic clusters [85], so in our opinion their direct application to bitumen represents an obvious and immediate step. This idea has been recently tested in preliminary works where the surfactants have been successfully used to prepare warm mix asphalt binders. The results showed that the use of the

surfactant-based additive reduces surface free energy. It increases after short-term (Rolling Thin Film Oven) and reduces after long-term (Pressure Aging Vessel) aging [86]. Moreover, the addition of DBSA (Dodecylbenzosulfonic acid) based surfactant enhanced viscoelastic response of bitumen and reduced glass transition temperatures since it promotes the association of asphaltene molecules/aggregates into larger clusters in bitumen [87].

6. Forefront/Vanguard Techniques Facing Complexity in Bitumen

6.1. Complexity

The aim of this last paragraph is to furnish some hints on the future developments of new techniques for the investigation of bitumen. To do so, it is advisable first to clarify the exact nature of such systems, so it is needed to shed light on what is meant with the concept of "complex systems". Complexity is based on a hierarchical relationship between constituents and objects. Just to introduce the topic by an example, elementary particles are somehow assembled to form atoms, atoms are assembled to form molecules, molecules can assemble to form living cell, opportunely organized living cells can constitute tissues, and insisting with such a kind of reasoning, tissues, organs, human beings, society, etc., can be consecutively considered in an escalation within the principle a high number of levels. What is called "constituents" can be assembled together to form a complex object which, in turn, can be one of the "constituents" making an even bigger (i.e., more complex) object. So, what are called "constituents" belong to a specific "level", but when they are assembled to form a "bigger" object, a successive level is reached. These are what are called levels of complexity, and it can be misleading to deal with "bigger" or "smaller" systems, because it is not a matter of size: it is correct to deal with different levels of complexity. The peculiar features possessed by the elements belonging to each level of complexity are the consequence of novel emerging and unexpected properties that can arise when passing from a level to the successive. Since constituents are interacting, in fact, the complex system is not the mere collection of its building blocks so that the overall properties cannot be obtained by simple extrapolation of the characteristics of their constituents. Interestingly, novel and unexpected emerging properties can arise when passing from a level to the successive. Complex materials exhibit, therefore, spatial correlations between their constituents at different scales.

6.2. Probing Complexity

Bitumen is certainly a complex system, due to the asphaltene aggregation taking place at different length-scales, and due to the specific molecular aggregation involving different chemical species (see Sections 1 and 2). As in micellar systems, there are structures living for milliseconds (micelles) which can also be spatially correlated at high concentrations, in a similar way the same can be expected for bitumen. The term "structure", obviously crucial for an adequate description of a complex system is to be intended as strictly related to the spatial correlation between the constituents of the system. On the other hand, it cannot be neglected that for applicative purposes, the study of material must advisably involve non-invasive techniques. This is exactly what scattering techniques probe. The structure factor is inherently contained in the output of a scattering experiment. Scattering techniques not only give direct information on the structure possessed by the system, but also give its synthetic fingerprint. Such information (characterization of the constituents and their correlation to longer scales) are crucial in order to establish the proper connection between nanoscale morphology and bulk properties in complex systems. Here we want to emphasize that the "structure" involved in complexity is exactly defined in terms of the direct observable through scattering techniques, i.e., the existence of preferred distances (spatial correlations) among specific constituents of the system and taking place at different length-scales [88] so will give, in the following paragraphs, some hints on the theoretical background at the basis of this technique. Of course, other methods, especially microscopy-based, are available, i.e., Atomic Force Microscopy (AFM), Scanning Electron Microscopy (SEM) and Fluorescence Microscopy were used to investigate bitumen doped by polymers. The AFM and SEM have been used in order to

study the structure of asphalt while Fluorescence Microscopy was used to aid in understanding the structural changes occurring when polymers are added to the asphalt. The Atomic Force Microscopy was able to study the only structures of the asphaltenes. On the contrary, the Fluorescence Microscopy can only reveal the presence of fluorescing molecules. Oil exhibits autofluorescence when irradiated with shorter wavelength light, such as UV light, but for bitumen, there is very little fluorescent light emission because the oil phase is mixed with an asphaltene and a resin phase which do not exhibit any autofluorescence [89]. Performances and rheological behavior of a bitumen, however, is also a consequence of the dynamics involved at the molecular basis. Whereas, the above-cited techniques essentially probe the structure, a vanguard method to probe the dynamics fit for accurate bitumen characterization must also be individuated. Therefore, after a presentation of the scattering techniques, it will be shown another vanguard technology that can be used to deeply analyze the bitumen dynamics: the Relaxometry NMR, consisting in the measurement of the ^{1}H-NMR relaxation times of bitumen at low magnetic fields.

6.2.1. Scattering Theory

Apart from the development of scattering techniques at the large-scale facilities, recent improvements in lab instrumentation and the related beam intensities have greatly enhanced the importance of scattering methods in the structural characterization of complex materials. The quality of the recorded spectra is becoming adequate to extract information even from complex systems as bitumen is. The fundamentals of scattering techniques are, therefore, now given with the only scope to show how they are able to furnish the synthetic view of the material structure [90] of any nature [88]. A typical scattering geometry is reported in Figure 26: an incident (monochromatic or monochromatized) beam from a given source (e.g., Neutrons, X-rays, visible light, electrons, etc.) with incident wavevector (k_0) impinges on the material system under investigation. The scattered radiation intensity I is collected by a detector at a given scattering angle 2θ with respect to the incident radiation direction. The difference between the scattered (k_F) and incident (k_0) wavevectors furnishes the scattering wavevector $q = |k_F - k_0| = (4\pi n/\lambda)\sin(\theta)$ (where n is the index of refraction of the medium and λ is the wavelength of the employed radiation). For light n = 1.33 for a water medium, whereas, for X-rays and neutron n is very close to unit. It is worth noticing that a scattering experiment furnishes information over distances that are of the same order, or bigger, than the wavelength λ of the source radiation. The scattering is generally described as arising from the constructive interference coming from objects that are embedded in a continuum medium (treated as constant background). The interaction of radiations with materials is characterized then by a scattering length b_i, and its scattering length density (SLD) which is given by $\rho(\boldsymbol{r}) = \sum_i \rho_i(\boldsymbol{r}) b_i$ where $\rho_i(\boldsymbol{r})$ is the local density of scatters of type i [91,92].

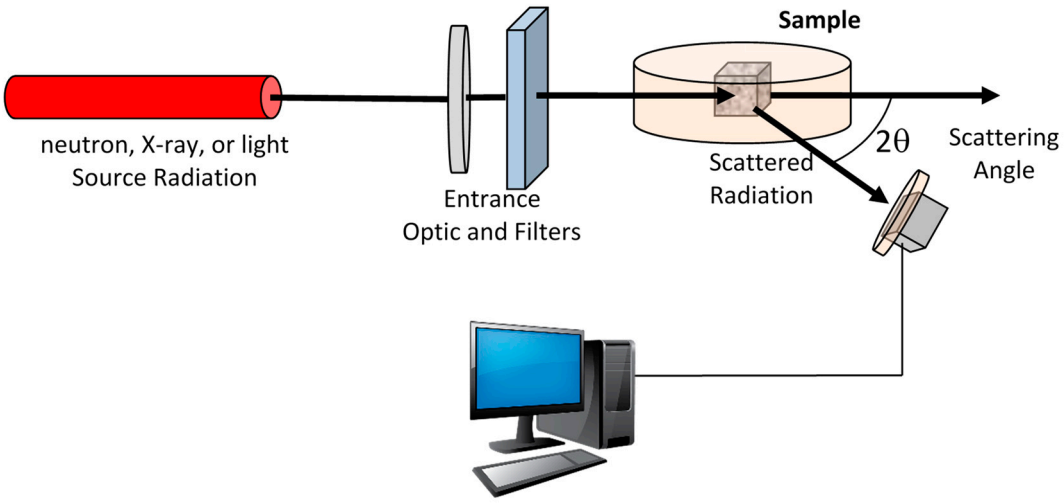

Figure 26. Schematic setup of a scattering experiment.

So, for example:

(i) neutron scattering arises through (short-range) nuclear interactions (or magnetically, if atoms have unpaired electron spins), while the scattering length depends on the nature of the nuclei of the reference atoms.
(ii) X-rays scattering comes from the interactions among all the electrons in the material under investigation. In this case, the scattering density can be traced back to the electron density.
(iii) In the case of Light photons, which have lower energy than X-rays ones, are scattered only by the outer part of the electronic cloud of an atom. In this case, the scattering length density is proportional to the polarizability of the materials.

Of course, different radiation (particle) sources give different sub-techniques. However, in the following, the different information that can be derived from the various scattering angle ranges, which in turn give different methods of analysis, will be shown.

6.2.2. Scattering of Neutrons (SANS), X-rays (SAXS) and Light

Scattering probes the statistical ensemble of the nano-structures and deals with the diffusion of electromagnetic (or particle) waves by heterogeneities in material systems [93]. At small angles 2θ, the (coherent) scattering intensity in the so-called "static approximation" is given by:

$$\boldsymbol{I}(\boldsymbol{q}) \propto \left[\sum_{\boldsymbol{i}} \boldsymbol{b_i}\, \boldsymbol{e}^{\boldsymbol{iqR}}\right]^2 \tag{2}$$

where b_i is the scattering length of the particle (chemical species) that occupy the position $\boldsymbol{R}$ in the material system. For SANS experiments the scattering length density $\rho(\boldsymbol{r})$ of the sample is defined as $\rho(\boldsymbol{r}) = \sum_i n_i(\boldsymbol{r}) b_i$, where b_i is the scattering length of the nucleus of type i, while $n_i(\boldsymbol{r})$ is the corresponding number density of such nuclei. For X-ray scattering $\rho(\boldsymbol{r}) = \left(\frac{e^2}{mc^2}\right) n_{el}(\boldsymbol{r})$, where $\left(\frac{e^2}{mc^2}\right)$ is the Thompson scattering length of the electron, and $n_{el}(\boldsymbol{r})$ is the electron number density.

By replacing b_i by a locally averaged scattering length density $\rho_i(\boldsymbol{r})$, (where r is a variable position vector), it is possible to perform an integration over the sample volume, V:

$$I(\boldsymbol{q}) \propto \left[\int_V \rho(\boldsymbol{r}) e^{i\boldsymbol{qR}} d^3\boldsymbol{r}\right]^2 \tag{3}$$

If isotropic samples are considered (i.e., where the orientation effects are averaged, due to the radial symmetry), the scattering intensity $I(q)$ can be expressed as:

$$I(q) \propto \int_0^\infty (\rho(r))^2 \frac{\sin qr}{qr} 4\pi r^2 dr \tag{4}$$

Very often, it is not immediate from the experimental Small Angle Scattering (SAS) intensity profile to obtaining direct information about the $\rho(\boldsymbol{r})$ function by inverse transform methods. In this case, SAS interpretation is based on the choice of suitable models expressed in terms of specified functions, which are capable of furnishing information on specific parameters connected to particular properties of the material system under consideration. The name of the technique is then further characterized by the probe which is used: if the probe is made of X-rays, then SAXS is considered; if the probe is a flux of neutrons, then SANS holds, etc. If the source is light, then it will obviously deal with light scattering. However, it must be noticed that, when dealing with light scattering, another technique, called dynamic light scattering (DLS) also known as photon correlation spectroscopy (PCS), is usually referred to. In such a method, time fluctuations of the scattering intensity as a consequence

of the Brownian motion of nano-scatters in a solution are recorded. Then, a time-dependent scattering function is derived to the diffusion coefficient of the particles (the scatters) dispersed in the liquid phase [94,95]. In contrast to this (more widely known) technique, the static light scattering (SLS) configuration resembles the typical scattering apparatus.

In the case of wide-angle scattering, higher $\boldsymbol{q}$ values are considered, which means that shorter distances are explored. In a typical Wide-Angle Scattering experiment, which can use in principle the same sources as small-angle, usually, the scatters are the atoms themselves. Typical interatomic distances are, therefore, probed: in the case of pure crystals, where positional order is dominant, this gives the famous Bragg law:

$$2\boldsymbol{d}\ \mathbf{sin}\boldsymbol{\theta} = \boldsymbol{n\lambda} \tag{5}$$

where n is an integer and d is the characteristic distance of reticular planes.

However, when the order is weak, the principle still holds, and wide-angle scattering can also be used for amorphous materials as in the case of bitumen. In this case, typical interatomic distances are unveiled: the interatomic first shell (which is often associated to the interatomic spacing typical of the liquid phase [96]) and other eventual longer-range peaks sometimes occurring as a consequence of intermolecular interactions [97]. In this situation, no sharp peak is observed, due to the disordered nature of the system. This disorder can be due to two effects:

(i) a polydispersion of the value of the interatomic distance represented by the peak. The intrinsically-disordered nature of the system (fluid) gives a peak broadening whose width gives the distance polydispersion. The order is partially lost at any distance.

(ii) Reduced size of the domain. The band broadening is due to the fact that the specific interatomic distance is only help at a certain length, called the correlation length. The order is lost beyond this length. The scattering domain size can be derived by the full width at half maximum (FWHM) of the band through the Debye-Sherrer formula:

$$\boldsymbol{\Delta} = \frac{\mathbf{K\lambda}}{\mathbf{FWHM\ cos\theta}} \tag{6}$$

where Δ is the average scattering domain size θ is the Bragg angle, λ is the wavelength of the incident beam, the FWHM (is expressed in radians and must be corrected for instrumental broadening, and K is a factor, approximately equal to unity, related to the domain shape [98].

This approach has proved to be effective in the structural analysis of structured molecular fluids [99,100], even in ionic liquids [101], and recently also in bitumen [1]

6.2.3. Applications of Scattering Techniques to Bitumen

Due to the high diffusion of X-ray scattering techniques and the development of lab-scale instrumentation giving adequate data quality, X-ray scattering was used for the analysis of bitumen even in the '60 [17]. Of course, when exploring the structure, taking into account values of typical length scales longer than a few nm small-angle scattering is best suitable [102]. However, in the wide angle range, the spectrum gives already a significant amount of information: it will be now briefly shown how to interpret it taking as an example of the representative spectrum, reported in Figure 27, as a function of a scattering vector $\boldsymbol{q}$ ($\boldsymbol{q}$ = (4π/λ) sinθ).

Let us pay attention to the following features:

1. A prominent broad band centered around 1.3 $Å^{-1}$ dominates the spectrum;
2. A weak and broad band around 3 $Å^{-1}$;
3. There is a tiny, but sharp, peak around 0.5 $Å^{-1}$, not always present;

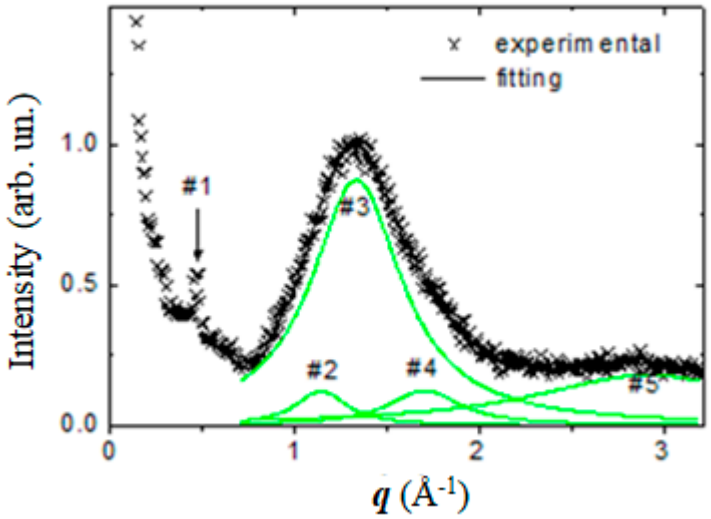

Figure 27. A typical X-ray scattering spectrum together with the Lorentzian deconvolution.

Different peaks (in Figure 27 indicated with progressive numbers) indicate that there are different characteristic distances belonging to various atomic and molecular organizations of different levels of complexity. The position of the center of each peak gives the characteristic distance (d), according to the Bragg law (Equation (7)) which, readapted, gives the following:

$$d = \frac{n\lambda}{2\sin\theta}. \quad (7)$$

As above, d is the interplanar distance, θ is the scattering angle, and λ is the wavelength of the incident radiation. Table 3 resembles the peculiarities and meaning of the peaks.

Table 3. Bands in the WAXS profile with the corresponding characteristics.

Position ($Å^{-1}$)	Features	Characteristic Distance (Å)	Meaning
1.3	Dominant and broad	~4.7	combination of various intermolecular distances between alkyl and aromatic parts: See text
2.9	Broad and weak	2.2	interatomic distance within asphaltene;
~0.5, varying	Not always present usually tiny	~13	supra-molecular aggregation: Repetition distance of aggregates of local asphaltene aggregates

The most prominent band centered at around 1.3 $Å^{-1}$ deserves some attention. In alkyl-based fluids, this band has been attributed to a characteristic intermolecular lateral distance of 4.4–4.7 Å [96,100,103] usually present in the conventional liquid (disordered) state [96,97,99–105]. Aromatic compounds are characterized by shorter distances, due to their tendency to form stacks, so they give the so-called graphene band (the lateral distance of about 3.6 Å) [22]. Due to the simultaneous presence of both aliphatic and aromatic compounds in the bitumen, it is reasonable to treat this band as a not-resolved superposition of these two contributions. Deconvolution in terms of bell-shaped curves is sometimes necessary to discriminate all the signals. Two noteworthy observations are due:

1. The fitting procedure will also help in analyzing the weaker band at higher angles (around 2.9 $Å^{-1}$ and which is a characteristic distance d of about 2.2 Å) which is sometimes partially overlapped;
2. The fitting allows to derive, from each curve, also the Full Width at Half Maximum (FWHM)

The shorter distance, of about 2.2 Å, can be surely attributed to some particular interatomic distance. The value is in the range of the typical distance between non-adjacent carbons reported for polycyclic aromatic compounds [106] so such attribution can be safely hypothesized. In the range

0.3–0.8 $Å^{-1}$ it can be present at a tiny peak. This would reveal the occurrence of a supra-molecular aggregation and would be, therefore, associated to a repetition distance between one asphaltene local aggregate and its neighboring one [22], suggesting the presence of aggregates of asphaltene aggregates, in accordance with a model of a complex system with different levels of complexity. Finally, in the low-angles range of the WAXS spectrum ($q < 0.3$ $Å^{-1}$), the fractal aggregation of the supra-aggregates of asphaltene clusters can be explored. The presence of self-similar, fractal structures, in fact, can be in principle possible in bitumen: in these cases, interfacial boundary is not sharp, and a scaling law between the mass M (or particle number N) and the enclosed volume is established, which furnishing an indication of how efficiently the particles are packed [107]. For a porous fractal cluster containing N identical primary units this scaling law is expressed as $N \sim R^{Df}$, were the fractal dimension D_f is connected with the involved aggregation mechanism. Since 1984 scattering techniques have been widely used for characterization of materials having fractal microstructures. The fractal dimension of a particle can be determined by analyzing the power-law regime of the scattered intensity $I(q) \sim q^{-\alpha}$, where the exponent α is related to the fractal dimension D_f of the scattering structures. For a mass fractal, it is possible to show that $\alpha = D_m$ and $1 < \alpha < 3$ in a three-dimensional space. In contrast, $\alpha = 6 - D_s$ for surface fractals. If $D_s = 2$ the well-known Porod's law $I(q) \sim q^{-4}$ for non-fractal structures with smooth interfaces is obtained.

So, the slope α can be, therefore, derived by linear fit, in an adequate region of the spectrum (see Figure 28 as reference), using the equation:

$$I(q) \propto q^{-\alpha} \tag{8}$$

However, self-similar hierarchical structures are seldom present or rarely probed in the literature, and, due to diversity of bitumen origin, chemical composition and age, this feature of the structure can change dramatically. Additives can change (i) the fractal structure, if present (ii) the band around 1.3 $Å^{-1}$ and (iii) the peak around 0.5 $Å^{-1}$, if present, but not the higher angle band around 2.2 $Å^{-1}$ because this distance refers to an intra-molecular distance, and it is not expected, therefore, to be changed by the presence of an additive.

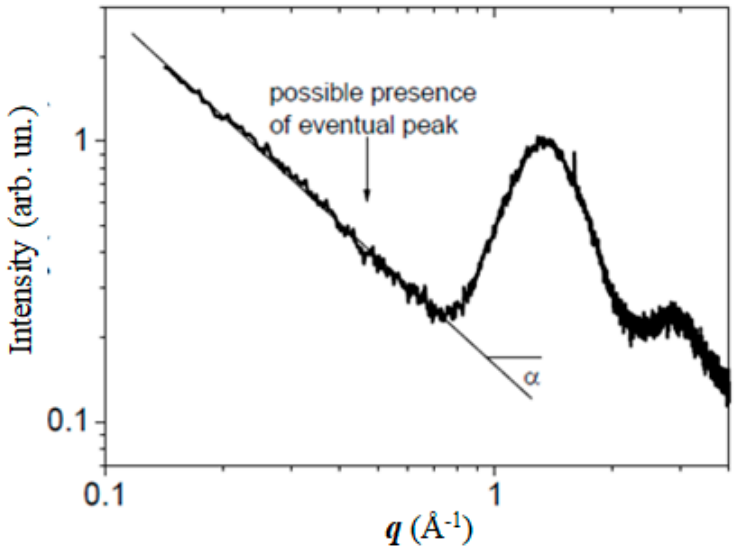

Figure 28. X-ray scattering spectrum of a bitumen showing fractal-like structure (see text for details).

6.2.4. Relaxometry Nuclear Magnetic Resonance Theory

The second vanguard technology that can be used to analyze the bitumen is the Relaxometry NMR. This method probes dynamic features and consists of measuring the ^{1}H-NMR relaxation times of bitumen at the low magnetic field. In the current high-resolution NMR technique, it is not

possible to obtain high resolution spectra because of their highly heterogeneous and low magnetic field strengths. In a basic NMR concept, at equilibrium, protons nuclei are distributed among the energy levels according to a Boltzmann distribution. Following any process that disrupts this distribution (e.g., absorption of radio frequency energy), the nuclear spin system returns to equilibrium with its surroundings (the "lattice") by a first-order relaxation process characterized by a time T_1 called the spin−lattice relaxation time. To account for processes that cause the nuclear spins to come to equilibrium with each other, a second time T_2 is required. T_2 is called the spin−spin relaxation time, because the relaxation is concerned with the exchange of energy between spins via a flip-flop type mechanism. In a perfectly homogeneous field, the NMR time constant of the decay would be T_2, but, in fact, the signal decays in a time T_2* that often is determined primarily by field inhomogeneity, since nuclei in different parts of the field precess at slightly different frequencies, and hence, quickly get out of phase with each other. Thus, the signal decays with a characteristic time T_2*. This decay directly measures the decrease in the transverse magnetization M_{xy}. The contribution of the magnetic field inhomogeneity to the free induction decay precludes the use of this decay time, T_2* as a measure of T_2. A method for overcoming the inhomogeneity problem is to apply the Carr−Purcell technique (CP) [108]. This method may be described as a 90°, τ, 180°, 2τ, 180°, 2τ, 180°, 2τ, ... pulse sequence. In Figure 29, experimental steps of bitumen, NMR Relaxometry are shown. Four hundred echoes have been obtained by Carr−Purcell sequence and analyzed by Inverse Laplace Transform (ILT).

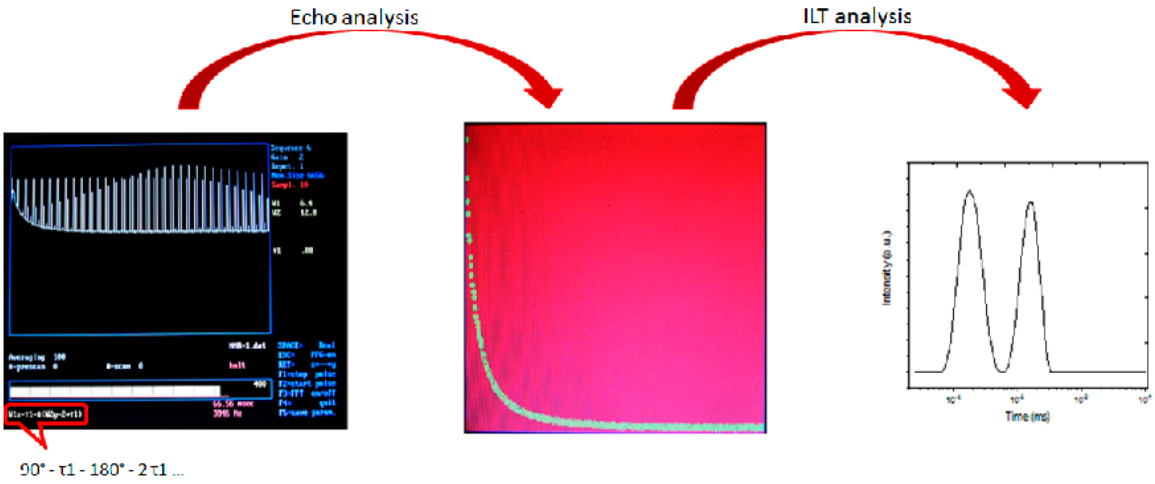

Figure 29. Schematic sequence of Echo and Inverse Laplace Transform (ILT) analysis in NMR Relaxometry.

The 180° pulses are applied at 90° phase difference relative to the initial 90° pulse, and the τ time delay was 0.05 ms. The main advantage of such a multiple echo technique is its quickness compared with other techniques based on single echoes. Consequently, it allows multiple accumulations of the echo train signal, which is an important issue in low-field experiments where the detection sensitivity is strongly reduced relative to the high-field experiments. If the CP envelope has a mono-exponential decay, the relaxation time T_2 of the sample can be obtained by fitting the n data to the following equation:

$$A_n = A_0 e^{-\frac{2n\tau}{T_2}} \quad (9)$$

where A_n is the amplitude of the nth echo in the echo train and A_0 is a constant depending on the sample magnetization, filling factor, and other experimental parameters. Usually, the T_2 relaxation time varies all over the sample because of the sample heterogeneity or surface relaxation differences; then a multiexponential attenuation of the CP envelope should be observed. Hence, if inside the sample, a continuous distribution of relaxation times exists, the amplitude of the nth echo in the echo train is given by:

$$A_n = A_0 \int_0^\infty P(T_2) e^{-\frac{2\pi\tau}{T_2}} dT_2, \tag{10}$$

where $P(T_2)$ is the T_2 relaxation time probability density.

Equation (10) suggests that the analysis of the experimental data using an inverse Laplace transform (ILT) might provide the relaxation time probability function. The ILT is a well-known mathematical tool, where it needs to face the inverse problem of estimating the desired function from the noisy measurements of experimental data. For convenience, the definition of the problem will be shortly recalled. Let $f(t)$ be a function defined for $t \geq 0$; the function $F(s)$ introduced by means of the expression:

$$F(s) = L\{f(t)\} = \int_0^\infty f(t) e^{-st} dt \tag{11}$$

is the real Laplace transform of $f(t)$. The inverse process, indicated by the notation $f(t) = L^{-1}[F(s)]$, is termed the inverse Laplace transform (ILT). $P(T_2)$ is the ILT of the unknown function that fit the echo amplitude curve. Hence, $P(T_2)$ can be understood as a distribution of rate (inverse of time) constants, strictly speaking, a Probability Density Function (PDF) that, among other things, could account for the different macro-structures that compose the bitumen binder [109]. This technique allows finding the PDF distribution, which associates with relaxation times that correspond to unrelated molecular aggregates inside the bitumen.

6.2.5. Applications of Relaxometry Nuclear Magnetic Resonance to Bitumen

Generally, regarding types of bitumen, the T_2 relaxation time distribution exhibits two peaks. Direct correlation can be made between T_2 and the rigidity of structures in these materials [43], as well as the molecular constraint, which causes dynamic hindrance [46]. The shorter T_2 times (around 10 ms) reasonably corresponds, therefore, to more rigid supra-molecular aggregates; hence, they are attributed to asphaltenes. Conversely, high T_2 times (around 100 ms) can be attributed to low intra-molecular interactions; they can be referred to the maltene fraction of the sample under examination. This finding supports the colloidal model of the bitumen. In fact, if the polar fluid model suggested by Christensen [110] were applicable to our system, the ILT result would demonstrate a sole broad peak referred to as a continuous T_2 time. Figure 30 shows a typical Probability Density Function obtained through an ILT transform of T_2 relaxation time data determined by analyzing neat and modified 100/130 penetration grade bitumen supplied by Highway Research Institute (Almaty, Kazakhstan) [111]. The measures of T_2 were made at a temperature 15 °C lower than transition temperature (solid-liquid) measured by dynamic temperature ramp test experiment. In Figure 30 the panels refer to the following samples: SD refers to PAV bitumen + 2 wt% HR (the green rejuvenator), SC refers to PAV bitumen + 2 wt% VO (Vegetable Flux Oil), SB PAV bitumen, SA Neat Bitumen.

The T_2 relaxation time distribution can be considered a structural fingerprint of the bitumen where changes in the T_2 relaxation times evidence modification in the structure of colloidal binder. In particular, the powerful ILT, applied to the echo decay, can be used to verify the effectiveness of the real rejuvenator. The same or better similar profile of T_2 relaxation times prove that the structure of aged bitumen has been regenerated reorganizing the same distribution of asphaltene micelles in the maltene phase. In general, by ILT NMR relaxometry it is possible to follow the structural evolution of bitumen when additives (polymer surfactants, etc.) are added, in fact, the relaxation distribution is strongly affected by the supramolecular organizations present in the colloids.

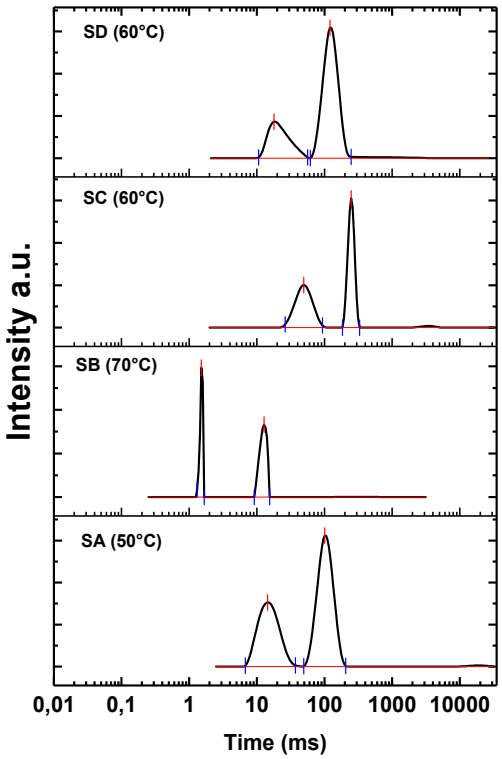

Figure 30. Inverse Laplace Transform (ILT) showing the Probability Density Function (PDF) of asphaltene and maltene aggregates of bitumen samples.

7. Concluding Remarks

1. Many materials are used for rejuvenating bitumen by lowering viscosity and stiffness. Since different physico-chemical mechanisms are involved in bitumen ageing (oxidation, evaporation, structural changes), different mechanisms of actions can be consequently exerted by the various rejuvenators (softening/fluxing, restoration of the pristine structure/properties). The distinction of the various mechanisms has been highlighted. These aspects have been shown in Sections 1–3.
2. The state-of-the-art constituted by the works carried out by several researchers in this field has been shown. Low-cost oils are generally added to increase the maltene fraction, but it should be noticed that an additive having complete rejuvenating function should also induce a reorganization of the chemical structure of asphaltenes and their assemblies. The restoring of the aged bitumen structure to the original conditions is not trivial, due to its complex organization at the supra-molecular scale. This has been extensively shown in Section 4.
3. Taking into account the complex chemistry involved in the bitumen rejuvenation, the additive performances can be improved by chemical manipulation/modification (paragraph 5.1). Some perspectives have been also presented (Section 5.2) considering for the complexity of the systems and suggesting the use of amphiphilic species as promising rejuvenator thanks to their simultaneous presence, within their molecular architecture of both polar and apolar moieties which permits their simultaneous interactions with polar (asphaltene clusters), apolar (maltene) and amphiphilic (resins) species of the bitumen.
4. Scattering techniques and nuclear magnetic relaxometry have been presented as vanguard and promising techniques deserving attention for deeper analyses in bitumen. In fact, they can probe the effectiveness of a rejuvenator in restoring the microstructure of bitumen after the aging process, whereas, mechanical properties, on their own, are not enough for investigating this aspect. A clear introduction to the physics of the techniques and applications to the study of bitumen has been presented.

5. With this work, we would like to share with the reader our belief that the detailed analysis of the physics of bitumen at the molecular basis extends the information taken from the commonly used empirical and quick tools. This allows to better understand the phenomena taking place in bitumen furnishing new tools for the piloted design of new and ever-performing rejuvenators.
6. We wanted to furnish a novel viewpoint for the study of bitumen based on the concepts of the complex systems in physics. According to this approach, the final behavior of the material is not only dictated by specific interactions, as usually assumed in most of the research papers, but also by collective contributions of many molecules interacting and aggregating themselves usually at different length scales in hierarchical structures generating emerging properties. We hope that this study can constitute a novel approach for the investigation of bitumen, and the improvements of its performances.

Author Contributions: P.C. (Pietro Calandra) conceptualization methodology and writing, P.C. (Paolino Caputo) conceptualization; M.P. editing correction and writing, V.L. conceptualization and research, R.A. conceptualization, and C.O.R. conceptualization and supervision.

Funding: This research received no external funding.

Conflicts of Interest: The authors declare no conflict of interest.

References

1. Calandra, P.; Caputo, P.; De Santo, M.P.; Todaro, L.; Turco Liveri, V.; Oliviero Rossi, C. Effect of additives on the structural organization of asphaltene aggregates in bitumen. *Constr. Build. Mater.* **2019**, *199*, 288–297. [CrossRef]
2. Rozeveld, S.; Shin, E.; Bhurke, A.; France, L.; Drzal, L. Network morphology of straight and polymer modified asphalt cements. *Microsc. Res. Technol.* **1997**, *38*, 529–543. [CrossRef]
3. Lesueur, D. The colloidal structure of bitumen: Consequences on the rheology and on the mechanisms of bitumen modification. *Adv. Colloid Interface Sci.* **2009**, *145*, 42–82. [CrossRef] [PubMed]
4. Petersen, J.C. Chemical composition of asphalt as related to asphalt durability: State of the art Transport. *Transp. Res. Rec.* **1984**, *999*, 13–30.
5. Yu, X.; Zaumanis, M.; dos Santos, S.; Poulikakos, L.D. Rheological, microscopic, and chemical characterization of the rejuvenating effect on asphalt binders. *Fuel* **2014**, *135*, 162–171. [CrossRef]
6. Copeland, A. Reclaimed asphalt pavement in asphalt mixtures: State of the practice. In *Report No. FHWA-HRT-11-021*; Federal Highway Administratio: McLean, WV, USA, 2011.
7. Firoozifar, H.; Foroutan, S.; Foroutan, S. The effect of asphaltene on thermal properties of bitumen. *Chem. Eng. Res. Des.* **2011**, *89*, 2044–2048. [CrossRef]
8. Filippelli, L.; Gentile, L.; Oliviero Rossi, C.; Ranieri, G.A.; Antunes, F.E. Structural change of bitumen in the recycling process by using rheology and NMR. *Indus. Eng. Chem. Res.* **2012**, *51*, 16346–16353. [CrossRef]
9. Gentile, L.; Filippelli, L.; Oliviero Rossi, C.; Baldino, N.; Ranieri, G.A. Rheological and H-NMR spin–spin relaxation time for the evaluation of the effects of PPA addition on bitumen. *Mol. Cryst. Liq. Cryst.* **2012**, *558*, 54–63. [CrossRef]
10. Yoon, S.; Durgashanker Bhatt, S.; Lee, W.; Lee, H.Y.; Jeong, S.Y.; Baeg, J.O.; Wee Lee, C. Separation and characterization of bitumen from Athabasca oil sand. *Korean J. Chem. Eng.* **2009**, *26*, 64–71. [CrossRef]
11. Altgelt, K.H.; Boduszynski, M.M. Compositional Analysis: Dream and Reality. In *Composition and Analysis of Heavy Petroleum Fractions*; Marcel Dekker: New York, NY, USA, 1994; pp. 9–39.
12. Zenke, G. Zum Löseverhalten von "Asphaltenen": Anwendung von Löslichkeitsparameter-Konzepten auf Kolloidfraktionen Schwerer Erdöl Produkte. Ph.D. Thesis, Technical University of Clausthal, German State, Germany, 1989.
13. Hurley, G.C.; Prowell, B.D. Evaluation of potential processes for use in warm mix asphalt. *J. Assoc. Asph. Paving Technol.* **2006**, *75*, 41–90.
14. Silva, H.M.R.D.; Oliveira, J.R.M.; Ferreira, C.I.G.; Pereira, P.A.A. Assessment of the performance of warm mix asphalts in road pavements. *Int. J. Pavement Res. Technol.* **2010**, *3*, 119–127.

15. Hakseo, K.; Soon-Jae, L. Rheology of warm mix asphalt binders with aged binders. *Constr. Build. Mater.* **2011**, *25*, 183–189.
16. Jamshidia, A.; Hamzaha, M.O. Performance of warm mix asphalt containing Sasobit®: State of the art. *Constr. Build. Mater.* **2013**, *38*, 530–553. [CrossRef]
17. Yen, T.F.; Erdman, J.G.; Pollak, S.S. Investigation of the Structure of Petroleum Asphaltenes by X-Ray Diffraction. *Anal. Chem.* **1961**, *33*, 1587–1594. [CrossRef]
18. Jäger, A.; Lackner, R.; Eisenmenger-Sittner, C.; Blab, R. Identification of Microstructural components of bitumen by means of Atomic Force microscopy (AFM). *Proc. PAMM Appl. Math. Mech.* **2004**, *4*, 400–401. [CrossRef]
19. Handle, F.; Füssl, J.; Neudl, S.; Grossegger, D.; Eberhardsteiner, L.; Hofko, B.; Hospodka, M.; Blab, R.; Grothe, H. The bitumen microstructure: A fluorescent approach. *Mater. Struct.* **2016**, *49*, 167–180. [CrossRef]
20. Zhang, F.; Hu, C.; Zhang, Y. Influence of poly (phosphoric acid) on the properties and structure of ethylene-vinyl acetate-modified bitumen. *J. Appl. Polym. Sci.* **2018**, *135*, 46553. [CrossRef]
21. Xu, X.; Yu, J.; Xue, L.; Zhang, C.; He, B.; Wu, M. Structure and performance evaluation on aged SBS modified bitumen with bi- or tri- epoxy reactive rejuvenating system. *Constr. Build. Mater.* **2017**, *151*, 479–486. [CrossRef]
22. Tanaka, R.; Sato, E.; Hunt, J.E.; Winans, R.E.; Sato, S.; Takanohashi, T. Characterization of Asphaltene Aggregates Using X-ray Diffraction and Small-Angle X-ray Scattering. *Energy Fuels* **2004**, *18*, 1118–1125. [CrossRef]
23. Kuang, D.; Ye, Z.; Yang, L.; Iu, N.; Lu, Z.; Che, H. Effect of Rejuvenator Containing Dodecyl Benzene Sulfonic Acid (DBSA) on Physical Properties, Chemical Components, Colloidal Structure and Micro-Morphology of Aged Bitumen. *Materials* **2018**, *11*, 1476. [CrossRef]
24. Sharma, B.K.; Adhavaryu, A.; Liu, Z.; Erhan, S.Z. Chemical modification of vegetable oils for lubrificant application. *J. Am. Oil Chem. Soc.* **2006**, *83*, 129–136. [CrossRef]
25. Thyrion, F. Asphalt Oxidation. In *Asphaltenes and Asphalts: Development in Petroleum Science 2000*; Elsevier: New York, NY, USA, 2000; pp. 445–474.
26. Calandra, P.; Turco Liveri, V.; Caputo, P.; Teltayev, B.; Oliviero Rossi, C. Wide Angle X-Ray Scattering as a Technique of Choice to Probe Asphaltene Hierarchical structures. *J. Nanosci. Nanotechnol.*. in press.
27. Lu, I.; Isacsson, U. Influence of styrene-butadiene-styrene polymer modification on bitumen viscosity. *Fuel* **1997**, *76*, 1353–1359. [CrossRef]
28. Edwards, Y. Influence of Waxes on Bitumen and Asphalt Concrete Mixture Performance. *Road Mater. Pavement Des.* **2009**, *10*, 313–335. [CrossRef]
29. Senise, S.; Carrera, V.; Navarro, F.J.; Partal, P. Thermomechanical and microstructural evaluation of hybrid rubberised bitumen containing a thermoplastic polymer. *Constr. Build. Mater.* **2017**, *157*, 873–884. [CrossRef]
30. Oliviero Rossi, C.; Ashimova, S.; Calandra, P.; De Santo, M.P.; Angelico, R. Mechanical Resilience of Modified Bitumen at Different Cooling Rates: A Rheological and Atomic Force Microscopy Investigation. *Appl. Sci.* **2017**, *7*, 779. [CrossRef]
31. Remišová, E.; Holý, M. Changes of Properties of Bitumen Binders by Additives Application. *IOP Conf. Ser. Mater. Sci. Eng.* **2017**, *245*, 032003. [CrossRef]
32. Abdullin, A.I.; Idrisov, M.R.; Emelyanycheva, E. Improvement of thermal-oxidative stability of petroleum bitumen using "overoxidation-dilution" technology and introduction of antioxidant additives. *Pet. Sci. Technol.* **2017**, *35*, 1859–1865. [CrossRef]
33. Roberts, F.L.; Kandhal, P.S.; Brown, E.R.; Lee, D.Y.; Kennedy, T.W. *Hot Mix Asphalt Materials, Mixture Design and Construction*, 2nd ed.; NAPA: Lanham, MD, USA, 1996; p. 576.
34. Lee, C.; Terrel, R.; Mahoney, J. Test for Efficiency of Mixing of Recycled Asphalt Paving Mixtures. In *Proceedings of the Transportation Research Record 911*; TRB: Washington, DC, USA, 1983.
35. Carpenter, S.; Wolosick, J. Modifier Influence in the Characterization of Hot-Mix Recycled Material. In *Proceedings of Transportation Research Record 777*; TRB: Washington, DC, USA, 1980.
36. Noureldin, S.; Wood, L. Rejuvenator Diffusion in Binder Film for Hot-Mix Recycled Asphalt Pavement. In *Proceeding of Transportation Research Record 1115*; TRB: Washington, DC, USA, 1987.
37. Huang, B.; Li, G.; Vukosavljevic, D.; Shu, X.; Egan, B. Laboratory Investigation of Mixing Hot-Mix Asphalt with Reclaimed Asphalt Pavement. In *Proceedings of Transportation Research Record 1929*; TRB: Washington, DC, USA, 2005.

38. Karlsson, R.; Isacsson, U. Investigations on Bitumen Rejuvenator Diffusion and Structural Stability. *J. Assoc. Asph. Paving Technol.* **2003**, *72*, 463–501.
39. Oliver, J. *Diffusion of Oils in Asphalts*; Report No. 9; Proceedings of Australian Road Research Board: Vermont South, Victoria, Australia, 1975.
40. Yousefi, A.A. Rubber-Modified Bitumens. *Iran. Polym. J.* **2002**, *11*, 303–309.
41. Radenberg, M.; Boetcher, S.; Sedaghat, N. Effect and efficiency of rejuvenators on aged asphalt binder—German experiences. In Proceedings of the 6th Eurasphalt & Eurobitume Congress, Prague, Czech Republic, 1–3 June 2016.
42. Airey, G.D.; Brown, S.F. Rheological Performance of Aged Polymer Modified Bitumens. *J. Assoc. Asph. Paving Technol.* **1998**, *67*, 66–100.
43. Barbosa, L.L.; Kock, F.V.C.; Silva, R.C.; Freitas, J.C.C.; Lacerda Jr, V.; Castro, E.V.R. Application of low-field NMR for the determination of physical properties of petroleum fractions. *Energy Fuels* **2013**, *27*, 673–679. [CrossRef]
44. Oliviero Rossi, C.; Caputo, P.; De Luca, G.; Maiuolo, L.; Eskandarsefat, S.; Sangiorgi, C. ^{1}H-NMR Spectroscopy: A Possible Approach to Advanced Bitumen Characterization for Industrial and Paving Applications. *Appl. Sci.* **2018**, *8*, 229. [CrossRef]
45. Caputo, P.; Loise, V.; Crispini, A.; Sangiorgi, C.; Scarpelli, F.; Oliviero Rossi, C. The efficiency of bitumen rejuvenator investigated through Powder X-ray Diffraction (PXRD) analysis and T_2 -NMR spectroscopy. *Colloids Surf. A Physicochem. Eng. Esp.* **2019**, *571*, 50–54. [CrossRef]
46. Osman, K.S.; Taylor, S.E. Insight into Liquid Interactions with Fibrous Absorbent Filter Media Using Low-Field NMR Relaxometry. Prospective Application to Water/Jet Fuel Filter−Coalescence. *Ind. Eng. Chem. Res.* **2017**, *56*, 14651–14661. [CrossRef]
47. Bocci, E.; Grilli, A.; Bocci, M.; Gomes, V. Recycling of high percentage of reclaimed asphalt using bio-rejuvenator—A case study. In Proceedings of the 6th Eurasphalt & Eurobitume Congress, Prague, Czech Republic, 1–3 June 2016.
48. Tine, T.; Lemoine, G.; Nösler, I.; Kloet, B. Influence of rejuvenating additives on recycled asphalt (RAP) properties. In Proceedings of the 5th Eurasphalt & Eurobitume Congress, Istanbul, Turkey, 13–15 June 2012.
49. Król, J.B.; Kowalski, K.J.; Niczke, L.; Radziszewski, P. Effect of bitumen fluxing using a bio-origin additive. *Constr. Build. Mater.* **2016**, *114*, 194–203. [CrossRef]
50. Somé, C.; Pavoine, A.; Chailleux, E.; Andrieux, L.; DeMArco, L.; Philippe Da, S.; Stephan, B. Rheological behaviour of vegetable oil-modified asphaltite binders and mixes. In Proceedings of the 6th Eurasphalt & Eurobitume Congress, Prague, Czech Republic, 1–3 June 2016.
51. Caputo, P.; Porto, M.; Calandra, P.; De Santo, M.P.; Oliviero Rossi, C. Effect of epoxidized soybean oil on mechanical properties of bitumen and aged bitumen. *Mol. Cryst. Liq. Cryst.* **2018**, *675*, 68–74. [CrossRef]
52. Zargar, M.; Ahmadinia, E.; Asli, H.; Karim, M.R. Investigation of the possibility of using waste cooking oil as a rejuvenating agent for aged bitumen. *J. Hazard. Mater.* **2012**, *233*, 254–258. [CrossRef]
53. Nayak, P.; Sahoo, U.C. Rheological, chemical and thermal investigations on an aged binder rejuvenated with two nonedible oils. *Road Mater. Pavement Des.* **2016**, *18*, 612–629. [CrossRef]
54. De la Roche, C.; Van de Ven, M.; Van den bergh, W.; Gabet, T.; Dubois, V.; Grenfell, J.; Porot, L. Development of a laboratory bituminous mixtures ageing protocol. In *Advanced Testing and Characterization of Bituminous Materials*, 1st ed.; Loizos, A., Partl, M.N., Scarpas, T., Al-Qadi, I.L., Eds.; CRC Press: AK Leiden, The Netherlands, 2009; Volume 1, pp. 331–345.
55. Lamontagne, J.; Dumas, P.; Mouillet, V.; Kister, J. Comparison by Fourier transform infrared (FTIR) spectroscopy of different ageing techniques: Application to road bitumens. *Fuel* **2001**, *80*, 483–488. [CrossRef]
56. Elkashef, M.; Williams, R.C.; Cochran, E. Thermal stability and evolved gas analysis of rejuvenated reclaimed asphalt pavement (RAP) bitumen using thermogravimetric analysis–Fourier transform infrared (TG–FTIR). *J. Anal. Calorim.* **2018**, *131*, 865–871. [CrossRef]
57. Cavalli, M.C.; Zaumanis, M.; Mazza, M.; Partl, M.N.; Poulikakos, L.D. Effect of ageing on the mechanical and chemical properties of binder from RAP treated with bio-based rejuvenators. *Compos. Part B Eng.* **2018**, *141*, 174–181. [CrossRef]
58. Marsac, P.; Piérard, N.; Porot, L.; Van den bergh, W.; Grenfell, J.; Mouillet, V.; Pouget, S.; Besamusca, J.; Farcas, F.; Gabet, T.; et al. Potential and limits of FTIR methods for reclaimed asphalt characterisation. *Mater. Struct.* **2014**, *47*, 1273–1286. [CrossRef]

59. Elkashef, M.; Podolsky, J.; Williams, R.C.; Cochran, E.W. Introducing a soybean oil-derived material as a potential rejuvenator of asphalt through rheology, mix characterisation and Fourier Transform Infrared analysis. *Road Mater. Pavement Des.* **2017**, *19*, 1750–1770. [CrossRef]
60. Zhu, H.; Xu, G.; Gong, M.; Yang, J. Recycling long-term-aged asphalts using bio-binder/plasticizer-based rejuvenator. *Constr. Build. Mater.* **2017**, *147*, 117–129. [CrossRef]
61. Elkashef, M.; Williams, R.C.; Cochran, E.W. Physical and chemical characterization of rejuvenated reclaimed asphalt pavement (RAP) binders using rheology testing and pyrolysis gas chromatography-mass spectrometry. *Mater. Struct.* **2018**, *51*, 12. [CrossRef]
62. Mokhtari, A.; Lee, H.D.; Williams, R.C.; Guymon, C.A.; Scholte, J.P.; Schram, S. A novel approach to evaluate fracture surfaces of aged and rejuvenator-restored asphalt using cryo-SEM and image analysis techniques. *Constr. Build. Mater.* **2017**, *133*, 301–313. [CrossRef]
63. Nahar, S.; Qiu, J.; Schmets, A.; Schlangen, E.; Shirazi, M.; van de Ven, M.; Schitter, G.; Scarpas, A. Turning Back Time: Rheological and Microstructural Assessment of Rejuvenated Bitumen. In Proceedings of the 93th Annual Meeting of the Transportation Research Board, Washington, DC, USA, 12–16 January 2014.
64. Kuang, D.; Yu, J.; Chen, H.; Feng, Z.; Li, R.; Yang, H. Effect of Rejuvenators on Performance and Microstructure of Aged Asphalt. *J. Wuhan Univ. Technol.* **2014**, *29*, 341–345. [CrossRef]
65. Sharma, B.K.; Doll, K.M.; Erhan, S.Z. Ester hydroxyl derivatives of methyl oleate. Tribological, oxidation and low temperature properties. *Bioresour. Technol.* **2008**, *99*, 7333–7340. [CrossRef]
66. King, J.W.; Holliday, R.L.; List, G.R.; Snyder, J.M. Hydrogenation of vegetable oils using mixture of supercritical carbon dioxide and hydrogen. *J. Am. Oil Chem. Soc.* **2001**, *78*, 107–113. [CrossRef]
67. Campanella, A.; Baltanas, M.A.; Capel-Sanchez, M.C.; Campos-Martin, J.M.; Fierro, J.L.G. Soybean oil epoxidation with hydrogen peroxide using an amorphous Ti/SiO2 catalyst. *Green Chem.* **2004**, *6*, 330–334. [CrossRef]
68. Xiang, S.; Chen, L.; Yang, X.; Zhang, P.; Zhu, L. Physiochemical and Tribological Properties of Triester Derivatives from Chemically Modified Waste Cooking Oil. *Biotechnology* **2015**, *141*, 1–8.
69. Maiuolo, L.; De Nino, A.; Merino, P.; Russo, B.; Stabile, G.; Nardi, M.; D'Agostino, N.; Bernardi, T. Rapid, efficient and solvent free microwave mediated synthesis of aldo- and ketonitrones. *Arab. J. Chem.* **2016**, *9*, 25–31. [CrossRef]
70. Bortolini, O.; Mulani, I.; De Nino, A.; Maiuolo, L.; Melicchio, A.; Russo, B.; Granchi, D. Synthesis of a novel class of gem-phosphonate-phosphates by reductive cleavage of the isoxazolidine ring. *Curr. Org. Synth.* **2014**, *11*, 461–465. [CrossRef]
71. Nardi, M.; Costanzo, P.; De Nino, A.; Di Gioia, M.L.; Olivito, F.; Sindona, G.; Procopio, A. Water excellent solvent for the synthesis of bifunctionalized cyclopentenones from furfural. *Green Chem.* **2017**, *19*, 5403–5411. [CrossRef]
72. Di Gioia, M.L.; Nardi, M.; Costanzo, P.; De Nino, A.; Maiuolo, L.; Oliverio, M.; Procopio, A. Biorenewable deep eutectic solvent for selective and scalable conversion of furfural into cyclopentenone derivatives. *Molecules* **2018**, *23*, 1891. [CrossRef] [PubMed]
73. Procopio, A.; Costanzo, P.; Dalpozzo, R.; Maiuolo, L.; Nardi, M.; Oliverio, M. Efficient ring opening of epoxides with trimethylsilyl azide and cyanide catalyzed by erbium(III) triflate. *Tetrahedron Lett.* **2010**, *51*, 5150–5153. [CrossRef]
74. Bortolini, O.; De Nino, A.; Garofalo, A.; Maiuolo, L.; Russo, B. Mild oxidative conversion of nitroalkanes into carbonyl compounds in ionic liquids. *Synth. Commun.* **2010**, *40*, 2483–2487. [CrossRef]
75. Nardi, M.; Di Gioia, M.L.; Costanzo, P.; De Nino, A.; Maiuolo, L.; Oliverio, M.; Olivito, F.; Procopio, A. Selective Acetylation of Small Biomolecules and Their Derivatives Catalyzed by Er(OTf)3. *Catalysts* **2017**, *7*, 269. [CrossRef]
76. Avisha, C.; Debarati, M.; Dipa, B. Biolubricant synthesis from waste cooking oil via enzymatic hydrolysis followed by chemical esterification. *J. Chem. Technol. Biotechnol.* **2013**, *88*, 139–144.
77. Okino-Delgad, C.H.; Zanoni do Prado, D.; Facanali, R.; Marques, M.M.O.; Nascimento, A.S.; da Costa Fernandes, C.J.; Zambuzzi, W.F.; Fleuri, L.F. Bioremediation of cooking oil waste using lipases from wastes. *PLoS ONE* **2017**, *12*, 1–17. [CrossRef] [PubMed]
78. Atkins, P.W.; de Paula, J.; Keeler, J. *Physical Chemistry*, 14th ed.; Oxford Press: Oxford, UK, 2011.
79. De Giorgio, V.; Corti, M. *Physics of Amphiphiles: Micelles*; Vesicles and Microemulsions: North-Holland, The Netherlands, 1985.

80. Lombardo, D.; Kiselev, M.A.; Magazù, S.; Calandra, P. Amphiphiles Self-Assembly: Basic Concepts and Future Perspectives of Supramolecular Approaches. *Adv. Condens. Matter Phys.* **2015**, *11*, 1–22. [CrossRef]
81. Calandra, P.; Longo, A.; Ruggirello, A.; Turco Liveri, V. Physico-Chemical Investigation of the State of Cyanamide Confined in AOT and Lecithin Reversed Micelles. *J. Phys. Chem. B* **2004**, *108*, 8260–8268. [CrossRef]
82. Calandra, P.; Giordano, C.; Ruggirello, A.; Turco Liveri, V. Physicochemical investigation of acrylamide solubilization in sodium bis(2-ethylhexyl)sulfosuccinate and lecithin reversed micelles. *J. Colloid Interface Sci.* **2004**, *277*, 206–214. [CrossRef]
83. Longo, A.; Calandra, P.; Casaletto, M.P.; Giordano, C.; Venezia, A.; Turco Liveri, V. Synthesis and physico-chemical characterization of gold nanoparticles softly coated by AOT. *Mater. Chem. Phys.* **2006**, *96*, 66–72. [CrossRef]
84. Calandra, P.; Giordano, C.; Longo, A.; Turco Liveri, V. Physicochemical investigation of surfactant-coated gold nanoparticles synthesized in the confined space of dry reversed micelles. *Mater. Chem. Phys.* **2006**, *98*, 494–499. [CrossRef]
85. Calandra, P.; Di Marco, G.; Ruggirello, A.; Turco Liveri, V. Physico-chemical investigation of nanostructures in liquid phases: Nickel chloride ionic clusters confined in sodium bis(2-ethylhexyl) sulfosuccinate reverse micelles. *J. Colloid Interface Sci.* **2009**, *336*, 176–182. [CrossRef]
86. Kakar, M.R.; Hamzah, M.O.; Akhtar, M.N. Surface free energy and moisture susceptibility evaluation of asphalt binders modified with surfactant-based chemical additive. *J. Clean. Prod.* **2016**, *112*, 2342–2353. [CrossRef]
87. Ortega, F.J.; Navarro, F.J.; García-Morales, M. Dodecylbenzenesulfonic Acid as a Bitumen Modifier: A Novel Approach to Enhance Rheological Properties of Bitumen. *Energy Fuels* **2017**, *31*, 5003–5010. [CrossRef]
88. Glatter, O.; Kratky, O. *Small-Angle X-ray Scattering*; Academic Press: London, UK, 1982.
89. Shirzad, S.; Hassan, M.M.; Aguirre, M.A.; Mohammad, L.N. Evaluation of Sunflower Oil as a Rejuvenator and Its Microencapsulation as a Healing Agent. *J. Mater. Civ. Eng.* **2016**, *28*. [CrossRef]
90. Fitter, J.; Gutberlet, T.; Katsaras, J. *Neutron Scattering in Biology Techniques and Applications*; Springer: Berlin, Germany, 2006; p. 560.
91. Zemb, T.; Lindner, P. *Neutron, X-rays and Light Scattering Methods Applied to Soft Condensed Matter*, 1st ed.; North-Holland (publisher): Amsterdam, The Netherlands, 2002; p. 552.
92. Feigin, L.A.; Svergun, D.I. *Structure Analysis by Small-Angle X-Ray and Neutron Scattering*, 1st ed.; Plenum Press: New York, NY, USA; London, UK, 1987; p. 335.
93. Magazù, S.; Migliardo, F.; Benedetto, A. Elastic incoherent neutron scattering operating by varying instrumental energy resolution: Principle, simulations, and experiments of the resolution elastic neutron scattering (RENS). *Rev. Sci. Instrum.* **2011**, *82*, 105115. [CrossRef] [PubMed]
94. Berne, B.J.; Pecora, R. *Dynamic Light Scattering*, 1st ed.; Wiley-Interscience: New York, NY, USA, 1976; p. 376.
95. Brown, W. *Light Scattering: Principles and Development*, 1st ed.; Clarendon: Oxford, UK, 1996; p. 544.
96. Nagana Gowda, G.A.; Chen, H.; Khetrapal, C.L.; Weiss, R.G. Amphotropic ionic liquid crystals with low order parameters. *Chem. Mater.* **2004**, *16*, 2101–2106. [CrossRef]
97. Calandra, P.; Ruggirello, A.; Mele, A.; Turco Liveri, V. Self-assembly in surfactant-based liquid mixtures: Bis(2-ethylhexyl)phosphoric acid/bis(2-ethylhexyl)amine systems. *J. Colloid Interface Sci.* **2010**, *348*, 183–188. [CrossRef] [PubMed]
98. Kumar, A.; Kuneida, H.; Vazquez, C.; Lopez-Quintela, M.A. Studies of domain size of hexagonal liquid crystals in C 12 EO 8 /water/alcohol systems. *Langmuir* **2001**, *17*, 7245–7250. [CrossRef]
99. Calandra, P.; Turco Liveri, V.; Ruggirello, A.; Licciardi, M.; Lombardo, D.; Mandanici, A. Anti-Arrhenian behaviour of conductivity in octanoic acid–bis(2-ethylhexyl)amine systems: A physico-chemical study. *J. Mater. Chem. C* **2015**, *3*, 3198–3210. [CrossRef]
100. Calandra, P.; Turco Liveri, V.; Riello, P.; Freris, I.; Mandanici, A. Self-assembly in surfactant-based liquid mixtures: Octanoic acid/Bis(2-ethylhexyl)amine systems. *J. Colloid Interface Sci.* **2012**, *367*, 280–285. [CrossRef]
101. Turco Liveri, V.; Lombardo, D.; Pochylski, M.; Calandra, P. Molecular association of small amphiphiles: Origin of ionic liquid properties in dibutyl phosphate/propylamine binary mixtures. *J. Mol. Liq.* **2018**, *263*, 274–281. [CrossRef]
102. Dickie, J.P.; Yen, T.F. Macrostructures of the Asphaltic Fractions by Various Instrumental Methods. *Anal. Chem.* **1967**, *39*, 1847–1852. [CrossRef]

103. Calandra, P.; Mandanici, A.; Turco Liveri, V. Self-assembly in surfactant-based mixtures driven by acid–base reactions: Bis(2-ethylhexyl) phosphoric acid–n-octylamine systems. *RSC Adv.* **2013**, *3*, 5148–5155. [CrossRef]
104. Calandra, P.; de Caro, T.; Caschera, D.; Lombardo, D.; Todaro, L.; Turco Liveri, V. Spectroscopic and structural characterization of pure and $FeCl_3$-containing tri-n-butyl phosphate. *Colloid Polym. Sci.* **2014**, *293*, 597–603. [CrossRef]
105. Cui, S.; de Almeida, V.F.; Hay, B.P.; Ye, X.; Khomami, B. Molecular dynamics simulation of Tri-n-butyl-phosphate liquid: A force field comparative study. *J. Phys. Chem. B* **2012**, *116*, 305–313. [CrossRef] [PubMed]
106. Charlesby, A.; Finch, G.I.; Wilman, H. The diffraction of electrons by anthracene. *Proc. Phys. Soc.* **1939**, *51*, 479–528. [CrossRef]
107. Bale, H.D.; Schmidt, P.W. Small-Angle X-Ray-Scattering Investigation of Submicroscopic Porosity with Fractal Properties. *Phys. Rev. Lett.* **1984**, *53*, 596–599. [CrossRef]
108. Carr, H.Y.; Purcell, E.M. Effects of Diffusion on Free Precession in Nuclear Magnetic Resonance Experiments. *Phys. Rev.* **1954**, *94*, 630. [CrossRef]
109. Oliviero Rossi, C.; Spadafora, A.; Teltayev, B.; Izmailova, G.; Amerbayev, Y.; Bortolotti, V. Polymer modified bitumen: Rheological properties and structural characterization. *Coll. Surf. A* **2015**, *480*, 390–397. [CrossRef]
110. Christensen, D.W.; Anderson, D.A. Rheological evidence concerning the molecular architecture of asphalt cements. *Proc. Chem. Bitum.* **1991**, *2*, 568–595.
111. Oliviero Rossi, C.; Caputo, P.; Loise, V.; Ashimova, S.; Teltayev, T.; Sangiorgi, C. A New Green Rejuvenator: Evaluation of Structural Changes of Aged and Recycled Bitumens by Means of Rheology and NMR. In *RILEM 252-CMB Symposium*; RILEM 252-CMB 2018; Poulikakos, L., Cannone Falchetto, A., Wistuba, M., Hofko, B., Porot, L., Di Benedetto, H., Eds.; Springer: Cham, Switzerland, 2018; Volume 20.

Chapter 6

The efficiency of bitumen rejuvenator investigated through Powder X-ray Diffraction (PXRD) analysis and T_2-NMR spectroscopy

Colloids and Surface A 2019, 571; doi:10.1016/j.colsufra.2019.03.059

Colloids and Surfaces A 571 (2019) 50–54

Contents lists available at ScienceDirect

Colloids and Surfaces A

journal homepage: www.elsevier.com/locate/colsurfa

The efficiency of bitumen rejuvenator investigated through Powder X-ray Diffraction (PXRD) analysis and T_2-NMR spectroscopy

Paolino Caputo[a], Valeria Loise[a,*], Alessandra Crispini[a], Cesare Sangiorgi[b], Francesca Scarpelli[a,*], Cesare Oliviero Rossi[a]

[a] Department of Chemistry and Chemical Technologies, University of Calabria, Via P. Bucci, Rende, CS, 87036, Italy
[b] DICAM-Roads, Dept. of Civil, Chemical, Environmental and Materials Engineering, University of Bologna, V. le Risorgimento 2, 40136, Bologna, Italy

GRAPHICAL ABSTRACT

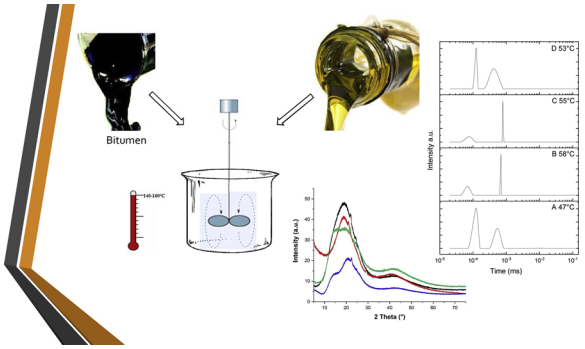

ARTICLE INFO

Keywords:
Rejuvenating agent
Biocompatible additive
Chemical structure
Powder X-ray diffraction (PXRD)
Nuclear Magnetic Spectroscopy (NMR)

ABSTRACT

Nowadays, many different materials are known to function, using different test methods, as rejuvenating agent when introduced into recycled asphalt pavements. However, it should be noticed that, an additive, which has a complete rejuvenating function, enables the chemical structure reorganization of the aged bitumen, otherwise not achieved by traditional methods. This rearrangement brings back the aged bitumen structure to the condition of the original one, restoring the elasticity and workability of the binder. In this study, two non-toxic and eco-friendly biocompatible additives have been tested to work as rejuvenators on an aged bitumen binder by means of Powder X-Ray Diffraction (PXRD) measurements and Nuclear Magnetic Spectroscopy (NMR). Powder X-ray diffraction (PXRD) analysis has been proved to be a very useful technique for assessing the structure of virgin, aged, and rejuvenating agent-added bitumen and for figuring out the chemical action of the additive in bitumen. All the test results were also supported by T2-NMR spectroscopy, which proves the validity of this method in chemical analysis.

1. Introduction

One of the principal factors that leads to the deterioration of asphalt pavements is the aging process during storage, mixing, transport and laying down, as well as in service life effect of aging on bitumen chemistry and rheology [1]. This phenomenon decreases the properties of asphalt pavements such as low-temperature cracking and shortens the lifespan of a pavement. In other words, the result of the processes is

* Corresponding authors.
E-mail addresses: valeria.loise@unical.it (V. Loise), francesca.scarpelli@unical.it (F. Scarpelli).

https://doi.org/10.1016/j.colsurfa.2019.03.059
Received 23 January 2019; Received in revised form 15 March 2019; Accepted 18 March 2019
Available online 21 March 2019
0927-7757/

an embrittlement of the asphalt which inevitably leads to phenomena of cracking and fracturing. From a rheological point of view, throughout the aging, the softening point temperature of bitumen increases. Consequently, pavement replacement is always required after a certain time of use.

The mechanism of bitumen aging is related to oxidation processes, which are extremely complex and still not completely clear. It has been shown that, during aging, ketones and carboxylic acids could be formed, as well as the formation of sulfoxides. Basically, there is an increase in the content of resins and asphaltenes [2,3]. This fact produces a decrease in molecular mobility, so that the molecules can no longer flow over one another and the system becomes harder (phenomena of cracking and fracturing can occur) [4–6].

Considering the principles of sustainability, Reclaimed Asphalt Pavement (RAP) has started to be increasingly used in the asphalt pavement industry, indeed containing valuable bitumen binder and therefore cannot any more be considered as a waste material [7]. Apparently, aged RAP asphalt binder has a lower penetration and is more viscous than the virgin one. Normally, the regeneration of bitumen is made by adding new binder, softer than those typically used to produce hot mixtures, or vegetable-based oils [8]. In the latter case, the real action appears not to be the one of a proper rejuvenating agent. Indeed, sometimes vegetable oils just soften bitumen, making it appear to match the mechanical parameters needed for engineering parameters [9].

Since oxidation increases the fragility and consequently decreases fatigue resistance, empirical parameters such as penetration and the softening point or viscosity are not enough to guarantee the real regeneration of the aged bitumen. For this reason, a complete rejuvenating product should be able to restore the original ratio of asphaltenes to maltenes, as well as reduce the rigidity of the aged bitumen. In this way, the rejuvenator can restore the aged binder properties to their original state. Hence, the choice of correct rejuvenator plays a key role in bitumen recycling, encouraging the reuse of the aged bitumen and RAP by enhancing the recycled asphalt concrete properties.

The present paper describes the structural characterization mainly based on a powder X-ray diffraction (PXRD) technique of a new class of restored bitumen containing a sustainable rejuvenator (HR) based on oleic acid, developed by the academic Spin-Off (Kimical SRL) of the University of Calabria. In particular, the aim of the paper is the comprehension of the physical-chemical interactions between the regenerating HR product, compared with normal vegetable oil and aged bitumen by means of powder X-ray diffraction analysis. Following the changes of the main diffraction peaks in the PXRD patterns observed before and after treating aged bitumen with the HR rejuvenator, it is possible to follow the restoring, if any, of the virgin asphalt properties. This technique can be considered as a powerful tool to characterize the microstructure organization of aged asphalt before and after the introduction of a rejuvenator [10,11]. Moreover, the PXRD analysis results are confirmed through NMR relaxometry. Typically, the checking of the relaxation time distributions of the aged bitumen after the addition of additives, is to be considered as the fingerprint of the system with or without shear [12,3,13,14].

2. Materials and methods

A 50/70 penetration grade bitumen (from a Venezuelan source) and two additives, a vegetable Flux Oil (OA) and an oleic acid-based rejuvenator (HR), were investigated in this research work. The vegetable Flux Oil (OA) was furnished by Baldini SRL and the HR rejuvenator was developed by the academic Spin-Off (Kimical SRL) operating at the University of Calabria, Italy. The rejuvenator is commercially named as HR Kimical, and all the technical information can be obtained from Kimical SRL Company. It is a reaction product between fatty acids and ammines

Table 1
Test materials and ID.

Bitumen	Additive and quantity	Sample ID
Base Bitumen	–	A
RTFOT Bitumen	–	B
RTFOT Bitumen	2% OA	C
RTFOT Bitumen	2% HR	D

2.1. Sample preparation and aging

Considering the targets of this study, the aged bitumen was blended with 2% (on the weight of bitumen) of the additives. For this purpose, in the first stage, the bitumen was aged by means of Rolling Thin Film Oven Test following (RTFOT) ASTM D2872 but with different time duration. It should be noted that RTFOT runs of 225 min, instead of 85 min were chosen, since they are based on the authors' previous research works [3,13], the approach was found suitable for simulating the chemical structure of the aged bitumen. The aged bitumen was then heated up to 150 ± 5°C and the testing rejuvenator was added. Then afterwards, the blends were mixed by a high-speed shear mixer at 400–600 rpm/min for 10 min. The provided blends were then poured into a small sealed can and were stored in a dark thermostatic chamber at 25°C in order to retain the obtained morphology. Table 1 represents the test materials and applied ID.

2.2. Bitumen characterization

The *penetration and softening point* (Ring and Ball) test methods were done following EN 1416 and 1427 European test methods respectively.

2.2.1. Asphaltene determination

The asphaltene fraction of the bitumen blends were extracted following the conventional method. For this purpose, in a vessel, an amount of bitumen in grams was carefully mixed and dissolved in $CHCl_3$ (e.g. 3 g of bitumen for 3 mL of $CHCl_3$). Then, n-pentane, forty times to the $CHCl_3$ was added to the solution. The compound was then kept in the dark and mixed occasionally. In the next stage, the precipitated asphaltenes were filtered in a funnel with paper filter by a vacuum (Whatman 42 ashless). The residue was washed several times with n-pentane until the solvent became colourless. The filter paper was dried in an oven at 80°C for three hours and consecutively the residue of the solvent was removed in a vacuum for two hours.

2.3. PXRD analysis

Powder X-Ray Diffraction (PXRD) patterns were acquired on a Bruker D2-Phaser equipped with a Cu Kα radiation (λ = 1.5418 Å) and a Lynxeye detector, at 30 kV and 10 mA, with step size of 0.01° and step time of 3 s, over an angular range of 5–75° 2θ. The obtained powder patterns were analysed with DIFFRAC.EVA diffraction software. Furthermore, in order to determine the area under the peaks, the peaks FWHM (full-width at half-maximum) and the backgrounds, the curves were deconvoluted by applying Voigt fitting procedure using Origin software. The residual error of the fit was calculated for each curve by mean of standard deviation (σ) and estimated within the range of 2–4%.

The interplanar distances (d) were calculated according to the Bragg equation:

$$n\lambda = 2d \sin\theta \quad (1)$$

The aromaticity (f_a), Eq. 4 and the crystallite parameters (the average diameter of the aromatic clusters perpendicular to the plane of the sheets, L_c, and the average diameter of the aromatic sheets, L_a) were estimated using the method proposed by Yen et al. [15].

$$f_a = A_{(002)}/(A_{(002)} + A_\gamma) \quad (2)$$

where:

$A_{(002)}$ represents the area under the (002) band (graphene band) and A_γ is the area under the γ-band.

The average thickness of the aromatic clusters (L_c) and the average diameter of the aromatic sheets (L_a) were determined using the Scherrer equation shown in Eq. 5

$$L_x = K_x \lambda / FWHM \cos\theta \quad (3)$$

Where:

λ is the X-Ray wavelength, θ is the Bragg angle of the reflection peak ((002)-band for L_c, (10)-band for La) and K_x is the shape factor (0.9 for the c-axis and 1.84 for the a-axis) [16].

Finally, the number of the aromatic sheets in a cluster was calculated using Eq. 6:

$$M = (L_c/dm) + 1 \quad (4)$$

Where:

L_c is the average thickness of the aromatic clusters and d_m is the d value of the (002)-band.

2.4. NMR relaxometry measurement and inverse laplace transform (ILT)

The Low Frequency NMR relaxation measurements were performed on a home-built NMR instrument with a resonance frequency of 15 MHz for protons. Measurements were performed at 5 °C lower than softening point temperatures of the blends, after a temperature conditioning time, required for equilibrium status. Transverse relaxation, T_2, was measured using the Carr-Purcell Meiboom-Gill sequence (CPMG), Eq. 1.

$$90^\circ_x - [\,| - (180^\circ_y - 2|)_k - 180^\circ_y - |- acq]_n \quad (5)$$

A CPMG sequence with an interpulse time of 160 μs provided the T_2 decay signal. The CPMG signals were made up of 400 echoes, with 128 averages, which provided a signal-to-noise level of circa 500 [17].

To study continuous distribution of relaxation time inside the sample, distributed exponential fitting analysis was performed using the UPEN algorithm, a widely applied method to analyse NMR data. This is a general-purpose program for inverting noisy linear algebraic and integral equations by means of the inverse Laplace transform, such as:

$$y(t_k) = \int_a^b G(t_k, \tau)s(\tau)d\tau + \beta_i \quad (6)$$

Where:

s(τ) is the unknown function to be solved;

y(tk) is the known function or the measurable relationship;

G (τ, tk) is a known kernel function depending on the physical meaning of the specific question;

and βi is a constant term. This analysis gives a plot $P(T_2)$ of relaxation amplitude for individual relaxation processes versus relaxation time.

3. Results and discussion

3.1. Penetration and softening point

The primary method for bitumen classification in the European standardisation framework is the physical/fundamental characterization of bitumen including penetration, softening point and asphaltene fraction. In this paper, these test methods are applied to assess the capability of the proposed rejuvenator in recovering the physical properties of aged bitumen.

The test results are shown in Table 2.

According to the results shown in Table 2, it can be seen that as expected, aging the bitumen resulted in an increase in the asphaltene fraction and softening point, while a decrease in penetration degree is obtained. Both tested additives decreased the asphaltene concentration of the blend and softened the material binder. It is noteworthy that the values obtained for the blends containing different additives, are found to be similar, proving that, by using these methodologies it is not possible to distinguish between real rejuvenator and a softener flux agent.

Table 2
Penetration, Softening point and Asphaltene fraction of sample A, B, C and D.

Sample	Penetration (mm) ± 1	Softening point (°C) ± 1	Asphaltene content in % (By the weight of test sample) ± 0.5
A	58	52	27.3
B	16	63	39.8
C	25	60	34.5
D	23	58	35.8

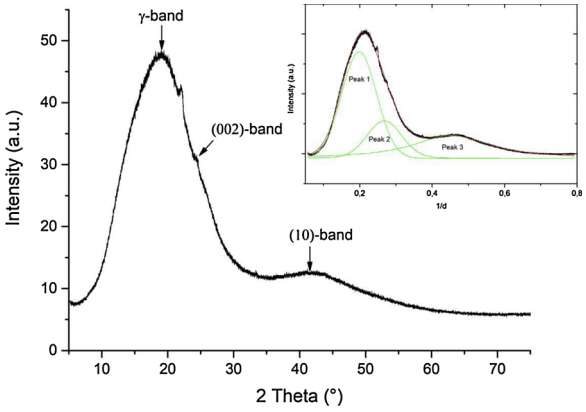

Fig. 1. XRD profile of neat (unaged) bitumen sample. Inset: deconvolution curves (green lines; peaks 1 and 2: predominant Gaussian character; peak 3: predominant Lorentzian character) and cumulative fit curve (red line) of Sample A XRD profile (For interpretation of the references to colour in this figure legend, the reader is referred to the web version of this article).

3.2. Powder X-Ray diffraction (PXRD)

The PXRD pattern of the neat (unaged) bitumen, together with its deconvolution curves, is reported in Fig. 1. It can be seen that the pattern shows a pronounced band approximately at 19° of 2θ (d_γ of 4.6 Å *ca.*), known as gamma (γ) band, superimposed to a peak centred at 2θ = 24° (d_m = 3.6 Å), commonly referred to as graphene (002) band and a weak band at 2θ of 42° *ca.*(*d* of 2.1 Å *ca.*), known as the (10) band. As already reported, while the γ-band arises from the packing distance of aliphatic chains or layers of condensed saturated rings, the graphene-band originates from the stacking of aromatic molecules [18,19] and the (10) band is due to the in-plane structure of the aromatic rings. Moreover, the PXRD pattern of the neat bitumen shows another reflection peak centred at 2θ of 22°*ca.* (*d* of 4.0 Å *ca.*), which according to the literature [19] can be reasonably assigned to a paraffinic order.

In order to investigate the changes in the aged bitumen microstructure before and after the addition of rejuvenating additives (OA and HR), PXRD patterns were recorded from samples B, C and D, and the obtained patterns were compared to the one obtained from the neat (unaged) bitumen sample, (sample A). Fig. 2, shows the diffractograms of the four samples and in Table 3 the related crystallite parameters are reported.

The PXRD pattern of the aged bitumen exhibits important differences with respect to that of the pristine bitumen sample (Fig. 2). The most important change occurs in the γ-band, which is shifted to a higher angle value, corresponding to a smaller *d* value (4.292 Å)

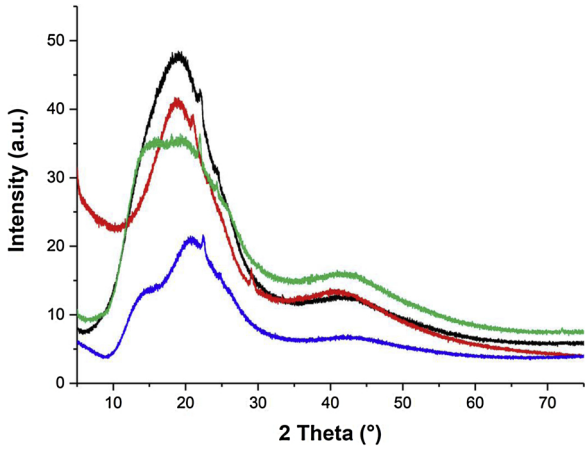

Fig. 2. XRD pattern of neat bitumen (black, sample A), aged bitumen (blue, sample B), aged bitumen containing OA (green, sample C), and age bitumen containing HR (red, sample D) (For interpretation of the references to colour in this figure legend, the reader is referred to the web version of this article).

Table 3
Crystallite and aromaticity parameters of tested blends.

Sample	d_γ(Å)	d_m (Å)	f_a	L_a (Å)	L_c (Å)	M
A (base bitumen)	4.670	3.657	0.256	11.95	12.6	4.4
B (RTFOT bitumen)	4.292	3.594	0.423	15.07	14.43	5.0
C (RTFOT bitumen + 2 wt% OA)	4.423	3.663	0.456	13.95	13.58	4.7
D (RTFOT bitumen + 2 wt% HR)	4.700	3.823	0.213	13.43	14.9	4.9

(Table 3), and splits into two broad reflections. The appearance of a new band indicates a new arrangement of molecules in a more organized structure. A more drastic change on the PXRD profile of aged bitumen has been recently reported by Fini et al. [10]. In this case, it is most probably due to oxidation processes on the specific type of bitumen used, the new reflection at low angle, appearing in the PXRD pattern of the aged sample at 2θ of 9.7°, has been attributed to the formation of graphene oxide (GO)-like molecular structure. Moreover, the (002)-band in the PXRD pattern of Sample B (Fig. 2) exhibits the same shift observed as for the γ-band; indeed, the (002)-band occurs at 3.657 Å for the fresh bitumen sample and at 3.594 Å in the aged bitumen sample.

These experimental data indicates that, after bitumen aging, the aliphatic chains and the aromatic rings of the asphaltene molecules become closer and more condensed. Furthermore, the increase in the calculated aromaticity parameter f_a, with respect to the fresh bitumen, can be explained in part considering the partial loss of the maltene fraction during the aging process, with subsequent decrease in the maltene/asphaltene ratio (Table 3). Consequently, the increased average diameter of the aromatic sheets (L_a) appears coherent with the increase in the aromaticity degree. The found growth of the average height of the aromatic clusters (L_c) can be explained considering that, upon loss of the maltene fraction and decreased distance of the aromatic sheets, a new aromatic sheet enter the cluster (see M), enlarging it (see Table 3).

The addition of the two additives, Oleic Acid (Sample C) and HR (Sample D) into the aged bitumen determines a variation of the PXRD patterns with an increase, in both cases, in the d_γ and d_m values, more pronounced for Sample D (Fig. 2). All the changes in terms of differences between d_γ and d_m values (Δd) calculated from the PXRD patterns of all examined samples are reported in Table 4. This comparison, in terms of Δ*d*, highlights the effects of the aging process on the neat bitumen, in which the *d* values were decreased compared to the neat bitumen (negative Δ*d*). It can be noticed that the addition of the two additives results in an increase in the *d* values with respect to the aged sample (positive Δ*d*).

Table 4
Δ*d* values of γ-band and (002)-band between: B–A (aged bitumen and fresh bitumen), C–B (aged bitumen + 2 wt% OA and aged bitumen), D–B (aged bitumen + 2 wt% HR and aged bitumen).

Peak	Δd_{B-A}	Δd_{C-B}	Δd_{D-B}
γ- **band**	−0.38	0.131	0.408
(002)-band	−0.063	0.069	0.229

As reported in Table 3, the test samples containing additives display a decrease in the crystallite parameters, L_a, L_c and M, with respect to the aged bitumen sample, even though the complete recovery of the initial values (neat bitumen) is not achieved. Although sample C (the aged bitumen sample containing OA) exhibits d_γ value larger than sample B (aged bitumen without additives) and d_m value rather similar to the neat bitumen sample, its PXRD pattern profile still resembles the profile of the aged bitumen, with the γ-band splitting into two broad signals. Furthermore, the aged bitumen doped with Oleic Acid presents an aromaticity value (f_a = 0.456) comparable to that of the aged bitumen sample (f_a = 0.423), indicating that this additive is not able to restore aged bitumen to the neat bitumen microstructure. On the other hand, the PXRD pattern of the aged bitumen doped with HR shows quasi-identical intensity reflections and shape features of the fresh bitumen sample (Fig. 2). It can be seen that the addition of HR additive results in a significant shift of both the γ-band and the graphene band *d*-spacing compared to the aged bitumen sample (sample B). Consequently, the increased distance between the aliphatic chains and the aromatic sheets of asphaltene molecules by addition of HR results in the formation of a more flexible material. Finally, the aromaticity value f_a of 0.213 found for the HR containing sample decreases to a value comparable to that of the fresh bitumen (f_a = 0.256).

3.3. Nuclear magnetic resonance - NMR relaxometry

In this research, ILT (Inverse Laplace Transform) analysis of the NMR echo signal decay was carried out to confirm the effect of the OA and HR additives on the structure of the aged bitumen and to confirm the results of the PXRD analysis. The application of the ILT to the echo decay allows finding the $P(T_2)$ distribution associated with the relaxation times referred to molecular aggregates presented in the analysed system. Fig. 3 shows the test results, in which the plots are the distribution $P(T_2)$ as a function of the relaxation time for the tested blends. In Fig. 3, two peaks corresponding to T_2 relaxation time distribution can be seen. The peak at shorter T_2 times represents the more rigid (asphaltenes), while the peak at longer T_2 times corresponds to the maltene fraction. This finding has been proved in several research works [3,12,13]. The ILT of the aged bitumen is particular, while the two peaks are observed, the times distribution of the maltene is sharper, this is mainly because the oxidation of bitumen reduces the maltene fraction and increases the asphaltene component. It is noteworthy that while the obtained profile of sample D is similar to the profile of sample A, the profiles of sample C is similar to sample B. This could show the effectiveness of HR additive as a rejuvenator compared to the OA one, since the addition of HR could restore the chemical structure of the aged binder. Related to this study, the authors' former research [13] also showed the effectiveness of NMR relaxometry for investigating the bitumen/additive chemical investigation, and in particular the influence of the rejuvenator on the aged binder.

4. Conclusions

Overall, comparing all the test results obtained from different test methods reported in this study, it can be concluded that the PXRD technique seems to be useful and powerful for investigating the

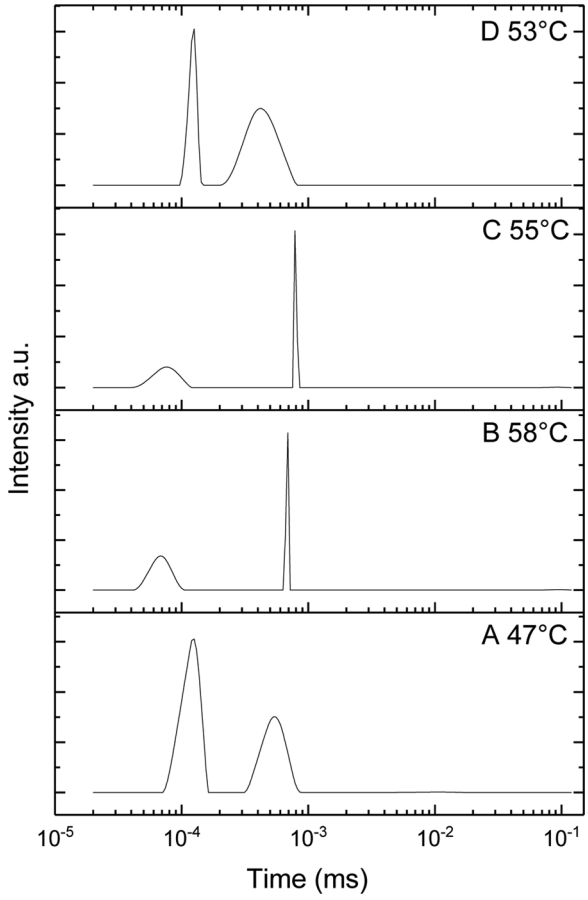

Fig. 3. ILT relaxation time distributions of blends at the temperature of 5 °C lower than transition temperature (sol-liquid) determined by dynamic temperature ramp test.

effectiveness of a rejuvenator in restoring the microstructure of bitumen after the aging process. In line with recent research works, this paper proves that mechanical properties, on their own, are not enough for investigating the effects of additives on bitumen. Indeed, only when a technique suitable to investigate the microstructure organization of aged asphalt before and after the introduction of a rejuvenator, such as X-ray powder diffraction, has it been possible to prove the real rejuvenating effects of the HR additive when compared to the Oleic Acid one. The HR additive has been found effective in restructuring the right balance between asphaltene/maltene, resulting in a reactive colloidal network. It is worth mentioning that, the validity of the obtained results were supported by ILT analysis of the NMR echo signal decay.

References

[1] X. Lu, U. Isacsson, Effect of ageing on bitumen chemistry and rheology, Constr. Build. Mater. 16 (1) (2002) 15–22.
[2] C. Oliviero Rossi, P. Caputo, S. Ashimova, A. Fabozzi, G. D'Errico, R. Angelico, Effects of natural antioxidant agents on the bitumen aging process: an EPR and rheological investigation, Appl. Sci. 8 (8) (2018) 1405–1419.
[3] N. Baldino, C. Oliviero Rossi, F.R. Lupi, D. Gabriele, Rheological and structural properties at high and low temperature of bitumen for warm recycling technology, Colloid Surf. A 532 (2017) 592–600.
[4] J.F. Branthaver, J.C. Petersen, R.E. Robertson, J.J. Duvall, S.S. Kim, P.M. Harnsberger, T. Mill, E.K. Ensley, F.A. Barbour, J.F. Schabron, Binder CharActerizationand Evaluation: Chemistry; SHRP-A-368 vol. 2, National Research Council, Washington, DC, 1993.
[5] Y.A. Tuffour, I. Ishai, The diffusion model and asphalt age-hardening, J. Assoc. Asphalt Paving Technol. 59 (1990) 73–92.
[6] J.C. Petersen, J.F. Branthaver, R.E. Robertson, P.M. Harnsberger, J.J. Duvall, E.K. Ensley, Effects of physicochemical factors on asphalt oxidation kinetics, Transport. Res. Record 1391 (1993) 1–10.
[7] G. Mazzoni, E. Bocci, F. Canestrari, Influence of rejuvenators on bitumen ageing in hot recycled asphalt mixtures, J. Traffic Transp. Eng. 5 (3) (2018) 157–168.
[8] M. Zaumanis, R.B. Mallick, L. Poulikakos, R. Frank, Influence of six rejuvenators on the performance properties of Reclaimed Asphalt Pavement (RAP) binder and 100% recycled asphalt mixtures, Constr. Build. Mater. 71 (2014) 538–550.
[9] M. Zargar, E. Ahmadinia, H. Asli, M.R. Karim, Investigation of the possibility of using waste cooking oil as a rejuvenating agent for aged bitumen, J. Hazard. Mater. 233–234 (2012) 254–258.
[10] F. Pahlavan, A.M. Hung, M. Zadshir, S. Hosseinnezhad, E.H. Fini, Alteration of π-electron distribution to induce deagglomeration in oxidized polar aromatics and asphaltenes in an aged asphalt binder, ACS Sustain. Chem. Eng. 6 (2018) 6554–6569.
[11] P. Calandra, P. Caputo, M.P. De Santo, L. Todaro, V. Turco Liveri, C. Oliviero Rossi, Effect of additives on the structural organization of asphaltene aggregates in bitumen, Constr. Build. Mater. 199 (2019) 288–297.
[12] L. Filippelli, L.Gentile C. Oliviero Rossi, G.A. Ranieri, F. Antunes, Structural change of bitumen in the recycling process by using rheology and NMR, Ind. Eng. Chem. Res. 51 (2013) 16346–16353.
[13] C. Oliviero Rossi, P. Caputo, V. Loise, S. Ashimova, B. Teltayev, C. Sangiorgi, A New Green Rejuvenator: Evaluation of Structural Changes of Aged and Recycled Bitumens by Means of Rheology and NMR vol. 20, Springer RILEM Bookseries, 2018, pp. 177–182.
[14] L. Coppola, L. Gentile, I. Nicotera, C. Oliviero Rossi, G.A. Ranieri, Evidence of formation of ammonium perfluorononanoate/2H 2O multilamellar vesicles: morphological analysis by rheology and Rheo-2H NMR experiments, Langmuir 26 (24) (2010) 19060–19065.
[15] T.F. Yen, J.G. Erdman, S.S. Pollack, Investigation of the structure of petroleum asphaltenes by X-Ray diffraction, Anal. Chem. 33 (1961) 1587–1594.
[16] S.I. Andersen, X-ray diffraction of subfractions of petroleum asphaltenes, Energy Fuels 19 (2005) 2371–2377.
[17] U. Bilardo, G.C. Borgia, V. Bortolotti, P. Fantazzini, E. Mesini, Magnetic resonance lifetimes as a bridge between transport and structural properties of natural porous media, J. Pet. Sci. Eng. 5 (1991) 273–283.
[18] M.N. Siddiqui, M.F. Ali, J. Shirokoff, Use of X-ray diffraction in assessing the aging pattern of asphalt fractions, Fuel 81 (2002) 51–58.
[19] L.B. Ebert, J.S. Scanlon, D.M. Mills, X-ray Diffraction of n-paraffins and stacked aromatic molecules: insights into the structure of petroleum asphaltenes, Liq. Fuels Technol. 2 (3) (1984) 257–286.

Chapter 7

Inverse Laplace Transform (ILT) NMR: A powerful tool to differentiate a real rejuvenator and a softener of aged bitumen

Colloids and Surfaces A 2019, 574; doi:10.1016/j.colsurfa.2019.04.080

Colloids and Surfaces A 574 (2019) 154–161

Contents lists available at ScienceDirect

Colloids and Surfaces A

journal homepage: www.elsevier.com/locate/colsurfa

Inverse Laplace Transform (ILT) NMR: A powerful tool to differentiate a real rejuvenator and a softener of aged bitumen

Paolino Caputo[a], Valeria Loise[a], Saltanat Ashimova[a], Bagdat Teltayev[b], Rosolino Vaiana[c], Cesare Oliviero Rossi[a,*]

[a] Department of Chemistry and Chemical Technologies, University of Calabria, Via P. Bucci, Cubo 14/D, Rende, CS, 87036, Italy
[b] Kazakhstan Highway Research Institute, Nurpeisova Str., 2A, Almaty, 050061, Kazakhstan
[c] Department of Civil Engineering, University of Calabria, Via P. Bucci, Cubo 46/B, Rende, CS, 87036, Italy

GRAPHICAL ABSTRACT

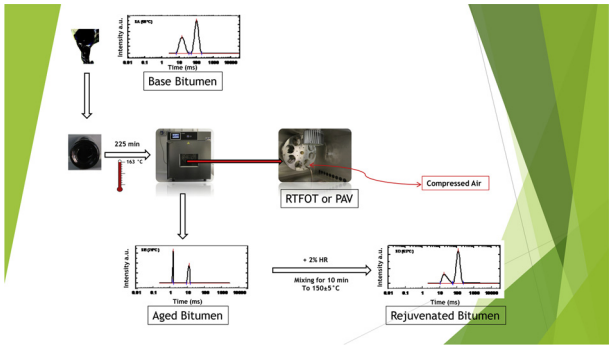

ARTICLE INFO

Keywords:
Aged bitumen
Rejuvenator
Rheological properties
ILT
Nuclear magnetic resonance (NMR)
spectroscopy
Scanning electron microscope (SEM)

ABSTRACT

ILT is particularly useful when the signal is characterized by multi-exponential decay, for example in spin relaxation or in the dephasing of the NMR spin echo signal associated with sopra molecular aggregation under the influence of pulsed magnetic or internal field gradients. As novel approach to observe the real rejuvenating effect of the potential additive, an Inverse Laplace Transform of the NMR spin-echo decay (T_2) was applied. The potentialities of a new, non-toxic and eco-friendly biocompatible additive on aged bitumen are explored for the first time as bitumen rejuvenator, by means of advanced rheological and Relaxometry-NMR measurements. Pristine, aged, and doped aged bitumen morphology have been investigated by SEM. The new rejuvenator helps to rearrange the structure of the aged bitumen (aiming at the original one), and this mechanism can be observed by ILTNMR analysis.

1. Introduction

The main use of bitumen is as a binder for mineral aggregates to produce asphalt mixes. Aging and adverse climatic events cause severe degradation phenomena and require the pavement replacement after a certain time in use [1]. However, the waste asphalt mixture contains valuable asphalt binder. The aged bitumen from this reclaimed asphalt pavement has a lower penetration and is more viscous than when first mixed [2].

It is becoming increasingly important to have a responsible

* Corresponding author.
E-mail address: cesare.oliviero@unical.it (C. Oliviero Rossi).

https://doi.org/10.1016/j.colsurfa.2019.04.080
Received 19 February 2019; Received in revised form 26 April 2019; Accepted 27 April 2019
Available online 28 April 2019
0927-7757/

approach and pay attention to the construction of asphalt roads. Especially considering the use of materials and energy necessary for the rebuilding of roads. For these reasons the research should aim at the reuse of "damaged" materials [3].

The regeneration methods employed include the addition of fresh binder, softer than those typically used to produce hot mixes, or the use of some vegetable oils [4]. However, often the action of the vegetable oil only softens hard bitumen bringing it to match the macroscopic mechanical parameters, but does not have a regenerating action. Indeed, as it is well known, the mechanism of bitumen aging, high temperatures used during production, storage, transport and laying (Short-Term Aging), involves volatilization and oxidation reactions of complex organic compounds in the bitumen, which lead to changes in the molecular structure [5]. Moreover, the aging process continues throughout the service life of the road pavement by oxidation processes also caused by atmospheric oxygen and UV radiation (Long-Term Aging) [6]. Oxidation leads to an increased fragility and, consequently, a decreased fatigue resistance involving the development of cracks in the asphalt layer [7,8]. Therefore, the regeneration of the aged bitumen is erroneously correlated with balancing penetration and softening point or viscosity.

A real rejuvenator modifies the chemical and physical structure of aged bitumen reducing its rigidity [9]. Thus, rejuvenators can be used to restore the aged binder properties to its original state, playing a crucial role in the bitumen recycling method, by ensuring the reusing of aged bitumen and a good performance of the reclaimed bitumen. Unfortunately, the rejuvenator mixtures have significant variability in terms of physical and chemical properties [10], and their behaviour and especially their action on the supramolecular structure arrangement of the bitumen is not well known yet [11].

With reference to the various mechanisms of ageing, at least two mechanisms for bitumen rejuvenation have been so far depicted:

1 addition of a softening agent: substances like flux oil, lube stock, slurry oil etc. can lower the viscosity of the aged binder
2 addition of a rejuvenator which helps to restore the physical and chemical properties and in particular to bring the aggregation process of asphaltenes backwards to the original state. In other words, a rejuvenator helps in finely re-disperse the aggregated asphaltenes [12]

The difference is subtle but important: a softening agent often consists of lubricating oil extracts and extender oils, which contain a high proportion of maltene constituents—napthenic or polar aromatic fractions—that help re-balance the composition of the aged binder that lost its maltenes during construction and service. On the other hand, rejuvenators should have a high proportion of aromatics, which are necessary to keep the asphaltenes dispersed, they should contain a low content of saturates, which are highly incompatible with the asphaltenes. This difference has been highlighted also by other authors. [13]

The bitumen can be depicted as a colloidal model where asphaltenes (dispersed phase) and maltenes (continuous phase) are the constituents in bituminous materials [14]. It is a real complex material where the simultaneous presence of different structures confers the material emerging and sometimes unexpected properties [15].

Using this model, the present research describes the physical chemical characteristics of a new green rejuvenator (HR) developed during our research activity, focusing on the understanding of the physical–-chemical interactions between a real regenerating substance and a simple vegetable oil (VO) and bitumen. Two different bitumen's were employed and, in an attempt to have more data, two different aging acknowledged methods were used for the bitumen [16].

The rejuvenator HR is green and based on oleic acid. The HR rejuvenators has been developed by the academic Spin-Off (Kimical SRL) of the University of Calabria.

All the bitumens were characterized by rheological tests, Relaxometry-NMR and Scanning Electron Microscope (SEM). The rheology is a useful technique to investigate the molecular aggregations with and without shear [17,18] as well as Inverse Laplace Transform to the spin-echo decay (T_2) [19]. Thus, the efficiency of the NMR and SEM techniques as an effective techniques to highlight the difference between a flux agent (softener) and a real rejuvenator are highlighted.

2. Experimental

2.1. Chemicals and materials

Two independent virgin bitumens from different sources are tested in this work: one with a penetration grade 100/130, produced in Kazakhstan and supplied by Kazakhstan Highway Research Institute (Almaty, Kazakhstan) and the second one with a penetration grade 50/70 sourced from Saudi Arabia and supplied by Loprete Costruzioni Stradali (Terranova Sappo Minulio, Reggio Calabria, Italy).

The two additives, a vegetable Flux Oil (VO) and an oleic acid-based rejuvenator (HR), were investigated in this research work. The vegetable Flux Oil (VO) was furnished by Fabiano SRL (Cosenza, Italy) and the HR rejuvenator has been developed by the academic Spin-Off (Kimical SRL) operating at the University of Calabria, Italy. The rejuvenator, is commercially named as HR Kimical, and all the technical information can be obtained by Kimical SRL Company. HR Kimical does not have carcinogenic risk and it can be carried safely by operators. Our research group remains at the disposition of interested parties for any technical advice on how to use the HR range for regeneration of aged bitumen.

2.2. Sample preparations

The modified bitumen was prepared by using a high shear mixing homogenizer (IKA model, USA). Firstly, bitumen was heated up to 150 ± 5 °C until it flowed fully, then a given part of HR or VO (2% of the weight of the base bitumen) was added to the melted bitumen under a high-speed shear mixer of 400–600 rpm/min. Furthermore, the mixture was kept under mechanical stirring at 150 °C for 10 min in a closed beaker to avoid oxidation. After mixing, the resulting bitumen was poured into a small sealed can and then stored in a dark chamber thermostated at 25 °C to retain the obtained morphology.

Table 1 represents all prepared samples and applied ID

2.2.1. Aging

2.2.1.1. RTFOT method (Saudi Arabia bitumen). According to ASTM D2872-04, the simulation of bitumen aging is carried out with Rolling Thin-Film Oven Test (RTFOT) [8]. Accordingly, a moving film of bitumen was heated in an oven for 85 min at 163 °C. The aging of bitumen is determined from changes in its physical and rheological properties, as measured before and after the oven treatment.

In this article, the same procedure (i.e. the RTFOT) was lengthened up to 225 min to acquire an ideal bitumen with a penetration grade 30/

Table 1
Samples and ID.

Kazak bitumen: Penetration grade 100/130	Sample ID
Base bitumen	KA
PAV bitumen	KB
PAV bitumen + 2 wt% VO	KC
PAV bitumen + 2 wt% HR	KD
Arabia Saudi bitumen: Penetration grade 50/70	**Sample ID**
Base bitumen	SA
RTFOT bitumen	SB
RTFOT bitumen + 2 wt% VO	SC
RTFOT bitumen + 2 wt% HR	SD

Table 2
Physical chemical parameters of investigated samples.

Sample	PN (mm) Penetration depth ± 1	R&B (°C) Softening point ± 1	X_A (wt%) Asphaltene content ± 0.5	T (°C) Transition ± 0.1
Sample KA	110	44	32.9	60.7
Sample KB	47	59	35.6	124.7
Sample KC	57	49	31.3	88.0
Sample KD	60	52	32.1	71.2
Sample SA	60	51	26.8	70.0
Sample SB	19	62	39.0	84.9
Sample SC	27	59	33.9	78.2
Sample SD	24	56	34.6	79.0

45, therefore making a quite-stiff material (sample SB, see Table 2) in order to simulate a different aging process with separated SARA fractions [20].

2.2.1.2. PAV method (Kazakhstan bitumen). With the Pressure Aging Vessel (PAV), the bitumen was simulated to in-service aging of the base bitumen after 5–10 years [8]. The binder was subjected to high pressure and heat for 20 h to give the effect of long-term oxidative aging. The apparatus was made up of a stainless-steel pressure container with encased band heaters and its own pressure and heat controls. A platinum resistance thermometer measures the internal test temperature to ± 0.1 °C. Selectable test temperatures (standard 90/100/110 °C) are controlled with a precision of ± 0.2 °C. Pressure is monitored by transducer and controlled at 2.1 ± 0.1 MPa. Temperature and pressure calibration were executed. The procedure was referenced according to AASHTO/ASTM T179.

2.2.2. Asphaltene determination

Asphaltenes were isolated from bitumens in the manner described elsewhere. [21].

2.2.3. S.A.R.A. determination

The Iatroscan MK 5 Thin Layer Chromatography (TLC) was used for the chemical characterization of bitumen by separating it into four fractions: Saturates, Aromatics, Resins and Asphaltenes (S.A.R.A) [19]. During the measurement, the separation took place on the surface of silica-coated rods. The detection of the amount of different groups were according to the flame ionization. The sample was dissolved in peroxide-free tetrahydrofurane solvent to reach a 2% (w/v) solution. Saturated components of the sample were developed in n-heptane solvent while the aromatics in a 4:1 mixture of toluene and n-heptane. Afterwards, the rods had to be dipped into a third tank, which was a 95 to 5% mixture of dichloromethane and methanol. That organic medium proved suitable to develop the resin fraction whereas the asphaltene fraction was left on the lower end of the rods.

2.3. Empirical characterization

The bitumen softening temperature (R&B T, ring and ball temperature) is determined with the ring and ball test (ASTM Standard D36) [22,23].

The bitumen consistency was evaluated by measuring the penetration depth (of a stainless-steel needle of standard dimensions under determinate charge conditions (100 g), time (5 s) and temperature (25 °C), according to the standard procedure (ASTM D946) [22,23].

2.4. Rheological characterization

Dynamic Shear Rheological (DSR) measurements on bitumen samples were carried out using a controlled shear stress rheometer (SR5, Rheometric Scientific, USA) equipped with a parallel plate geometry (gap 2 mm, φ = 25 mm within the temperature range 25–150 °C, gap 2 mm, φ = 8 mm within the temperature range from 25 to −20 °C) and a Peltier system (± 0.1 °C) for temperature control.

Dynamic experiments were performed within the linear viscoelastic region where measured material features are independent of the amplitude of applied load and are the only function of microstructure of material [24,25].

Aimed at investigating the material phase transition, temperature sweep tests were performed at 1 Hz with heating rate 1 °C/min and applying the proper stress values to guarantee linear viscoelastic conditions (previously determined by stress sweep tests) at all tested temperatures.

More details about the mechanical characterization can be found elsewhere. [26]

2.5. NMR measurement and inverse laplace transform (ILT)

Relaxation experiments were effected at 15 °C lower than transition temperature (sol-liquid) each where each sample underwent a dynamic temperature ramp test experiment by means of a custom-built NMR instrument that operates at a proton frequency of 15 MHz.

A CPMG sequence with an interpulse time of 160 μs provided the T_2 decay signal. The CPMG signals were made up of 400 echoes, with 128 averages, which provided a signal-to-noise level of circa 500 [27].

Heterogeneity usually causes the T_2 relaxation time to vary all over the sample, surface relaxation effects other then magnetic field in homogeneities [28]. Therefore, in general the obtained NMR signal is analysed in terms of sum exponentials, or, more realistically, allowing a continuous distribution of relaxation times to be observed [29]. Hence, if there is a continuous distribution of relaxation time inside the sample, the amplitude A_n of the n^{th} echo in the echo train is given by:

$$A_n = A_0 \int_0^\infty P(T_2) e^{-2n\tau/T_2} dT_2 \quad (1)$$

where A_0 is a constant,τ is the half echo time and $P(T_2)$ is the ILT of the unknown function that fits the echo amplitude curve. Moreover, $P(T_2)$ can be seen to be a distribution of rate (inverse of time) constant. Expressly, a Probability Density Function (PDF) which, in addition, could explain the different macro-structures composing the bitumen binder [30].

In this paper, ILT computation was operated by means of UpenWin, which is a Windows software written in C++ and released by the University of Bologna, which implements the UPEN algorithm [31]. UPEN allows obtaining distributions of relaxation time without multiple peaks which does not require separation by the data to prevent physical misinterpretation of data [32].

2.6. Morphological analysis

The Asphaltenes of each investigated bitumen were observed by a Scanning Electron Microscope (SEM) (Cambridge Stereoscan 360, Cambridge Instruments, UK). Sample specimens were successively sputter coated with a thin gold film prior to SEM.

3. Results and discussion

3.1. Mechanical behaviour

The hard consistency of the samples is strongly affected by aging processes. This is as a result of the oxidized aged bitumen. During the oxidative aging, the concentration of polar functional groups becomes high enough to render inactive an excessive number of molecules through intermolecular association. Furthermore, the molecules or molecular agglomerates lose enough mobility to flow past one another under thermal or mechanical stress. The resulting embrittlement of the

Table 3
Shows the composition of the tested neat and aged bitumens.

	SATURATES	AROMATICS	RESINES	ASPHALTENES
Sample KA	7.1	41.7	19.1	32.1
Sample KB	6.3	26.5	32.4	34.8
Sample SA	6.8	50.7	16.6	25.9
Sample SB	6.2	34.7	21	38.1

asphalt makes it susceptible to fracturing or cracking and resistant to healing. After that, the penetration depth decreases according to the additives content and the aging steps as long as on the contrary, the softening points escalate. Finally, the viscoelastic-liquid transition temperatures step-up with the aging process.

Using standardized tests, the penetration depth (PN), softening point (R&B) and the asphaltene content were determined (Table 2).

Although each bitumen displays a unique role, a good correlation exists between bitumen hardness and asphaltenes content for each of the investigated bitumens. Some points can be inferred from the data in Tables 2 and 3. The asphaltenes fraction seems to be the dominant component that is controlling hardness of the bitumen. Oxidation of a bitumen significantly increases the asphaltene and resins contents and reduces the aromatic fraction. Obviously, the incorporation of oxygen increases polar molecules contents consequently changes in polarity are sufficient to influence asphaltene fraction.

The asphaltene content (35.6 and 39.0% for the samples KB and SB respectively, Table 2) as well as the softening points increases with the aging step (59 and 62 °C for the KB an SB respectively). The values for the samples containing HR and VO are similar. These empirical data do not allow distinguishing the real efficiency of the rejuvenator.

3.2. Rheology

Rheology temperature-sweep experiments have been exploited to obtain some information on the structural changes induced by temperature, trying to better define a transition temperature range. In fact, in this experiment, the evolution of the loss tangent (tanδ) is monitored continuously during a temperature ramp at a constant heating rate (1 °C/min) and at a frequency of 1 Hz. In Fig. 1, the time cure tests of Kazak and Saudi bitumens are shown.

The transition temperature is evidenced when the loss tangent (tanδ) is plotted as a function of temperature. The initial trend is almost linear with temperature, when the material mainly behaves like a viscoelastic system. The subsequent sharp increase occurs in correspondence to the transition toward a liquid-like behaviour (tanδ diverges). Even though the typical trend is quite similar for the different samples, a discrepancy in transition temperatures is clearly obtained.

The aged bitumens (samples KB and SB) show much higher transition temperatures than the fresh material. This effect is due to an increased fraction of asphaltenes resulted from oxidation of the soft unsaturated organic part. This asphaltene enrichment causes a stronger rigidity and connectivity when compared to the less dense network of the virgin bitumen where the asphaltene domains are poorly connected to each other. It must be noted that the aggregation pattern of asphaltene is quite complex since asphaltene spontaneously tend to self-assemble hierarchically with formation of aggregates of different sizes and at different levels of complexity [33]

As a result of the aggregation-based process of modification of this complex pattern, however, Both VO and HR induce a shift toward lower transition temperatures from the viscoelastic to the liquid regime compared to the aged bitumen (Table 2). In another way, they also inflate the values of loss tangent, thus establishing the system more viscous than the simply aged binder. For the Kazak system, on the contrary of VO, the additive HR has an enormous effect in terms of loss

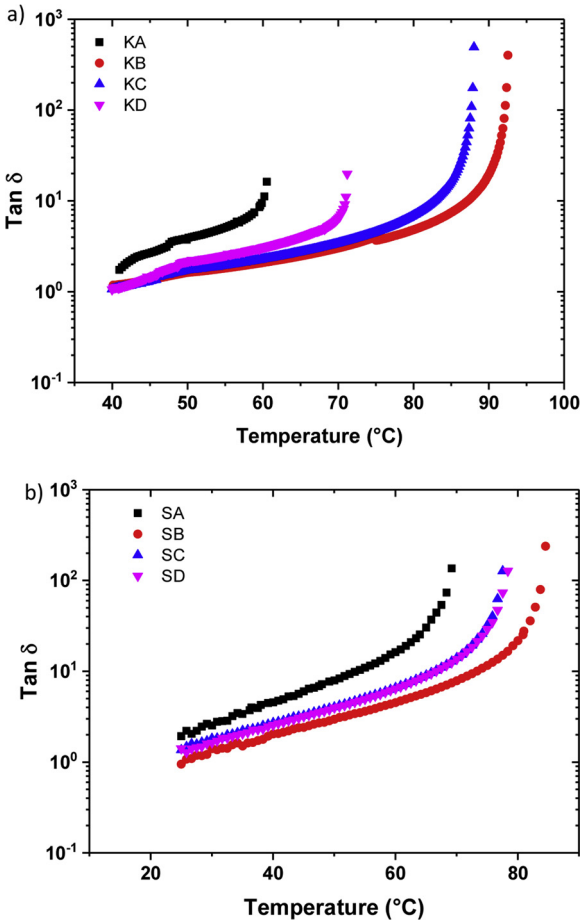

Fig. 1. Semi-log plot of high temperature ramp test for a) KA; KB; KC and KD and b) SA, SB, SC and SD. Left axis: loss tangent, tan. δ.

of rigidity. This additive possesses an amphiphilic nature. We believe that this behaviour might reduce the associative interactions between the asphaltene particles by interposing itself between the asphaltenes and the maltenes. This phenomenon might be alike to the one found in the deactivation of hydrophobic cross-links in hydrophobically modified polymers by surfactants [31]. Another mechanism concurrently present can be the formation of direct interactions between the surfactant polar headgroup and polar parts of asphaltene. In fact, it has been recently highlighted that, in addition to polar and apolar interactions, further specific interactions between surfactant and clusters of organic molecules, [34,35] or of ionic materials [36,37] and between surfactants and other surfactants with consequent peculiar self-assembly processes [38,39] dictating the final overall aggregation pattern [40]. and the (usually slowed-down) dynamics [41].

Among the wide scenario of possible interactions, in our systems specific interplay can be reasonably envisaged in the H-bonds and acid-base interactions between the carboxylic oleic acid headgroup and the basic functional groups of asphaltenes like carbonyl and amines)

As a result, the colloidal network can be weakened, which in turn may express a rise to a lowering of the transition temperature.

Consistently, VO, which has not surfactant nature, does not exert such an effect in this bitumen, thus justifying our vision of the mechanisms involved.

For the Saudi system, both VO and HR influence a shift toward lower transition temperatures, but in this case, VO and HR present reduced differences in the trends of tanδ. This phenomenon endures a typical situation where the analysis of the mechanical properties alone is not enough to distinguish between flux effect and regeneration effect.

In Fig. 2, the temperature sweep experiments at low temperatures

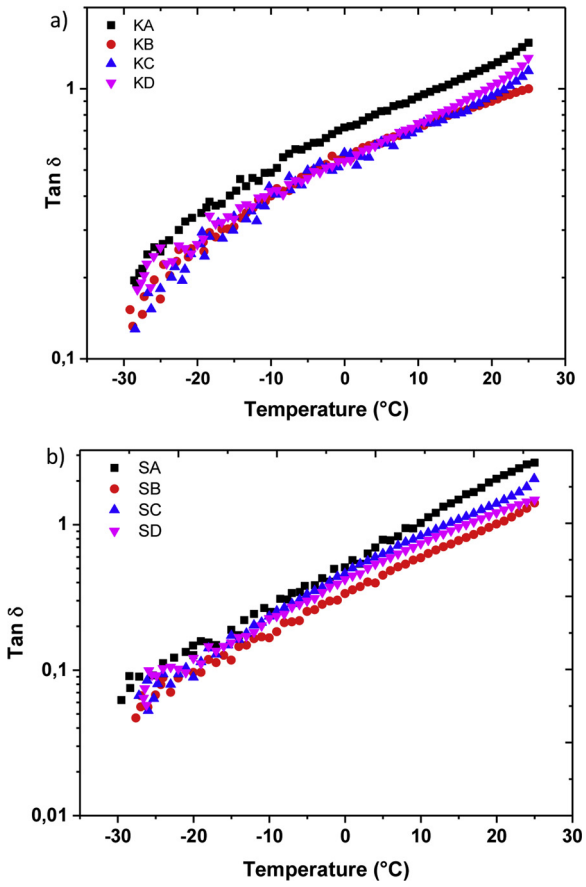

Fig. 2. Semi-log plot of low temperature ramp test for the samples a) KA; KB; KC and KD and b)SA; SB; SC and SD. Left axis: loss tangent, tan. δ.

are presented.

Similar trends of tan δ are observed for two kind of bitumens. The neat bitumens (KA and SA) are softer, whilst the aged (KB and SB) bitumens are harder. Considering the doped samples, the bitumen containing VO and HR reveal higher tan δ than aged ones. The dynamic mechanical analysis at low temperature reproduces what we observed at higher temperature where it is impossible to distinguish the effect of VO and HR.

Table 4
T_2 relaxation time of the two peaks of the samples.

ID Sample	Time (ms) ± 1	
ID		
SA	14	101
SB	2	13
SC	50	247
SD	18	121
KA	9	99
KB	3	10
KC	–	258
KD	2	24

3.3. NMR study

The analyses NMR has been effected to show the real effectiveness of HR as regenerating. Due to the time cure tests could be identified the sol-liquid transition temperature of each samples. As it is known, the temperature plays a fundamental role on the colloidal structure of the bitumen, so much that with the increase of it there is a progressive decreasing of the elastic ability of the system [42]. For this reason, the analysis performed by a custom built NMR instrument, that operates at a proton frequency of 15 MHz, were perfermed at 15 °C below the transition temperature of each sample.

This choice ensures us to be within the viscoelastic region of the material and to have samples with a certain structural homogeneity.

The Inverse Laplace Transform (ILT) analysis of the NMR echo signal decay has been implied to achieve the T_2 relaxation time distributions. This technique allows finding the PDF (Probability Density Function) distribution, which associates with relaxation times that correspond to unrelated molecular aggregates inside the samples. The results are presented in Fig. 3a and b, where the plots are the distribution PDF as a function of the relaxation time for the K and S bitumens are shown (Table 4).

The T_2 relaxation time distribution exhibits two peaks. Direct

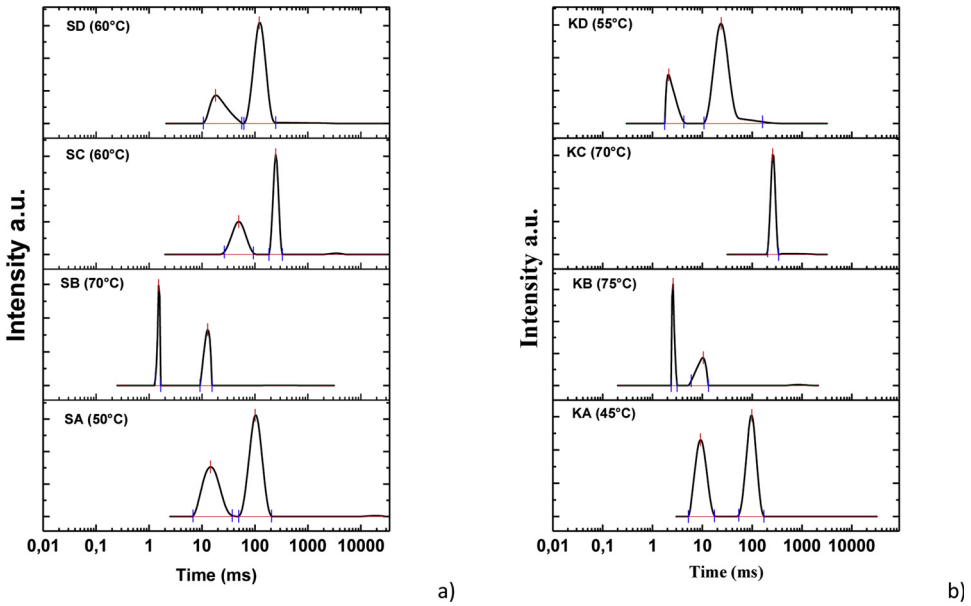

Fig. 3. ILT relaxation time distributions of S(a) and K (b) bitumen samples measured at the temperature of 15 °C lower than transition temperature (sol-liquid) determined by dynamic temperature ramp test experiment for each sample.

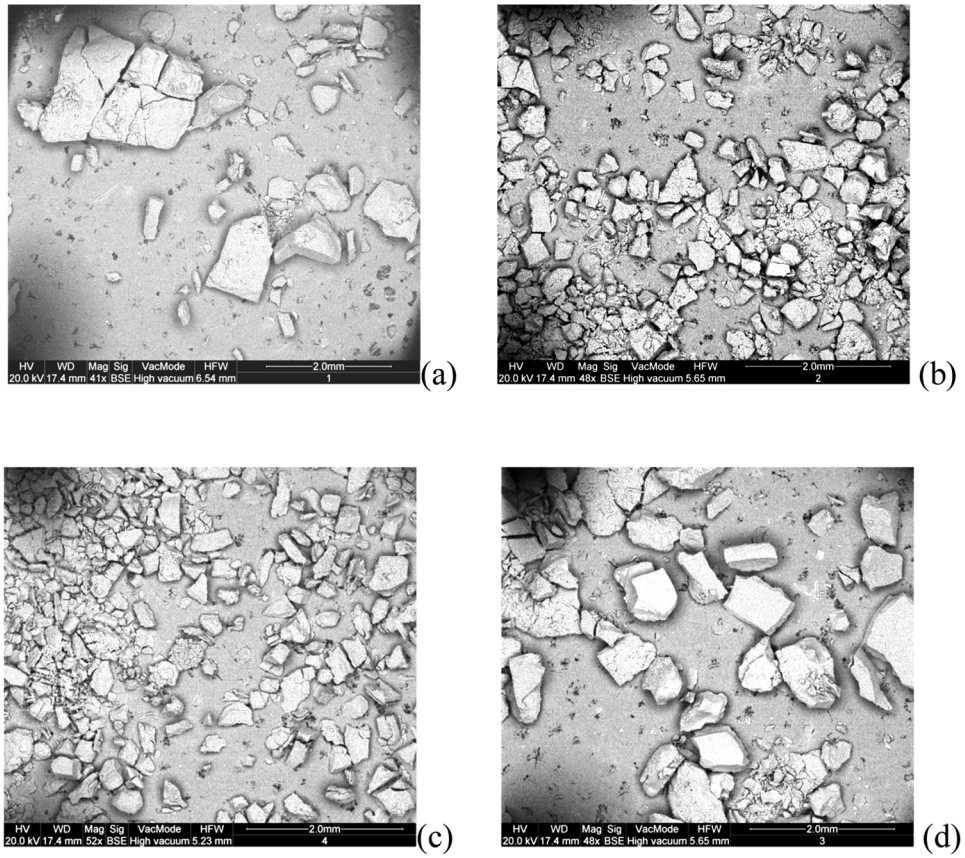

Fig. 4. SEM image of SA (a); SB (b); SC (c) and SD (d) samples.

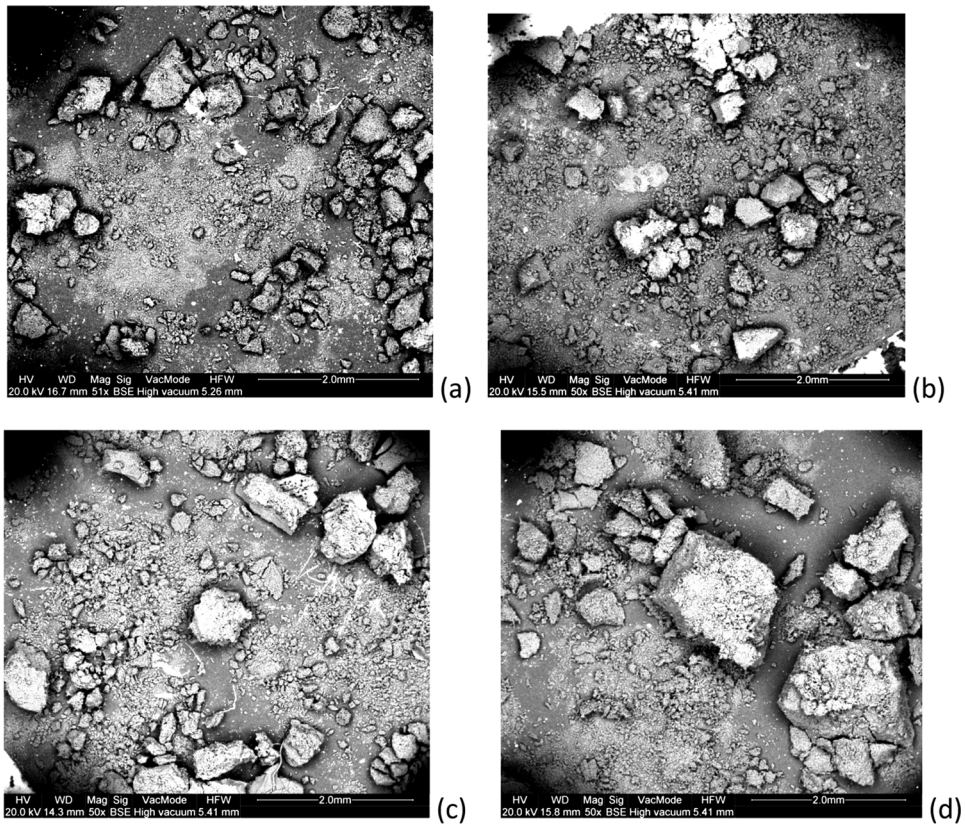

Fig. 5. SEM image of KA (a); KB (b); KC (c) and KD (d) samples.

correlation can be made between T_2 and the rigidity of structures in these materials [19] as well as the molecular constrain causing dynamic hinderance [43].

The shorter T_2 times (around 10 ms) reasonably corresponds, therefore, to more rigid supra-molecular aggregates, hence they are attributed to asphaltenes. Conversely, high T_2 times (around 100 ms) can be attributed to low intra-molecular interactions, they can be referred to the maltene fraction of the sample under examination. This finding supports the colloidal model of the bitumen. In fact, if the polar fluid model suggested by Anderson [44] was applicable to our system, the ILT result would demonstrate a sole broad peak referred to as a continuous T_2 time.

The ILT of the aged bitumen again discloses two shifted peaks toward shorter times (more potent effect as the aging step is increased) and present profoundly distinctive shapes. This probably indicates a gradual rise of the materials rigidity with the on-going oxidation process. In particular, the asphaltene peaks are now close to 1–2 ms for the aged S and K bitumens (see Table 3).

The addition of VO and HR to the aged bitumen shift the asphaltene peaks to longer T_2 times compared with the aged bitumen. In particular, the addition of HR (sample SC and KC) shows similar distribution profiles and the mean values of the T_2 relaxation time distributions are similar to those of pristine bitumen. Moreover, analysing the graphics in detail, evidence of differences in the action of the two additives emerges clearly. In both samples containing VO the T_2 relaxation times are significantly shifted respect to pristine bitumen. It is worth noting that only one T_2 value is present in the KC sample, this is the confirmation of the flux action of this additive and its action on the high penetration grade bitumen.

3.4. Morphology characterization

Images of the pristine bitumen, aged one and of those containing HR and VO. were acquired with the SEM

The SEM photographs of the S and K type bitumens are shown in Figs. 4 and 5 respectively.

The effect of aging on the bitumen asphaltenes is evident. The amount of asphaltenes increases through the oxidation process (Table 2) but it is worth noting that the aging leads to a sort of “mincing” of the asphaltenes for all the sample (Figs. 4b and 5 b). Indeed, for all the samples, the asphaltenes distributions shows two different situations between virgin and aged bitumen: the asphaltenes of the aged bitumens are more numerous and characterized by smaller sizes than the virgin ones. It is evident that the addition of VO to the aged bitumen does not bring any change to the size and distribution of asphaltenes (Figs. 4c and 5 c). Conversely, the addition of HR to the aged bitumen has the effect of aggregating again the asphaltenes, reconstructing a similar distribution of the pristine bitumen.

The sequence of images clearly shows how the HR, being a real rejuvenation for the aged bitumen, affects the structure of asphaltenes, while the presence of VO, which is a simple flux, does not affect the structure of asphaltenes.

4. Conclusions

This article shows the effectiveness of the HR additive for regenerating bitumen, acting as rejuvenator. This green additive is obtained by a simple method from two low-cost and eco-friendly precursors. HR tends to restore the mechanical properties of the oxidized bitumen, acting on the structure of the bitumen, having a restructuring effect on the altered colloidal network of the aged bitumen binder.

In the present work, we once more contributed to supporting the colloidal view of the bitumen structure. Moreover, the article demonstrates the necessity of testing the regenerated bitumen using structural techniques in order to distinguish between bitumen with flux or a real regenerating. Thus, bituminous systems can have like macroscopic (ring and ball) or rheological properties but unique supramolecular structure.

As expected, the fluxing action of VO reduces the temperature transitions for both systems. This can be explained by an increase of the maltene part, and we could call it “Solvent effect”. In the case of Saudi bitumen, the bitumen with flux can be mistakenly considered as a real regenerating according to the ring and ball test or rheological investigations. However, using the ILT analysis of the NMR echo signal decay, distinction between a real rejuvenator and a simple softener can be made.

References

[1] B. Hofko, A. Cannone Falchetto, J. Grenfell, L. Huber, X. Lu, L. Porot, L.D. Poulikakos, Z. You, Effect of short-term ageing temperature on bitumen properties, Road Mater. Pavement Des. 18 (2017) 108–117.

[2] S.R. Bearsley, R.G. Haverkamp, Age hardening potential of tall oil pitch modified bitumen, Road Mater. Pavement Des. 8 (2007) 467–481.

[3] P. Jitsangigam, W. K. Biswas, M. Compton, Sustainable utilization of lime kiln dust as active filler in hot mix asphalt with moisture damage resistance, Sustain. Mater. Technol. 17 (2018).

[4] M. Simonen, T. Blomberg, T. Pellinen, M. Makowska, J. Valtonen, Curing and ageing of biofluxed bitumen: a physicochemical approach, Road Mater. Pavement Des. 14 (2013) 159–177.

[5] Q. Quin, J.F. Schabron, R.B. Boysen, M.J. Farrar, Field aging effect on chemistry and rheology of asphalt binders and rheological predictions for field aging, Fuel 121 (2014) 86–94.

[6] J. Hu, S. Wu, Q. Liu, M. García Hernández, Z. Wang, S. Nie, G. Zhang, Effect of ultraviolet radiation in different wavebands on bitumen, Constr. Build. Mater. 159 (2018) 479–485.

[7] N. Baldino, D. Gabriele, C. Oliviero Rossi, L. Seta, F.R. Lupi, P. Caputo, Low temperature rheology of polyphosphoric acid (PPA) added bitumen, Constr. Build. Mater. 36 (2012) 592–596.

[8] J.P. Planche, Insights into binder chemistry, microstructure, properties relationships—usage in the real world, in: Y.R. Kim (Ed.), Asphalt Pavements, CRC Press, 2014.

[9] X. Yu, M. Zaumanis, S. dos Santos, L.D. Poulikakos, Rheological, microscopic, and chemical characterization of the rejuvenating effect on asphalt binders, Fuel 135 (2014) 162–171.

[10] T.B. Moghaddam, H. Baaj, The use of rejuvenating agents in production of recycled hot mix asphalt: a systematic review, Constr. Build. Mater. 114 (2016) 805–816.

[11] J.B. Kròl, K.J. Kowalski, L. Niczke, P. Radziszewski, Effect of bitumen fluxing using a bio-origin additive and a rejuvenator, Constr. Build. Mater. 114 (2016) 194–203.

[12] F. Roberts, P. Kandhal, E.R. Brown, D.Y. Lee, T. Kennedy, Hot Mix Asphalt Materials, Mixture Design and Construction, 2nd ed., NAPA, Lanham, MD, 1996.

[13] M. Radenberg, S. Boetcher, N. Sedaghat, Effect and efficiency of rejuvenators on aged asphalt binder – German experiences, 6th Eurasphalt & Eurobitume Congress 1-3 June 2016 (2019), https://doi.org/10.14311/EE.2016.051.

[14] L. Jin, H. Xiaosheng, Z. Yuzhen, X. Meng, Bitumen colloidal and structural stability characterization, Road Mater. Pavement Des. 10 (2009) 45–59.

[15] P. Calandra, D. Caschera, V. Turco, L.D. Lombardo, How self-assembly of amphiphilic molecules can generate complexity in the nanoscale, Colloids Surf. A Physicochem. Eng. Asp. 484 (2019) 164–183.

[16] A. Grilli, M. Iorio Gnisci, M. Bocci, Effect of ageing process on bitumen and rejuvenated bitumen, Constr. Build. Mater. 163 (2017) 474–481.

[17] L. Gentile, C. Oliviero Rossi, U. Olsson, G.A. Ranieri, Effect of Shear Rates on the MLV Formation and MLV Stability Region in the C12E5/D2O System: rheology and Rheo-NMR and Rheo-SANS Experiments, Langmuir 27 (6) (2011) 2088–2092.

[18] L. Coppola, L. Gentile, I. Nicotera, C. Oliviero Rossi, G.A. Ranieri, Evidence of formation of ammonium perfluorononanoate/2H 2O multilamellar vesicles: morphological analysis by rheology and Rheo-2H NMR experiments, Langmuir 26 (24) (2010) 19060–19065.

[19] L.L. Barbosa, F.V.C. Kock, R.C. Silva, J.C.C. Freitas, V. Lacerda Jr., E.V.R. Castro, Application of Low-Field NMR for the determination of physical properties of petroleum fractions, Energy Fuels 27 (2013) 673–679.

[20] N. Baldino, C. Oliviero Rossi, F.R. Lupi, D. Gabriele, Rheological and structural properties at high and low temperature of bitumen for warm recycling technology, Colloids Surf. A Physicochem. Eng. Asp. 532 (2017) 592–600.

[21] C. Oliviero Rossi, P. Caputo, G. De Luca, L. Maiuolo, S. Eskandarsefat, C. Sangiorgi, ^{1}H-NMR spectroscopy: a possible approach to advanced bitumen characterization for industrial and paving applications, Appl. Sci. (2018).

[22] K.H. Altgelt, M.M. Boduszynski, Composition and Analysis of Heavy Petroleum Fractions, Marcel Dekker Inc., New York, 1994.

[23] C. Oliviero Rossi, P. Caputo, V. Loise, D. Miriello, B. Teltayev, R. Angelico, Role of a food grade additive in the high temperature performance of modified bitumens, Colloids Surf. A Physicochem. Eng. Asp. 532 (2017) 618–624.

[24] H.A. Barnes, J.F. Hutton, K. Walters, An Introduction to Rheology, Elsevier Science, Amsterdam, 1989.

[25] J.C. Jansen, M. Macchione, C. Oliviero Rossi, R. Mendichi, G.A. Ranieri, E. Drioli, Rheological evaluation of the influence of polymer concentration and molar mass distribution on the formation and performance of asymmetric gas separation membranes prepared by dry phase inversion, Polymer 46 (2005) 11366–11379.

[26] F.R. Lupi, A. Shakeel, V. Greco, C. Oliviero Rossi, N. Baldino, D. Gabriele, A

rheological and microstructural characterisation of bigels for cosmetic and pharmaceutical uses, Mater. Sci. Eng. C 69 (2016) 358–365.
[27] H.Y. Carr, E.M. Purcell, Effects of diffusion on free precession in nuclear magnetic resonance experiments, Phys. Rev. 94 (3) (1954) 630–638.
[28] L. Gentile, L. Filippelli, C. Oliviero Rossi, N. Baldino, G.A. Ranieri, Rheological and H-NMR spin-spin relaxation time for the evaluation of the effects of PPA addition on bitumen, Mol. Cryst. Liq. Cryst. 558 (2012) 54–63.
[29] A. Muhammad, R.B.D.V. Azeredo, ^{1}H NMR spectroscopy and low-field relaxometry for predicting viscosity and API gravity of Brazilian crude oils – A comparative study, Fuel 130 (2014) 126–134.
[30] V. Bortolotti, R.J.S. Brown, P. Fantazzini, UpenWin: A Software to Invert Multi-exponential Relaxation Decay Data, Distributed by the University of Bologna, 2009, villiam.bortolotti@unibo.it.
[31] C. Oliviero Rossi, A. Spadafora, B. Teltayev, G. Izmailova, Y. Amerbayev, V. Bortolotti, Polymer modified bitumen: rheological properties and structural characterization, Colloids Surf. A Physicochem. Eng. Asp. 480 (2015) 390–397.
[32] F.E. Antunes, E.F. Marques, M.G. Miguel, B. Lindman, Polymer – vesicle association, Adv. Colloid Interface Sci. 147 – 148 (2009) 18–35.
[33] P. Calandra, P. Caputo, M.P. De Santo, L. Todaro, V. Turco Liveri, C. Oliviero Rossi, Effect of additives on the structural organization of asphaltene aggregates in bitumen, Constr. Build. Mater. 199 (2019) 288–297.
[34] P. Calandra, A. Longo, A. Ruggirello, V. Turco Liveri, Physico-Chemical Investigation of the State of Cyanamide Confined in AOT and Lecithin Reversed Micelles, J. Phys. Chem. B 108 (24) (2004) 8260–8268.
[35] P. Calandra, C. Giordano, A. Ruggirello, V. Turco Liveri, Physicochemical investigation of acrylamide solubilization in sodium bis(2-ethylhexyl)sulfosuccinate and lecithin reversed micelles, J. Colloid Interface Sci. 277 (2004) 206–214.
[36] P. Calandra, G. Di Marco, A. Ruggirello, V. Turco Liveri, Physico-chemical investigation of nanostructures in liquid phases: Nickel chloride ionic clusters confined in sodium bis(2-ethylhexyl) sulfosuccinate reverse micelles, J. Colloid Interface Sci. 336 (2009) 176–182.
[37] P. Calandra, T. de Caro, D. Caschera, D. Lombardo, L. Todaro, V. Turco Liveri, Spectroscopic and structural characterization of pure and FeCl3-containing tri-n-butyl phosphate, Colloid Polym. Sci. 293 (2015) 597–603.
[38] P. Calandra, A. Ruggirello, A. Mele, V. Turco Liveri, Self-assembly in surfactant-based liquid mixtures: Bis(2-ethylhexyl)phosphoric acid/bis(2-ethylhexyl)amine systems, J. Colloid Interface Sci. 348 (1) (2010) 183–188.
[39] P. Calandra, V. Turco Liveri, P. Riello, I. Freris, A. Mandanici, Self-assembly in surfactant-based liquid mixtures: Octanoic acid/Bis(2-ethylhexyl)amine systems, J. Colloid Interface Sci. 367 (2012) 280–285.
[40] P. Calandra, A. Mandanici, V. Turco Liveri, Self-assembly in surfactant-based mixtures driven by acid–base reactions: bis(2-ethylhexyl) phosphoric acid–n-octylamine systems, RSC Adv. 3 (2013) 5148–5155.
[41] P. Calandra, A. Mandanici, V. Turco Liveri, M. Pochylski, F. Aliotta, Emerging dynamics in surfactant-based liquid mixtures: Octanoic acid/bis(2-ethylhexyl) amine systems, J. Chem. Phys. 136 (6) (2012) 064515.
[42] Eva Remišová, V. Zatkaliková, F. Schlosser, Study of rheological properties of bituminous binders in middle and high temperatures, Civ. Environ. Eng. 12 (1) (2016) 13–20.
[43] K.S. Osman, S.E. Taylor, Insight into liquid interactions with fibrous absorbent filter media using low-field NMR relaxometry. Prospective application to water/jet fuel filter – coalescence, Ind. Eng. Chem. Res. 56 (2017) 14651–14661.
[44] D.W. Christensen, D.A. Anderson, Rheological evidence concerning the molecular architecture of asphalt cements, Proc. Chem. Bitumen 2 (1991) 568–595 Rome.

Chapter 8

NMR Diffusiometry Spectroscopy, a Novel Technique for Monitoring the Micro-Modifications in Bitumen Ageing

Applied Sciences 2020, 10; doi:10.3390/app10165409

applied sciences

MDPI

Article

NMR Diffusiometry Spectroscopy, a Novel Technique for Monitoring the Micro-Modifications in Bitumen Ageing

Paolino Caputo [1], Dlshad Shaikhah [2,3], Michele Porto [1,*], Valeria Loise [1,*], Maria Penelope De Santo [4] and Cesare Oliviero Rossi [1]

1 Department of Chemistry and Chemical Technologies, University of Calabria, 87036 Arcavacata di Rende (CS), Italy; paolino.caputo@unical.it (P.C.); cesare.oliviero@unical.it (C.O.R.)
2 Institute of Functional Surfaces, School of Mechanical Engineering, University of Leeds, Woodhouse Lane LS2 9JT, UK; D.M.Shaikhah@leeds.ac.uk
3 Department of Chemistry, College of Science, Salahaddin University-Erbil, Erbil 44002, Kurdistan
4 Department of Physics and CNR-Nanotec, University of Calabria, via Bucci 31C, 87036 Arcavacata di Rende (CS), Italy; maria.desanto@fis.unical.it
* Correspondence: michele.porto@unical.it (M.P.); valeria.loise@unical.it (V.L.); Tel./Fax: +39-0984492045

Received: 9 July 2020; Accepted: 29 July 2020; Published: 5 August 2020

Abstract: In the past three decades, several conventional methods have been employed for characterizing the bitumen ageing phenomenon, such as rheological testing, ultraviolet testing, gel permeation chromatography (GPC), gas chromatography (GC), atomic force microscopy (AFM), X-ray scattering, and Fourier transform infrared spectroscopy (FTIR). Nevertheless, these techniques can provide only limited observations of the structural micro-modifications occurring during bitumen ageing. In this study, Fourier transform nuclear magnetic resonance self-diffusion coefficient (FT-NMR-SDC) spectroscopy, as a novel method, was employed to investigate and compare the microstructural changes between virgin bitumen (pristine bitumen) and aged bitumen. The virgin bitumen was aged artificially using two standard ageing tests: Rolling Thin-Film Oven Test (RTFOT) and Pressure Ageing Vessel (PAV). For a comprehensive comparison and an assessment of the validity of this method, the generated samples were studied using various methods: rheological test, atomic force microscopy, and optical microscopy. Significant differences were obtained between the structure and ageing patterns of virgin and aged bitumen. The results indicate that the modification of maltenes to asphaltenes is responsible for the ageing character. When compared with the other methods' findings, FT-NMR-SDC observations confirm that the asphaltene content increases during ageing processes.

Keywords: aged bitumen; NMR diffusiometry; rheology; AFM

1. Introduction

The most widely used road material in the world is asphalt. As this product possesses the desired industrial characteristics (waterproof and excellent thermoplasticity), it is widely employed in the construction industry, mainly in road construction and other paved areas [1]. From the chemical point of view, an asphalt is defined as a heterogenous system consisting of macro-meter-sized inorganic particles, known as aggregates, and a binder material called bitumen [2]. Bitumen is a heavy hydrocarbon material, and it is the by-product of the fractural refinement process of crude oil, which removes the lighter fractions (i.e., liquid petroleum gas, gasoline, and diesel) [3].

Traditionally, bitumen is defined as a colloidal system consisting of micelles of high polarity and molecular mass known as asphaltene; these are the solid particles behaving as adhesive aggregates.

Richardson defined the asphaltenes as insoluble in naphtha but soluble in carbon tetrachloride and also introduced the term "carbenes" for the fraction insoluble in carbon tetrachloride but soluble in carbon disulphide [4]. The word "carboids" for the part insoluble in carbon disulphide is also seldom used [5] (although not used by Richardson [4]). In all cases, these two additional fractions are present in very limited amounts in paving-grade bitumen [6] and are generally not mentioned in the road industry. Asphaltene aggregates remain in an oily apolar environment of lower molecular weight, known as maltenes, granting fluidity [7]. The apolar maltene phase, in turn, is composed of saturated paraffins, aromatic oils, and resins. Figure 1 shows a schematic splitting of bitumen into its main components. The proposed model of bitumen in the literature is that the asphaltene, in the form of polar nano-aggregates, remains dispersed as a peninsula or group of peninsulas within a more apolar continuous maltene phase [8]. In the conventional colloidal model, the resins-to-asphaltenes ratio characterizes the bitumen behavior to a specific path if the bitumen is in solution (sol). Sol bitumen is due to a high maltene concentration that leads to rapid relaxation modes (a liquid-like system), while the bitumen is gelatinous (gel) when the asphaltene concentration is dominant, resulting in slow relaxation modes [9].

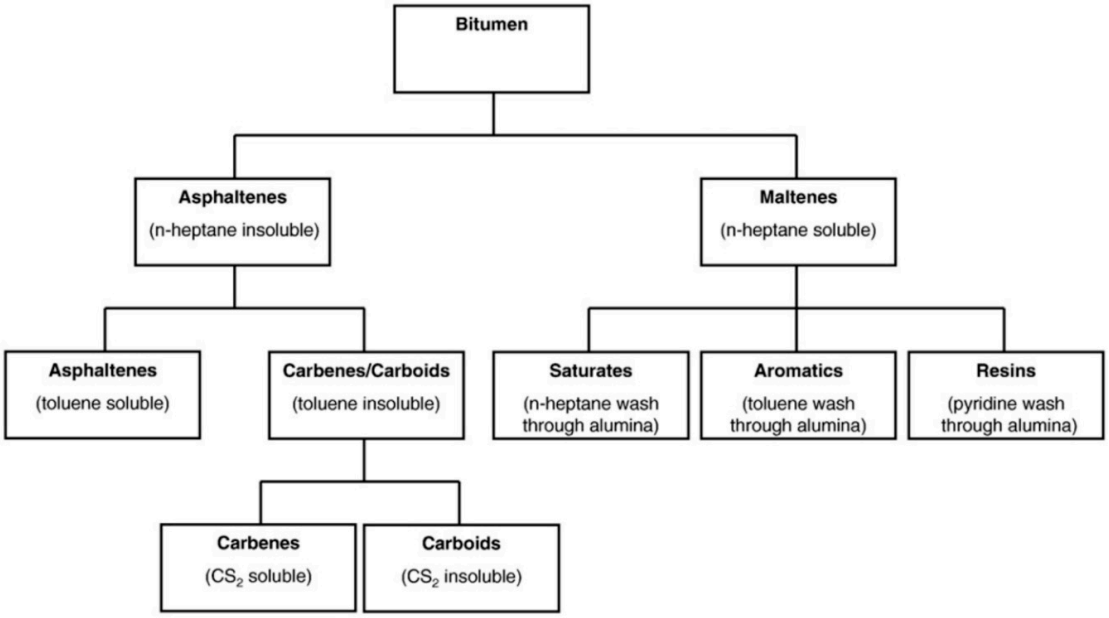

Figure 1. Bitumen separation into its various constituents, highlighting the SARA (saturates, aromatics, resins, asphaltenes) distribution, reproduced from [10], Copyright Elsevier, 2020.

In bitumen, resins are the dispersing agents for asphaltene molecules, combining them with aromatics and saturates; this produces the conditions for asphaltic flow. In fact, the chemistry of bitumen is the key element to defining its physical properties: following the analogy with reversed micelles in water-in-oil microemulsions [11], the stabilization of the polar domains is of pivotal importance for determining both the structure and the properties of the overall aggregates of organic-based materials [12,13], even if, it must be pointed out, the stabilization mechanism is quite general, spanning from organic materials to inorganic complexes [14] and even nanoparticles [15]. Due to these strict relationships between intermolecular interactions, the aggregates' structure, and their dynamic properties, the rheology (ductility at a given temperature/frequency) and behavior of bitumen are dependent not only on its structure, but also on the maltene's glass transition temperature and the effective asphaltene content [10].

When it comes to the bitumen structure, the microstructural model offers a typical point of view. It describes the system as a complex solution of evenly distributed molecules, classifying them according to their molecular weight and polarity; these behaviors are the key to grasping whether

the bitumen is modified. As there are millions of such constituents within the bitumen, its chemical analysis is usually performed based on the molecular structure type, not by studying the constituents individually [16]. Any technique, therefore, that differentiates the types of molecules or fractions within narrower properties would be a more effective form of analysis.

The stiffness and viscosity of asphalt pavement and its corresponding bitumen increase with time while it is in service; this is called the ageing phenomenon. As this phenomenon is responsible for the chemical modifications occurring in each fraction of bitumen, it is one of the most important factors impacting the bitumen structure. Asphalt research is currently directed towards the construction of new road pavements using milled reclaimed asphalt pavement (RAP) with consequent advantages both economically and environmentally. To use RAP in a bituminous conglomerate, it is necessary to add additives termed "Rejuvenating". The search for these additives is simply based on the evaluation of their effect on the mechanical performance of the final conglomerate. Having more information on the effect of the bitumen ageing process will make it possible to design these additives by identifying molecules containing functional groups which can interact in a targeted manner with aged bitumen components, thus regenerating them.

Generally, the ageing process is divided into two stages: short-term ageing and long-term ageing [17]. The former results from the loss of volatile components from the bitumen's maltene due to mixing at high temperature in the pristine paving process or during asphalt construction. The latter, in turn, occurs in the field, owing to the following factors: oxidation of bitumen components by atmospheric oxygen, evaporation of low-molecular-weight components of maltene, and polymerization between the bitumen's components. These processes induce greater stiffness and viscosity of the bitumen, which ultimately hardens the material, causing potential cracking and loss of its binding efficiency [16].

In the laboratory, different artificial standard methods for simulating the ageing phenomenon have been introduced. The Rolling Thin-Film Oven Test (RTFOT) and Thin-Film Oven Test (TFOT) techniques are considered short-term ageing as they simulate bitumen ageing during storage, mixing, transport, and placing as pavement. Meanwhile, to simulate long-term ageing, ultraviolet testing (UV) and Pressure Ageing Vessel (PAV) are employed. In this study, RTFOT and PAV are used as short- and long-term ageing simulation techniques, respectively [18].

As the outcome of ageing is crucial, a vast number of studies, using various perspectives and theories, have explored a range of parameters or factors relating to this phenomenon. Different in situ techniques have been used in the laboratory to evaluate, analyze, and identify what actually occurs inside bitumen during the ageing process [9]. These studies or techniques, however, are mainly measuring a specific factor of a material; this raises a challenge to identify all the feasible variables and forms of the material to study the bitumen ageing process, for either short-term ageing or long-term ageing.

The ageing phenomenon impacts not only the rheology of binders but also the structural chemistry; thus, there are numerous techniques to characterize this phenomenon, such as softening point (EN 1427 [19]), penetration test (EN 1426 [20]), and viscosity (EN 13302 [21]). As explained above, the process of ageing causes an increase in stiffness and viscosity but reduces the bitumen penetration grade. Thus, from this point of view, it is feasible to establish an ageing index by measuring the variation of the abovementioned physical properties (before and after ageing). This parameter has proven to be the most exemplary measure with regard to the results observed in the field [22].

It is important to note that assessing bitumen's physical and mechanical properties allows indirect macro-structural analysis of the binder. To measure these properties, the most commonly used techniques are dynamic shear rheology (DSR), softening point test, penetration test, and Brookfield or rotational viscosity determination [9]. Additionally, a variety of perspectives are utilized through a range of evaluation techniques to explain changes in asphalt materials after ageing. These techniques include Fourier transform infrared spectroscopy (FTIR) [23], spectrophotometry [24], X-ray scattering spectroscopy [25,26], gel permeation chromatography (GPC) [27], thin-layer chromatography with

flame ionization detection (TLC-FID) [28], atomic force spectroscopy (AFM) [29] and self-diffusion Pulsed Field Gradient Spin-Echo (PGSE) nuclear magnetic resonance (NMR) [30]. NMR spectroscopy is one of the most authentic and efficient techniques used to characterize complex materials i.e., bitumen. It is a conventional tool in the characterization of synthetic and natural products, wherein the structural and conformational behavior of their flexible molecules are investigated using anisotropic media [31]. In dynamic NMR characterization, the determination of self-diffusion coefficients can provide data about self-assembly [32,33], molecular dynamics, and spatial dimensions of cavities [34] and aggregates [35–38].

In this study, Fourier transform (FT) NMR self-diffusion coefficient measurements were performed on bitumen samples in order to have a better understanding of their molecular mobility and microstructure modification due to ageing; then, the measurements were compared with the results of rheological testing, AFM, and optical microscopy for validation. Ultimately, obtaining more information on the ageing process will provide consequent advantages in the design of rejuvenating additives and in understanding the structural organization of aged bitumen.

2. Materials

The pristine bitumen (PB) was kindly supplied by Total Italia S.p.A. (Italy) and produced in Saudi Arabia. It was used as a fresh standard with penetration grade 50/70 as measured by the usual standardized procedure [39]. Essentially, the standard needle is loaded with a weight of 100 g, and the length travelled into the bitumen specimen is measured in tenths of a millimeter for a known time, at a fixed temperature.

The chemical composition of the bitumen in terms of saturates, aromatics, resins, and asphaltenes (SARA) is reported in Table 1.

Table 1. Group composition of pristine bitumen.

Sample	% *w/w*
Saturates	4
Aromatics	51
Resins	22
Asphaltenes	23

2.1. Sample Preparation

In order to produce simulated short-term and long-term ageing samples, pristine bitumen (PB) was aged artificially via two conventional techniques: Rolling Thin-Film Oven Test (RTFOT) and Pressure Ageing Vessel (PAV). The RTFOT simulation was used for three ageing terms (75 min, 150 min, and 225 min) as per ASTM D2872, whereas the PAV simulation was performed on the virgin binder for a long term as specified in ASTM D6521. The sample IDs of RTFOT-aged binders were adopted based on their ageing time (BRTFOT-75, BRTFOT-150, and BRTFOT-225), while the PAV-aged binder was named BPAV.

2.2. Asphaltene and Maltene Separation (Modified Conventional Method)

To perform optical microscopy measurements, asphaltenes were isolated from the bitumen in the manner described elsewhere [40]. Chloroform and n-pentane were used as solvents to separate the maltenes and the asphaltenes.

3. Methodology

3.1. Rheological Characterization

The performance grades of the binders were determined using a dynamic shear rheometer (DSR) to quantify the viscoelastic properties in the temperature range 25–100 °C. The rheological

measurements were performed by utilizing a shear-stress-controlled rheometer (DSR5000, Rheometrics Scientific, Piscataway, USA), set up with a plate geometry (gap = 2 mm and diameter ∅ = 25 mm). The temperature of the system was controlled by a Peltier system (±1 °C).

Temperature sweep (time cure) rheological tests were performed to analyze the mechanical response of modified bitumens versus temperature. Bitumen exhibits aspects of both elastic and viscous behaviors and is thus classified as a viscoelastic material [41,42]. DSR is a common and standard technique used to study the rheology of asphalt binders at high and intermediate temperatures [43,44].

Operatively, a bitumen sample was sandwiched between two parallel plates, one standing and one oscillatory. The oscillating plate was rotated accordingly with the sample and the resulting shear stress was measured.

During the tests, a periodic sinusoidal stress at constant frequency of 1 Hz was applied to the sample, and the resulting sinusoidal strain was measured in terms of amplitude and phase angle as the loss tangent (tan δ).

All experiments were conducted during the heating of the bitumen sample. The study of rheological characteristics, complex shear modulus, and phase angle was performed in a time cure test (1 Hz) with a heating ramp rate of 1 °C/min. Information on the linear viscoelastic character of materials was provided by small-amplitude dynamic tests through characterization of the complex shear modulus [45]:

$$G^*(\omega) = G'(\omega) + iG''(\omega) \quad (1)$$

where $G^*(\omega)$ is the complex shear modulus, $G'(\omega)$ is the storage (in-phase) component (Pascal, Pa), $G''(\omega)$ is the loss (out-of-phase) component (Pascal, Pa), and i is the imaginary parameter of the complex number. The definitions of the parameters are as follows:

- $G'(\omega)$ represents elastic and reversible energy;
- $G''(\omega)$ represents irreversible viscous dissipation of mechanical energy.

The linear response regime was acquired by reducing the applied stress amplitude for the viscoelastic measurements. All rheological analyses were achieved by applying stress within the viscoelastic region.

3.2. Optical Microscopy

A polarized Leica Digital Microscope Light Polarized (DMLP) Research Microscope equipped with a Leica DFC280 digital camera was utilized to track the melting behaviors and morphologies of the asphaltenes. A Mettler FP82 HThot stage with a Mettler FP90 temperature controller was applied to control the temperature profile. The sample was kept at constant temperature, for each investigated temperature, for 10 min before taking images.

3.3. Nuclear Magnetic Resonance (NMR) Characterization

NMR characterization was conducted using a Bruker 300 spectrometer. A range of temperatures—from 90 to 130 °C in 10 °C increments—was chosen to conduct NMR experiments to determine the self-diffusion coefficient (D) for each binder.

Using Fourier transform, the acquired NMR spectra were derived from the free induction decay (FID). In Figure 2, a typical ^{1}H-NMR spectrum of the bitumen is presented. The number of scans used in the pulsed NMR experiment was 8 with pulse width equal to $\pi/2$. The measurements of D were conducted using a Diff30 NMR probe. As the transverse relaxation time (T_2) is much shorter than the longitudinal relaxation time (T_1), the Pulsed Gradient Stimulated Spin Echo (PFG-STE) sequence was utilized [46,47]. This sequence comprises three radiofrequency (RF) pulses of 90 ($\pi/2$-τ_1-$\pi/2$-τ_m-$\pi/2$) and two gradient pulses that are performed after the first and third pulse RF. τ_1 and τ_m are the time

intervals between RF pulses (milliseconds). The echo appears at $2\tau_1 + \tau_m$, and the ECHO amplitude attenuation was derived from the equation below:

$$I\,(2\tau_1 + \tau_m) = I_0 e^{-\left[\frac{\tau_m}{T_1} + \frac{3\tau_1}{T_2} + (\gamma g \delta)^2\ \mathrm{D}(\Delta - \frac{\delta}{3})\right]} \quad (2)$$

where D is the self-diffusion coefficient, and I and I_0 are the signal intensities in the presence and absence of gradient pulses. The NMR characterization parameters applied in the experiments to investigate the samples were as follows: δ (2 ms), the gradient length pulse; Δ, diffusion delay time (30 ms); and g, the gradient amplitude (from 100 to 900 gauss/cm). The number of scans increased due to an increment in the number of repetitions. This NMR has a very low fitting standard deviation and good reproducibility of measurements, where the uncertainty of D is approximately 3%.

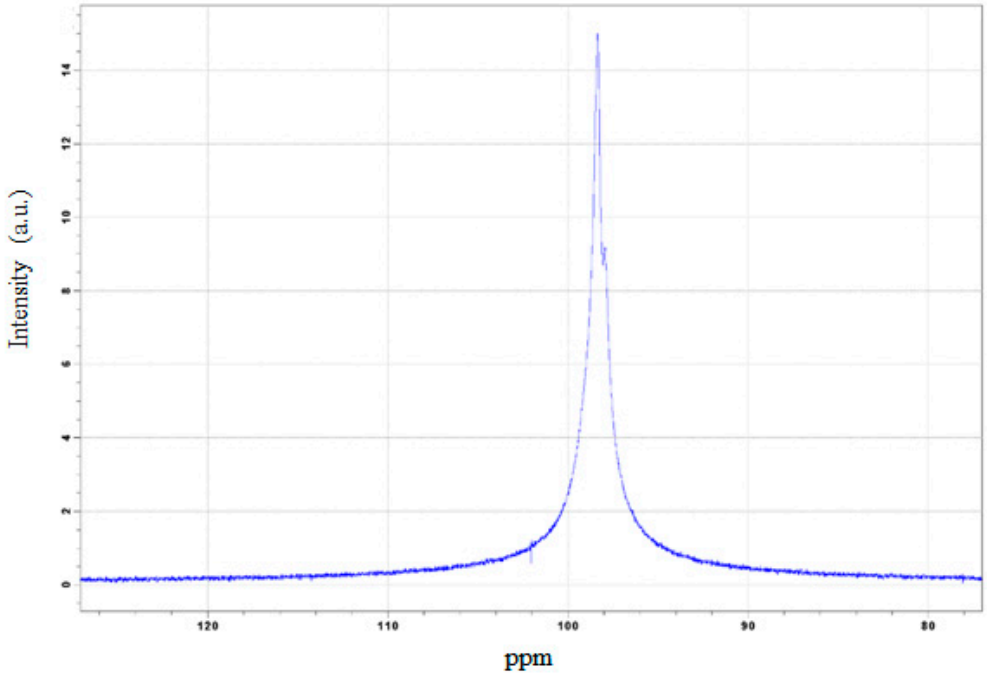

Figure 2. FT-NMR spin echo spectrum for the virgin bitumen.

According to the colloidal model, bitumen is generally composed of two principal constituents: asphaltene and maltene. The asphaltene is the rigid and polar part, which is characterized by high melting points. The maltene, in turn, is the soft and oily part that disperses the asphaltenes. Considering the low T_2 relaxation times of the asphaltenes [48], the self-diffusion coefficients can be attributed to the oily part of the bitumen; in fact, the NMR signal of asphaltenes relaxes during the pulse's application [49].

3.4. Atomic Force Microscopy (AFM)

Atomic force microscopy (AFM) was carried out using a Nanoscope VIII Bruker microscope which was operated in tapping mode. In this mode, the cantilever oscillates close to its resonance frequency (150 kHz) [50]. Since the cantilever oscillates up and down, the tip is in contact with the sample surface intermittently. When the tip is brought close to the surface, the vibration of the cantilever is influenced by the tip–sample interaction. The shift in the phase angle of the cantilever vibration implies energy dissipation in the tip–sample ensemble, so it depends upon the specific mechanical properties of the sample underlying the tip. For the measurements, cantilevers with elastic constants of 5 N/m and 42 N/m were used. Antimony-doped silicon probes (TAP150A, TESPA-V2, Bruker) with resonance

frequencies 150 kHz and 320 kHz, respectively, and nominal tip radius of curvature 10 nm were used. Phase images were acquired simultaneously with the topography.

4. Results and Discussion

4.1. Rheology

The below rheological plots illustrate consistent viscoelastic transition temperature (TR) trends among the binders (see Figures 3 and 4). It is worth noting that at low temperatures, PB shows a higher phase angle value when compared with aged samples; this indicates that PB has lower rigidity. The TR for each of the studied aged binders increased with ageing, which implies an increase in hardness. The effect of ageing on pristine bitumen shifted the TR depending on the duration of ageing; for instance, the TR values of the most-aged binders, BRTFOT-225 and BPAV, increased by approximately 25 °C in comparison with the neat bitumen. The phase angle, tan δ, increased with temperature, signalling a reduction in material consistency, which means that the prevalent liquid-like character is inclined with temperature [41]. In order to have a clearer image of the bitumen TR range and the structural modifications, temperature-sweep experiments were plotted in terms of the elastic modulus G'. This experiment was conducted at a frequency of 1 Hz and at a constant heating rate (1 °C/min). The binder's elastic modulus was observed continuously during a temperature ramp.

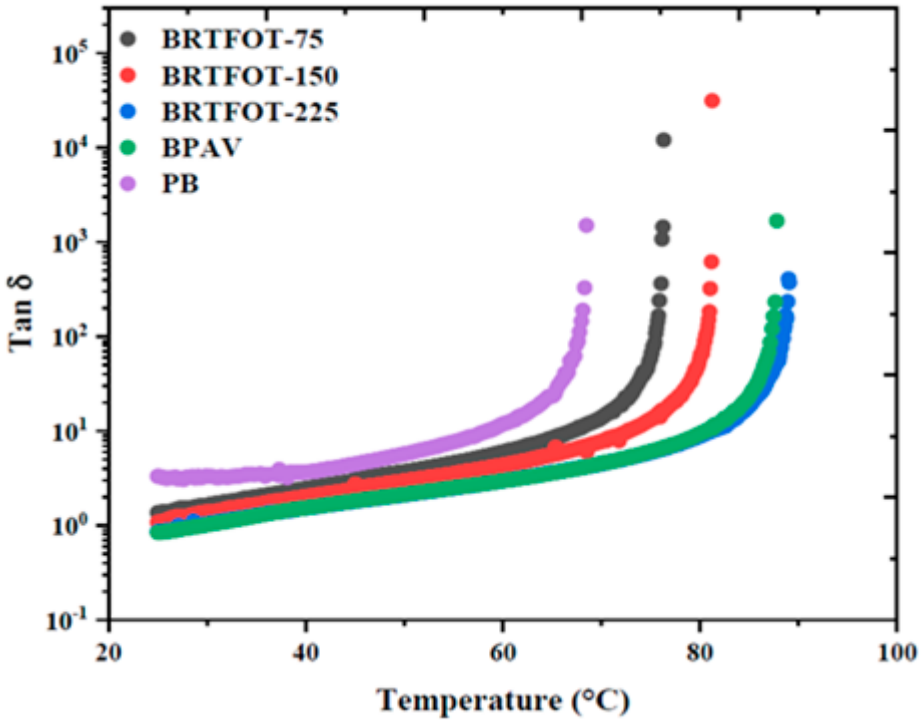

Figure 3. Temperature dependence (in the range 25 to 100 °C) of the loss tangent for pristine (PB) and aged bitumen samples (BRTFOT-75; BRTFOT-15; BRTFOT-225 and BPAV).

Figure 4 depicts the elastic modulus $G'(\omega)$ against temperature for all studied samples, in the temperature range 25 to 100 °C. In the temperature range 25–45 °C, the BRTFOT-75 and BRTFOT-150 binders had overlapped $G'(\omega)$ values, meaning their rigidity character is similar. At elevated temperatures, however, the aged binders showed higher $G'(\omega)$ values depending on their degree of ageing. For instance, PB had the lowest $G'(\omega)$ value in correlation with its tan δ value. After 60 °C for virgin bitumen and after 70 °C for aged binders, nonlinearity tended to appear in the trends, indicating the starting point of the TR region. When the elastic modulus is no longer detected, the transition

process from viscoelastic to a liquid regime can be considered complete, and this proves that the liquid-like behavior increases with temperature.

Interestingly, the viscoelastic responses of the PAV and RTFOT binders show similar rheological behavior. This analysis should prompt thinking that the two kinds of ageing processes (RTFOT 225 and PAV) could have similar effects on the structure and self-assembling properties of the binder.

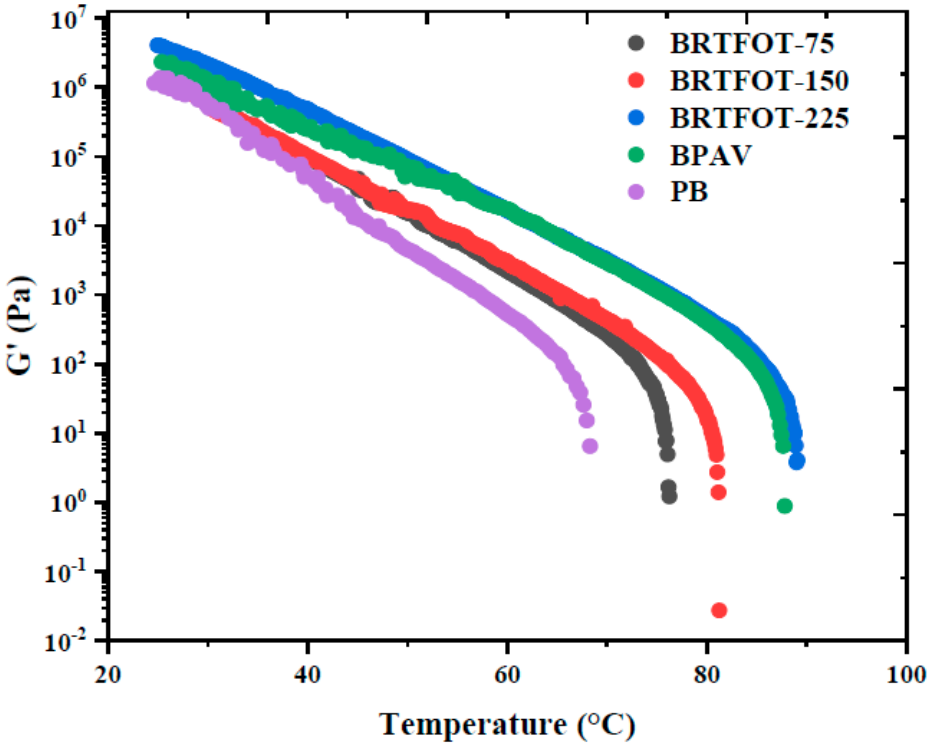

Figure 4. Temperature dependence (in the range 25 to 100 °C) of the elastic modulus for pristine and aged bitumen samples.

4.2. Optical Microscopy

The PB and BPAV samples were studied under optical microscopy since they were the softest and hardest samples among the investigated samples. In Figure 5, images of the PB and PAV asphaltenes are presented. The results imply that the BPAV binder is harder than the PB binder due to a higher concentration of asphaltenes.

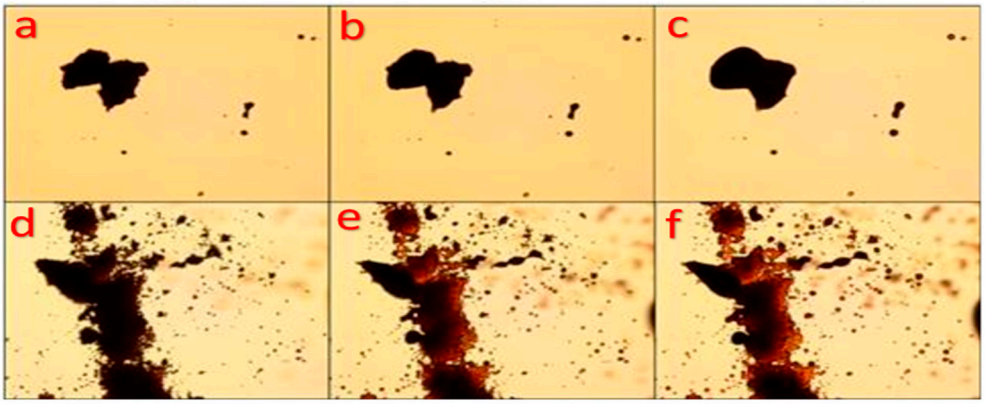

Figure 5. Optical microscopy (20×) images of PB (**a**–**c**) and PAV (**d**–**f**) asphaltenes at high temperature.

These images, obtained at 150 (a and d), 160 (b and e), and 165 °C (c and f), show the materials at different crystallization stages. The high-temperature stage of the experiment also shows the melting point of the crystallized material near 160 °C for the PB asphaltenes, while the material is partially melted at 165 °C for the BPAV sample, where the crystals are almost lost.

These novel results reveal two crucial points: First, the asphaltenes are solid at temperatures lower than 150 °C. Secondly, the asphaltene phase of virgin bitumen holds a different assembling structure to aged bitumen.

4.3. Fourier Transform NMR Self-Diffusion Coefficient Test

An advanced molecular investigation was conducted using NMR in order to analyze the chemical ageing processes and microstructural modification. As previously mentioned, Fourier transform (FT) NMR self-diffusion coefficient (SDC) allows insight into the bitumen microstructure by detecting the long-range mobility of the mixture constituents. The determination of motion over long distances, in comparison with ideal micelles, provides a sensitive probe for the state of aggregates [47,51]. It is crucial to note that the SDC values of asphaltene molecules cannot be detected owing to the short transverse relaxation times of their protons; so, hereafter, the measured SDC values are related to the maltene phase.

The observation of self-diffusion is based on the mobility of molecules. The motion of these molecules can be hindered due to the obstruction they face during their mobility in media. These typical data, observed where the motion occurs, can be considered as a fingerprint of the microstructural behavior.

In this study, the SDC data for each sample were investigated within the temperature range of 90–130 °C, increasing in increments of 10 °C at a time, as per Figure 6. The SDC data are related to the maltene part since at this temperature the asphaltenes are solid, meaning that their signals are not visible on the NMR spectrum after a spin echo sequence. According to this chart, the SDC values for binders decreased with ageing at each specific temperature. This effect is due to the stronger rigidity in aged bitumen which unavoidably involves stronger intermolecular connectivity when compared to the less dense network of the virgin bitumen, where the asphaltene domains are poorly connected to each other. As a result of this aggregation-based process/modification, a progressive shift from the viscoelastic toward the liquid regime dominating the highest temperatures occurs. In this picture, the resin molecules, due to their amphiphilic nature, will tend to reduce the associative interactions between the asphaltene particles by interposing themselves between the asphaltenes and the maltenes. This phenomenon might be like that found in the deactivation of hydrophobic cross-links in hydrophobically modified polymers by surfactants [43].

The interaction of the apolar part of the resin (its apolar moiety) with the maltene phase drags the latter to more-hindered dynamics typical of the stiffened asphaltene-dominated structure. Another mechanism concurrently present may be the formation of direct interactions between the surfactant polar headgroup and polar parts of asphaltene. In fact, it has been recently highlighted that, in addition to polar and apolar interactions, further specific interactions between surfactants themselves with consequent peculiar self-assembly processes [52,53] dictate the final overall aggregation pattern [54] and the (usually slowed-down) dynamics [55,56]. As an overall result of the two processes above described, maltene molecules in aged binders showed lower SDC values. What remains to be seen is the reproducibility of this gradual difference between virgin and aged binders at even higher temperatures in future experiments. It is worth noting that the BPAV bitumen's SDC value is a little bit higher than that of BRTFOT-225. This result could be due to the different dimensions of the asphaltenes or different structural network morphology. The BRTFOT-225 asphaltenes are expected to be bigger and to provide a strong obstruction to the maltene molecules' mobility. This difference in behavior is also visible in both ageing techniques (RTFOT and PAV). This is an interesting finding, and it could be hypothesized that the FT-NMR-SDC technique can be used to investigate the effects induced by the ageing phenomenon in bitumen. In order to confirm this hypothesis, AFM morphological images

were employed. By raising the temperature, we also observed upward trends in SDC values for all binders; this can be attributed to the incremental liquefying (melting) of the solid constituents, which inclines the motion of molecular protons. Although there was a steady rise in SDC measurements by a degree for each 10 °C increment, they increased dramatically at 130 °C, reaching twice the values of the respective binders at 120 °C. The results mentioned above are the most relevant findings and perhaps the most significant, confirming that the FT-NMR-SDC technique can be utilized as a fingerprint for the characterization of microstructural behaviors of bitumen.

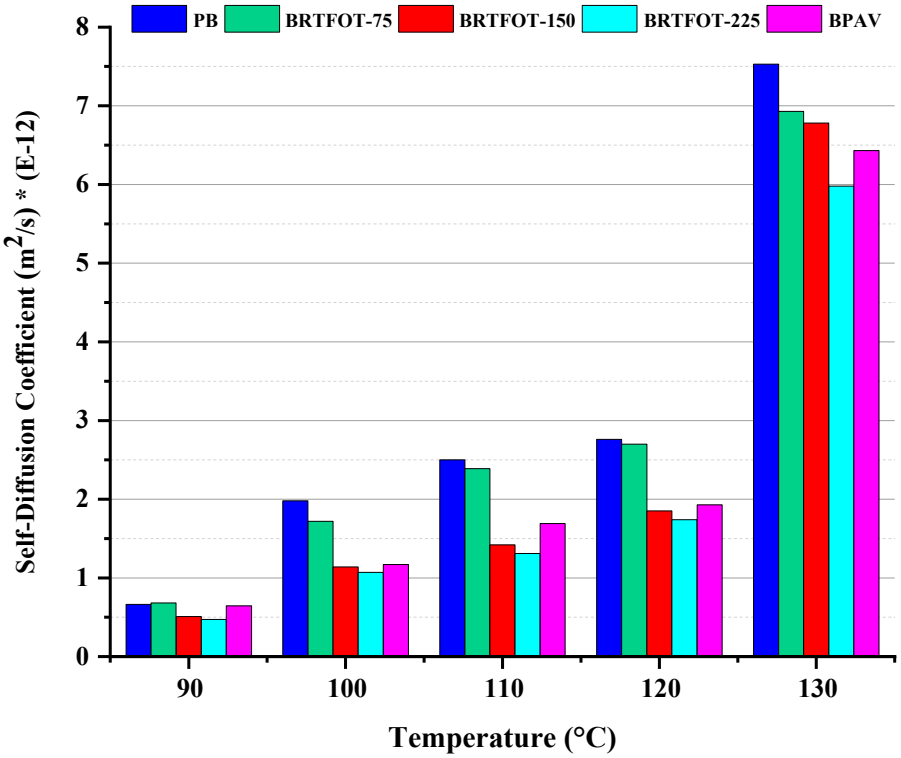

Figure 6. NMR self-diffusion coefficient characterization in the temperature range 90–130 °C for the different samples (PB, BRTFOT-75, BRTFOT-150, BRTFOT-225, and BPAV).

4.4. Atomic Force Microscopy (AFM)

AFM has been found to be a useful technique in bitumen microscopic analysis. In this work, we aimed to analyze the AFM images regardless of the correlations between the bitumen structures at different ageing processes in AFM images.

AFM characterization was performed in tapping mode at room temperature in air on a Multimode 8. The AFM system equipped with a Nanoscope V controller (Bruker) provided simultaneous topography and phase imaging of the sample. The measurements of bitumen were performed using probes with a conical tip of nominal end radius 10 nm and a resonance frequency of 150 kHz.

Phase images can show the sample's viscoelastic properties and are useful for bitumen microscopic analysis because materials with different viscoelasticity are clearly distinguishable: soft domains appear dark, while the hard ones appear bright.

The AFM measurements in Figure 7 show that with increasing exposure time (RTFOT), the morphological structure of asphaltenes changes. More specifically, in the aged samples, we note the arising of progressively more oscillations in the AFM signal within each single cluster, a feature which is known as "bee structure" [57] and which denotes structuring of asphaltene clusters at the micrometer-length scale [50]. Moreover, the asphaltene domain size increased with ageing time. For instance, at BRTFOT-225, the domains were about 10 microns in length and 5 microns in width;

the AFM image of PAV bitumen instead revealed asphaltene domains smaller than those observed in BRTFOT-225, homogeneously dispersed on the sample surface.

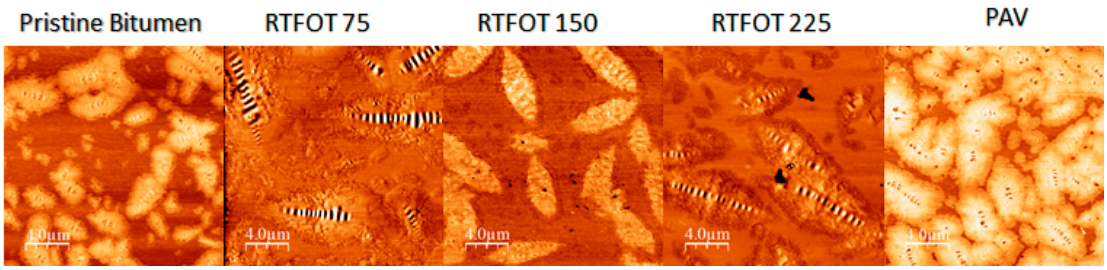

Figure 7. AFM phase images of PB, BRTFOT-75, BRTFOT-150, BRTFOT-225, and BPAV.

It must be pointed out that asphaltene clusters as they are seen by optical microscopy (length scales of micrometers) are the overall, long-range result of asphaltene molecules' hierarchical aggregation occurring at different length scales [50], for which different kinds of intermolecular interactions, from strong and short-range to weak and long-range, are involved. Among these, however, polar–polar interactions are expected to play the major role, since amphiphilic molecules can effectively bind, through their polar moiety, the polar groups of the dispersed molecules or the interfacial polar groups if the molecules are dispersed as clusters, as in the case of asphaltenes in the bitumen. So, a change of the cluster structure can be expected if the polar interactions are strong enough to trigger competition between asphaltene–asphaltene interactions and asphaltene–additive interactions, competition which has been found to be typical at the nanoscale in complex systems [58]. In light of this observation, atomic force microscopy can be seen additionally as a technique to indirectly probe the interactions taking place at shorter length scales, allowing us to explain, in the present work, the trends observed by FT-NMR-SDC. AFM images show the structural morphology of the bitumen, and they allow us to understand where maltene molecular mobility occurs. Considering the RTFOT ageing, the decrease in self-diffusion coefficients at all temperatures is apparently due to an increase in the size of asphaltenes, while the BPAV image clearly shows a different structural morphology from that in the image of BRTFOT-225.

5. Conclusions

In summary, ageing produces fundamental modifications in the colloidal structure of bitumen. Ageing also causes oxidation of bitumens and, consequently, increases the content of large molecules and the bitumen's molecular weight; these changes increase with ageing time. The two conventional ageing processes (RTFOT and PAV) modified the colloidal system of the bitumen, and both showed a certain level of asphaltene content. The RTFOT ageing, for different exposure times, changed the asphaltene structure in a consistent way, while the PAV ageing created a new colloid structural network. From the tangent loss and elastic modulus results, the rheological properties of the aged binders were found to be dependent on bitumen oxidation and changes in microstructures. The impact of these varies with the amount of ageing.

From the optical microscopy results, we concluded that the microstructural assembly of asphaltenes in unaged and aged bitumen is different, which is consistent with our FT-NMR-SDC observations. The core of this investigation was focused on using FT-NMR-SDC to track changes in the chemical functionalities of an unmodified binder and four types of aged binders manufactured with the same bitumen subjected to RTFOT/PAV ageing conditions. Most interestingly, this technique showed strong ability to monitor the ageing processes and to highlight the structural differences induced during ageing. The AFM results indirectly confirmed what was obtained via the FT-NMR-SDC technique by showing that the size of asphaltenes in aged bitumens is increased when compared with the size of asphaltenes in unaged bitumen.

The latter results provide new information in addition to that already present in the scientific literature regarding the subject, providing a more complete picture of the ageing process, in particular, on how the ageing techniques used in the laboratory affect the chemical structure of bitumen. This new information can be used in future research for the creation of new rejuvenating additives that are even higher performance than those currently on the market.

Author Contributions: Conceptualization, M.P. and C.O.R.; Writing-Original draft preparation P.C. and D.S.; Writing-review and Editing M.P.; Formal analysis V.L. and M.P.D.S.; Investigation P.C. and M.P.D.S.; Supervision C.O.R. All authors have read and agreed to the published version of the manuscript.

Funding: This research received no external founding.

Conflicts of Interest: The authors declare no conflicts of interest.

References

1. Huang, S.C.; Di Benedetto, H. *Advances in Asphalt Materials*; Elsevier: Dordrecht, The Netherlands, 2015. [CrossRef]
2. Speight, J.G. *Asphalt Materials Science and Technology*; Elsevier: Dordrecht, The Netherlands, 2016. [CrossRef]
3. Fahim, M.A.; Alsahhaf, T.A.; Elkilani, A. *Fundamentals of Petroleum Refining*; Elsevier: Dordrecht, The Netherlands, 2010. [CrossRef]
4. TH, B. The modern asphalt pavement. *Nature* **1905**, *72*, 316. [CrossRef]
5. Speight, J.G. *The Chemistry and Technology of Petroleum*; CRC Press: Boca Raton, FL, USA, 2014. [CrossRef]
6. Fischer, K.A.; Schram, A. The constitution of asphaltic bitumen. In Proceedings of the 5th World Petroleum Congress, New York, NY, USA, 30 May–5 June 1959; pp. 259–271.
7. Thurston, R.R.; Knowles, E.C. Asphalt and Its constituents. Oxidation at service temperatures. *Ind. Eng. Chem.* **1941**, *33*, 320–324. [CrossRef]
8. Loise, V.; Caputo, P.; Porto, M.; Calandra, P.; Angelico, R.; Oliviero Rossi, C. A Review on bitumen rejuvenation: Mechanisms, materials, methods and perspectives. *Appl. Sci.* **2019**, *9*, 4316. [CrossRef]
9. Tauste, R.; Moreno-Navarro, F.; Sol-Sánchez, M.; Rubio-Gámez, M.C. Understanding the bitumen ageing phenomenon: A review. *Constr. Build. Mater.* **2018**, *192*, 593–609. [CrossRef]
10. Lesueur, D. The colloidal structure of bitumen: Consequences on the rheology and on the mechanisms of bitumen modification. *Adv. Colloid Interface Sci.* **2009**, *145*, 42–82. [CrossRef] [PubMed]
11. Cautela, J.; Giustini, M.; Pavel, N.V.; Palazzo, G.; Galantini, L. Wormlike reverse micelles in lecithin/bile salt/water mixtures in oil. *Colloids Surf. A Physicochem. Eng. Asp.* **2017**, *532*, 411–419. [CrossRef]
12. Calandra, P.; Giordano, C.; Ruggirello, A.; Turco Liveri, V. Physicochemical investigation of acrylamide solubilization in sodium bis(2-ethylhexyl)sulfosuccinate and lecithin reversed micelles. *J. Colloid Interface Sci.* **2004**, *277*, 206–214. [CrossRef]
13. Calandra, P.; Longo, A.; Ruggirello, A.; Turco Liveri, V. Physico-chemical investigation of the state of cyanamide confined in AOT and lecithin reversed micelles. *J. Phys. Chem. B* **2004**, *108*, 8260–8268. [CrossRef]
14. Calandra, P.; Di Marco, G.; Ruggirello, A.; Liveri, V.T. Physico-chemical investigation of nanostructures in liquid phases: Nickel chloride ionic clusters confined in sodium bis(2-ethylhexyl) sulfosuccinate reverse micelles. *J. Colloid Interface Sci.* **2009**, *336*, 176–182. [CrossRef]
15. Longo, A.; Calandra, P.; Casaletto, M.P.; Giordano, C.; Venezia, A.M.; Liveri, V.T. Synthesis and physico-chemical characterization of gold nanoparticles softly coated by AOT. *Mater. Chem. Phys.* **2006**, *96*, 66–72. [CrossRef]
16. Petersen, J.C. *A Review of the Fundamentals of Asphalt Oxidation: Chemical, Physicochemical, Physical Property, and Durability Relationships*; Transportation Research Board: Washington, DC, USA, 2009. [CrossRef]
17. Ashimova, S.; Teltayev, B.; Oliviero Rossi, C.; Caputo, P.; Eskandarsefat, S. Organic-based recycling agents for road paving applications in cold-climate regions. *Int. J. Pavement Eng.* **2020**, 1–9. [CrossRef]
18. Caputo, P.; Loise, V.; Ashimova, S.; Teltayev, B.; Vaiana, R.; Oliviero Rossi, C. Inverse laplace transform (ILT) NMR: A powerful tool to differentiate a real rejuvenator and a softener of aged bitumen. *Colloids Surf. A Physicochem. Eng. Asp.* **2019**, *574*, 154–161. [CrossRef]

19. European Committee for Standardization. *EN 1427, Bitumen and Bituminous Binders—Determination of the Softening Point—Ring and Ball Method*; European Committee for Standardization: Brussels, Belgium, 2015; p. 18.
20. European Committee for Standardization. *EN 1426, Bitumen and Bituminous Binders—Determination of Needle Penetration*; European Committee for Standardization: Brussels, Belgium, 2007.
21. European Committee for Standardization. *EN 13302, Bitumen and Bituminous Binders—Determination of Dynamic Viscosity of Bituminous Binder Using a Rotating Spindle Apparatus*; European Committee for Standardization: Brussels, Belgium, 2010; p. 16.
22. Lin, J.; Hong, J.; Liu, J.; Wu, S. Investigation on physical and chemical parameters to predict long-term aging of asphalt binder. *Constr. Build. Mater.* **2016**, *122*, 753–759. [CrossRef]
23. Yao, H.; Dai, Q.; You, Z. Fourier transform infrared spectroscopy characterization of aging-related properties of original and nano-modified asphalt binders. *Constr. Build. Mater.* **2015**, *101*, 1078–1087. [CrossRef]
24. Hou, X.; Xiao, F.; Wang, J.; Amirkhanian, S. Identification of asphalt aging characterization by spectrophotometry technique. *Fuel* **2018**, *226*, 230–239. [CrossRef]
25. Tanaka, R.; Sato, E.; Hunt, J.E.; Winans, R.E.; Sato, S.; Takanohashi, T. Characterization of asphaltene aggregates using X-ray diffraction and small-angle X-ray scattering. *Energy Fuels* **2004**, *18*, 1118–1125. [CrossRef]
26. Caputo, P.; Loise, V.; Crispini, A.; Sangiorgi, C.; Scarpelli, F.; Oliviero Rossi, C. The efficiency of bitumen rejuvenator investigated through Powder X-ray Diffraction (PXRD) analysis and T2-NMR spectroscopy. *Colloids Surfaces A Physicochem. Eng. Asp.* **2019**, *571*, 50–54. [CrossRef]
27. Lee, S.-J.; Amirkhanian, S.N.; Shatanawi, K.; Kim, K.W. Short-term aging characterization of asphalt binders using gel permeation chromatography and selected Superpave binder tests. *Constr. Build. Mater.* **2008**, *22*, 2220–2227. [CrossRef]
28. Masson, J.-F.; Price, T.; Collins, P. Dynamics of bitumen fractions by thin layer chromatography/flame ionization detection. *Energy Fuels* **2001**, *15*, 955–960. [CrossRef]
29. Allen, R.G.; Little, D.N.; Bhasin, A. Structural characterization of micromechanical properties in asphalt using atomic force microscopy. *J. Mater. Civ. Eng.* **2012**, *24*, 1317–1327. [CrossRef]
30. Menapace, I.; Masad, E.; Papavassiliou, G.; Kassem, E. Evaluation of ageing in asphalt cores using low-field nuclear magnetic resonance. *Int. J. Pavement Eng.* **2016**, *17*, 847–860. [CrossRef]
31. Pauli, G.F.; Jaki, B.U.; Lankin, D.C. Quantitative 1 H NMR: Development and potential of a method for natural products analysis §. *J. Nat. Prod.* **2005**, *68*, 133–149. [CrossRef] [PubMed]
32. Cozzolino, S.; Galantini, L.; Leggio, C.; Pavel, N.V. Correlation between small-angle X-ray scattering spectra and apparent diffusion coefficients in the study of structure and interaction of sodium taurodeoxycholate micelles. *J. Phys. Chem. B* **2005**, *109*, 6111–6120. [CrossRef] [PubMed]
33. Galantini, L.; Giglio, E.; Leonelli, A.; Pavel, N.V. An integrated study of small-Angle X-ray scattering and dynamic light scattering on cylindrical micelles of sodium glycodeoxycholate. *J. Phys. Chem. B* **2004**, *108*, 3078–3085. [CrossRef]
34. Corain, B.; D'Archivio, A.A.; Galantini, L.; Lora, S.; Isse, A.A.; Maran, F. Electrochemical, pulsed-field-gradient spin-echo NMR spectroscopic, and ESR spectroscopic study of the diffusivity of molecular probes inside gel-type cross-linked polymers. *Chem. A Eur. J.* **2007**, *13*, 2392–2401. [CrossRef]
35. Aroulanda, C.; Celebre, G.; De Luca, G.; Longeri, M. Molecular ordering and structure of quasi-spherical solutes by liquid crystal NMR and Monte Carlo simulations: The case of norbornadiene. *J. Phys. Chem. B* **2006**. [CrossRef]
36. Celebre, G.; Concistré, M.; De Luca, G.; Longeri, M.; Pileio, G. Intrinsic information content of NMR dipolar couplings: A conformational investigation of 1,3-Butadiene in a nematic phase. *ChemPhysChem* **2006**, *7*, 1930–1943. [CrossRef]
37. Di Pietro, M.E.; Aroulanda, C.; Merlet, D.; Celebre, G.; De Luca, G. Conformational investigation in solution of a fluorinated anti-inflammatory drug by NMR spectroscopy in weakly ordering media. *J. Phys. Chem. B* **2014**, *118*, 9007–9016. [CrossRef]
38. Angelico, R.; Ceglie, A.; Olsson, U.; Palazzo, G.; Ambrosone, L. Anomalous surfactant diffusion in a living polymer system. *Phys. Rev. E* **2006**, *74*, 031403. [CrossRef]
39. Read, J.; Whiteoak, D.; Hunter, R.N. *The Shell Bitumen Handbook*, 5th ed.; Thomas Telford Ltd.: London, UK, 2003. [CrossRef]

40. Oliviero Rossi, C.; Caputo, P.; De Luca, G.; Maiuolo, L.; Eskandarsefat, S.; Sangiorgi, C. 1H-NMR spectroscopy: A possible approach to advanced bitumen characterization for industrial and paving applications. *Appl. Sci.* **2018**, *8*, 229. [CrossRef]
41. Barnes, H.A.; Hutton, J.F.; Walters, K. *An Introduction to Rheology*; Elsevier: Dordrecht, The Netherlands, 1989; Volume 3.
42. Olsson, U.; Börjesson, J.; Angelico, R.; Ceglie, A.; Palazzo, G. Slow dynamics of wormlike micelles. *Soft Matter* **2010**, *6*, 1769–1777. [CrossRef]
43. Oliviero Rossi, C.; Spadafora, A.; Teltayev, B.; Izmailova, G.; Amerbayev, Y.; Bortolotti, V. Polymer modified bitumen: Rheological properties and structural characterization. *Colloids Surf. A Physicochem. Eng. Asp.* **2015**, *480*, 390–397. [CrossRef]
44. Oliviero Rossi, C.; Caputo, P.; Loise, V.; Miriello, D.; Teltayev, B.; Angelico, R. Role of a food grade additive in the high temperature performance of modified bitumens. *Colloids Surf. A Physicochem. Eng. Asp.* **2017**, *532*, 618–624. [CrossRef]
45. Jansen, J.C.; Macchione, M.; Oliviero, C.; Mendichi, R.; Ranieri, G.A.; Drioli, E. Rheological evaluation of the influence of polymer concentration and molar mass distribution on the formation and performance of asymmetric gas separation membranes prepared by dry phase inversion. *Polymer* **2005**, *46*, 11366–11379. [CrossRef]
46. Stejskal, E.O.; Tanner, J.E. Spin diffusion measurements: Spin echoes in the presence of a time-dependent field Gradient. *J. Chem. Phys.* **1965**, *42*, 288–292. [CrossRef]
47. Coppola, L.; Oliviero, C.; Olsson, U.; Ranieri, G.A. Characterization of a reverse hexagonal lyomesophase by a PGSE NMR water self-diffusion study. *Langmuir* **2000**, *16*, 4180–4184. [CrossRef]
48. Filippelli, L.; Gentile, L.; Rossi, C.O.; Ranieri, G.A.; Antunes, F.E. Structural change of bitumen in the recycling process by using rheology and NMR. *Ind. Eng. Chem. Res.* **2012**, *51*, 16346–16353. [CrossRef]
49. Chidichimo, D.; De Fazio, G.A.; Ranieri, M.; Terenzi, M. Self-diffusion of water in a lamellar lyotropic liquid crystal: A study by pulsed field gradient NMR. *Chem. Phys. Lett.* **1985**, *117*, 514–517. [CrossRef]
50. Calandra, P.; Caputo, P.; De Santo, M.P.; Todaro, L.; Turco Liveri, V.; Oliviero Rossi, C. Effect of additives on the structural organization of asphaltene aggregates in bitumen. *Constr. Build. Mater.* **2019**, *199*, 288–297. [CrossRef]
51. Coppola, L.; Oliviero, C.; Pogliani, L.; Ranieri, G.A.; Terenzi, M. A self-diffusion study in aqueous solution and lyotropic mesophases of amphiphilic block copolymers. *Colloid Polym. Sci.* **2000**, *278*, 434–442. [CrossRef]
52. Calandra, P.; Ruggirello, A.; Mele, A.; Liveri, V.T. Self-assembly in surfactant-based liquid mixtures: Bis(2-ethylhexyl)phosphoric acid/bis(2-ethylhexyl)amine systems. *J. Colloid Interface Sci.* **2010**, *348*, 183–188. [CrossRef] [PubMed]
53. Calandra, P.; Turco Liveri, V.; Riello, P.; Freris, I.; Mandanici, A. Self-assembly in surfactant-based liquid mixtures: Octanoic acid/Bis(2-ethylhexyl)amine systems. *J. Colloid Interface Sci.* **2012**, *367*, 280–285. [CrossRef] [PubMed]
54. Calandra, P.; Mandanici, A.; Liveri, V.T. Self-assembly in surfactant-based mixtures driven by acid–base reactions: Bis(2-ethylhexyl) phosphoric acid–n-octylamine systems. *RSC Adv.* **2013**, *3*, 5148. [CrossRef]
55. Calandra, P.; Mandanici, A.; Turco Liveri, V.; Pochylski, M.; Aliotta, F. Emerging dynamics in surfactant-based liquid mixtures: Octanoic acid/bis(2-ethylhexyl) amine systems. *J. Chem. Phys.* **2012**, *136*, 064515. [CrossRef]
56. Calandra, P.; Mandanici, A.; Liveri, V.T. Dynamical properties of self-assembled surfactant-based mixtures: Triggering of one-dimensional anomalous diffusion in bis(2-ethylhexyl)phosphoric acid/ n -octylamine systems. *Langmuir* **2013**, *29*, 14848–14854. [CrossRef]
57. Jäger, A.; Lackner, R.; Eisenmenger-Sittner, C.; Blab, R. Identification of microstructural components of bitumen by means of atomic force microscopy (AFM). *PAMM* **2004**, *4*, 400–401. [CrossRef]
58. Calandra, P.; Caschera, D.; Turco Liveri, V.; Lombardo, D. How self-assembly of amphiphilic molecules can generate complexity in the nanoscale. *Colloids Surf. A Physicochem. Eng. Asp.* **2015**, *484*, 164–183. [CrossRef]

Chapter 9

Unravelling the role of a green rejuvenator agent in contrasting the aging effect on bitumen: A dynamics rheology, nuclear magnetic relaxometry and self-diffusion study

Colloids and Surfaces A 2020, 125182; doi:10.1016/j.colsufra.2020.125182

Colloids and Surfaces A 603 (2020) 125182

Contents lists available at ScienceDirect

Colloids and Surfaces A

journal homepage: www.elsevier.com/locate/colsurfa

Unravelling the role of a green rejuvenator agent in contrasting the aging effect on bitumen: A dynamics rheology, nuclear magnetic relaxometry and self-diffusion study

Valeria Loise[a], Paolino Caputo[a,*], Michele Porto[a,*], Bagdat Teltayev[b], Ruggero Angelico[c], Cesare Oliviero Rossi[a]

[a] Department of Chemistry and Chemical Technologies, University of Calabria, 87036, Arcavacata Di Rende, CS, Italy
[b] Kazakhstan Highway Research Institute, Nurpeisova Str., 2A, Almaty, 050061, Kazakhstan
[c] Department of Agricultural, Environmental and Food Sciences (DIAAA), University of Molise, Via De Sanctis 86100, Campobasso, CB, Italy

GRAPHICAL ABSTRACT

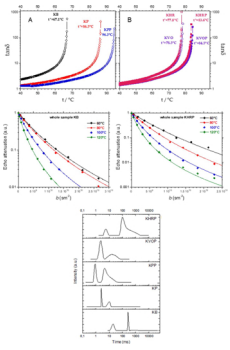

ARTICLE INFO

Keywords:
Recycled aged bitumen
Rejuvenator
Physical chemistry techniques
Reuse waste bituminous materials
RAP

ABSTRACT

This paper evaluated the potentialities of a green and biocompatible rejuvenator agent (HR) in conferring an appreciable resistance against the effects caused by artificial aging on a given bitumen. Both neat and aged bitumens were analyzed and compared to analogous samples modified with HR. Control samples containing a vegetable oil as softening agent were also tested for comparison. The tested samples were subjected to a second aging cycle. Structural differences between the samples were carried out through an inverse Laplace transform of the NMR spin-echo decay (T_2) and self-diffusion measurements by pulsed gradient spin echo nuclear magnetic resonance (PGSE-NMR) spectroscopy. In addition, dynamic rheological analyses were conducted to determine the dependence of the gel-sol transition temperature on both the type of additive and ageing process. The present study clearly highlighted the fact that artificial ageing, realized here by the rolling thin film oven test (RTFOT) and the pressure ageing vessel (PAV) test, induced important structural modifications. The analysis of relaxation times and self-diffusion coefficients indicated that ageing promoted the formation of molecular populations characterized by a shift of the distribution toward higher molecular weights compared to unaged bitumen. Diffusion data showed also an Arrhenius-like temperature dependence. A correlation between all the data was

* Corresponding authors.
E-mail addresses: paolino.caputo@unical.it (P. Caputo), michele.porto@unical.it (M. Porto).

https://doi.org/10.1016/j.colsurfa.2020.125182
Received 20 April 2020; Received in revised form 13 June 2020; Accepted 15 June 2020
Available online 16 June 2020

attempted to understand the role of the investigated additives. The eco-friendly biocompatible rejuvenator helped not only to restore the structure of the aged bitumen, but even slowed down the processes of a second aging (aiming at the first aged sample).

1. Introduction

One of the phenomena most responsible for the deterioration of the performance of road surfaces in the bituminous conglomerate is the oxidation of the binder, which occurs both during installation and throughout the lifetime of the road pavement [1]. Furthermore, in recent decades, the increase in traffic and the need to economically and ecologically dispose of material from old road pavements have led to searching for new materials and methods for recycle the road surface. Nowadays, one of the most important concern is the production of waste. The scientific community is working to make waste products recirculated. When aging, wear and adverse climatic events make the asphalts no longer safe, so the pavement must be replaced after a certain time in use [2]. The scarifying of the road surface produces the reclaimed asphalt binder, which is often regarded as a waste to dispose of. Fortunately, the waste asphalt mixture still contains valuable asphalt binder. The aged bitumen from this reclaimed asphalt pavement (RAP), has a lower penetration degree and is more viscous than when all pristine components are used [3]. However, the effect of aging can be delayed by using rejuvenating agents that have a distinct role from common softening agents [4]. Indeed, it is known by now that it is possible to exploit RAP using a rejuvenator capable to reduce stiffness, viscosity, brittleness, and restore the right balance between asphaltenes and maltenes characteristic of unaged bitumen.

Considering the accelerated aging methods, by aging thin films of bitumen in an oven at 163 °C, the rolling thin film oven test (RTFOT) simulates short-term aging in the laboratory that represents aging before the material is placed in the road [5]. The pressure aging vessel (PAV) uses temperature of 90–110 °C and a pressure 2.10 MPa to simulate long-term aging in the laboratory [6].

According to the classical colloidal model of bitumen, its general composition can be broadly subdivided into higher molecular weight asphaltenes dispersed in lower molecular weight maltenes, the latter being the n-heptane soluble part of bitumen, sometimes called deasphaltened bitumen [7]. Those class of compounds, collectively indicated as SARA (saturates, aromatics, resins and asphaltenes) fractions, are characterized by different sizes, aromaticity, and polarity, which can be hardly analysed individually [8]. Asphaltenes form a black powder and decompose when heated above 350 °C. The asphaltene fraction consists of large molecules containing hetero atoms like oxygen, nitrogen, sulphur and metal atoms. Resins are a black solid at room temperature and liquefy at higher temperature whereas saturates are a colourless viscous liquid, the amount of which (5 − 20 wt%) is not altered during ageing. Aromatics or naphthene aromatics appear yellow to dark brown, they constitute 30 − 60 wt% of bitumen and are more viscous than saturates. Their average molecular weight is of the order of a few thousands of Da and the averaged structure is composed by lightly condensed aromatic and naphthenic rings with side chains. All these ingredients are organized in supra-molecular assemblies whose structure resembles that of reversed micelles: clusters of asphaltene molecules piled in stacks (polar domains) are stabilized by resins (amphiphilic part) and dispersed in saturates and aromatics (apolar matrix). The role of resin is essential in the delicate equilibrium of intermolecular interactions (polar-polar, polar-apolar and van deer Waals interactions) which holds up the overall structure, since amphiphilic molecules are well-known to bind from a side the polar molecules clusters and from the other side the apolar phase [9,10].

In this framework, the chemical reactivity towards oxidation processes and loss of volatile hydrocarbons activated by heat, lead to a significant change in composition within the SARA fractions characterized by an increasing content of asphaltenes and decreasing content of aromatics during ageing, [11–14]. Moreover, due to oxidative aging, the molecular interactions change as well. The combined effect of these two processes affects the mechanical performances of bitumen and asphalt mixture behaviour [15]. As a consequence, insights on the microstructure evolution over the strength of oxidative treatment (steric hardening) could be monitored by measuring molecular dynamic properties such as NMR relaxation times and self-diffusion coefficients [16–18]. On the other hands, changes in bulk rheological properties, such as viscosity and sol-gel transition temperature turn to be useful for verifying the effect of age hardening and for controlling the rejuvenating action of specific additives [19,20].

The present paper aims to investigate the ability of the green rejuvenator HR, developed by the academic Spin-Off Kimical SRL (University of Calabria, Italy), to compensate for the microstructural deterioration effects observed in a bitumen subjected to multiple artificial aging processes. This study is important to understand the rejuvenating effect of a green additive specially designed to reduce the disposal of aged asphalt and promote sustainable practices for the recycling of reclaimed asphalt binder. Therefore, the potential use of HR in increasing the useful life cycle of the RAP is deeply described.

To highlight the real rejuvenating effect, control samples containing a vegetable oil (flux oil) were also tested.

All the bitumens were characterized by rheological time cure tests and NMR techniques such as proton relaxometry and measurements of self-diffusion coefficients. The inverse Laplace transform to the spin-echo decay (T_2) was carried out.

2. Experimental

2.1. Chemicals and materials

A pristine bitumen with a penetration grade 100/130 produced in Kazakhstan and supplied by Kazakhstan Highway Research Institute (Almaty, Kazakhstan) has been tested in this work. The vegetable oil VO and the rejuvenator eco-friendly additive HR were provided by Kimical SRL (Rende, Italy). HR was prepared by a direct reaction between low cost and green materials such as oleic acid and urea [21].

2.2. Sample preparations

Samples with differently ageing treatments, with or without VO and HR additives, were produced to allow a direct comparison of results. The analysed samples were initially subjected to artificial aging consisting of RTFOT + PAV according, respectively, to the standard methods ASTM D2872-04 and AASTHO/ASTM T179. Subsequently, the bitumen thus obtained was heated and mixed with the selected additives for 10 min under mechanical stirring. Finally, the samples were subjected to a further PAV aging cycle. For various states and aging conditions KB means virgin bitumen; KP and KPP mean, respectively, bitumen aged with the first treatment of RTFOT + PAV and subsequently subjected to a second PAV aging; KVO and KVOP mean, respectively, bitumen modified with VO (2 wt%) after being aged with RTFOT + PAV, and subjected to a second PAV treatment; KHR and KHRP mean, respectively, bitumen modified with HR (2 wt%) after being aged with RTFOT + PAV, and subjected to a second PAV treatment. A second series of samples consisted of maltene fractions (deasphaltened bitumens) extracted from the correspondent whole samples. In the text $(KB)^M$ means the maltene fraction extracted from KB sample; $(KP)^M$ and $(KPP)^M$ mean the maltene fractions extracted from samples

KP and KPP, respectively, and so on. The dosage of 2 wt% of additive was chosen according the literature data. In fact, it is a typical percentage for the modification of the bitumen [22]

2.2.1. Aging

The bitumen samples were artificially aged by means of the Rolling Thin Film Oven Test (RTFOT) according to ASTM D1754 with thermal treatment for 5 h at 163 °C, followed by 20 h of a pressure aging vessel PAV test according to ASTM D6521 (at 100 °C, 2.1 MPa). Details of the RTFOT and PAV method of aging is based on a previous research work done by the authors [21]. This procedure should mimic the aging process that would take place during the hot mixing of asphalt binder with aggregates, followed by the pavement construction phase and then the in-service life of asphalt pavement.

2.3. Empirical characterization

The bitumen softening temperature (R&B T, ring and ball temperature) is determined with the ring and ball test (ASTM Standard D36).

The bitumen consistency was evaluated by measuring the penetration depth (of a stainless-steel needle of standard dimensions under determinate charge conditions (100 g), time (5 s) and temperature (25 °C), according to the standard procedure (ASTM D946).

2.4. Rheological characterization

Temperature sweep (time cure) rheological characterization of the samples was performed by means of sinusoidal oscillatory experiments conducted through a controlled shear stress rheometer (SR5, Rheometric Scientific, USA) equipped with a parallel plate geometry (gap 2 mm, ø = 25 mm) and a Peltier system (± 0.1 °C) for temperature control. In a temperature sweep test, the frequency and the oscillation amplitude were kept constant, while the temperature was increased in some progression. The analysis of the mechanical behaviour of the selected binders was carried out within the Linear Visco-Elastic (LVE) region by measuring the complex modulus G* and viscosity η* and phase angle δ as a function of the temperature in the range 25–120 °C with a ramp of 1 °C/min and constant frequency of 1 Hz.

2.5. NMR measurement and inverse laplace transform (ILT)

The method is based on the application of the Carr-Purcell-Meiboom-Gill (CPMG) spin-echo pulse sequence as described in ref. [23]. ^{1}H NMR relaxation experiments were conducted at 15 and 30 °C both below and above the gel-sol the transition temperature (t*) determined for each sample through dynamic temperature ramp tests. Relaxation experiments were carried out by means of a custom-built NMR instrument that operates at a proton frequency of 15 MHz. In general, two peaks corresponding to T_2 relaxation time distribution can be observed, one peak at shorter T_2 times corresponding to the more rigid (asphaltenes), while other one at longer T_2 times corresponding to the maltene fraction. This finding has been proved in several research works. All details of the experimental procedure can be found in the following references [24–26].

2.6. PGSE NMR self-diffusion

The Pulsed Gradient Spin Echo (PGSE) NMR experiments performed on a Bruker 300 spectrometer have been described in detail elsewhere. The magnetic field gradient unit is electronically controlled and produces gradients g between 0 and 10 $T{\cdot}m^{-1}$ (0 and 1000 $G{\cdot}cm^{-1}$) with typical duration δ of 2 − 4 ms, and a diffusion observation time Δ typically of 20 − 30 ms. Experimental measurements of the self-diffusion coefficient (D) directly were made using a Diff30 NMR probe. The experiments were run in the PFG-STE (Pulsed Field Gradient Stimulated-Echo) echo version, using three 90° radio frequency pulses [17], because the transverse relaxation time (T_2) was much shorter than the longitudinal relaxation time (T_1). In an experimental run, δ and δ are kept constant and g is varied. Sixteen different values for g give 10 signal intensities measured as the area, after Fourier transformation of the free induction decay (FID) that are fit to the Eq. (4) to determine the mean self-diffusion coefficient, $\langle D \rangle$.

3. Results and discussion

3.1. Mechanical behaviour

The aging of the bitumen leads to an embrittlement of the binder, making it susceptible to fractures or cracking. From a microscopic point of view, the aging process leads to a loss of oily bitumen components,

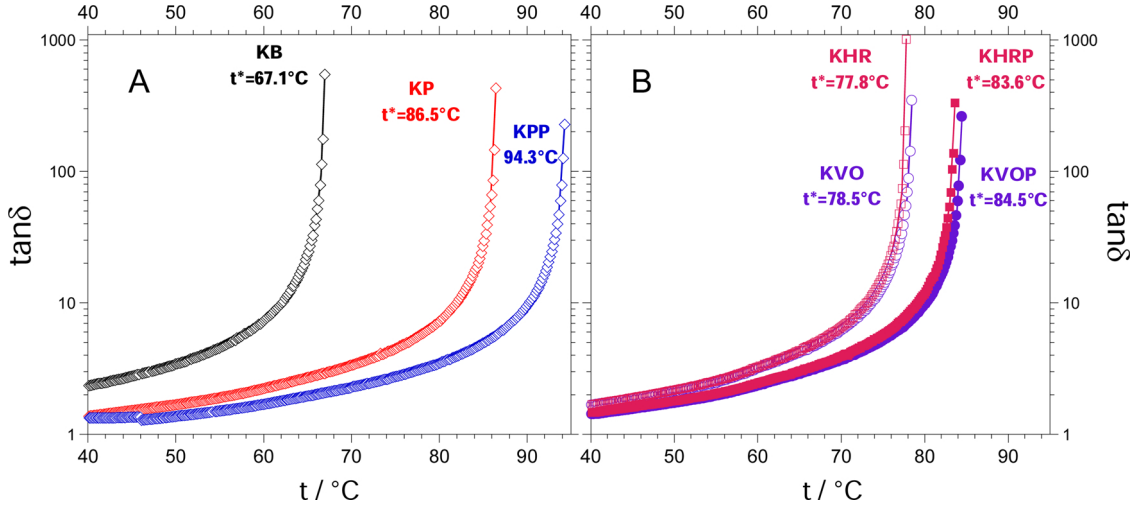

Fig. 1. (A) Temperature sweep (time cure) tests performed on the pristine bitumen (KB) and on the same sample after a first (KP) and second cycle (KPP) of artificial aging. The gel-sol transition temperature t*, estimated from the asymptotic value of the tangent of phase angle δ, is reported close to each curve. **(B)** Time cure tests for bitumens modified with 2 wt% of rejuvenating HR (hollow and full squares for KHR and KHRP, respectively) and softening VO (hollow and full circles for KVO and KVOP, respectively) additives. Hollow symbols indicate samples subjected to RTFOT + PAV aging whereas full symbols refer to the subsequent second PAV treatment. The gel-sol transition temperature t* is reported close to each curve.

due to the volatility or absorption by the porous aggregates. In addition, polar compounds increase due to polar groups containing oxygen. This is the cause of a loss of mobility on the part of molecules or molecular aggregates, which are no longer free to flow one on top of the other [27]. From the macroscopic point of view, a decrease in penetration depth is observed, while the softening point increases [28]. Moreover, the viscoelastic-liquid transition temperature increases with the aging process. In this research the dynamic material properties of bitumen samples have been tested through dynamic shear rheometer (DSR) analysis. The response to a mechanical stress-strain on materials such as bitumen are characterized by their elastic (G') and viscous (G") moduli. The loss factor tanδ is defined as the ratio between the viscous G" and elastic moduli G'. All these parameters depend on the temperature, in fact as the temperature increases tanδ increases too and diverges upon reaching a certain critical temperature value, called gel-sol transition temperature t*. This trend is due to the loss of the elastic component G' by the system, and consequently the viscous component G" becomes predominant. Fig. 1A and B show the time cure tests of the investigated samples in which the dependence of tanδ on the temperature is evident. In particular, t* shifts towards higher values along the sequence: untreated bitumen, bitumen aged by the first heating treatment (RTFOT + PAV) and bitumen aged by the second heating treatment PAV. Resins can be more polar than asphaltenes and govern the rheological properties together with asphaltenes [29]. Therefore, upon ageing, the bitumen is oxidized and as a consequence the polarity of the medium increases leading to increased interaction forces between the molecules. These conditions would favour the aggregation of asphaltenes by forming large molecular structures and causing a considerable hardening of the binder. As illustrated in Fig. 1A for bitumen not modified with additives, ageing causes a shift of t* towards higher temperatures, indicating a change in rheological behaviour which consists in a stiffness increase accompanied by an enhancement of elastic response (see the sequence KB→KP→KPP).

In Fig. 1B, the time cure tests for KHR and KHRP bitumens mixed with HR additive are compared to those modified with the softening agent VO (KVO and KVOP) at same 2 wt% dosage.

It is evident that both the one-step (KHR and KVO) and second-step (KHRP and KVOP) ageing treatments yield a similar rejuvenating effect since both additives are able to reduce t* by 8 − 9 °C and 10 − 11 °C in relation to the first (KP) and second (KPP) aging step, respectively.

3.2. NMR study

3.2.1. Diffusion coefficient

PGSE NMR self-diffusion measurements have been carried out for both the series of whole samples and maltene fractions, after one- and two-steps oxidative artificial treatments, to evaluate the effect of a rejuvenator additive on the observed molecular translational motion. We premise that the molecular species that contribute to the observed average self-diffusion coefficients and transversal relaxation times should be identified in the lighter components of the maltene fraction [30]. Previous studies have reported that a significant amount of the latter class of compounds tends to decrease with aging, converting to more polar and heavier molecules such as resins and asphaltenes [12,14,31]. Other works have revealed that after short- and long-term aging the content of resins in the bitumen remained practically constant whereas the oil content reduced up to 7 wt% and concomitantly the increase in asphaltenes content could reach about 6 wt% [32]. Therefore, the contribution to the observed translational diffusion can be reasonably attributed to the mobility of the oil components of maltene, namely, saturates and aromatics, which are liquid at the experimental temperatures in the range 60 − 120 °C whereas resins and asphaltenes constitute solid nuclei embedded in the oil. Owing to the molecular complexity of maltene, the correspondent NMR echo attenuation cannot be described by a single exponential function. Indeed, an exact explicit solution of the Bloch-Torrey equation is only available for unrestricted diffusion in the whole space for which the echo attenuation NMR signal *S(b)* takes the classical mono-exponential form [33]:

$$S(b) = S_0 e^{-bD} \tag{1}$$

where S_0 is the reference signal (without diffusion-weighting gradient), and the *b*-value is defined as $b = (\gamma g \delta)^2(\Delta - \delta/3)$ according to the Stejskal-Tanner profile, where $\Delta - \delta/3$ is the observation time. Varying either the gradient pulse strength (g) or pulse duration (δ) or Δ, one can access the diffusion coefficient *D* of freely diffusing molecules from the slope of a semi-logarithmic representation of Eq. (1). Any deviation from the mono-exponential decay of *S(b)* may be interpreted in terms of a phenomenological anomalous diffusion model [34]. Generally, the echo attenuation shows non-linear behaviour for molecules with a large degree of polydispersity. For polydisperse species which cannot be resolved due to their chemical shift, it is assumed that the signal attenuation is multi-exponential as a result of the mass-weighted distribution of diffusion coefficients.

Here, we apply a model where the *D*-values are distributed according to the following probability density function:

$$P_{\Gamma}(D, \kappa, \theta) = \frac{D^{\kappa-1}}{\theta^{\kappa}\Gamma(\kappa)} e^{-\frac{D}{\theta}} \tag{2}$$

where κ and θ are, respectively, the shape and scaling parameters and Γ is the Gamma function. Previous works [35,36] have discussed the usefulness of the Gamma model with regard to performance and consistency for the analysis of PFG NMR data, in comparison to more established approaches based on the stretched exponential and the log-normal distribution model. Assuming that *S(b)* can be described by an integral over a multi-exponential decay with self-diffusion coefficients *D* that respect the probability distribution of Eq. (2), one would have the following:

$$S(b, \kappa, \theta) = S_0 \int_0^{\infty} P_{\Gamma}(D, \kappa, \theta) e^{-bD} dD \tag{3}$$

where S_0 is the signal intensity for $b = 0$. As described in details in ref. [35], the analytical expression of the NMR signal attenuation can be obtained in a closed form to be used directly in a non-linear best-fitting

Table 1
Mean self-diffusion coefficient $\langle D \rangle_{t°C}$ and standard deviation $\sigma_{t°C}$ for whole samples at various temperatures, calculated from non-linear fits of the NMR echo decays (see Eq. (4)) according to the gamma distribution model. Data are expressed in 10^{-10} units. The last column shows the transition temperatures derived from rheological time cure tests. Legend: KB = pristine bitumen; KP = RTFOT + PAV bitumen; KVO = KP + VO (2 wt%); KHR = KP + HR (2 wt%); KPP = RTFOT + PAV aging, followed by a second PAV treatment; KVOP = KVO subjected by a second PAV; KHRP = KHR subjected by a second PAV.

whole sample	$\langle D \rangle_{60°C}/\sigma_{60°C}$	$\langle D \rangle_{80°C}/\sigma_{80°C}$	$\langle D \rangle_{100°C}/\sigma_{100°C}$	$\langle D \rangle_{120°C}/\sigma_{120°C}$	$t_{gel \rightarrow sol}$ (°C)
KB	2.3 / 1.0	2.5 / 1.1	4.0 / 2.0	7.1 / 3.8	67.1 (0.1)
KP	–	2.0 / 1.1	3.5 / 2.0	6.5 / 3.9	86.5 (0.1)
KVO	–	1.7 / 1.2	3.7 / 2.2	7.1 / 4.5	78.5 (0.1)
KHR	–	2.4 / 1.1	4.0 / 2.1	7.5 / 4.5	77.8 (0.1)
KPP	2.5 / 1.1	3.8 / 1.5	5.9 / 2.6	–	94.3 (0.1)
KVOP	1.0 / 0.7	1.7 / 1.2	3.6 / 5.2	9.1 / 12	84.5 (0.1)
KHRP	2.1 / 0.8	3.1 / 1.3	5.3 / 2.6	8.9 / 4.9	83.6 (0.1)

procedure with respect to the experimental data:

$$S(b, \kappa, \theta) = \frac{S_0}{(1 + \theta b)^{\kappa}} \quad (4)$$

Then, from the calculated best-fit parameters, namely, κ (dimensionless) and θ (m^2s^{-1}), the mean self-diffusion coefficient $\langle D \rangle = \kappa\theta$ and the distribution width or standard deviation $\sigma = \theta\sqrt{\kappa}$ can be obtained. Tables 1 and 2 collect both $\langle D \rangle$ and σ at various temperatures and referred, respectively, to the whole samples and to their correspondent maltene fractions. In Supporting Material, several plots showing the temperature dependence of $\langle D \rangle$ together with error bars correspondent to the width of distributions σ, have been collected for a better comparison between diffusion data illustrated in Tables 1 and 2.

Regarding the analysis of the echo attenuations, typical examples of the good agreement between NMR PFG signals and Gamma diffusion model are illustrated in Fig. 2 (whole samples) and Fig. 3 (maltene fractions), respectively. By comparing the data shown in Table 1 with the ones in Table 2, it is found that $\langle D \rangle < \langle D \rangle^M$ for all the samples at each explored temperature, with the exception of KHRP and $(KHRP)^M$ at t = 60 °C. This is the evidence that the molecular transport of oil within the whole bituminous samples is more hindered than the diffusive transport that occurs in the corresponding maltene fractions. It is plausible, in fact, that the diffusivity decreases through more restrictive structural regions such as the large supramolecular aggregates of asphaltenes and resins, which are instead absent in the maltene fractions.

From the analysis of diffusion data within the series of whole samples without additives, it can be noted that the datasets of both the unaged bitumen (KB) and bitumen subjected to one-step aging treatment (KP) match substantially the same $\langle D \rangle$ values when considering the width of the respective distributions as error bars ($\sigma_{t°C}$) (see Fig. S1A in Supporting Material). Besides, $\langle D \rangle$ for KPP appear shifted towards higher values with respect to both KB and KPP samples. The latter effect can be explained considering first that with aging, there is a drastic variation in the chemical composition and colloidal structure of the bitumen attributed to an increase in the content of asphaltenes, which in turn is a consequence of the conversion of polar aromatic molecules. During the oxidative ageing process, the concentration of polar functional groups increases, resulting in an immobilisation of large asphaltene molecules through intermolecular association. As it has been described before, this association promotes the formation of much larger molecular agglomerates and significantly increase the apparent molecular weight leading to higher viscosity. Besides, the high molecular weight populations increase slightly after RTFOT and significantly after PAV ageing. This behaviour is confirmed by the probability density profiles of the relaxation time distributions illustrated in the next Fig. 5 (see 3.3.1 NMR relaxometry), where the samples KP and KPP show two peaks shifted toward shorter times, the displacement of the peaks being greater with increasing the aging treatment. This behaviour indicates a gradually rise of the materials rigidity with the on-going of the oxidation process. Therefore, according to the above description, it can be argued that after the second accelerated aging treatment (KPP), the only species that possess high translational mobility and contribute most to the observed molecular transport should be low MW saturated compounds, which are inert to oxidation. However, in both KB and KP (mild aged) samples, the contribution of a significant fraction of larger molecules to the observed diffusional process is not negligible and causes a lowering of the mean diffusion coefficients.

The effect of type of additive on the artificially aged whole samples, can be inferred by comparing the diffusion data of Table 1 as well as by checking the graphical trends as a function of temperature (see Figs. S2A–S3A in Supporting Material). As far as VO additive is concerned, while no appreciable differences can be revealed between KVO, KP and KB, the two-step aging results to a decrease of diffusion data for KVOP sample with respect to the reference KB, especially at relatively low temperatures (KVOP < KB for both $\langle D \rangle_{60°C}$ and $\langle D \rangle_{80°C}$). This fact could indicate a substantial difference between the microstructures of both unaged KB and double-aged KVOP samples. Therefore, VO could not be classified as a real rejuvenating additive.

Different trends are observed for the samples modified with HR (KHR and KHRP) whose diffusion data as a function of temperature are also plotted together with those of virgin bitumen and bitumen aged without additive (KB, KP and KPP) as illustrated in Fig. S3A of Supporting Material. Here, the data for KHR match with those of KB while $\langle D \rangle$ values of KHRP are closer to KB data (compare $\langle D \rangle_{80°C}$ values in Table 1) than the sample without additives and subjected to same aging treatment (KPP). This evidence is consistent with a rejuvenating action exerted by the additive HR, which is able to disperse the large molecular agglomerations produced with the two-step aging, making the colloidal microstructure similar to that of virgin bitumen. Concerning the maltene fractions, data shown in Table 2 (see also the graphs illustrated in Figs. S2B–S3B in Supporting Material), reveal that $\langle D \rangle^M$ values obtained in presence of either VO or HR and relating to both stages of aging, coincide with those of the KP sample. On the other hands, the most evident differences are found for the maltene fractions derived from samples in absence of additives, where the diffusion data follow the sequence KB > KPP > KP (see also Fig. S1B in Supporting Material).

As a final observation, from the calculated standard deviations $\sigma_{t°C}$ of the correspondent Gamma distributions, it is observed that each whole sample shows an amplitude of the dispersion of $\langle D \rangle$ which widens with increasing temperature (see Table 1). A similar behaviour is reflected for $\langle D \rangle^M$ as well (see Table 2).

3.3. Temperature dependence

It is evident that the mean self-diffusion coefficients increase with increasing temperature as expected by the temperature dependence of diffusion described by the Arrhenius model. The Arrhenius equation expressed in its logarithmic form is:

$$ln\langle D \rangle = lnA - \frac{E_A}{RT} \quad (5)$$

where A is a pre-exponential factor assumed to be independent of absolute temperature T, E_A is the activation energy and R is the gas constant. The agreement to the Arrhenius behaviour within the explored range of temperatures is verified by analysing the semi-log plots of $\langle D \rangle$ *vs* T^{-1} as in Fig. 4A (whole samples) or $\langle D \rangle^M$ *vs* T^{-1} as in Fig. 4B (maltene fraction), respectively.

Due to the multicomponent origin of the self-diffusion coefficients determined for our samples, only mean activation energies $\langle E_A \rangle$ could be calculated from the slope of each Arrhenius plot. In the present context, $\langle E_A \rangle$ may be defined as the energy barrier that should be overcome when the oil component of bitumen (saturates and aromatics) moves from one surrounding environment to the another.

For the whole samples, $\langle E_A \rangle$ varies between 23 and 53 KJ·mol^{-1} whereas for the maltene fractions an average value of 40 ± 2 KJ·mol^{-1}

Table 2
Mean self-diffusion coefficient $\langle D \rangle^M_{t°C}$ and standard deviation $\sigma^M_{t°C}$ for maltene samples at various temperatures, calculated from non-linear fits of the NMR echo decays (see Eq. (4)) according to the gamma distribution model. Data are expressed in 10^{-10} units. Legend: each label identifies the maltene fraction extracted from the correspondent sample.

maltene fraction	$\langle D \rangle^M_{60°C}/\sigma^M_{60°C}$	$\langle D \rangle^M_{80°C}/\sigma^M_{80°C}$	$\langle D \rangle^M_{100°C}/\sigma^M_{100°C}$	$\langle D \rangle^M_{120°C}/\sigma^M_{120°C}$
$(KB)^M$	9.4 / 5.5	18 / 9.5	29 / 15	40 / 20
$(KP)^M$	2.0 / 1.8	3.7 / 2.5	7.9 / 5.2	16 / 11
$(KVO)^M$	1.7 / 1.5	4.5 / 4.0	–	16 / 12
$(KHR)^M$	2.5 / 2.2	4.2 / 2.8	8.8 / 6.0	17 / 12
$(KPP)^M$	3.3 / 2.1	7.8 / 4.7	15 / 8.2	28 / 14
$(KVOP)^M$	1.9 / 1.1	4.0 / 2.2	8.1 / 4.4	17 / 8.4
$(KHRP)^M$	1.6 / 0.9	4.7 / 2.1	9.8 / 4.9	19 / 8.9

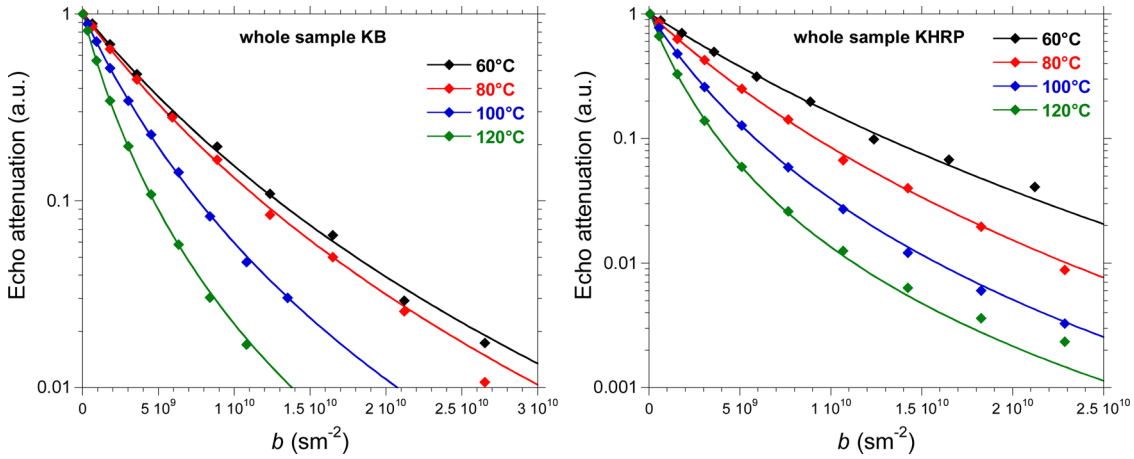

Fig. 2. Examples of semi-logarithmic plots of normalized experimental NMR PFG echo attenuations *vs* $b = (\gamma g \delta)^2(\Delta - \delta/3)$, acquired at various temperatures from the whole samples, respectively, KB (left) and KHRP (right). Solid lines represent non-linear best fits ($R^2 > 0.999$) using the Gamma distribution model (see Eq. (4)).

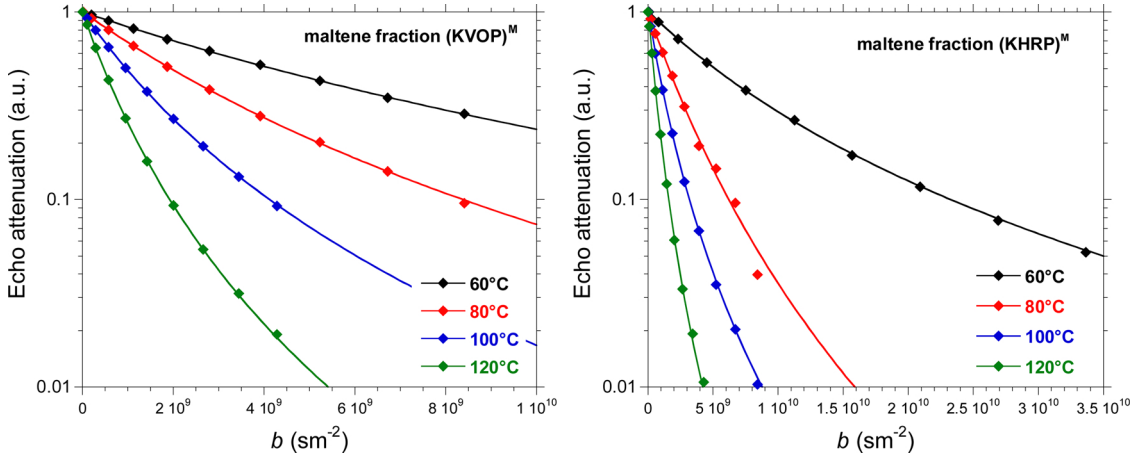

Fig. 3. Examples of semi-logarithmic plots of normalized experimental NMR PFG echo attenuations *vs* $b = (\gamma g \delta)^2(\Delta - \delta/3)$, acquired at various temperatures from the maltene fractions, respectively, $(KVOP)^M$ (left) and $(KHRP)^M$ (right). Solid lines represent non-linear best fits ($R^2 > 0.999$) using the Gamma distribution model (see Eq. (4)).

is estimated between all the values except that calculated for the original KB sample, as shown graphically in Fig. 4B by the parallelism of the straight lines. Since the fractions of maltene are devoid of the heavier molecular components, such as resins and mainly asphaltenes, it can be argued that the marked variability of $\langle E_A \rangle$ observed for the whole samples (Fig. 4A) may be attributable to the asphaltene/oil interactions, regarded as the major factor dictating the energy barrier of the diffusion. The rejuvenating effect promoted by the HR additive can

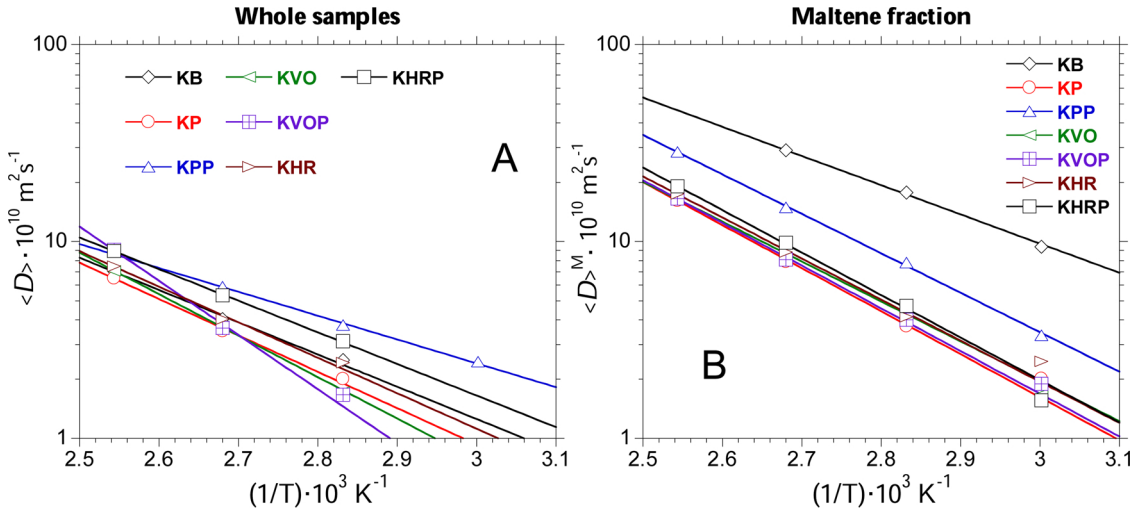

Fig. 4. Plot of the logarithm of the mean self-diffusion coefficients *vs.* the reciprocal of the absolute temperature for whole samples **(A)** and maltene fractions **(B)**, respectively. The straight lines were obtained from the Arrhenius fit with Eq. (5) and the mean activation energies were calculated from the respective slopes.

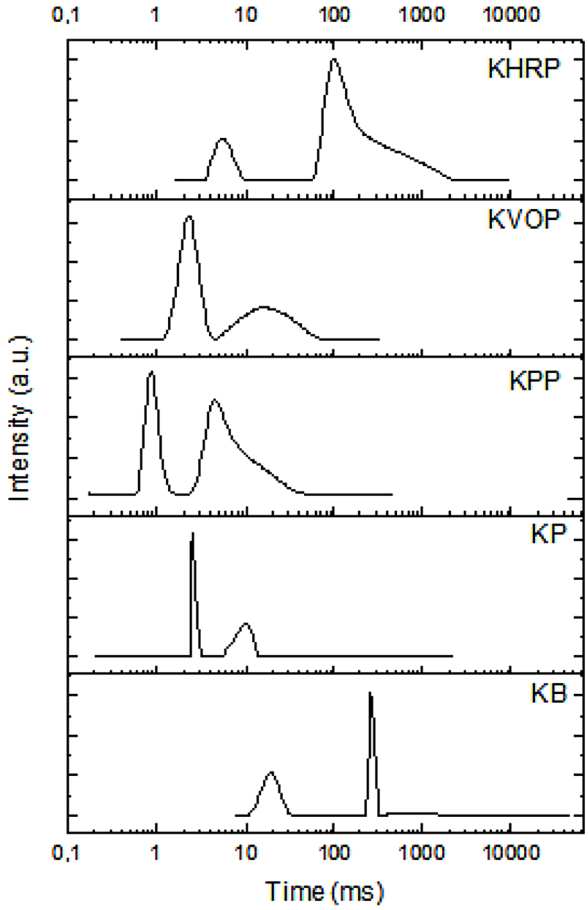

Fig. 5. Probability Density Function (PDF) distributions of T_2 relaxation times for the whole samples KB, KP, KPP, KVOP and KHRP determined at t* + 15 °C (**C**) where t* is the gel-sol the transition temperature for each sample.

be checked by comparing $\langle E_A \rangle$ of the pristine bitumen KB (31 ± 2 KJ·mol^{-1}) with those determined, respectively, for the KHR sample after the first RTFOT + PAV aging (34 ± 3 KJ mol^{-1}) and KHRP sample after the second PAV aging process (31 ± 1 KJ mol^{-1}). This means that upon artificial oxidation, HR is capable to restore in some way the interactions between the asphaltenic and maltenic phase typical of the unaged bitumen, confirming the clues derived from the diffusion coefficient data. In contrast, bitumen samples modified with the softening agent VO gave 40 ± 1 and 53 ± 4 KJ mol^{-1}, after the first RTFOT + PAV (KHR) and second PAV (KHRP) aging treatments, respectively.

In the light of all these results, it can be stated that the effective rejuvenating action exerted by HR with respect to the flux oil, can be interpreted as a consequence of the chemical nature of HR. Thanks to its complex/amphiphilic characteristic, HR would tend to reduce the associative interactions between the asphaltene particles by interposing itself between the asphaltenes and the maltenes. Such phenomenon can be considered similar to that exerted by the rheological modifier polyphosphoric acid (PPA), which has been found able to stabilize the hydrophobic interactions between asphaltene molecules, leading to a reduction of the macro-aggregate sizes [27].

It can be argued, taking for example the self-assembly properties of amphiphilic molecules, that the additive can effectively interact with the resins, competing with them for the interactions with asphaltenes and maltenes. Specific interactions between surfactants can in fact bring to peculiar self-assembly processes [37,38] giving extended amphiphilic network [39,40], which could help in dispersing/stabilizing asphaltene clusters restoring their original distribution.

3.3.1. NMR relaxometry

By applying the ^{1}H NMR relaxometry technique, the transverse (T_2) relaxation times have been determined for the whole bitumen samples subjected to the second PAV ageing treatment (KPP, KVOP and KHRP) as well as for the native bitumen and for the first RTFOT + PAV ageing treatment (KB, KP). In fluid systems, T_2 is dominated by molecular rotations and is sensitive to the local dynamics of the molecule that the proton is attached to (spin-spin interactions) and therefore reveals inhomogeneities in the system [41]. For our systems, the NMR echo decays are characterized by a multi-exponential behaviour and have been analysed by applying the Inverse Laplace Transform (ILT) to derive the T_2 distributions directly from the experimental signals. Fig. 5 collects the calculated Probability Density Function (PDF) distributions as a function of T_2 at a reference temperature characteristic for each of investigated samples, namely, at 15 °C above the gel-sol transition temperature t*.

Almost all the T_2 distributions exhibited two variously narrow or wide peaks, which could be ascribed to the more or less rigidity of supramolecular aggregates as well as to the molecular constrain causing dynamic hindrance [42]. In bitumen, supramolecular aggregates of asphaltene and resins possess average sizes of a few nanometers, as observed by several small-angle neutron and X-ray scattering measurements [43,44]. Therefore, the shorter T_2 may be reasonably attributed to the rigid supra-molecular aggregates constituted by asphaltenes and resins, while longer T_2 could be referred to the rotational dynamics of the lighter components of maltene fraction (saturates and aromatics) [23].

Since the aging process is responsible for shifting the distributions towards higher molecular weights and, that is, towards shorter relaxation times, bitumen modified with the HR agent appeared to benefit from its rejuvenating effect. At higher temperatures above the gel-sol transitions the samples are outside the viscoelastic region of the material and present various structural heterogeneities giving rise to more complicated T_2-distribution patterns.

The PDF distribution of the aged bitumens (KP and KPP) shows two peaks shifted toward shorter times, the displacement of the peaks being greater with increasing the aging process. This behaviour indicates a gradually rise of the materials rigidity with the on-going of the oxidation process.

The effect exerted by the two additives, VO and HR, is to move the peaks towards T_2 values higher than those of aged bitumens. In more details, the peak attributable to the asphaltenes of the KVOP sample is considerably more intense than that one referred to the maltenes and it is centred on asphaltenic peak of the KP sample. This indicates a softening effect of VO but no rejuvenating action occurs since the huge asphaltene peak does not change. On the other hand, KHRP and KB bitumen have similar distribution profiles. This indicate a sort of antioxidant effect of HR additives.

4. Conclusions

In this paper, the dynamic properties of bitumen samples subjected to different artificial aging processes have been tested through dynamic shear rheometer (DSR) analysis, NMR relaxometry and NMR diffusion measurements. The aim of this study was to develop a fundamental understanding on the role played by a rejuvenating green additive (HR) to compensate for the microstructural deterioration effects observed in a bitumen subjected to multiple artificial aging processes. Analogous control samples containing a softening agent (VO) were also tested as term of comparison between the performances exhibited by both the additives. The measurements of bulk rheological properties, such as viscosity and sol-gel transition temperature, were not sufficient to identify the real functionality of an additive. In fact, according to the rheological profiles, both the tested additives were found equally capable of counteracting the bitumen hardening induced by ageing processes.

NMR methodologies employed for investigating translational diffusion coefficients and relaxation times have been found useful to differentiate between the rejuvenating and antioxidant effect of HR compared to the mere fluxing effect of VO. Indeed, the analysis of the temperature dependence of diffusion data gave the indication that in response to artificial oxidation, HR was capable to restore somehow the interactions between the polar asphaltene molecules and maltene phase, typical of the unaged bitumen. As a consequence, a more efficient dispersion of large macro-molecular aggregates produced during the aging treatments was achieved for bitumen mixed with HR rather than VO. That property was confirmed by analysing the Probability Density Function (PDF) distributions acquired through Inverse Laplace Transform, as a function of relaxation times T_2 at a reference temperature above the gel-sol transition temperature t* characteristic for each of investigated samples. Indeed, the presence of HR in aged bitumen promoted a certain downsizing effect of the asphaltenes aggregates, identified by an evident shift of relaxation times to longer values. Such effect was not detected in the profile of the relaxation time distributions for aged samples in presence of VO, indicating the inability of VO to restore the initial colloidal distribution of bitumen. Overall, the results of the present work reinforce the potential use of the green rejuvenator HR in increasing the useful life cycle of the reclaimed asphalt pavement (RAP) and furnish more reliable and rigorous methodological approaches as useful tools for a correct interpretation of the effective action exerted by this important class of additives for asphalt binders.

CRediT authorship contribution statement

Valeria Loise: Investigation, Conceptualization. **Paolino Caputo:** Data curation, Methodology. **Michele Porto:** Data curation, Methodology. **Bagdat Teltayev:** Supervision. **Ruggero Angelico:** Writing - original draft. **Cesare Oliviero Rossi:** Supervision.

Declaration of Competing Interest

No affiliations with or involvement in any organization or entity with any financial interest (such as honoraria; educational grants; participation in speakers' bureaus; membership, employment, consultancies, stock ownership, or other equity interest; and expert testimony or patent-licensing arrangements), or non-financial interest (such as personal or professional relationships, affiliations, knowledge or beliefs) in the subject matter or materials discussed in this manuscript.

Appendix A. Supplementary data

Supplementary material related to this article can be found, in the online version, at doi:https://doi.org/10.1016/j.colsurfa.2020.125182.

References

[1] O. Sirin, D.K. Paul, E. Kassem, State of the art study on aging of asphalt mixtures and use of antioxidant additives, Adv. Civ. Eng. (2018), https://doi.org/10.1155/2018/3428961.

[2] M.F.C. Van De Ven, K.J. Jenkins, J.L.M. Voskuilen, R. Van Den Beemt, Development of (half-) warm foamed bitumen mixes: state of the art, Int. J. Pavement Eng. (2007), https://doi.org/10.1080/10298430601149635.

[3] M.C. Cavalli, M.N. Partl, L.D. Poulikakos, Measuring the binder film residues on black rock in mixtures with high amounts of reclaimed asphalt, J. Clean. Prod. (2017), https://doi.org/10.1016/j.jclepro.2017.02.055.

[4] V. Loise, P. Caputo, M. Porto, P. Calandra, R. Angelico, C.O. Rossi, A review on Bitumen Rejuvenation: mechanisms, materials, methods and perspectives, Appl. Sci. (Switzerland) 9 (2019), https://doi.org/10.3390/app9204316.

[5] ASTM, Effect of heat and air on a moving film of asphalt (rolling thin-film oven test), Standard Test Method for Effect of Heat and Air on a Moving Film of Asphalt (Rolling Thin-Film Oven Test), (2004), https://doi.org/10.1520/D2872.

[6] ASTM D6521, Standard practice for accelerated ageing of asphalt binder using a pressurized ageing vessel (PAV), Annual Book of American Society for Testing Materials Standards, (2008), https://doi.org/10.1520/D6521-08.Copyright.

[7] D. Lesueur, The colloidal structure of bitumen: consequences on the rheology and on the mechanisms of bitumen modification, Adv. Colloid Interface Sci. (2009), https://doi.org/10.1016/j.cis.2008.08.011.

[8] J.G. Speight, The Chemistry and Technology of Petroleum, (2006), https://doi.org/10.1201/9781420008388.

[9] P. Calandra, A. Longo, A. Ruggirello, V.T. Liveri, Physico-chemical investigation of the state of cyanamide confined in AOT and lecithin reversed micelles, J. Phys. Chem. B (2004), https://doi.org/10.1021/jp0492422.

[10] P. Calandra, C. Giordano, A. Ruggirello, V.T. Liveri, Physicochemical investigation of acrylamide solubilization in sodium bis(2-ethylhexyl)sulfosuccinate and lecithin reversed micelles, J. Colloid Interface Sci. (2004), https://doi.org/10.1016/j.jcis.2004.04.021.

[11] X. Lu, U. Isacsson, Effect of ageing on bitumen chemistry and rheology, Constr. Build. Mater. (2002), https://doi.org/10.1016/S0950-0618(01)00033-2.

[12] M. Paliukaitė, A. Vaitkus, A. Zofka, Influence of bitumen chemical composition and ageing on pavement performance, Balt. J. Road Bridge Eng. (2015), https://doi.org/10.3846/bjrbe.2015.12.

[13] S. Dessouky, C. Reyes, M. Ilias, D. Contreras, A.T. Papagiannakis, Effect of preheating duration and temperature conditioning on the rheological properties of bitumen, Constr. Build. Mater. (2011), https://doi.org/10.1016/j.conbuildmat.2010.12.058.

[14] V. Mouillet, F. Farcas, E. Chailleux, Physico-chemical techniques for analysing the ageing of polymer modified bitumen, Polymer Modif. Bitumen (2011), https://doi.org/10.1016/B978-0-85709-048-5.50012-2.

[15] J.C. Petersen, A review of the fundamentals of asphalt oxidation (E-C140), Transp. Res. Rec.: J. Transp. Res. Board (2009).

[16] W.S. Price, NMR Studies of Translational Motion, (2009), https://doi.org/10.1017/CBO9780511770487.

[17] R. Angelico, S. Murgia, G. Palazzo, Reverse wormlike micelles: a special focus on nuclear magnetic resonance investigations, RSC Soft Matter (2017), https://doi.org/10.1039/9781782629788-00031.

[18] M. Porto, P. Caputo, V. Loise, B. Teltayev, R. Angelico, P. Calandra, C.O. Rossi, New experimental approaches to analyse the supramolecular structure of rejuvenated aged bitumens, News of the National Academy of Sciences of the Republic of Kazakhstan, Ser. Geol. Tech. Sci. 6 (2019), https://doi.org/10.32014/2019.2518-170X.181.

[19] C.O. Rossi, S. Ashimova, P. Calandra, M.P. De Santo, R. Angelico, Mechanical resilience of modified bitumen at different cooling rates: a rheological and atomic force microscopy investigation, Appl. Sci. (Switzerland) (2017), https://doi.org/10.3390/app7080779.

[20] C.O. Rossi, P. Caputo, S. Ashimova, A. Fabozzi, G. D'Errico, R. Angelico, Effects of natural antioxidant agents on the bitumen aging process: an EPR and rheological investigation, Appl. Sci. (Switzerland) (2018), https://doi.org/10.3390/app8081405.

[21] H. Cui, S. Siva, L. Lin, Ultrasound processed cuminaldehyde/2-hydroxypropyl-β-cyclodextrin inclusion complex: Preparation, characterization and antibacterial activity, Ultrason. Sonochem. (2019), https://doi.org/10.1016/j.ultsonch.2019.04.001.

[22] C. Oliviero Rossi, P. Caputo, V. Loise, S. Ashimova, B. Teltayev, C. Sangiorgi, A new green rejuvenator: evaluation of structural changes of aged and recycled bitumens by means of rheology and NMR, © RILEM (2019), https://doi.org/10.1007/978-3-030-00476-7_28 L. D. Poulikakos et al. (Eds.): RILEM 252-CMB 2018, RILEM Bookseries 20, pp. 177–182, 2019.

[23] P. Caputo, V. Loise, S. Ashimova, B. Teltayev, R. Vaiana, C.O. Rossi, Inverse Laplace Transform (ILT)NMR: a powerful tool to differentiate a real rejuvenator and a softener of aged bitumen, Colloids Surf. A Physicochem. Eng. Asp. (2019), https://doi.org/10.1016/j.colsurfa.2019.04.080.

[24] A. Muhammad, R.B.D.V. Azeredo, ^{1}H NMR spectroscopy and low-field relaxometry for predicting viscosity and API gravity of Brazilian crude oils – a comparative study, Fuel (2014), https://doi.org/10.1016/j.fuel.2014.04.026.

[25] L. Gentile, L. Filippelli, C.O. Rossi, N. Baldino, G.A. Ranieri, Rheological and H-NMR spin-spin relaxation time for the evaluation of the effects of PPA addition on bitumen Mol, Cryst. Liq. Cryst. (2012), https://doi.org/10.1080/15421406.2011.653679.

[26] P. Caputo, V. Loise, A. Crispini, C. Sangiorgi, F. Scarpelli, C.O. Rossi, The Efficiency of Bitumen Rejuvenator Investigated Through Powder X-ray Diffraction (PXRD) Analysis and T_2-NMR Spectroscopy Colloids and Surfaces a: Physicochemical and Engineering Aspects, (2019), https://doi.org/10.1016/j.colsurfa.2019.03.059.

[27] C.O. Rossi, A. Spadafora, B. Teltayev, G. Izmailova, Y. Amerbayev, V. Bortolotti, Polymer modified bitumen: rheological properties and structural characterization, Colloids Surf. A Physicochem. Eng. Asp. (2015), https://doi.org/10.1016/j.colsurfa.2015.02.048.

[28] S. Saoula, K. Soudani, S. Haddadi, M.E. Munoz, A. Santamaria, Analysis of the rheological behavior of aging bitumen and predicting the risk of permanent deformation of asphalt, Mater. Sci. Appl. (2013), https://doi.org/10.4236/msa.2013.45040.

[29] P. Redelius, H. Soenen, Relation between bitumen chemistry and performance, Fuel (2015), https://doi.org/10.1016/j.fuel.2014.09.044.

[30] P. Caputo, M. Porto, V. Loise, B. Teltayev, C.O. Rossi, Analysis of mechanical performance of bitumen modified with waste plastic and rubber (SBR) additives by rheology and PGSE NMR experiments, Eurasian Chem. J. 21 (2019), https://doi.org/10.18321/ectj864.

[31] M. Le Guern, E. Chailleux, F. Farcas, S. Dreessen, I. Mabille, Physico-chemical analysis of five hard bitumens: identification of chemical species and molecular organization before and after artificial aging, Fuel (2010), https://doi.org/10.1016/j.fuel.2010.04.035.

[32] A.A.A. Molenaar, E.T. Hagos, M.F.C. van de Ven, Effects of aging on the mechanical

characteristics of bituminous binders in PAC, J. Mater. Civ. Eng. (2010), https://doi.org/10.1061/(ASCE)MT.1943-5533.0000021.
[33] G.H. Sørland, Dynamic pulsed-field-Gradient NMR, Springer Ser. Chem. Phys. (2014), https://doi.org/10.1007/978-3-662-44500-6.
[34] R. Angelico, A. Ceglie, U. Olsson, G. Palazzo, L. Ambrosone, Anomalous surfactant diffusion in a living polymer system, Phys. Revi. E - Stat. Nonlinear Soft Matter Phys. (2006), https://doi.org/10.1103/PhysRevE.74.031403.
[35] M. Röding, D. Bernin, J. Jonasson, A. Särkkä, D. Topgaard, M. Rudemo, M. Nydén, The gamma distribution model for pulsed-field gradient NMR studies of molecular-weight distributions of polymers, J. Magn. Reson. (2012), https://doi.org/10.1016/j.jmr.2012.07.005.
[36] N.H. Williamson, M. Nydén, M. Röding, The lognormal and gamma distribution models for estimating molecular weight distributions of polymers using PGSE NMR, J. Magn. Reson. (2016), https://doi.org/10.1016/j.jmr.2016.04.007.
[37] P. Calandra, A. Ruggirello, A. Mele, V.T. Liveri, Self-assembly in surfactant-based liquid mixtures: Bis(2-ethylhexyl)phosphoric acid/bis(2-ethylhexyl)amine systems, J. Colloid Interface Sci. 348 (2010) 183–188, https://doi.org/10.1016/j.jcis.2010.04.031.
[38] P. Calandra, V.T. Liveri, P. Riello, I. Freris, A. Mandanici, Self-assembly in surfactant-based liquid mixtures: Octanoic acid/Bis(2-ethylhexyl)amine systems, J. Colloid Interface Sci. 367 (2012) 280–285, https://doi.org/10.1016/j.jcis.2011.10.015.
[39] P. Calandra, A. Mandanici, V.T. Liveri, Self-assembly in surfactant-based mixtures driven by acid-base reactions: Bis(2-ethylhexyl) phosphoric acid-n-octylamine systems, RSC Adv. 3 (2013) 5148–5155, https://doi.org/10.1039/c3ra23295f.
[40] P. Calandra, I. Nicotera, C.O. Rossi, V.T. Liveri, Dynamical properties of self-assembled surfactant-based mixtures: triggering of one-dimensional anomalous diffusion in Bis(2-ethylhexyl)phosphoric acid/ n -octylamine systems, Langmuir (2013), https://doi.org/10.1021/la403522q.
[41] W.S. Price, Spin Dynamics: Basics of Nuclear Magnetic Resonance, 2nd ed., Concepts in Magnetic Resonance Part A, 2009, https://doi.org/10.1002/cmr.a.20130.
[42] L.L. Barbosa, F.V.C. Kock, R.C. Silva, J.C.C. Freitas, V. Lacerda, E.V.R. Castro, Application of low-field NMR for the determination of physical properties of petroleum fractions, Energy Fuels (2013), https://doi.org/10.1021/ef301588r.
[43] J. Eyssautier, P. Levitz, D. Espinat, J. Jestin, J. Gummel, I. Grillo, L. Barré, Insight into asphaltene nanoaggregate structure inferred by small angle neutron and X-ray scattering, J. Phys. Chem. B (2011), https://doi.org/10.1021/jp111468d.
[44] M.P. Hoepfner, H.S. Fogler, Multiscale scattering investigations of asphaltene cluster breakup, nanoaggregate dissociation, and molecular ordering, Langmuir (2013), https://doi.org/10.1021/la403531w.

Chapter 10

Rejuvenating vs. Softening Agents; A Rheological and Microscopic Study

Book of proceedings Firs Macedonian Road Congress, 7-8 November 2019, Skopje (Republic of North Macedonia)

REJUVENATING VS. SOFTENING AGENTS; A RHEOLOGICAL AND MICROSCOPIC STUDY

Valeria Loise[1], Cesare Oliviero Rossi[2], Loretta Venturini[3], Shahin Eskandarsefat[4],Lorenzo Sangalli[5]
[1]Ph.D. Candidate, University of Calabria, Italy,valeria.loise@unical.it
[2]Associated Professor, University of Calabria, Italy,cesare.oliviero@unical.it
[3]Technical Manager, Iterchimica S.r.l., Italy,loretta.venturini@iterchimica.it
[4]Scientific Technical Development, Iterchimica S.r.l., Italy, shahin.eskandarsefat@iterchimica.it
[5]Technical Area Manager, Iterchimica S.r.l., Italy,lorenzo.sangalli@iterchimica.it

Апстракт

Во денешно време, нема потреба да се потенцираат непроценливите придобивки од поплочен асфалтен коловоз (РАП) при производство на одржливи асфалтни коловози, бидејќи тоа е докажано со многу истражувачки работи и практични искуства. Како и да е, треба да се напомене дека во мешавините што содржат голема количина на RAP, нивото на успех зависи многу од видот и количината на користениот агенс за подмладување. Презентираниот труд се занимава со техниките, кои во моментот се користат за испитување на средства за подмладување / омекнување. Се покажа дека иако некои материјали се ефикасни во обновувањето на реолошките својства, тие не се ефикасни во обновувањето на хемиските компоненти на стариот битумен, што значително влијае на трајноста и својствата на рециклираните асфалтни мешавини. За таа цел, различни агенси за подмладување / омекнување беа испитани со користење на различни проценти додадени на стариот битумен со помош на ролна за тенок филм (RTFO) и садови под притисок (ПАВ). Планот за тестирање се состоеше од реолошка и микроскопска анализа со помош на динамичен реметар на сноп (ДСР) и микроскопија на атомска сила (АФМ), соодветно.

Клучни зборови

Обновен асфалтен коловоз (RAP), средства за подмладување / омекнување, ролна со тенок филм (РТФО), садови за стареење на притисок (ПАВ), динамички стриминг реометар (ДСР), атомска сила микроскопија (АФМ).

Abstract

Nowadays, there is no need for highlighting the uncountable benefits of Reclaimed Asphalt Pavement (RAP) in producing sustainable asphalt pavements, since it has been proven with many research works and practical experiences. However, it should be noted that within the mixtures containing high amount of RAP the level of success is highly depended on the type and quantity of the used rejuvenating agent. The presented paper deals with the techniques, which are currently being used for investigating rejuvenating/softening agents. It has been shown that while some materials are effective in recovering the rheological properties, they are not effective in restoring the chemical components of the aged bitumen, which significantly affects the durability and properties of the recycled asphalt mixtures. For this purpose, different rejuvenating/softening agents were investigated using different percentages added to an aged bitumen by means of Rolling Thin Film Oven (RTFO) and Pressure Aging Vessel (PAV). The test plan consisted of rheological and microscopic analysis by means of Dynamic Shear Rheometer (DSR) and Atomic Force Microscopy (AFM), respectively.

Key words

Reclaimed Asphalt Pavement (RAP), rejuvenating/softening agents, Rolling Thin Film Oven (RTFO), Pressure Aging Vessel (PAV), Dynamic Shear Rheometer (DSR), Atomic Force Microscopy (AFM).

1. INTRODUCTION

While the economic and environmental advantages of usingreclaimed asphalt pavement (RAP) in asphalt mixes have been recognized for decades, with increasing environmental awareness and rising costs of virgin binders it has become the first choice for sustainable pavements. RAP binders have been aged to different extents during pavements' service life hence adding recycling agents provides a practical means for restoring the mechanical properties of the aged binders reducing the needed additional virgin binder.In this regards, many research works and practical experiences have shown that the final properties of the recycled asphalt mix, in particular those of high-RAP containing are highly depended on the type and amount of the recycling agent used in it. While many additives have been used to modify the properties of aged bituminous materials to ensure long-term durability in highly recycled pavements, many of them are just capable of reducing the stiffness and not restoring the lost components of the aged binder.It should be noted that it is not only important to have a balanced mix design for volumetric and physical indices but also to ensure that the design will provide long term performance without increased rutting and/or premature cracking. This makes difference between a softening agent and rejuvenating agent.It is believed that rejuvenating agents affect both the physical and chemical properties of the virgin bitumen binder and the RAP binder in the mix design [1] the softening agents modify just the physical and rheological properties.In fact,there is no consensus on the definition of recycling agents and associated mechanism.Perhaps, one of the most useful descriptions in this respect has been offered by Tabatabaee and Kurth, 2017[2]:

The most useful categorization for discriminating between recycling agents would need to be based on the bitumen fraction most affected by the additive and expected mechanism of affecting that compatible fraction upon adding to aged bitumen.

In another words, it can be said that all the additives that are being used for recycling purposes could be considered as recycling agents, however, not all of rejuvenating agents. Recycling agents could be either softening agent or rejuvenating agent with complete action. While rejuvenating agents are capable of modifying aged binder in both chemical and physical way, softening agents just work on physical properties in different extents.Considering the mentioned issues, the authors aimed for developinga new approach for investigating the mechanism of rejuvenation useful fordiscriminating rejuvenators with softening agents.

6. LITERATURE REVIEW

To analyse the effective mechanism of rejuvenators in the aged bitumen, one must first describe the bitumen chemical composition and aging mechanism. However, bitumen consists of a complex continuum of compounds. For this purpose, to date, awide range of test methods have been introduced and adopted by researchers. Bitumen well known SARA fractionation methods, different means of spectroscopy including Nuclear Magnetic Resonance (NMR) [3-5] and infrared spectroscopy (IR)[6-8], and microscopic analysis mostly by means of Atomic Force Microscopy(AFM)[9-11]are some these efforts. Amongst these methods, AFM has been shown to be a promising method for bitumen chemical structure analysis. Straightforward sample preparation and test procedure besides tangible results got attentions of researchers for bitumen studies. Depending on the type of measurement(non-contact mode (NCM) or pulsed-force mode(PFM)), the results can be presented either by surface topographyimage or phase image with which the mechanical properties can be identified. Within AFM images, aging mechanism of the bitumen can be easily seen with increased roughness of surface topography of bitumen or increased bitumen [12&13].

From another point of view, it cannot be denied that the first step for investigating the effectiveness of any type of recycling agent is physical modification. In this regards, while conventional test methods are use forevaluating the physical and rheological properties of bitumen at a specific temperature, Dynamic Shear Rheometer (DSR) can provide a reliable data on rheological properties of bitumen over a wide range of temperatures and frequencies. To date many research works have shown that the addition of different types of recycling agents modifies the stiffness and viscoelastic properties of aged bitumen binders to different extents[14&15]. However, the quantity and the effectiveness of any type of recycling agent based on just rheological analysis does not necessarily certify the expected durabilityof the final the asphalt mixture. This is mainlybecause of the lost bitumen constituents ofaged bitumen compared to virgin condition.

3. MATERIALS ANS METHODS

3.1 Materials

In this study, a 50/70 pen-graded bitumen binder was selected as for the base bitumen binder. As for recycling agents,seven different commercial products both including rejuvenating agents and softening agents were investigated anonymously in this research. The considered dosages of recycling agentsin the bitumen were2, 4, and 6% (on the weight of bitumen), which were added to the aged binder (after RTFO+PAV) after heating at 160±5˚C. It is worth mentioning thatthe mixing was manually and continueduntil getting a homogeneous compound.

3.2 Methods

Considering the objectives of the present research, the authors aimed forintroducing an approach distinguishing the rejuvenating agents with those of softening agents, which both groups could be considered as recycling agent. For this target at the first stage the base bitumen was subjected to short-term aging by means of Rolling Thin Film Oven (RTFO) and long-term aging by means of Pressure Aging Vessel (PAV). This bitumenwere then considered as references bitumen for investigating the performance of testing material. The recycling agents were then added in three different dosages to the aged bitumen in three different dosage, also evaluating the influence of its quantity on the rejuvenation mechanism. The experimental works consisted of rheological analysis by means of DSR and microscopic analysis by means of AFM.

4. RESULTS AND DISCUSSIONS

4.1 Dynamic Shear Rheology (DSR)

The DSR tests here consisted of temperature sweep tests from 25˚C to 80˚C.The tests have been done under constant amplitude of 1% at a constant frequency of1.59 Hz and temperature rate of 1˚C/min.Considering the temperature range in this study, the 25mm plate was applied for the tests considering 1 mm of gap.Figure 1 represents the test results represented in terms of Loss tangent (tan δ) versus temperature.The loss tangent, tan(δ)as shown in Equation 1, is commonly used to describe material losses, which indicates the softness ofthe material. The loss modulus G" is a measureof the lost deformation energy and therefore characterizes theliquid part (the viscous part) of the sample. The storage modulus G' is a measure of the deformationenergy stored in the system. It reflects the solid character (theelastic part) of the sample.As the viscous component increases,G ’’, the tangent δ increases and its divergenceindicates the gel-sol transition.The G’-G ’’ equilibrium (Tan δ profile) indicates thestructure of the material. Therefore, rheologicalanalysis can be considered as a valid technique forinvestigating the behaviour of a regeneratingadditives for bitumen binders.

$$Tan\,\delta = \frac{G''}{G'} \quad (1)$$

where:

G” is loss modulus and G’ is storage modulus.

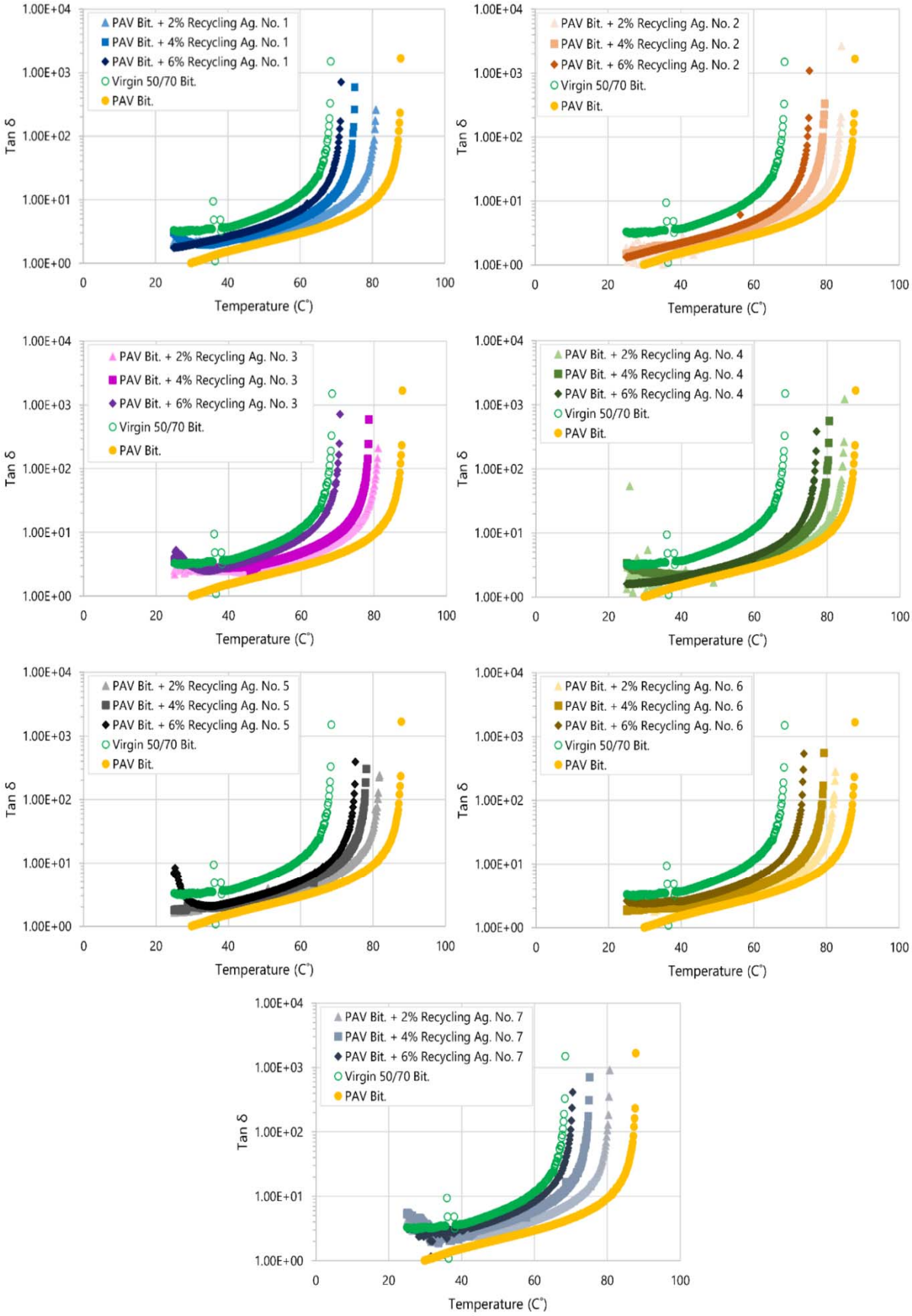

Fig. 1: Tanδ vs. Temperature

According to the figures, it can be seen that regardless of the recycling agent type (whether it is rejuvenating agent or softening agent), the more the recycling agent, the better the performance is and all the rested materials were effective somehow. Hence it can be said that all are softening agents. However, not all the compounds even with highest content of these recycling agents showed a comparable performance compared to the virgin neat bitumen. It can be seen that amongst the seven studied recycling agents, just three of them: number 1, 3, and 7 (with the highest quantity) were effective in changing the rheological properties of the aged binder close to the virgin neat bitumen.

In addition to tan δ, Table 1, represents the G* and G*/sin δ at 60˚C according to the Superpave binder specifications.G* is defined as the ratio of maximum (shear) stress to maximum strain and provides a measure of the total resistance to deformation when the bitumen is subjected to shear loading. Superpave considers the complex modulus (G*) as the stiffness of the binder including its viscosity and its elastic properties. On the other hand, G*/sin δ is measured at 1.592 Hz (10 rad/s) and is used for the prediction of pavement's resistance to permanent deformation. It is worth mentioning that the parameter has been determined at the temperature of 60˚C. In general, greater G*/sin δ values have been obtained for the PmBs compared to the neat binders. As expected the PAV aged bitumen showed the highest stiffness and adding all the recycling agents could reduce the stiffness significantly. However, it is clear that recycling agents no. 1, 3, and 7 were performed more effective than other tested materials.

Overall it can be claimed that from physical rheological point of view all the tested materials could be considered as a softening agent to some extent.

Table 1.G and rutting parameter*

Compound	G* at 60˚C (Pa)	G*/sin δ @ 1.592 Hz (kPa)
Virgin 50/70 Bit.	6228.1	6.3
PAV 50/70 Bit.	53989.5	57.0
PAV 50/70 Bit. + 6% Recycling Agent No. 1	6339.4	6.4
PAV 50/70 Bit. + 6% Recycling Agent No. 2	10573.9	10.8
PAV 50/70 Bit. + 6% Recycling Agent No. 3	6763.3	6.8
PAV 50/70 Bit. + 6% Recycling Agent No. 4	11489.9	11.8
PAV 50/70 Bit. + 6% Recycling Agent No. 5	10596.1	10.8
PAV 50/70 Bit. + 6% Recycling Agent No. 6	8145.1	8.3
PAV 50/70 Bit. + 6% Recycling Agent No. 7	6576.0	6.6

4.2 Atomic Force Microscopy (AFM)

Using AFM, four phases are typicallyobserved in bitumen AFM images:I) Catana phase consists of topographicfeatures known as bee like structures, II)Peri phase consists ofthe region surrounding the bee structures, III) Para phase as thepredominant smooth matrix, and IV) Sal phase as very small dots. In the literature with regards to bitumen's colloidal structure, the recognized phases in AFM images could be corresponded to the four well-known chemical fractions of bitumen consisted of Saturates, Aromatics, Resins, and Asphalene(SARA). The asphaltene are referred to the bee structures (In some contexts also referred to crystallized paraffin content of bitumen). The impression of "bees" stems from alternating higher and lower parts in the surface topography of bitumen. Resins as the region surrounding the bee-structures, and aromatics and saturates as the smooth matrix [14-19]. However, from the review of bitumen AFM imaging and analysis, it can be found that there is evident differences between interpretations of the researchers, who have worked on this topic. Even though the interpretation of AFM images might be difficult, they do contain a good deal of useful information.

Fig. 2 and Fig. 3 show the AFM images of the virgin bitumen, the aged sample, and the tested compounds.

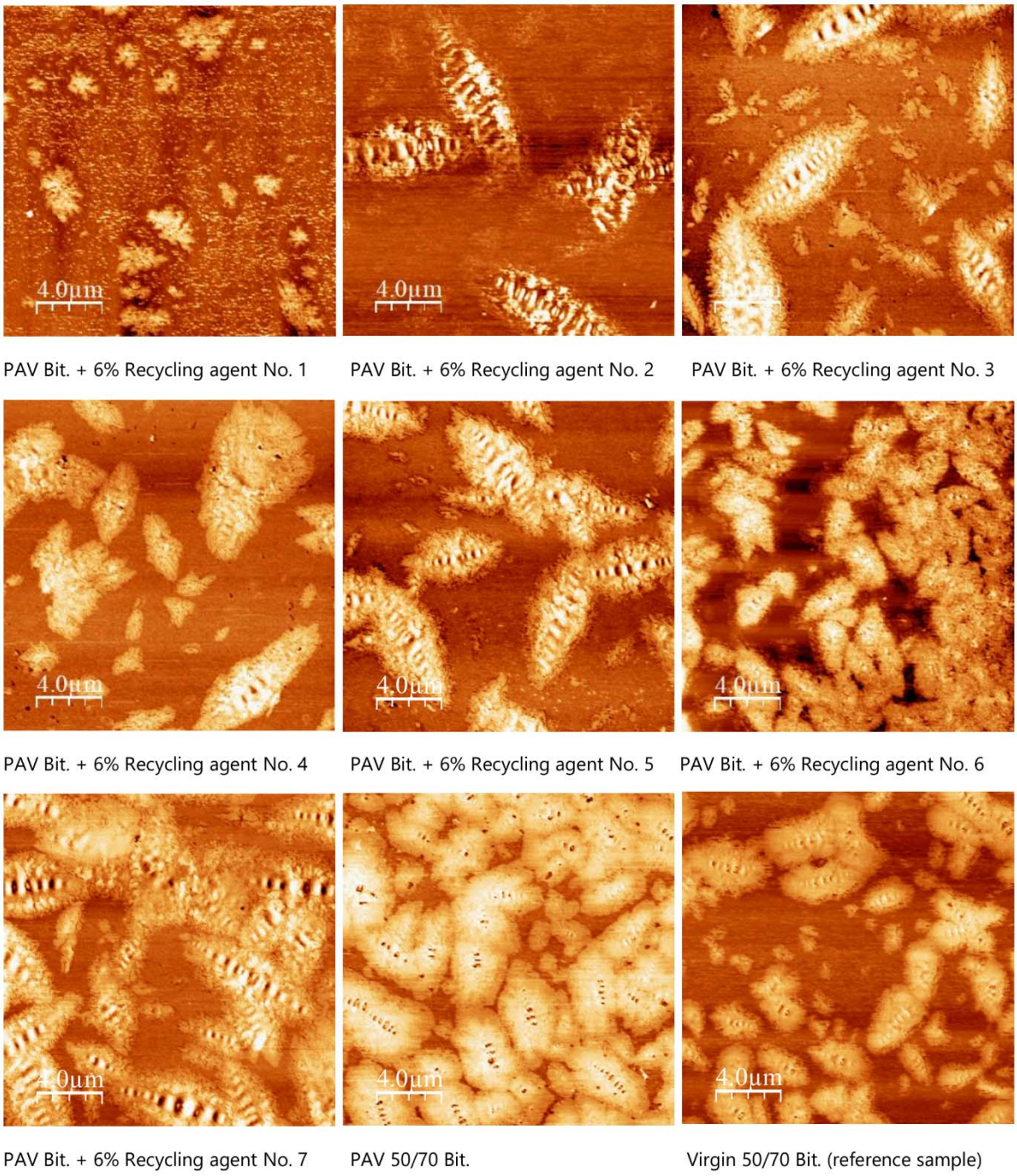

Fig. 2: AFM phase images (PFM)

According to the obtained AFM images shown in, the effect of aging on the virgin bitumen mainly can be seen by extended Peri phase, diminished Para phase, and rougher Catana phase. From the rejuvenation point of view, it can be seen that apart from the physical rheological properties the recycling agents affect the chemical micro structure of bitumen significantly. It is noteworthy that among the seven recycling agents, which were studied in this research, same to the rheological analysis the recycling agent no. 1, 3, and 7 showed more effective in terms of recovering chemical structure of aged binder. In addition to these recycling agents, no. 6 also shows an apparent improvement in chemical properties of aged bitumen. This has been also notified by 6% addition of this recycling agents.

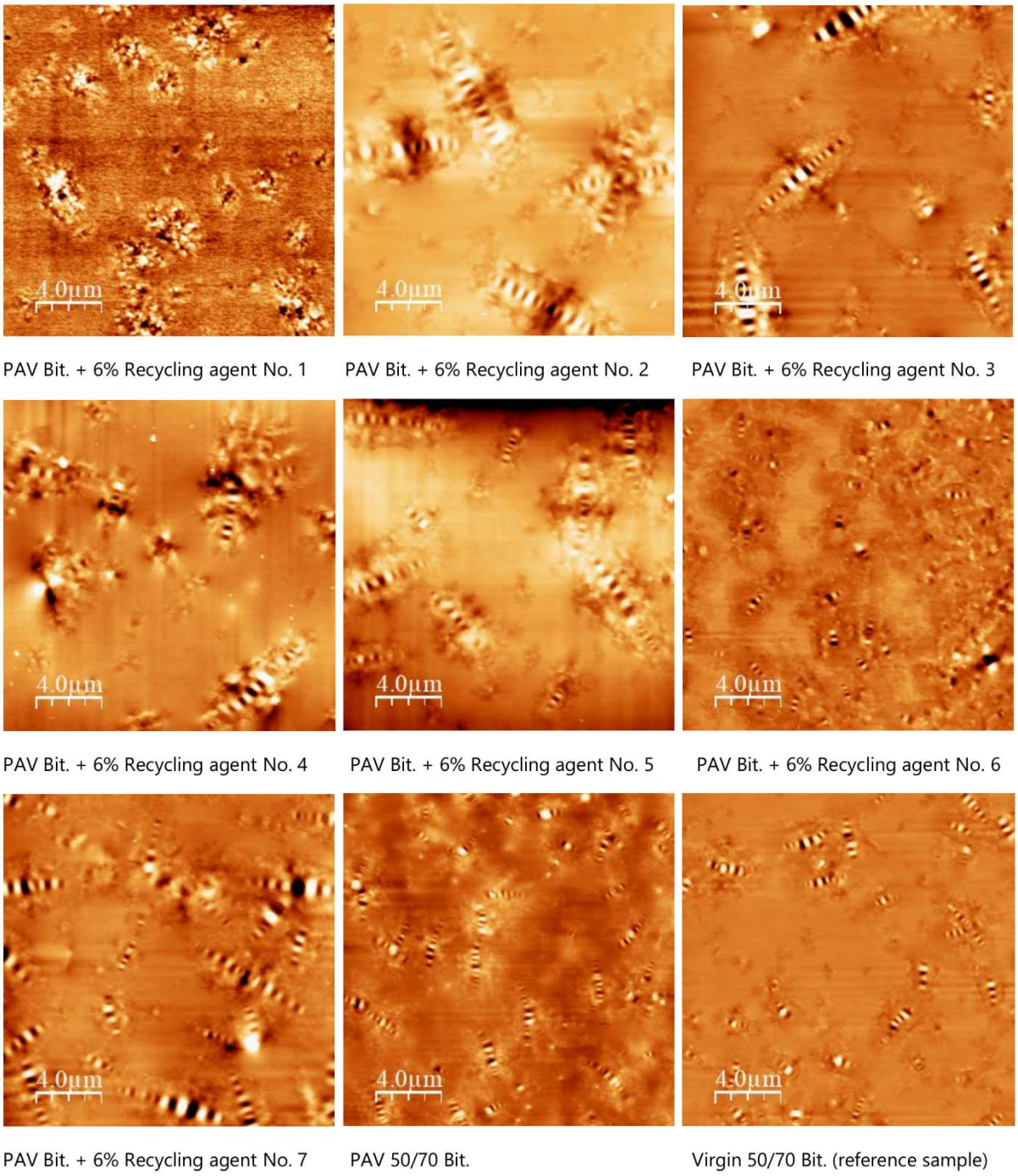

Fig. 3: AFM topography images (NCM)

5. CONCLUSIONS

In the current paper 7 different recycling (either softening agent or rejuvenating agent that provides both physical and chemical modification action) agents have been investigated using DSR analysis and AFM as forstudying the physical and chemical effectiveness of the recycling agents on the aged bitumen, respectively. Overall,in the light of the test results of this study, it can be declared that the not all the recycling agents are capable of rejuvenating function. It is clear that besides the early age mechanical and performance properties of a recycled mixture, the durability is highly depended on the chemical rejuvenation.The findings in this study can be concludedas followings:

- All the tested recycling agents in this study could reduce the stiffness in different extent however, few of them could reach to similar rheological properties to the virgin bitumen.
- It has been notified that the higher the used dosage was added, the better the performance was obtained. This was regardless of the type of recycling agent (softening agent/rejuvenating agent).

- AFM was found a useful tool and user friendly method for investigating the chemical rejuvenation of recycling agents, showing the influence of these materials on chemical structure of bitumen.
- Overall, considering the rheological analysis together with microscopic investigations, it can be said that recycling agents no. 1, 3, and 7 could act as a rejuvenator.

6. REFERENCES

[117]. Holly Frontier. Rejuvenating agents vs. recycling agentsin hot mix asphalt (HMA) design. (on-line) available at:https://www.hollyfrontierlsp.com/SiteData/docs/Rejuvenati

[118]. Tabatabaee H. A., Kurth T. L.(2017). Analytical investigation of the impact of a novel bio-based recycling agent on the colloidal stability of aged bitumen. Road materials and pavement design, Vol. 18, No. S2, 131-140.DOI: 10.1080/14680629.2017.1304257

[119]. Oliviero Rossi C., CaputoP., De LucaG., MaiuoloL., EskandarsefatS., SangiorgiC. (2018). 1H-NMR Spectroscopy: A Possible Approach toAdvanced Bitumen Characterization for Industrialand Paving Applications. Applied Sciences 8(2). DOI: 10.3390/app8020229

[120]. Caputo P., Loise V., Ashimova S., Teltayev B., Vaiana R., Oliviero Rossi C. (2019). Inverse Laplace Transform (ILT) NMR: a powerful tool to differentiate a real rejuvenator and a softener of aged bitumen. Colloid and Surface, 154-161. DOI: 10.1016/j.colsurfa.2019.04.080

[121]. Caputo P., Loise V., Crispini A., Sangiorgi C., Scarpelli F., Oliviero Rossi C.(2019).The efficiency of bitumen rejuvenator investigated through Powder X-ray Diffraction (PXRD) analysis and T 2 -NMR spectroscopy. Colloids and Surfaces, 50-54. DOI:10.1016/j.colsurfa.2019.03.059

[122]. Dony A., Ziyani L., Drouadaine I., S. Pouget, Faucon-Dumont S., Simard D., Mouillet V., Eric Poirier J., Gabet T., Boulange L., Nicolai A., Gueit C. (2016). MURE National Project: FTIR spectroscopy study to assess ageing of asphalt mixtures. Proceedings of E&E Congress 2016, 6th Eurasphalt&Eurobitume Congress. DOI: 10.14311/EE.2016.154

[123]. Ahmed F. (2016) Diffusion of the rejuvenators into bitumen studied by FTIR-ATR as a function of temperature and bitumen properties. Master's thesis, Aalto University.

[124]. Mikhailenko P., Bertron A., Ringot E. (2015). Methods for analyzing the chemical mechanisms of bitumen aging and rejuvenation with FTIR spectrometry. 8th RILEM International Symposium on Testing and Characterization of Sustainable and Innovative Bituminous Materials, RILEM Bookseries. DOI: 10.1007/978-94-017-7342-2_17

[125]. Aguiar-Moya J. P., Salazar-Delgado J., García A., Baldi-Sevilla A., Bonilla-Mora V., Loría-Salazar L. G. (2017). Effect of aging on micromechanical properties of bitumen by means of atomic force microscopy. Road materials and pavement design, Vol. 18, No. S2, 203-215. DOI: 10.1080/14680629.2017.1304249

[126]. Nahar S.N., Qiu J., Schmets A.J.M., Schlangen E., Shirazi M., Van de Ven M. F. C., Schitter G., Scarpas A. (2014).Turning Back Time: Rheological and microstructural assessment of rejuvenated bitumen. 93th Annual Meeting of the Transportation Research Board, Washington, D.C.

[127]. Oliviero Rossi C., Ashimova S., Calandra P., Penelope De Santo M. and Angelico R. (2017). Mechanical resilience of modified bitumen at different cooling rates: a rheological and atomic force microscopy investigation. Appl. Sci. DOI: 10.3390/app7080779

[128]. JvdMSteyn W. (2011). Analysis of bitumen properties during ageing using Atomic Force Microscopy. Conference paper in Geotechnical Special Publication. DOI: 10.1061/47634(413)4

[129]. Großegger D. (2016). Microstructural aging of bitumen.E&E Congress 2016, 6th Eurasphalt&Eurobitume Congress, Prague, Czech Republic. DOI: dx.doi.org/10.14311/EE.2016.135

[130]. Zaumanis M.,Mallick R. B, PoulikakosL., FrankR. (2014). Influence of six rejuvenators on the performance properties of reclaimedasphalt pavement (RAP) binder and 100% recycled asphalt mixtures. Construction and Building Materials, 538–550,DOI:10.1016/j.conbuildmat.2014.08.073

[131]. Koudelka T., Coufalik P., Fiedler J., Coufalikova I., Varasus M., Yin F. (2019).Rheological evaluation of asphalt blends at multiple rejuvenation and aging cycles.Road materials and pavement design, Vol. 20, No. S1, DOI: 10.1080/14680629.2019.1588150

[132]. LesueurD. (2009). The colloidal structure of bitumen: Consequences on the rheology and on the mechanisms of bitumen modification. Advances in Colloid and Interface Science.

[133]. Pauli A.T., Branthaver J.F., Robertson R.E., Grimes W., Eggleston C.M. (2001). Atomic force microscopy investigation of SHRP asphalts: Heavy oil and reside compatibility and stability. Prepr. Am. Chem. Soc. Div. Pet. Chem.

[134]. Loeber L., Sutton O., Morel J.V.J.M, Valleton J.M., Muller G. (1996). New direct observations of asphalts and asphalt binders by scanning electron microscopy and atomic force microscopy. J. Microsc.

[135]. Jäger A., Lackner R., Eisenmenger-Sittner C., Blab R. (2004). Identification of microstructural components of bitumen by means of atomic force microscopy (AFM). PAMM.